The antiviral siRNA interactome in Drosophila melanogaster

Karim Majzoub

Université de Strasbourg (UdS) **Institut de Biologie Moléculaire et Cellulaire (IBMC)**

Année 2013

ECOLE DOCTORALE DES SCIENCES DE LA VIE ET DE LA SANTÉ DE STRASBOURG

Thèse

Présentée à l'Université de Strasbourg
pour l'obtention du grade de Docteur en Sciences

Spécialité : Biologie Moléculaire

Karim MAJZOUB

The antiviral siRNA interactome *in Drosophila melanogaster*

Soutenue publiquement le 23 Septembre 2013 devant
le jury d'examen

Prof. Eric WESTHOF
Dr. Monsef BENKIRANE
Prof. Eric MISKA
Prof. Jean-Luc IMLER (Directeur de Thèse)

Aknowledgements

The work presented hereafter wouldn't have been possible without the support of many people that I would like to gratefully thank.

I am thankful to Pr. Jean-Marc Reichhart, director of the UPR9022 of the CNRS (Réponse Immunitaire et Développement chez les insectes), who hosted me in his laboratory. I would like also to aknowledge my PhD supervisor
Pr. Jean-Luc Imler who guided me throughout my thesis. Pr. Imler investement in my project was full of important advice and ideas. His great knowledge, experience and sens of perfection contributed in shaping my scientific thinking during the past four years. I would like also to thank professors Jules Hoffmann and Charles Hetru who submerged me with their wisdom each time I talked to them.
I would like to also thank my laboratory colleagues with whom I had a very pleasent and productive time : Gloria, Hide, Vincent, Akira, Basti, Francois and Estelle.
Dr. Nicolas Matt and Dr. Carine Meignin were always very supportive and the discussion we had were full of good advice.
I would like to thank my father, mother and sister who always loved me and supported me and contributed indirectly to this work. My friends : Eli, Housam, Julien, Alex, Niccolo and Simon who constituted my adoption family in Europe.
Finally, I would like to thank my patient and beautiful wife, Laure, for supporting me throughout all these years, and for giving me my lovely daughter, Maya.
Apart from being definitely the best result I obtained during my PhD years, Maya, reinforced my fascination for Life. Giving me an additonal reason for asking lively questions and trying to answer them.

Table of Contents

The ribosomal protein RACK1 is a specific host factor required for IRES-mediated translation of fly and human viruses

I- Introduction

We live in a dangerous world. Living organisms have evolved facing constant existential threats. Environmental changes and competition for survival, inherent to life on earth, have consequently shaped our defense systems.

The first line of defense, of all organisms, against microbial pathogens is their physical barrier, which delimits the “self“ from the “outside world“. However, if the pathogen breaches such a barrier, a layered immune response is employed to counter the invasion. The recognition of the pathogen via the Pathogen Associated Molecular Patterns (PAMPs) by the host’s innate immune system leads to an immediate but non-specific response. Such innate immune systems are found in all plants and animals. Vertebrates possess a second layer of protection consisting of the adaptive immunity. Albeit its need for innate immunity for activation, the adaptive response is more tailored and specific. Moreover, this specific response can be retained after the elimination of the pathogen, constituting an “immune memory“.

Immune systems, are not only important for the defense against invading cellular pathogens, they are also crucial for the preservation of the organism’s genetic integrity from foreign selfish genetic elements such as viruses. The control of viral replication constitutes a challenge for the host immune system for many reasons. First, unlike other classical pathogens, viruses offer very few intrinsic PAMPs to the immune system for detection. Additionally, viruses are able to replicate, mutate and spread very rapidly, escaping immune surveillance. Their intimate interaction and dependence on various host cellular compartments and machineries makes them difficult targets. Moreover, viruses often encode proteins that attempt to neutralise immune responses. Therefore, an elaborate immune antiviral arsenal is constantly being selected throughout evolution, creating an ever-escalating arms race between host and virus.

The study of model organisms in biology has contributed greatly to the understanding of how an efficient immune response is mounted. Important discoveries of fundamental defense processes in plants, insects, worms and mammals were carried out in model

organisms such as *Arabidopsis thaliana, Drosophila melanogaster, Caenorhabditis elegans and Mus musculus*.

The fruit fly *D. melanogaster* have been, historically, the model of choice of my host laboratory to study immune mechanisms in insects. Amongst the animal kingdom *D.melanogaster* offer non-negligible advantages for researchers. Its small size, fast generation time and easy handling make it a very attractive model. Consequently, drosophila have been studied by biologists for over a century, therefore an immense volume of data concerning fly's biology has accumulated and many genetic tools have been developed.

During the last two decades Pr. Jules Hoffmann's group and others have been able to characterize different pathways governing fly's immunity. This work depicted not only basic principles of the fly's innate immune response, but it also paved the way for a better understanding of general innate immunity in other organisms, including human beings.

1. Innate Immunity in *Drosophila melanogaster*

1.1 An inducible anti-fungal and anti-bacterial response

In 1996, the discovery of the involvement of *Dm* Toll receptor in the flies' immunity answered a riddle that vertebrate immunologists have theoretically posed.

Towards the end of the 1980s, Charles Janeway has proposed what was then an unorthodox belief that the immune system evolved not simply to discriminate "self" from "non-self", but "non-dangerous self " from "dangerous non-self". This idea implied the conceptual existence of cellular Pattern Recognition Receptors (PRRs), capable of recognizing conserved pathogenic signatures (Janeway, 1989). The discovery of cellular receptors, like *Dm* Toll, capable of sensing a pathogen's invasion proved that such a theory was correct. Moreover, the signalling cascade subsequent to Toll activation turned out to be very conserved between insects and vertebrates.

In Drosophila, the hallmarks of innate immunity activation are the recognition of pathogens by germline-encoded, non-rearranging receptors, and rapid effector mechanisms that involve phagocytosis, activation of proteolytic cascades and synthesis

of potent antimicrobial peptides (Hoffmann, 2003) .Two pathways are major players in *Drosophila* immunity : The Toll and the IMD pathways.

Toll pathway activation constitutes the main anti-fungal and anti-Gram+ bacteria immune response in *Drosophila*. A proteolytic cascade of extra-cellular proteins is initiated early after infection, which leads to the cleavage of the Spaëtzle protein. Cleaved forms of Spaëtzle binds then as a dimer to the ectodomain of the transmembrane receptor Toll. The conformational change induced by this binding is relayed by the intracytoplasmic TIR domain of Toll, which permits its interaction with three cytoplasmic adaptor proteins such as the conserved Myd88. The ultimate result of Toll signalling is the dissociation of the NF-kB protein from the protein Cactus, a homologue of mammalian IkBs. This dissociation leads to NF-kB translocation to the nucleus, and the activation of an immune transcriptional program. The result of such an activation is the synthesis of potent and broad spectrum antibiotics known as anti-microbial peptides (AMPs) (e.g. Drosomycin) (Hoffmann, 2003).

The second pathway controlling the response against Gram- bacteria in Drosophila is the IMD pathway. This pathway is similar in many aspects to the mammalian TNF-α receptor signaling pathway. Activation of the IMD pathway requires proteins members of the peptidoglycan-recognition proteins (PGRP) family like PGRP-LC and PGRP-LE. In contrast to Dm Toll receptor and similar to Toll-like receptors (TLRs) in mammals PGRPs are able to recognise PAMPs on their own. This recognition leads to the activation of a signalling cascade involving proteins with known mammalian homologues (e.g. FADD, caspase-8, TAK1 and IKK signalosome proteins). Similar to the Toll pathway, IMD pathway activation leads ultimately to the synthesis of AMPs (e.g. Attacin, Diptericin) in a NF-kB dependant manner (Hoffmann, 2003).

Many functional parallels can be drawn between innate immune responses in different animals: first is the recognition of the “Pathogen“ or “Danger “ by cellular receptors, second is the transmission of such an information to the nucleus, third is the response with specific transcriptional programs and finally the synthesis of signalling or effector molecules that will fight the infection. The striking sequence similarities of genes governing these responses between Drosophila and vertebrates demonstrates the evolutionary ancient character of such defense mechanism.

1.2 An inducible antiviral response

In insects, some viral infections also induce a transcriptional response able to restrict virus replication (Deddouche et al., 2008; Dostert et al., 2005; Paradkar et al., 2012). The response, in this case, is different and less characterized than the one triggered by bacteria and fungi. Interestingly, this response does not seem to be the only strategy employed by insects to fight viral infections. Another broader mechanism, involving programmed viral RNA targeting, termed as "RNA interference" (RNAi), seems to constitute the central antiviral arsenal in the fly. However, a closer look at the inducible antiviral response, hints to a certain connection to RNAi. Moreover, a careful examination of this inducible response reveals many parallels with the antiviral IFN system in vertebrates.

Infection of drosophila by the picorna-related virus Drosophila C Virus (DCV) triggers the upregulation of at least one hundred genes (Dostert et al., 2005), whereas infection of *Aedes* mosquitoes with Flaviviruses (dengue or West-Nile virus) leads to induction of a couple of hundred genes (Colpitts et al., 2011). The existence of such an inducible response raises two major questions concerning (1) the nature and function of the effector molecules induced by viral infections; and (2) the identity of the receptors sensing viral infection and triggering such a response.

The analysis of the promoter of the DCV and Flock House Virus (FHV) induced gene vir-1 (virus-induced RNA1) revealed the importance of DNA motifs recognized by the transcription factor STAT92E, the only STAT factor present in flies (Dostert et al., 2005). Importantly, *vir-1* and other DCV-induced genes are not transcribed following viral infection in *hopscotch (hop)* flies, mutants for the *Dm* JAK kinase. In addition, *hop* $^{-/-}$ mutant flies succumb more rapidly, with higher viral loads, compared to control flies, when infected with DCV. It has also been shown that the JAK/STAT pathway participates in the control of Dengue virus infections in *Aedes* mosquitoes (Souza-Neto et al., 2009). The JAK/STAT activation seems to be dependant on the Domeless receptor, which implies the presence of a secreted cytokine-like ligand induced after viral sensing. The involvement of the JAK/STAT pathway in the antiviral immune

defense in insects allows to draw a first parallel with the mammalian antiviral IFN system. The induction of many antiviral Interferon-Stimulated Genes (ISGs) depend on IFN α/ β binding to IFNAR receptor followed by the JAK-dependant STAT dimerization and its translocation to the nucleus to serve as a transcription factor (Shuai and Liu, 2003).

Another interesting marker for this inducible response is the up-regulation of the gene *Vago* (Deddouche et al., 2008; Paradkar et al., 2012). The expression of the gene *Vago* is observed after DCV or Sindbis virus (SINV) infection of fruit flies or West Nile Virus (WNV) infection of *Culex* mosquitoes. Importantly, independant research groups (including ours) , have shown that the expression of the Vago protein is able to control DCV replication in the flies' fat body or to restrict WNV infection in mosquito cells. Curiously, the expression of *vago* is JAK/STAT- independent and seems to depend on Dicer-2 protein. Moreover, the induction of the antiviral gene *vir-1* in mosquitoes seem to require secreted Vago, placing this molecule as the potential cytokine-like, responsible of the antiviral JAK/STAT activation(Paradkar et al., 2012). Unfortunately, the signalling pathway linking Dicer-2 to *vago* remains completely unknown, but some experiments hint that dsRNA is required to activate such a pathway (Deddouche et al., 2008).

Dicer-2 is a known RNase III able to cleave long viral double-stranded RNA (dsRNA) intermediates into small interfering RNAs (siRNAs) *in vitro* (Lee et al., 2004; Ye and Liu, 2008) Apart from the unquestionable involvement of the two RNase III domains of this protein in the antiviral RNAi, Dcr-2 also possesses in its N-terminal a DExD/H-box helicase domain (Deddouche et al., 2008). This molecule is, therefore, not only an antiviral effector but is a typical sensor of viral RNA. Strikingly, Dcr-2's helicase domain shares important phylogenetic similarity with DExD/H-box helicase of known mammalian viral sensors, namely the RIG-I-Like-Receptors (RLRs). RLRs, like RIG-I or MDA-5, sense conserved viral signatures, like 5' triphosphates or dsRNA duplexes, and are then able, through their caspase recruitment domains (CARD), to activate a signaling cascade leading to interferon production (Takeuchi and Akira, 2008).

The structural similarity between the DExD/H-box helicase domain that the mammalian RLRs and *Dm* Dicer-2, added to their common functional role in sensing viral RNAs, constitute another striking parallel between the mammalian antiviral IFN system and the

inducible antiviral response in *drosophila*. It also hints to an evolutionary conserved role of such domains in antiviral immunity (Takeuchi and Akira, 2008).

Importantly, all the cited examples hereupon about the involvement of an inducible antiviral response in *Drosophila,* concern only certain virus-specific responses. As mentioned before, the inducible response does not seem to be the general antiviral mechanism in Drosophila but it appears to rather constitute a special battalion amongst a greater antiviral armada.

There are undoubtedly biochemical and genetic evidence showing that siRNA pathway components are the main antiviral players in *Drosophila melanogaster*.
The importance of the siRNA pathway for the control of viral infections is best illustrated by the high susceptibility of *Dicer-2*$^{-/-}$, *AGO2*$^{-/-}$ and *r2d2*$^{-/-}$ mutant flies to viral infections. Mutant flies die more rapidly than wild-type controls, with higher viral loads, following infection by a large number of viruses. This includes double stranded RNA viruses like Drosophila X Virus (DXV) or single-stranded viruses of positive polarity like Drosophila C Virus (DCV), Cricket Paralysis Virus (CrPV), Flock House Virus (FHV) and Sindbis Virus (SINV) or negative polarity like Vesicular Stomatitis Virus (VSV) (Galiana-Arnoux et al., 2006; Mueller et al., 2010; van Rij et al., 2006; Wang, 2006; Zambon et al., 2006). Furthermore it has been recently shown that mutants in these proteins are also more susceptible to a DNA virus infection, the iridescent IIV-5 virus (Bronkhorst et al.; Kemp et al., 2013). It is therefore clearly established that the siRNA pathway plays a major role in the control of virus infections in *Drosophila*.

Hereafter, I will try to review what is known about RNAi function in different organisms, stressing the importance of this mechanism in general genome defense in plants, invertebrates and more particularly *Drosophila* species.

2. RNA interference and genome defense

The discovery of the RNA interference mechanism constituted one of the major discoveries in biology of the last twenty years. The discovery of such a mechanism brought to light an unappreciated role of small RNA molecules in different aspects of genome defense, maintenance and gene regulation.

The first observation that a specific small anti-sense oligonucleotides can regulate negatively gene expression was made in 1978 when Zamecnik and Stephenson succeeded in inhibiting the replication of Rous Sarcoma Virus (RSV) in chick embryo fibroblasts, by artificially introducing 13 anti-sense nucleotides molecules which can potentially hybridize with the viral terminal sequences. The authors of this study proposed many models that could explain such a phenomenon, involving DNA:DNA, DNA:RNA or RNA:RNA duplexes) (Stephenson and Zamecnik, 1978; Zamecnik and Stephenson, 1978). During the early 1980's, different groups reported the phenomenon of negative regulation of gene expression (either of a transgene or of an endogenous gene) thanks to artificially introduced anti-sense RNA transcripts. Importantly, this finding was observed in a variety of model organisms including *Xenopus*, *Dictyostelium*, *Drosophila,* plant and mammalian cells (Crowley et al., 1985; Izant and Weintraub, 1984; 1985; Kim and Wold, 1985; Melton, 1985; Rosenberg et al., 1985; Van der Krol et al., 1990; 2004a). Later, this mechanism was termed Post-Transcriptional Gene Silencing (PTGS) in plants. Studies in *Petunia* and *Nicotiana benthamiana* demonstrated, thanks to nuclear run-on experiments, that the silencing phenomenon did not affect transcription of target RNAs but rather affected a later step in gene expression (de Carvalho Niebel et al., 1995; Elmayan and Vaucheret, 1996; Stam et al., 1997).

Interestingly, all the experiments observing gene silencing performed till that time were artificially induced by transgenesis. Towards the end of the 1990's, parallel findings in different model organisms (*A.thaliana, Nicotiana benthamiana, C.elegans)* succeeded in explaining the action of such a conserved silencing mechanism in natural contexts.
In a series of papers, David Baulcombe's laboratory showed that viruses can initiate an RNA silencing response (Covey, 1997; Ratcliff et al., 1997; Voinnet and Baulcombe, 1997). Importantly, they showed that such a response is maintained by a cellular mechanism that is able to amplify it and spread it through the whole plant (Voinnet and

Baulcombe, 1997). Moreover, they showed that viruses try to counter this silencing mechanism by supressing it, providing compelling evidence that PTGS represents a natural mechanism for plant protection against viruses (Voinnet et al., 1998) . At the same time, Fire, Mello and colleagues showed that double-stranded RNA is able to induce potent and specific genetic interference in *C.elegans* (Tabara et al., 1998). Furthermore, the authors were able to select two *C.elegans* mutants resistant to RNAi. The mapping of mutations in these lines enabled them to identify for the first time genes (*rde-1, rde-4*) involved in this "mysterious" silencing mechanism (Tabara et al., 1999). The authors characterized the *rde-1* gene molecularly, and found out that it produces a protein, which is a member of the *piwi/argonaute/zwille* gene family, conserved from plants to vertebrates. Interestingly, they also observed a mobilisation of the endogenous transposons in some of these RNAi resistant lines. This led them to propose another natural function for RNAi which is transposon silencing (Tabara et al., 1999)

The studies in plants and worms were not only able to explain the natural duty of such a conserved silencing mechanism, but they were also able to pinpoint effector genes controlling it. These findings elicited great excitement and interest in the scientific community, which is illustrated by the overwhelmingly rich literature published on the RNAi mechanism during the last decade. Significant efforts have been made in order to gain more insight into the structural and functional molecular details of RNAi, but many questions remain unresolved.

RNAi turned out to be a very conserved mechanism amongst different species. This mechanism involves the production of small double stranded RNA duplexes by Dicer proteins and sometimes independently of Dicer. These small RNA are then loaded onto argonaute proteins that are part of a larger protein complex called the RNA Induced Silencing Complex or "RISC". The loaded small RNA programs the RISC and directs it in a sequence specific manner to complementary RNA. Some argonaute proteins are able to endonucleotically cleave target RNAs (Slicer competent), inhibiting their expression. Other argonaute proteins are "Slicer" incompetent but are nevertheless able to recruit different cellular factors (e.g. GW proteins, exonucleases) that interfere with the translation of target mRNAs, resulting ultimately in the silencing of the target gene.

Two small RNAs associated mechanisms, namely the siRNA and the PIWI-interacting piRNA pathways, are involved in genome defence against exogenous or endogenous

selfish genetic elements in many species. A third small RNA associated mechanism termed the microRNA pathway, co-exist with the first two in different organisms. This microRNA plays an important role in development and in various aspects of cell physiology by fine-tuning gene expression. I will try next to briefly review our actual knowledge on the RNAi mechanism, emphasizing its role in genome defence in different species including plants, drosophila, nematodes and mammals.

3. Viruses and RNA silencing in plants

The model plant *Arabidopsis thaliana* encodes four Dicer-like proteins (DCL1 to DCL4). DCL1 essentially synthesizes small ~22 nucleotides microRNAs, originating from endogenously transcribed small imperfectly matched hairpin RNA structures DCL2, DCL3, and DCL4 process long dsRNA molecules of various cellular origins into siRNA populations that are 22, 24, and 21 nucleotides in length, respectively (Brodersen and Voinnet, 2006; Moissiard and Voinnet, 2006). DCL4 generates 21-nt-long siRNAs that mediate post-transcriptional silencing of some endogenous genes trans-acting (ta)–siRNAs(Gasciolli et al., 2005),and of trans- genes mediating RNA interference (Dunoyer et al., 2005). DCL2 synthesizes stress-related natural-antisense-transcript (nat)–siRNAs (Borsani et al., 2005). Once a plant is infected DCL4 and DCL2 exhibit specific, hierarchical antiviral activities switching their substrate to viral dsRNA intermediates. DCL4 is the primary antiviral Dicer against different (+) single stranded RNA viruses but it can be replaced by DCL2 when genetically removed (Deleris, 2006). The combined action in antiviral defense, of both DCL2 and DCL4, is best illustrated in the hyper-susceptibility of plants where both enzymes were genetically depleted. DCL1 has been also shown to be antiviral in some cases, for example with the *Cauliflower mosaic virus (CMV)* infection. This DNA virus possesses a *35S leader* RNA structure that mimics a miRNA that is likely excised by DCL1, facilitating its subsequent processing by other DCLs (Ding and Voinnet, 2007). DCL3-dependent 24 nucleotide siRNAs recruit AGO4 to transcriptionally silence transposons and DNA repeats *in-cis* through chromatin modifications and DNA methylation (Marí-Ordóñez et al., 2013; Matzke and Birchler, 2005).

Concerning argonautes, *A. thaliana* genome encodes 10 of those proteins (AGO1 to AGO10). Half of those are not well characterized. *AGO1* mutants have the most severe developmental phenotype compared to other AGO mutants that present only limited or

no obvious developmental defects (Vaucheret, 2008). AGO1 protein is crucial for the miRNA pathway and seems to behave as a competent Slicer (Zhang et al., 2006). AGO1 hypomorphic mutant plants are hyper-susceptible to *Cucumber Mosaic Virus* (CMV) infection, suggesting a role of this protein in antiviral defense. Moreover, two viruses encode proteins that counter AGO1 action. The cucumovirus 2b protein inhibits AGO1 Slicer activity (Zhang et al., 2006) and the polerovirus P0 protein targets AGO1 for degradation. Other AGOs like AGO7 have been involved in ta-siRNA related silencing. The function of other argonaute proteins is under intense investigation. Like the DCLs, the ten argonaute proteins of *A. thaliana* are expected to have many functional redundancies and specializations (Vaucheret, 2008). Whether slicing of target viral RNA is the only antiviral mechanism that plant argonautes employ to counter viral replication remains, nevertheless, an open question.

One hallmark of plant antiviral RNAi is the signal amplification mechanism. At least two small RNA amplification loops, which are not mutually exclusive, are present in *A. thaliana*. Both involve RNA-Dependant RNA Polymerases (RdRps). Primary siRNA originating from the dicing of viral dsRNA intermediates recruits RdRps to homologous ssRNA. The siRNAs prime the RdRp on the single stranded target RNA, which is subsequently amplified and diced leading to a secondary siRNAs population. This process requires the RdRp RDR6, the coiled-coil protein SGS3 and the RNA-helicases SDE3 or SDE5 together with AGO1 (Ding and Voinnet, 2007). Another RdRp-dependant pathway that does not seem to have any antiviral role involves RDR2-dependant amplification of DCL-3 products for transposon silencing by DNA methylation (Marí-Ordóñez et al., 2013). Interestingly, the secondary siRNA can move from cell to cell through plasmodesmata and over long distances through the phloem (Voinnet, 2005). Remarkably, this mechanism primes an immunization process in uninfected plant tissue.

Finally, an eloquent evolutionary evidence stressing how important is the siRNA pathway in plant antiviral defenses is the invention by plant viruses of Viral Suppressors of RNAi (VSRs). More than 35 individual VSRs encoded by many different plant viruses have been identified, unravelling a necessary and general counterstrategy (Li and Ding, 2006). An example of a well-characterized VSR is the P19 protein encoded by the *Cymbidium ringspot virus.* P19 head-to tail homo-dimers form a “siRNA clamp” that specifically sequesters DCL4-dependent 21 bp RNA duplexes (Vargason et al., 2003; Ye et al., 2003). Another example is the geminivirus VSR AC4 that seems to prevent

holoRISC assembly by capturing single-stranded small RNAs preventing them from binding to AGOs. Each characterized plant VSR seem to have evolved to antagonize a specific step in the RNAi pathway (Li and Ding, 2006).
Interestingly some VSRs, constituted very valuable research tools that permitted scientists to decipher different steps in the RNAi mechanism(Deleris, 2006).
All together, the data obtained in plants unquestionably indicate that the RNA interference mechanism is the major antiviral immune pathway in these organisms. This observation led researchers working on other model organisms to ask the following question: Are orthologous RNAi components (Dicers, Argonautes) also antiviral in organisms like flies, worms and mammals?

4. RNA silencing in *Drosophila* and its antiviral function

Similar to plants, the *Drosophila* genome encodes many Dicers, Argonautes and dsRNA binding proteins involved in different RNAi pathways. Only a subset of these proteins has been shown to be important for the fly's antiviral defense. Indeed, *Drosophila* possesses two Dicer proteins, Dcr-1 and Dcr-2, and five argonautes, AGO1, AGO2, AGO3, Piwi and Aubergine. Dcr-1, AGO1 and a dsRNA binding protein Loquacious (Loqs) are believed to be important players in the microRNA pathway (Ghildiyal and Zamore, 2009). Dcr-2, AGO2 and another dsRNA binding protein known as R2D2 constitute the main arsenal of the siRNA pathway. AGO3, PIWI and Aubergine are involved in the PIWI-interacting RNAs (piRNAs) pathway, which requires no Dicer proteins. Intersestingly, the molecular seperation between these three pathways is influenced by the lenght and the thermodynamic properties, of the small RNA duplexes. These parameters seem to dictate the sorting fate of the small RNAs into argonaute proteins. Therefore the existence of some functional cross-talks amongst these pathways is not surprising.

4.1 The microRNA pathway

Like in plants, the microRNA pathway in drosophila is a general gene expression regulation mechanism, occurring post-transcriptionally. MicroRNAs regulate the expression of proteins involved in a variety of basic biological mechanisms including cell cycle, apoptosis, differentiation, and development. This is best illustrated by the embryonic lethality of homozygous mutants of core components of this pathway (*AGO1*$^{-/-}$, *Dcr-1*$^{-/-}$ and *Loqs*$^{-/-}$). MicroRNAs are therefore essential for the general physiology of the fly(Ambros, 2003).

MicroRNAs derive from precursor transcripts called primary miRNAs (pri-miRNAs) which are typically transcribed by RNA polymerase II (RNA Pol II) (Ghildiyal and Zamore, 2009). The pri-miRNA is then sequentially cleaved by two RNase III endonucleases onto a ~22 nucleotides microRNA. First, the pri-miRNA is processed in the nucleus into a 60–70-nucleotides pre-miRNA by Drosha, assisted by its dsRNA-binding domain (dsRBD) partner protein Pasha. The resulting pre-miRNA has a hairpin structure (a loop flanked by base-paired arms that form a stem). The nuclear exportin, Exportin-5, is responsible of transporting the pre-miRNA to the cytoplasm through the nuclear pore, in a Ran-GTP dependant manner (Ghildiyal and Zamore, 2009). Once in the cytoplasm, the two symmetrical RNase domains of Dcr-1 supported by its dsRBD partner protein Loqs cleave the pre-miRNA. Importantly, like argonaute proteins and unlike Drosha, Dcr-1 contains a PAZ domain, which is believed to allow it to bind the two nucleotides 3' -overhanging end of the pre-miRNA, left by Drosha. Cleavage by Dcr-1 generates a ~22 nucleotides duplex containing two strands, termed miRNA and miRNA*, corresponding to the two sides of the base of the stem. Importantly, this cleavage leaves 3'OH overhanging nucleotides. Some miRNAs are produced by an alternative pathway where the pre-mRNA splicing pathway replaces the Drosha processing step in the nucleus (Ruby et al., 2007). These pre-miRNA-like introns are called mirtrons and require an additional lariat-debranching enzyme for their nuclear processing. The mirtrons subsequent cytoplasmic processing involves Dcr-1, similar to classical miRNA.

The mechanism by which a small RNA will regulate its target mRNA, is dictated by the specific argonaute protein into which the small RNA is loaded, which is by itself, influenced by the thermodynamic stability of the small RNA duplex. Convergent models

suggest that two major parameters influence the Loqs or R2D2-assisted sorting of the small RNA into argonautes (Czech et al., 2009; Förstemann et al., 2007; Kawamata et al., 2009; Okamura et al., 2009). First is the complementarity status of the 9th and 10th base pair of the miRNA/miRNA* duplex, and second, is the 5'end pairing status of one strand with the 3'end of the other. A duplex with a 9th and 10th base pair mismatch or G:U wobble and a 5'end unpaired uridine, is preferentially loaded onto AGO1. A duplex presenting more matching base pairs in general and especially at the 9th and the 10th position, together with a paired 5' end, is more likely loaded into AGO2.

As the majority of miRNAs form bulgy imperfect stems, and harbours at their 5'end an unpaired uridine, most of them are loaded into AGO1. Rare miRNAs forming near-perfect complementary duplexes, like mir-277, are indeed loaded into AGO2 (Förstemann et al., 2007). This also explains, why the vast majority of the perfectly matched Dcr-2 derived siRNAs are loaded into AGO2.

The AGO1/AGO2 sorting decision seems to be an important crossroad, dictating the subsequent silencing fate. Once loaded in argonaute proteins, the small RNA duplex is unwound, one strand is kept and the other is discarded. Neither the rules of this unwinding step nor all the factors involved in it are completely known to date (Czech et al., 2009). However, it is clear that the remaining small RNA strand is crucial for directing the argonautes to complementary RNA. The small RNA /AGO1 complex can either bind to the 5' or the 3' Untranslated Region (UTR) of target mRNA or to ORF regions. In *Drosophila*, most miRNAs pair with their targets through only a limited region of sequence at their 5′ end called the "seed region". A minimal 7 to 8 baispairs region followed by a bulge then a variable complementarity region seems to apply to most miRNA/target interactions (Bartel, 2009). This binding is believed to recruit factors that inhibit translation.

Unlike AGO2, AGO1 seems to have lost its endonucleotic RNase-H residues, and is believed to rely on GW182 to inhibit translation. *In vitro* experiments from different groups agree on a model where GW182 will either inhibit the initiation of translation at a step after CAP recognition (Iwasaki et al., 2009), or recruit deadenylases and exonucleases like the CCR4/Not complex causing RNA decay (Eulalio et al., 2007; Fabian and Sonenberg, 2010; Fabian et al., 2009). Intriguingly, some data coming from mammals suggest that the nuclear transcriptional history of an mRNA target influences

whether the miRNA represses its translation at the initiation or post-initiation (Kong et al., 2008).

On the other hand, AGO2 “slicer“ activity is sufficient for the endonucleotic cleavage of the target RNA, causing its degradation. Interestingly, a recent study elegantly shows that AGO2 sits a long time on its target, whereas the mouse Ago-2 , which is the drosophila AGO1 orthologue, have faster association/dissociation rates from its target, this is partly explained by the extent of complementarity of the small RNA to its target (Wee et al., 2012).

4.2 The exo-siRNA pathway and antiviral defense

Demonstration of the critical role of RNAi as a potent antiviral mechanism in drosophila is based on three main lines of evidence. First, genetic experiments show that RNAi pathway mutants (*AGO2*$^{-/-}$, *Dcr-2*$^{-/-}$ and *R2D2*$^{-/-}$) are hypersensitive to RNA virus infections and succumb with increased viral loads when compared to controls (Ding, 2010; Galiana-Arnoux et al., 2006; van Rij et al., 2006). The second line of evidence is the identification of VSRs encoded by fly viruses that counteract this silencing mechanism (Chao et al., 2005; Nayak et al., 2010), and the third one, is the presence of siRNAs of viral origin (vsiRNAs) in infected cells and flies (Aliyari et al., 2008; Mueller et al., 2010).

First, *Dicer-2*, *AGO2* or *R2D2* homozygous null mutants are viable. Their hyper susceptibility to a variety of viral infection: CrPV (Dicistroviridae), FHV (Nodaviridae) and SINV (Alphaviridae) indicates that the siRNA pathway mediates a broad antiviral defense in flies (Kemp and Imler, 2009). It has recently been shown that Dcr-2 and AGO2 mutants are more susceptible to a DNA virus, IIV-6 iridescent virus (Bronkhorst et al.; Kemp et al., 2013).

Interestingly, resistance to the virus Drosophila X virus (DXV; Birnaviridae) and West-Nile virus (WNV; Flaviviridae) seems to involve AGO2, but not Dicer-2 (Chotkowski et al., 2008; Zambon et al., 2006). Second, RNAi is believed to exert an evolutionary pressure on viruses. This agrees with the fact that many VSRs have been identified in insect RNA viruses (Chao et al., 2005; Nayak et al., 2010; van Mierlo et al., 2012). Two of these, B2 from FHV and 1A from DCV interact with dsRNA, preventing the dsRNA

recognition and cleavage by Dicer-2. Unlike DCV-1A, which only binds long dsRNAs, FHV-B2 can interact with both long dsRNA and siRNAs. Thus, FHV-B2 can potentially inhibit both the dicing and the loading steps, whereas DCV-1A only blocks the dicing of long dsRNAs. This may partly explain the stronger suppression of RNAi exerted by B2 compared to DCV-1A (Berry et al., 2009; Chao et al., 2005). A third example of VSRs is the 1A from CrPV. This protein antagonizes AGO2 preventing its proper function (Nayak et al., 2010). Interestingly, the existence of VSRs in insect viruses targeting key players of the siRNA pathway is indirectly supported by the rapid evolution of these host genes. Indeed, *dicer-2*, *AGO2* and *R2D2* are among the 3% fastest evolving genes in drosophila, which contrasts with the slow evolution of their cousins of the miRNA pathway *dicer-1*, *AGO1* and *Loqs* (Obbard et al., 2009).

The third observation confirming the involvement of the siRNA pathway in antiviral immunity is the presence of Dcr-2 derived 21 nt-siRNA in infected animals or cells. Like in plants these siRNAs are able to confer specific resistance to the uncontrolled viral replication. Indeed, flies carrying a transgene directing expression of FHV dsRNA are protected against a challenge by FHV, but not by DCV (Galiana-Arnoux et al., 2006). In a natural infectious context, many indications suggest that these vsiRNAs originate from long dsRNA viral replication intermediates and to be Dcr-2-dependant. First, high-throughput sequencing of small RNAs produced in the course of a viral infection in flies and mosquitoes confirms that the virus derived siRNAs have a size of 21nt, as expected for the products of the Dicer-2 enzyme (Aliyari et al., 2008; Mueller et al., 2010; Myles et al., 2008). Second, the production of the vsiRNAs is strongly reduced or abolished in *Dicer-2*$^{-/-}$ mutant flies(Mueller et al., 2010). Third, the vsiRNAs cover the whole length of the viral genome and the ratio between the number of siRNAs matching the (+) strand and the (-) strand of the genome is close to one (Aliyari et al., 2008; Mueller et al., 2010).

As the Dcr-2 derived vsiRNAs form perfectly complimentary duplexes, the Dcr-2/R2D2 heterodimer assists their preferential loading into AGO2 (Cenik et al., 2011; Liu, 2003; Liu et al., 2006). In AGO2 these vsiRNAs are 2'O-methylated at their 3'end by the methyl-transferase Hen1 (Aliyari et al., 2008). This methylation is thought to protect them from mechanisms such as tailing and trimming, responsible of recycling the miRNAs (Ameres et al., 2010). Once loaded these vsiRNAs guide the siRISC complex

toward target viral RNA molecules. AGO2 is then able to cleave the viral RNA through its slicer activity.

Interestingly, this mechanism may also be used to immunize cells that have not yet been infected. Indeed, insect cells in culture can take up exogenous dsRNA molecules, through scavenger receptor mediated endocytosis (Saleh et al., 2006). One interesting study suggests that even thought there doesn't seem to be a RdRp-dependant vsiRNA amplification step in *drosophila,* viral dsRNA molecules released following lysis of virus-infected cells can be taken up by non-infected cells and induce RNA interference, protecting them against future challenges with the virus (Saleh et al., 2009). Intriguingly, a very recent study shows that some parts of the RNA viruses genome can be retro-transcribed to DNA by an unknown mechanism (Goic et al., 2013). This DNA form of viral sequences may represent an ideal template for a potential RdRp-independant amplification of vsiRNAs in *Drosophila* (Voinnet, 2013).

4.3 The endo-siRNA pathway : a defence mechanism against transposons in somatic tissues. .

The endo-siRNAs were discovered in *C.elegans* and plants (Ambros et al., 2003; Hamilton, 2002). The prefix "endo" refers to the origin of the long dsRNA from which the siRNAs are produced. These endo-siRNAs can arise from structured loci that can pair intramolecularly to produce long dsRNA, complementary overlapping transcripts or bidirectionally transcribed loci (Ghildiyal and Zamore, 2009). Deep sequencing of small RNAs from germline and somatic tissues of *Drosophila* and of AGO2 immunoprecipitates revealed a population of small RNAs that could be distinguished from miRNAs and piRNAs (Chung et al., 2008; Czech et al., 2008; Kawamura et al., 2008; Okamura and Lai, 2008; Okamura et al., 2008; Siomi et al., 2008; Wu et al., 2010). These small RNAs are nearly always exactly 21 nucleotides, are present in both orientations (sense and anti-sense), they have methylated 3'-ends and, unlike miRNAs and piRNAs, are not biased towards starting with uracil, and are loaded into AGO2. Production of the 21-mers requires Dcr-2, although in the absence of Dcr-2 a remnant of the endo-siRNA population inexplicably persists, implying that in some cases the production of endo-siRNAs can be Dcr-2-independant.

Drosophila endo-siRNAs are found to derive from transposons, heterochromatic sequences, intergenic regions and long RNA transcripts with extensive structure and from mRNAs. Expression of many transposons, like 297, Blood or Roo mRNAs increases in both *Dcr-2* and *AGO2* mutants. Interestingly, the generation of many endo-siRNAs requires Loqs , which is the typical dsRBD-containing partner of Dcr-1 in the miRNA pathway, but not R2D2, the partner of DCR-2 (Czech et al., 2008; Okamura and Lai, 2008). All together the published data indicate that endo-siRNAs might be the main mechanism for silencing 'selfish' genetic elements in most somatic tissues, which lack the piRNA pathway.

4.4 The piRNA pathway: a germline defense mechanism against transposable elements and (maybe) viruses?

The piRNAs were first discovered in flies and proposed to ensure germline stability by repressing transposons. A class of ~24 to 30 nucleotides was first shown to be associated with silencing of repetitive elements (Aravin et al., 2001). Later, these 'repeat associated small interfering RNAs' were found to be relatively distinct from classical micro or siRNAs. First, because they bind to argonautes belonging to the Piwi-clade (AGO3, Piwi and Aubergine). Second, piRNAs do not seem to require Dcr-1 or Dcr-2 for their production, unlike miRNAs and siRNAs (Saito et al., 2006; Vagin, 2006). Third, they are 2'-O-methylated at their 3' termini, unlike miRNAs but similar to siRNAs (Saito et al., 2007). Fourth, their sizes range between ~24 and ~ 30nts as opposed to the sharp 21nts species that characterize the siRNAs.

Two mechanisms depending on different factors seem to generate piRNAs either in germline cells or somatic follicle cells. The germline piRNAs can be generated throught an amplification loop. The current model for piRNA biogenesis in the germline was deduced from the sequences of piRNAs that are bound to Piwi, Aubergine and AGO3 (Aravin et al., 2007; Brennecke et al., 2007). piRNAs bound to Piwi and Aubergine are typically antisense to transposon mRNAs, whereas AGO3 is loaded with piRNAs corresponding to the transposon mRNAs themselves. Remarkably, the first 10

nucleotides of antisense piRNAs are frequently complementary to the sense piRNAs found in AGO3. This intriguing sequence complementarity has been proposed to reflect a feed-forward amplification mechanism — 'piRNA Ping-Pong'— that is activated only after transcription of transposon mRNA. Many aspects of the Ping-Pong model remain nevertheless speculative. Interestingly, a distinct ping-pong-independent piRNA pathway seem to operate in germline and somatic follicle cells. Analysis of piRNA profiles in somatic cells reveal that this primary piRNA pathway depends on Piwi and not AGO3, nor Aubergine(Ishizu et al., 2012).

Genetic experiments conclude that the Piwi-clade argonautes are indispensable for germline development in many animals, and more particularly in *Drosophila*. Piwi is found only in the nucleus of *Drosophila* germ cells and adjacent somatic cells. Piwi is required to maintain germline stem cells and to promote their division. Aubergine is required for the silencing of the repetitive Stellate locus, which would otherwise cause male sterility (Vagin, 2006). However, the presence and role of piRNAs outside the germline, in all flies' somatic tissues is a debated question. Indeed, all the piRNAs identified in somatic cells originated from very specialized follicle cells that envelop the gonads. It is not clear if piRNAs are produced in other somatic cells. Interestingly, a very recent report shows that the loss of piRNA proteins (e.g Aub, AGO3) in the *Drosophila* brain correlates with elevated transposon expression. Depletion of one of these proteins resulted in more than 200 de novo transposon insertions in the neurons, including insertions into memory-relevant loci. This is the first report, implicating the piRNAs in a genome plasticity mechanism in non-ovarian somatic cells (Perrat et al., 2013).

The piRNAs and endo-siRNAs repress transposons in the germ line, where mutations caused by transposition would propagate to the next generation. Philip Zamore proposes a cross-talk between the endo-siRNA and piRNA systems. Zamore believes that the siRNA pathway provide probably a rapid response to the introduction of a new transposon into the germline, a challenge similar to a viral infection. By contrast, the piRNA system is believed to provide a more robust, permanent solution to the acquisition of a transposon (Ghildiyal and Zamore, 2009). However, the presence of piRNAs in some somatic cells implies that perhaps in the absence of endo-siRNAs, piRNAs are produced somatically and resume transposon surveillance.

Likewise, the evidence of a cross-talk between the piRNA and the siRNA pathways is observed in the viral infection scenario. Many reports have observed, by deep sequencing, virally derived piRNAs, in either *Drosophila* OSS cells (Wu et al., 2010), or the C6/36 mosquito cell line lacking a functional Dcr-2 enzyme. The small RNA profiles retrieved from the the C6/36 cells after various viral challenges (e.g Dengue virus-2, cell fusing agent virus), revealed predominantly 27 nucleotides long small RNAs without an obvious peak at 21 nt (Hjelle et al., 2010; Mudge et al., 2010). More recent reports implicate functionally these piRNA-like 27 nucleotides in the antiviral defense in mosquitoes (Léger et al., 2013; Morazzani et al., 2012). One report presents evidence that suggests that virus-derived Ping-Pong-dependent piRNA-like molecules are capable of modulating the pathogenesis of alphavirus infections in *Dicer-2* null mutant mosquito cell lines defective in viral siRNA production in the mosquito soma (Morazzani et al., 2012). In another report the authors compare the small RNA profiles from different mosquito cell lines infected with *Rift Valley fever virus* (RVFV) (Léger et al., 2013). They show that whereas 21-nucleotide (nt) Dicer-2 viRNAs were prominent during early infection, the population of 24- to 27-nt piRNAs increased progressively and became predominant later during persistence phase. The authors observed that in Aag2 and U4.4 cells, the combined actions of the Dicer-2 and Piwi pathways triggered an efficient antiviral response allowing establishment of persistence. Furthermore, they showed that in C6/36 cells, Piwi-mediated RNA interference (RNAi) appeared to be sufficient to mount an antiviral response against a secondary infection with a superinfecting virus. This functional redundancy between the piRNA and the siRNA suggest that these two antiviral systems can co-exist but are modulated tissue-specifically. This may represent a functional specialization of RNA silencing specific to animals. This hypothesis is consistent with the early observations that Piwi and Aub *Drosophila* mutants exhibit enhanced virus susceptibility (Chotkowski et al., 2008; Zambon et al., 2006). However, piRNA pathway mainly acts to repress transposons and repeat elements in the germline, which RNA viruses do not seem to invade. Does this suggest a role for the piRNA pathway to prevent viral invasion into the germline and to inhibit viral vertical transmission or a role in antiviral defense in the soma?

More experiments need to be performed in the future to tackle this question, but such a question puts the finger on a fundamental aspect in immunology concerning the genetic

identity preservation. The implication of RNAi-like systems in an evolutionary ancient genetic defence mechanism is discussed later in this introduction.

5. RNAi's antiviral function in *C.elegans*

Although the first discovered RNAi pathway enzyme was found in *C.elegans* (Tabara et al., 1999) and although the first microRNA (lin-4) was also discovered in this organism (Ambros et al., 2003), the involvement of RNAi in antiviral defense against a natural worm virus, has not been proven until very recently (Félix et al., 2011).

The first indication implicating *C.elegans* RNAi in an antiviral function came from an artificial FHV replicon system, mimicking a positive-strand RNA virus replication. The replicon comprised the coding regions of the FHV RdRP and GFP. When expressed, the RdRP recognizes its RNA and allows a replication cycle to take place. Components of the RNAi pathway, namely DICER and RDE-1 were shown to be required to limit the accumulation of GFP (Lu et al., 2005). Similarly, VSV was shown to induce antiviral silencing in adult worms and embryonic cells respectively, and detection of VSV-specific viRNAs was reported (Schott et al., 2005; Wilkins et al., 2005) .

The recent isolation of a worm virus named Orsay showing a (+) polarity ssRNA bi-partite genome, constituted a valuable asset to test RNAi mutant's susceptibility to natural infection. Orsay virus can naturally infect wild and laboratory *C.elegans* species (Félix et al., 2011). Two lines of evidence suggest the involvement of the worm's RNAi pathway in the defense against Orsay virus infection. First, argonaute protein RDE-1 mutants are infected approximately 100-fold more than the N2 WT strain. Of note, RDE-1 enzyme is essential for secondary siRNA production in the worm. Second, in infected N2 animals, both primary and secondary virus-derived ~ 22nt siRNA were detected (Félix et al., 2011).
These findings suggest that both primary and secondary siRNAs are important for antiviral defence in *C.elegans*.

Although the activity of the only *C.elegans* DICER on the viral genome is expected to limit viral infection by generating primary siRNAs, secondary siRNAs generated in N2 are also clearly important because *rde-1* mutants, with no secondary siRNAs (but still able to generate primary siRNAs) show increased sensitivity to viral infection (Félix et al., 2011) .

Although *C.elegans'* genome encodes only one DICER protein, it also encodes three Dicer-like helicase (DRH-1,2,3) proteins, similar to vertebrate RLRs, with a homologous N-terminal helicase domain but with no CARD domain. The DRH molecules function in the RNAi silencing pathway, and two of them have been molecularly characterized. DRH-3 is a core component of a cellular RNA-dependent RNA polymerase (RdRP) complex that produces secondary siRNAs (Gu et al., 2009).
It may be also involved in the release of siRNA duplexes from Dicer (Matranga and Pyle, 2010). DRH-1 also acts downstream of Dicer. Interestingly, this molecule has been proven to be involved in antiviral RNAi in nematodes, helping in the control viral RNA replication (Lu et al., 2009). Finally, the role of DRH-2 is molecularly less clearly defined, but this factor appears to play a negative regulatory role in antiviral defenses (Lu et al., 2009). Although one DICER is present in the worms, it is however proven that *C. elegans* DICER co-exist in different protein complexes. A logical question would be which DICER containing complex recognizes the Orsay virus?

Given that the RNAi response to the Orsay virus requires rde-1, it seems likely that the DICER–RDE-1–RDE-4–DRH-1 axis of the exo-RNAi complex is the one required for the sensing of viral dsRNA rather than the ERI–DICER complex that is involved in endo-RNAi. This raises an intriguing possibility that might explain the function of DRH-1 within this complex. The role of DRH-1 in the complex might be to specifically sense viral dsRNA. Interestingly some cited experiments about the involvement of DRH-1 in a strong primary siRNA response, with no role in the secondary response, suggest that the DRH-1, like RLRs, is able to recognize dsRNA with a 5'triphosphate, activating subsequently a specific antiviral response (Sarkies and Miska, 2013). Whether DRH-1 is involved in a specific signalling antiviral response in *C.elegans*, reminiscent to the inducible Dcr-2-dependant antiviral response in *drosophila*, or the RLR-dependant IFN response in vertebrates, is an open question for future studies.

6. Is the mammalian RNAi pathway antiviral?

The vertebrate genome and more particularly the mammalian one encode only one dicer protein. The mammalian Dicer share more important sequence homology with *Drosophila* Dcr-1 than Dcr-2. Expectedly, this protein have been shown to be involved in the micro-RNA pathway (Bartel, 2009). A null homozygous mutation of Dicer in mice is embryonically lethal, which is expected, knowing the important role of the miRNA pathway in development. Viable mice with hypomorphic mutations for this gene exist and may constitute a powerful research tool (Otsuka et al., 2007). The mammalian genome also encodes four argonaute proteins (Ago-1,2,3,4). The involvement of AGO2 protein, the only mammalian argonaute with a Slicer activity, in the microRNA has also been proven(Liu et al., 2004). Other mammalian argonautes have not been well characterized to date, and they are the aim of intense investigation. The question of whether these proteins confer antiviral immunity in mammals excited many biologists during the last decade. However, the answer to this question is still not so clear to date.

6.1 The microRNA pathway and viruses

Undoubtedly, the miRNA pathway is involved in the life cycle of certain mammalian viruses. Many DNA viruses and especially those from the *Herpesviridae* family, have been shown to encode miRNAs that target cellular genes, helping the virus in its replication strategy (Pfeffer et al., 2005; Umbach et al., 2008). For instance, viruses like Kaposi's Sarcoma-associated Herpesvirus (KSHV) and Epstein Barr virus (EBV encode miRNAs that can play a subtle role in preventing apoptosis by targeting pro-apoptotic host genes, thus extending the longevity of infected cells (Subramanian and Steer, 2010). Indeed, KSHV miRNAs can regulate the latent/lytic switch of this virus (Grundhoff and Sullivan, 2011). The KSHV encodes two miRNAs: miR-K12-9-5p and miR-K12-7-5p have been shown to directly regulate the transcript of the master lytic switch protein (RTA) (Bellare and Ganem, 2009; Lin et al., 2011). Another function of virally encoded miRNAs, is promoting persistent infections. For example, the deletion of two murine cytomegalovirus (MCMV) miRNAs, resulted in reduced titers in the salivary glands of mice. Interestingly, the phenotype was reverted in mice that were defective in both the adaptive and innate arms of the immune response through the depletion of NK

cells and CD4+ T-cells (Dölken et al., 2010),. This observation further supports a role of viral microRNAs in evading the immune response.

In contrast to DNA viruses, no RNA virus encoded miRNA, have been observed to date. However, a recent report was able to engineer an artificial miRNA in the 3'end of an infectious SINV virus (tenOever, 2013). This demonstrates that miRNA structures in RNA genomes do not necessarily interfere with viral encapsidation, as proposed earlier.

Some RNA viruses, on the other hand can, use cellular miRNAs for their own sake. An eloquent example of this scenario is the interaction between the abundant liver miR-122 and the Hepatitis C Virus (HCV) RNA. Indeed, HCV replication is greatly facilitated by the presence of mir-122. mir-122 can seed-match at two distinct positions of the very beginning of the 5' UTR of HCV. This interaction is thought to have a dual role: one in stimulating the IRES-dependant translation of HCV proteins and the other in masking the 5'end phosphate of this virus from RLRs, enabling it to evade immune detection (Machlin et al., 2011; Roberts et al., 2011).

The role of miRNAs in viral life cycles seems to be of a modulatory nature. This is consistent with the idea of the fine-tuning regulation exerted by the microRNA pathway. However, in all these examples the RNAi pathway is pro-viral, which does not answer the initial asked question: can the mammalian RNAi be antiviral?

6.2 The siRNA pathway and viruses

The artificial introduction of a perfectly complementary siRNAs to mammalian cells, is able to down-regulate the expression of target genes. Moreover, if the siRNA targets a viral genome, the RNAi machinery is able to inhibit the translation/replication of mammalian viruses (Scherer and Rossi, 2003). This means that the molecular machinery able to target viral genomes is potentially functional. However, if the RNAi constitute an antiviral strategy, viral infection should be able to generate virus-derived siRNA-like species. Moreover, these vsiRNA are supposed to be able to target the viral genome.

An interesting paper published in 2005, reported the existence of one single virally derived siRNA in HIV-1-infected cells. The investigators argue that this single viral siRNA could inhibit HIV-1 replication by binding to the Rev Response Element (RRE).

Furthermore, they find that the HIV-1 Tat protein can act as a mammalian VSR (Bennasser et al., 2005). Many reports have nevertheless doubted the validity of these findings. First, this siRNA appears to be expressed at very low levels, if expressed at all. Indeed, more recent studies were unable to detect this siRNA by small RNA cloning and deep sequencing (Cullen, 2009) . Second, the authors did not show that a target reporter is repressed by an HIV-1 infection. In an infectious context, the expression level of the vsiRNA is functionally more significant than the over-expression of the vsiRNA as a small hairpin RNA (shRNA). Third, the overexpression of an unspecific RNA binding protein like Tat, can give a VSR-like phenotype when tested on a reporter genes (Lichner, 2003). Indeed, apart from HIV-1 tat, many other groups claim the identification of VSRs encoded by mammalian viruses, including influenza NS1, vaccinia virus E3L (Li, 2004), Ebola virus VP35 (Haasnoot et al., 2007) and primate foamy virus (PFV) Tas (Lecellier, 2005). This would argue indirectly that the RNAi is antiviral. Like in the HIV-1 tat case, the question of specificity is crucial here, since it has been demonstrated that prokaryotic proteins containing a dsRNA-binding domain can also exhibit an VSR-like phenotype when overexpressed (Lichner, 2003). The question of specificity and physiological relevance is especially pertinent since the VSR activities of NS1, E3L, and VP35 have all been assigned to their dsRNA-binding domains.

Recently, the new high throughput sequencing technology enabled many groups to have an in depth view on the small RNA profiles of mammalian infected cells. Indeed, deep sequencing in cells infected with HIV-1, DENV, VSV, polio virus, HCV and WNV (Lefebvre et al., 2011; Parameswaran et al., 2010; Yeung et al., 2009) enabled the detection of a low number of vsiRNAs. Virus-specific RNAs appear to constitute in mammalian-infected cells between ~0,1 % to ~1% of the total small RNA population, whereas virus-specific RNAs can accumulate to ~20% of the total of small RNA pool in plants (Qi et al., 2009). The functional relevance of such non-abundant small RNA populations in silencing the viral genome still needs to be demonstrated.

In conclusion, the answer of whether the RNAi is antiviral in mammalian cells is still far from being clear. Importantly, the status of expression of the IFN pathway components have not always been carefully considered in all the studies that looked for virally derived small RNAs (Parameswaran et al., 2010; Yeung et al., 2009). Why would a cell, that already expresses an elaborate antiviral arsenal like the IFN, rely on the vestiges of

an ancestral antiviral system like RNAi? And even if there were an RNAi antiviral response, would not it be masked by the IFN response? Very interestingly, endogenous siRNAs have been cloned from mouse oocytes and embryonic stem (ES) cells, demonstrating that mammalian Dicer is capable of generating siRNAs through the progressive cleavage of long dsRNAs (Babiarz et al. 2008; Tam et al. 2008). These dsRNAs were derived from several sources, including bidirectional transcription of a single locus, endogenous hairpin RNAs, and pairing of near-complementary pseudogene RNAs. Such substrates are similar to those used to generate antiviral siRNAs in plants and invertebrates. It should be noted, that oocytes and ES cells are unusual in that the IFN pathway is not functional in these cells (Wianny and Zernicka-Goetz 2000; Yang et al. 2001). Maybe, looking for an antiviral RNAi in this kind of cells, using the right virus, would give more answers concerning involvement of RNAi in antiviral defences in mammals.

Finally, there is clear evidence that the endo- siRNA in mammals is indeed a defense mechanism against selfish genetic elements like retrotransposons in mouse oocytes, ES cells and murine spermatogenic cells (Babiarz et al., 2008; Song et al., 2011).
Even though its antiviral function in mammals have not been proven to date, altogether, the above findings suggest that the RNAi pathway seems to be a very ancient mechanism, playing a crucial role in general genome defence. The preservation of an organism's genetic identity is a fundamental issue in life on earth. Indeed, as mentioned in the very first page, defense systems, are not only important in the classical immunity mechanisms against invading cellular pathogens, they are also crucial for the preservation of the organism's genetic integrity from foreign selfish genetic elements. Such defense systems are conceptually likely to be very ancient in evolution. Assuming the existence of primitive cells with simple "replicators" early in life (Dawkins, 2006)systems controlling the spread of selfish genetic elements would be crucial to determine, which element must be combatted and which one is selected and maintained. We can comfortably propose that an RNAi-like system is always needed, and would be conceptually crucial in shaping the genetic identity of organisms during evolution.

7. Why studying the antiviral siRNA interactome in *Drosophila*?

Forward genetics experiments in different model organisms (*A.thaliana, C.elegans, D.melanogaster*) were crucial to elucidate the basic players of the RNAi pathway. Nevertheless, the post-genomic area is characterized by the emergence of very powerful tools, enabling new in-depth biological read-outs. Transcriptomics, proteomics and metablomics techniques brought in new angles, from which biological interactions can be seen. These techniques are vey useful to grope for unknown players in incompletely defined pathways. This is typically the case of the siRNA pathway in *Drosophila*. We decided, therefore, to undertake a comprehensive proteomic study followed by a reverse-genetic screen of the *Drosophila* antiviral siRNA interactome.

Although the main three players (AGO2, Dcr-2 and R2D2) of the antiviral siRNA pathway in *Drosophila* are well defined, many questions concerning their function and interaction networks remain unanswered. First, an inducible antiviral response that is Dcr-2 dependant and that is operating in parallel to RNAi, suggests the existence of important and unknown antiviral Dcr-2 partners that do not necessary participate in classical RNAi. Second, all the mechanistic details, describing how the siRNA pathway targets the viral genome, are either the result of indirect observations, or are inferred by *in vitro* experiments. Defining new molecular partners of AGO2, Dcr-2 and R2D2 in an infectious context *in vivo*, may reveal how *Drosophila* cells deal with viral infection. Indeed, the identification of protein complexes assembling around these three molecules upon viral stimulation would permit the identification of new potential antiviral sensors and/or effectors. Third, the RNAi response to different viruses does not seem to be always the same. For example, only DCV induced the antiviral protein *vago*. Along the same line, VSV, but not FHV or DCV, generates a very low quantity of siRNAs that seem to be nevertheless functional. Therefore, we thought that a comparison of the siRNA interactome after a challenge with different viruses would be very informative. Finally, the molecular redundancy between the exo-siRNA and the endo-siRNA pathways, added to the functional redundancy between the siRNA and the piRNA pathways, suggest the existence of cross talks between these pathways. Similarly, the identification of the exo-siRNA pathway protein niche would help defining the molecular nodes governing these different pathways.

II- Chapter 1

The siRNA pathway interactome in *Drosophila melanogaster*

Fig. 1

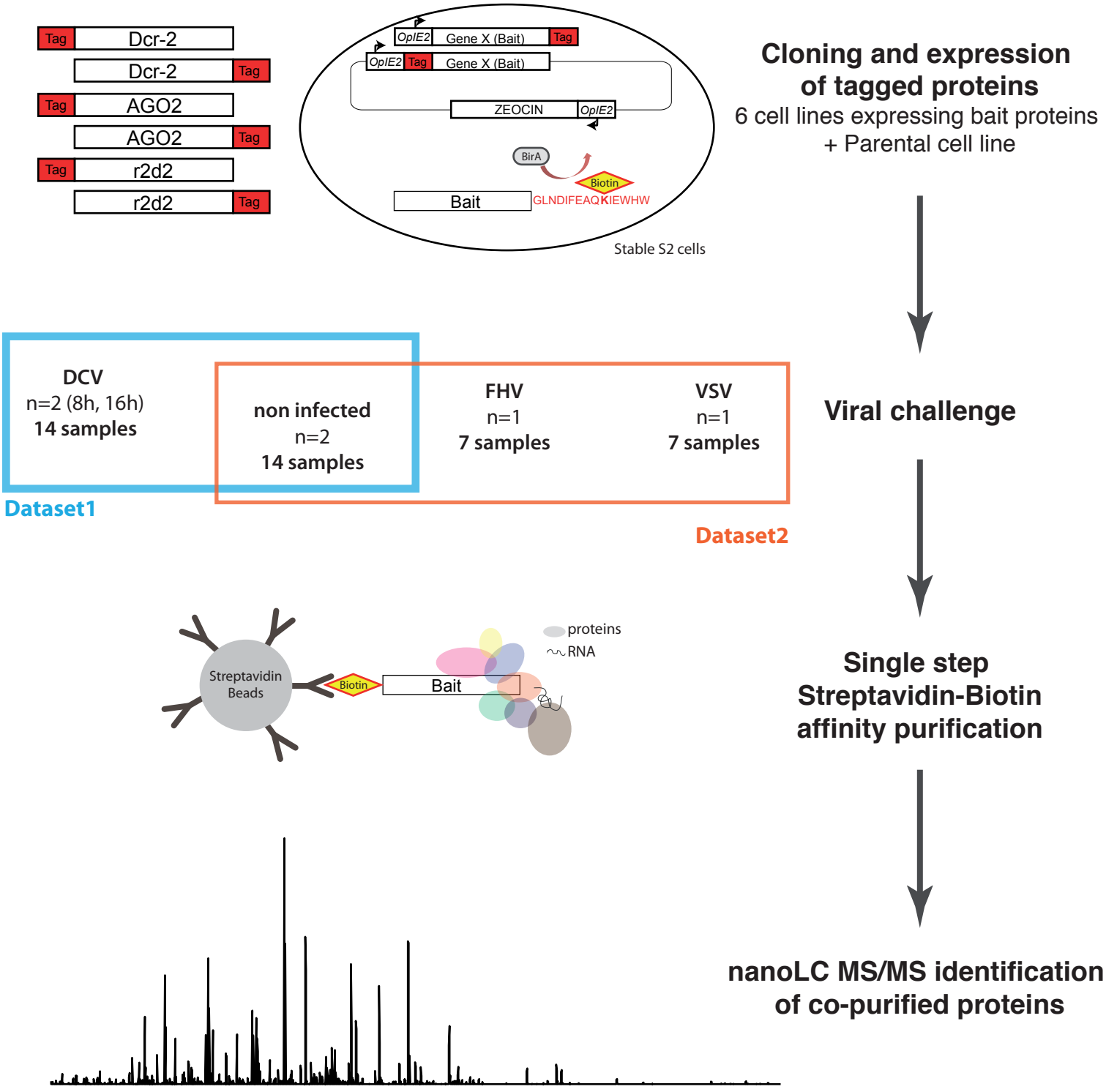

Fig.1 Strategy used to define the siRNA pathway interactome. The bait proteins (Dcr-2, AGO2 and r2d2) were tagged at their amino- or carboxy-terminal extremities with a 15 amino-acid biotinylation target sequence (in red, with modified Lys in bold). S2 cells epressing the bacterial biotin ligase BirA were stably transfected with the corresponding expression constructs. Cells were then either non-infected or infected with DCV (8h and 16h), FHV (16h) or VSV (48h). Cell lysates were affinity purified in a single step on streptavidin beads, digested with trypsin, and analyzed by nanoLC MS/MS on a FT ICR mass spectrometer.

II- Chapter 1

1. A proteomic analysis of the siRNA pathway in an infectious context

1.1 Experimental strategy

To identify the proteins interacting with the core components of the siRNA pathway, we used a biotin-tag affinity purification system, which allows high efficiency recovery of molecules expressed at physiological levels in drosophila cells, using the exceptionally high affinity of streptavidin for biotin. Dicer-2, R2D2 and AGO2 were tagged at the N- or C-terminus with a 15 amino-acid sequence, and stably expressed in a hemocyte-like Drosophila S2 cell line expressing the bacterial biotin-ligase BirA, which mediates biotinylation (Fukuyama et al., 2012) (Fig. 1). Expression of the tagged bait proteins is controlled by the baculovirus OpIE2 immediate early promoter, which is moderately active in drosophila cells. BirA expressing cell lines transfected with the six expression plasmids (three proteins, tagged at their N- or C-terminal extremities) were selected for stable expression of the proteins of interest at a moderate level (see Materials & Methods).

The tagged proteins and their associated partners were extracted from cells either mock treated (2 independent controls) or infected by the RNA viruses Drosophila C virus (DCV; 8h or 16hpi), Flock House Virus (FHV; 16hpi) or Vesicular Stomatitis Virus (VSV; 48hpi) (Figure 1). Samples ((6 cell lines + 1 control cell line) x 6 conditions = 42 in total) were collected and biotinylated proteins were recovered in a single step affinity purification on Streptavidin coupled beads (see Materials & Methods). The pulled down proteins were digested on-beads (de Boer et al., 2003; Fukuyama et al., 2012) with trypsin and processed by NanoLC-FT ICR mass spectrometry at the ESPCI (PatisTech) in collaboration with the group of Dr. Joelle Vinh (Fig. 1).

1.2 Mass Spectrometry Data Analysis

1.2.1 Partners identification and validation

The MS analysis was performed on a FT ICR mass spectrometer. The MS/MS Spectra from the 42 samples were analyzed and assigned to correspondent peptides as described in Material and Methods. Validation was performed on proteins identified using two filters: (1) only proteins identified with a False Discovery Rate (FDR) <1% (Peptide Validator Mascot significance threshold) and at least 1 peptide score above 30 were selected; (2) only proteins identified with 2 distinct sequences with ion score above 30, or 1 sequence with ion score above 30 and a MudPIT score above 49. Proteins identified by a peptide matching another protein were not taken into account and were filtered out (See Materials and Methods).

After selecting all the proteins that passed these filters we discarded proteins that are detected due to unspecific binding. These proteins are detected in the samples derived from the parental 1F3 cell-line, which only expressed BirA. Proteins detected in samples from 1F3-Control, 1F3-DCV, 1F3-FHV or 1F3-VSV were considered as unspecific interactants when they were detected in Dcr-2, AGO2 or R2D2 samples.

The data obtained from this analysis are presented in Table 1. The first sheet “Summary of MS results“ recapitulates the detection status of all identified proteins: columns A, B and C contain the gene name, the protein accession number and the corresponding description. Columns D, E, F, G and H contain the different conditions the cells were subjected to (infection status or control).

Each line harbors a gene/protein name, and whenever the D letter is present in a certain condition this means that the protein passed the filters described earlier and was considered as “detected“ (e.g.: in lane 99, the RACK1 gene has a D letter only in the DCV columns, which means it was detected only in this condition).

The second sheet in this Excel table (MSMS scores All conditions) follows the same logic. The lines contain the detected proteins and the columns the different conditions. This sheet has more extensive information, as all 42 conditions are listed (e.g. 016_RC_8h is the following condition: R2D2 tagged C-term infected with DCV for 8h).

This sheet contains all detected proteins with their correspondent MudPit scores and the number of corresponding peptides detected.

Fig. 2 Overlap between the identified proteins in each condition

A) Venn Diagram showing the numbers of identified interacting proteins with the 3 baits (AGO2,Dcr-2 and R2D2), in the two genrated datasets (non-infected conditions). B) Venn Diagramm showing the numbers of identified interacting proteins with each bait, influence of the Tag position (N-ter or C-ter) are showed in salmon and blue respectively. C) Venn Diagramm of the total interacting proteins with the 3 baits, all conditions merged (Non-infected, DCV, VSV, FHV).

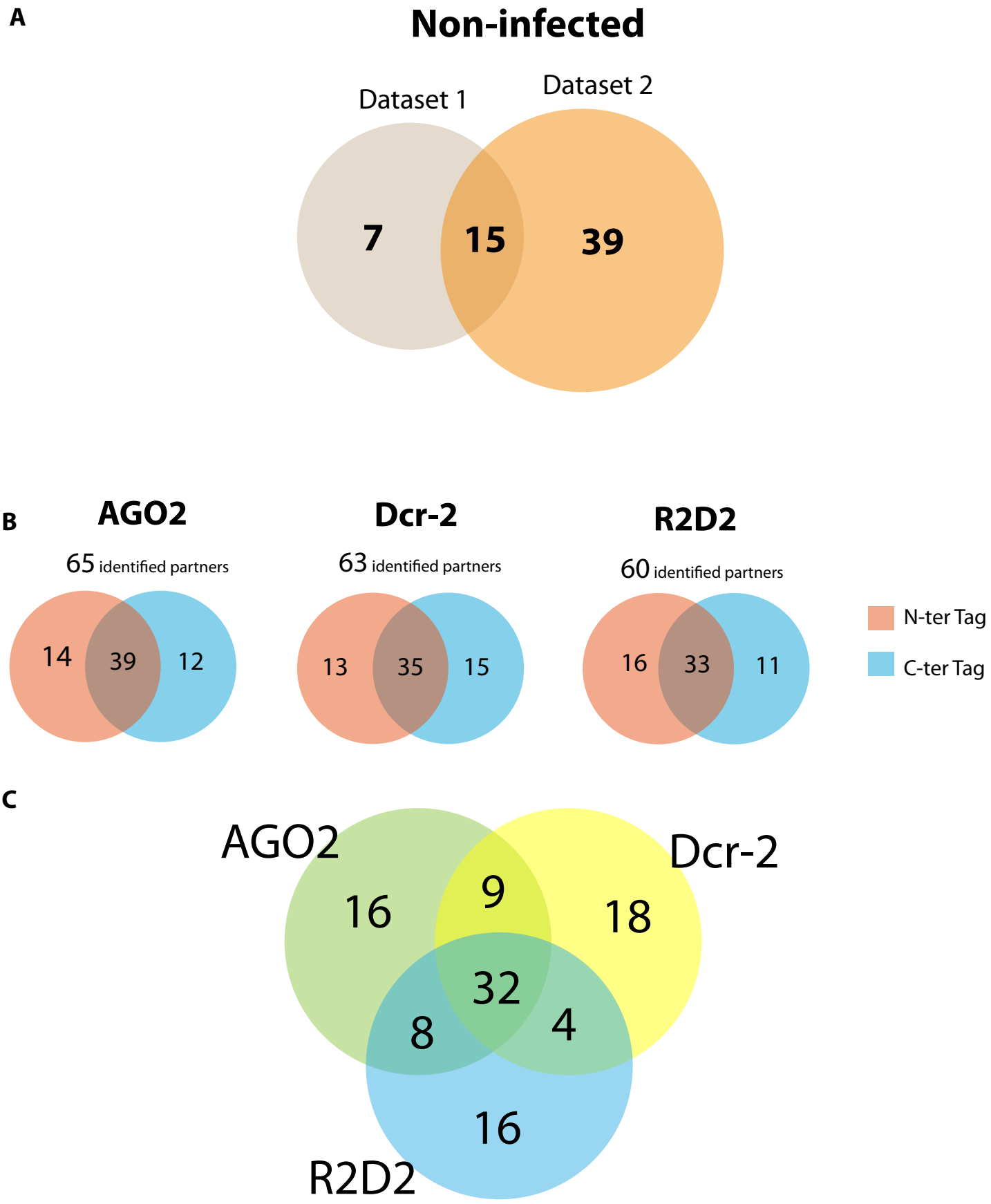

1.2.2 Dataset-1 vs. Dataset 2

This interactome analysis, which involves a large number of samples, was split in two for practical reasons. First, we compared uninfected cells to cells infected by DCV (Dataset 1); and second we compared uninfected cells to cells infected by FHV or VSV (Dataset 2) (Fig. 1 and 2). The comparison of the uninfected samples in Dataset 1 and 2 enabled us to evaluate accuracy and reproducibility of the method (Figure 2).

In non-infected condition, the first dataset revealed a network of 22 proteins interacting with AGO2, Dcr-2 or R2D2 whereas the second dataset revealed a network of 54 interacting proteins in the same condition (Figure 2A). 15 out of 22 proteins identified in dataset 1 (68%) were present in dataset 2, hinting at an acceptable reproducibility of the method and strengthening the confidence in the identity of the partners. The large number of interactants identified in dataset 2, but not in dataset 1 (39 out of a total of 54), most likely reflects the higher number of proteins identified in the second dataset (54 vs. 22 only for dataset 1). We have no clear explanation for this discrepancy, as the purification method used to generate the two datasets was strictly the same. The difference might result from changes in default settings of the FT ICR machine, which underwent maintenance during these four months, which might be responsible for the increased sensitivity.

Overall, although the second set of experiments was more sensitive than the first one, the fact that more than two-thirds of interactants identified in dataset 1 were again identified in dataset 2 attest of the reliability of the method.

1.2.3 Influence of the tag position on the recovered partners

We then wanted to compare the influence of the position from the Biotin-tag (Nter or Cter) on the pulled-down protein complexes. When all the generated data are pooled together (dataset 1 and 2, infected and non-infected), we observed that for the three baits, more than 50% of the identified proteins interact with both versions of the bait. By contrast, less than 25% of the interactants interact specifically with the N- and the C-tagged versions of the baits (Fig. 2B). The overall good reproducibility (55 to 60%) between the N- and C-ter tags for the three baits again attests of the reliability of the approach, even though the position of the tag (N-ter or C-ter) appears to influence the

recovery of some partners. In particular, the reduced number of interactants identified with the C-terminus tagged version of R2D2 may reflect a critical role for this extremity of the protein in interaction with co-factors. In order not to miss some significant co-factors, we decided to include all identified proteins, including N- or C-ter specific interactants in our subsequent functional analysis.

1.2.4 Influence of the baits on the recovered partners

Next, we wanted to assess the influence of the purified bait protein on the identity of the pulled-down co-factors. A total of a 103 proteins were identified as co-factors of either Dcr-2, AGO2 or R2D2. As previously reported (Cenik et al., 2011; Liu et al., 2006), Dcr-2 and R2D2 were always found pulled-down together in our analysis. Importantly, the tag position (N- or C- terminal) in both proteins did not seem to perturb their intimate interaction. Indeed, regardless of the condition, in every sample where R2D2 was pulled-down Dcr-2 was detected and vice versa. Interestingly, roughly one third of these were found with the three baits (Fig. 2C). These 32 common interacting factors might represent the core constituents of the siRNA pathway molecular machinery.

This analysis also shows that 16 factors interact specifically with AGO2, 18 with Dcr-2 and 16 with R2D2. These factors in contrast to the previously mentioned 32 common factors, may be involved in a non-core molecular function of the classical RNAi. Moreover, they might represent important players in the RNAi-independent mechanisms in which AGO2, Dcr-2 or R2D2 could be involved (Cernilogar et al., 2011; Deddouche et al., 2008; Fukuyama et al., 2012; Moshkovich et al., 2011).

Fig. 3 **Overlap between the identified *Dm* factors and RNAi-components identified in proteomic studies in other organisms.**

A) List of the identified *C.elegans* or *H.spaiens* DCR-1, Ago-2 or TRBP interacting partners that were also identified in the *Dm* siRNA interactome (Left panel), Venn Diagram showing the numbers of identified proteins in *C.elegans/H.sapiens vs. D.melanogaster* with the respective baits (Right panel). B) Pie chart illustrating the percentage of the independently reported RNAi purified co-factors in (*C.elegans or H.sapiens*) , the percentage of RNAi related factors identified in earlier studies in *D.m* and the newly uncovered RNAi co-factors.

A

DCR-1 interactome in *C.elegans* (Duchaine et al, Cell 2006)

Gene name in *C.elegans*	Gene Name in *D.melanogaster*	Found with
HSP-70	Hsp70	**Dcr-2**, *AGO2,R2D2*
HSP-3	Hsc70-3	**Dcr-2**, *AGO2,R2D2*
HSP-4	Hsc70-4	**Dcr-2**, *AGO2,R2D2*
HRP-2	CG17838 (Syncrip)	**Dcr-2**
CCT-2	CG7033	**Dcr-2**, *AGO2,R2D2*
CCT-7	Tcp-1eta	**Dcr-2**, *AGO2,R2D2*
CCT-1	T-cp1	**Dcr-2,** *AGO2*
NST-1	ns1	**Dcr-2**
FRL-1	CG32138	**Dcr-2**, *AGO2*
RDE-1	*AGO2*	*R2D2*
EFT-2	*ef2b*	*AGO2*

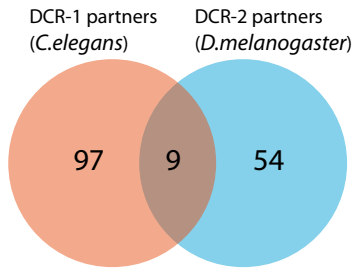

Argonaute-2 interactome in *Homo sapiens* (Frohn et al, Molecular and Cellular Proteomics 2012)

Gene name in *H.sapiens*	Gene Name in *D.melanogaster*	Found with
RS14	Rps14	**AGO2**
RS5	RpS5	**AGO2**, *Dcr-2*
RS3	RpS3A	**AGO2**, *Dcr-2, R2D2*
PABP1 and PABP4	Pabp	**AGO2**
DICER	*Dcr-2*	*R2D2*

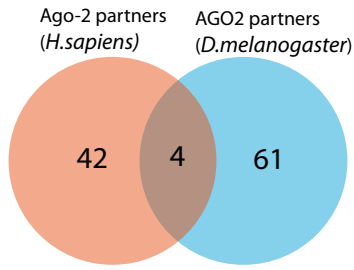

TAR-RNA Binding Protein (TRPBP) interactome in *Homo sapiens* (Chi et al, Cell & Bioscience 2011)

Gene name in *H.sapiens*	Gene Name in *D.melanogaster*	Found with
CPB	cct gamma	**R2D2**, *Dcr-2, AGO2*
RL22	RpL22	**R2D2**, *Dcr-2, AGO2*
RL23	RpL23	**R2D2**, *Dcr-2, AGO2*
RL7A	RpL7A	**R2D2**, *Dcr-2, AGO2*
RS17	RpS17	**R2D2**, *Dcr-2*
RS3A	RpS3A	**R2D2**,*Dcr-2, AGO2*
RS5	RpS5	**R2D2**, *Dcr-2*
GNL3	*ns1*	*Dcr-2*
TCPB	*T-cp1*	*Dcr-2, AGO2*
RS15A	*RpS15a*	*Dcr-2*
RS14	*RpS14*	*AGO2*
RL3	*RpL3*	*AGO2*
HNRPQ (SYNCRIP)	*CG17838 (Syncrip)*	*Dcr-2*

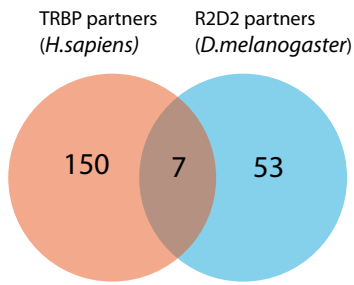

B

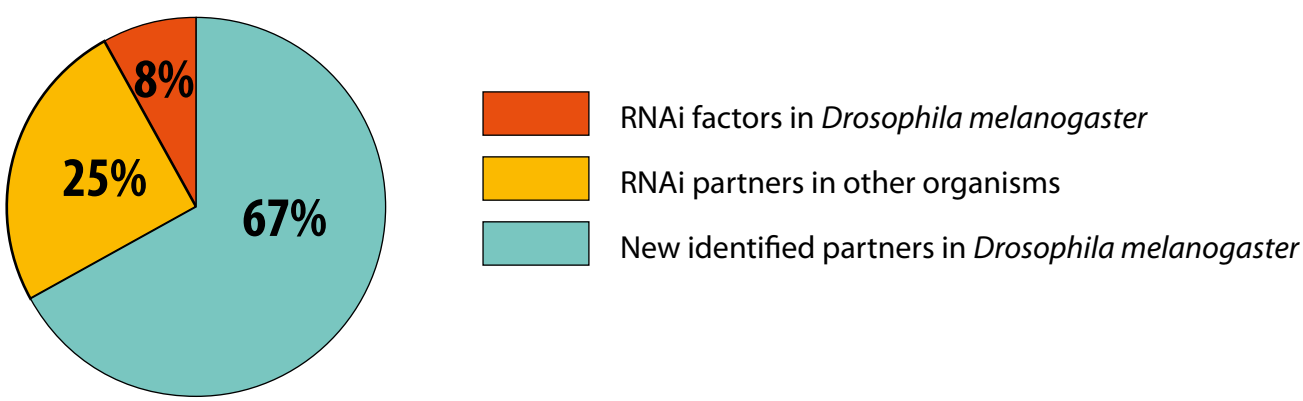

1.3 The identification of the (si)RNA pathway protein niche

1.3.1. Evolutionary conservation of the identified interactions in the RNAi mechanism.

The core components of the RNAi pathway (e.g. Dicer, Argonautes, dsRBP) are well conserved among eukaryotic species. Previous studies have attempted to identify co-factors of these molecules in other species. We took advantage of three independent published proteomic studies performed on the constituents of this pathway in *C.elegans* and *H.sapiens* (Chi et al., 2011; de Boer et al., 2003; Duchaine et al., 2006; Frohn et al., 2012; Fukuyama et al., 2012) to look for putative evolutionarily conserved interactants (Fig. 3).

The first dataset we used for this comparison was generated by a functional proteomic analysis of DCR-1's biochemical niche in *C.elegans* (Cenik et al., 2011; Duchaine et al., 2006; Liu et al., 2006). This study identified 106 interacting partners of DCR-1 in both worm embryos and gravid adults. Eleven of those had orthologs in our Drosophila interactome dataset (Fig. 3A), nine of which interacted with Dcr-2. Amongst these 9 factors six were protein chaperones belonging to two sub-families: heat-shock/cognate proteins (Hsp70, Hsc70-3 and Hsc70-4), and T-cp1-like chaperonins (T-cp1, T-cp1eta and CG7033), one RNA binding protein (Syncrip) and a GTP-binding protein (nucleostemin1) (Fig. 3A).

The two other datasets compared to our interactome were generated from two proteomic studies on the binding partners of human Ago-2 and the TAR-RNA Binding Protein, TRBP (an ortholog of R2D2) (Chi et al., 2011; Frohn et al., 2012). Among the 46 proteins found with human Ago-2, four were detected in with *dm*AGO2 (RpS3,RpS14, RpS5 and the poly-A binding protein (PABP)). Likewise, 6 ribosomal proteins found to interact with TRBP were found with R2D2 (RpL22, RpL23, RpL7A, RpS17, RpS3a and RpS5). Moreover, one T-cp1 like chaperone (CCT gamma), found with TRBP was detected with R2D2 (Fig. 3A).

Overall, this comparison between species shows reveals that 25% of the identified factors in our study have orthologs in worms or humans, which also interact with components of the RNAi pathway in those species. Interestingly, another search of the literature, this time within the drosophila species, revealed in our interactome, in addition to Dcr-2, AGO2 and R2D2, three newly identified factors with RNAi related functions (SoYb, Vret and Blanks) (Gerbasi et al., 2011; Handler et al., 2011). Finally,

Fig. 3.5 **Parrallel between the *Human* type I IFN interactome from (*Li et al*, Immunity 2011) , and the *Drosophila* siRNA pathway interactome :**
Amongst the 260 High-confidence interactants of the innate immunity protein interaction network regulating type I interferon production identified by **(*Li et al*,** Immunity 2011**) ,** only 8 proteins are depicted. These 8 proteins have homologs in the *Dm* siRNA interactome network composed of 101 proteins .
The baits are represented as squares and the identified partners represented as circles.

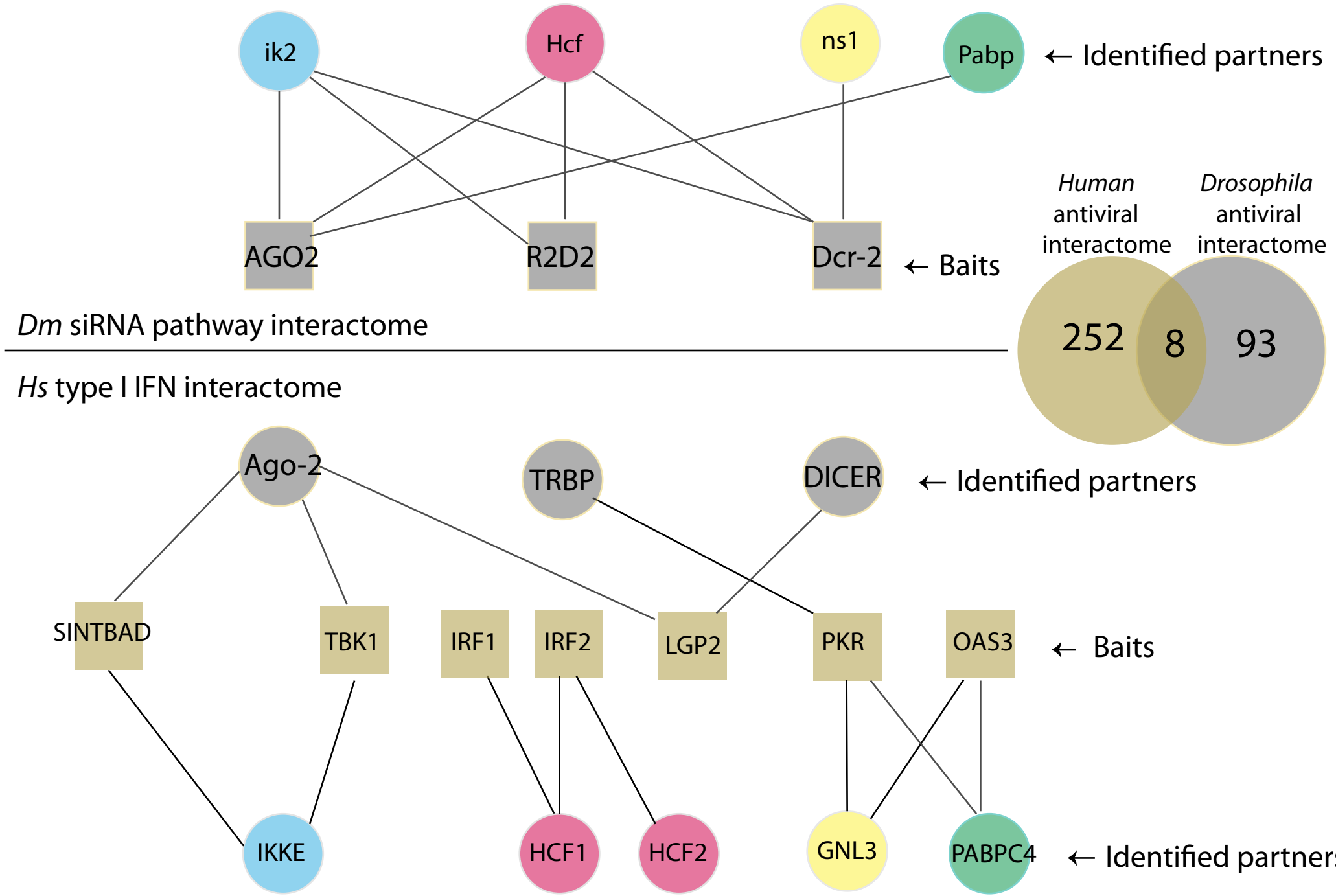

67% of the proteins we have identified have never been related to the RNAi machinery before (Fig. 3B).

In conclusion, the overlap in the identified factors between these various studies and ours, reveals some functional conservation of the RNA interference pathway network, it further provides a validation of our experimental system.

1.3.2. Evolutionary conservation of the identified interactions in antiviral immunity.

Because the siRNA pathway represents the major antiviral host-defense mechanism in flies, we next compared its interactome with the antiviral innate immunity interactome in mammalian cells, to see if common interactors could be identified. We took advantage of a comprehensive proteomic analysis published in 2011 (Li et al., 2011) that aimed to map the dynamic innate immunity protein interaction network regulating type I interferon production. Briefly, in this study the authors purified fifty-eight proteins known to be involved in the type I interferon system (sensors, signal transducers and effectors). 260 non-redundant high-confidence candidate interacting proteins (HCIP), constituting the human interferon proteome, were identified.

We compared the 103 factors identified in Drosophila to the list of these 260 HCIP. Only seven proteins were found in both the drosophila and the human antiviral IFN interactomes (Fig. 3.5). Intriguingly, orthologues of the three core components of the drosophila siRNA pathway were found in the human antiviral interactome. Human DICER was found to interact with one viral RNA sensor (LGP2); human Ago-2 also interacts with LGP2, as well as with two proteins involved in the signal transduction leading to interferon production (TBK1 and SINTBAD) (Fig. 3.5); TRBP was found to interact with Protein Kinase R (PKR), a known virally stimulated sensor involved in general translation shutdown. Interestingly, four other proteins found in *Dm* antiviral interactome were identified in this study. First, we note the Host Cell Factor (Hcf); a nuclear protein involved in transcription regulation in drosophila and pulled down with our three baits. Two human orthologues of this protein, HCF1 and HCF2, co-purify with IRF1 and IRF2, which are transcription factor regulating expression of various antiviral genes including IFN beta in response to viral challenge (Harada et al., 1989; Heylbroeck et al., 1998; Miyamoto et al., 1988; Weaver et al., 1998). Second, we note the presence of *Dm* Ik2 protein, found to interact with the three baits (Dcr-2, AGO2 and R2D2). This

Fig.4 Interactome of Dcr-2, R2D2 and AGO2 in Mock and Virus infected cells.

A schematic representation of all detected interactions (merged data from non-infected, DCV-, FHV- and VSV-infected cells) is shown. Colored nodes indicate to which Gene Ontology term (Molecular Function) the protein is assigned. The pie-chart represents the percentage of identified proteins for a given GO term.

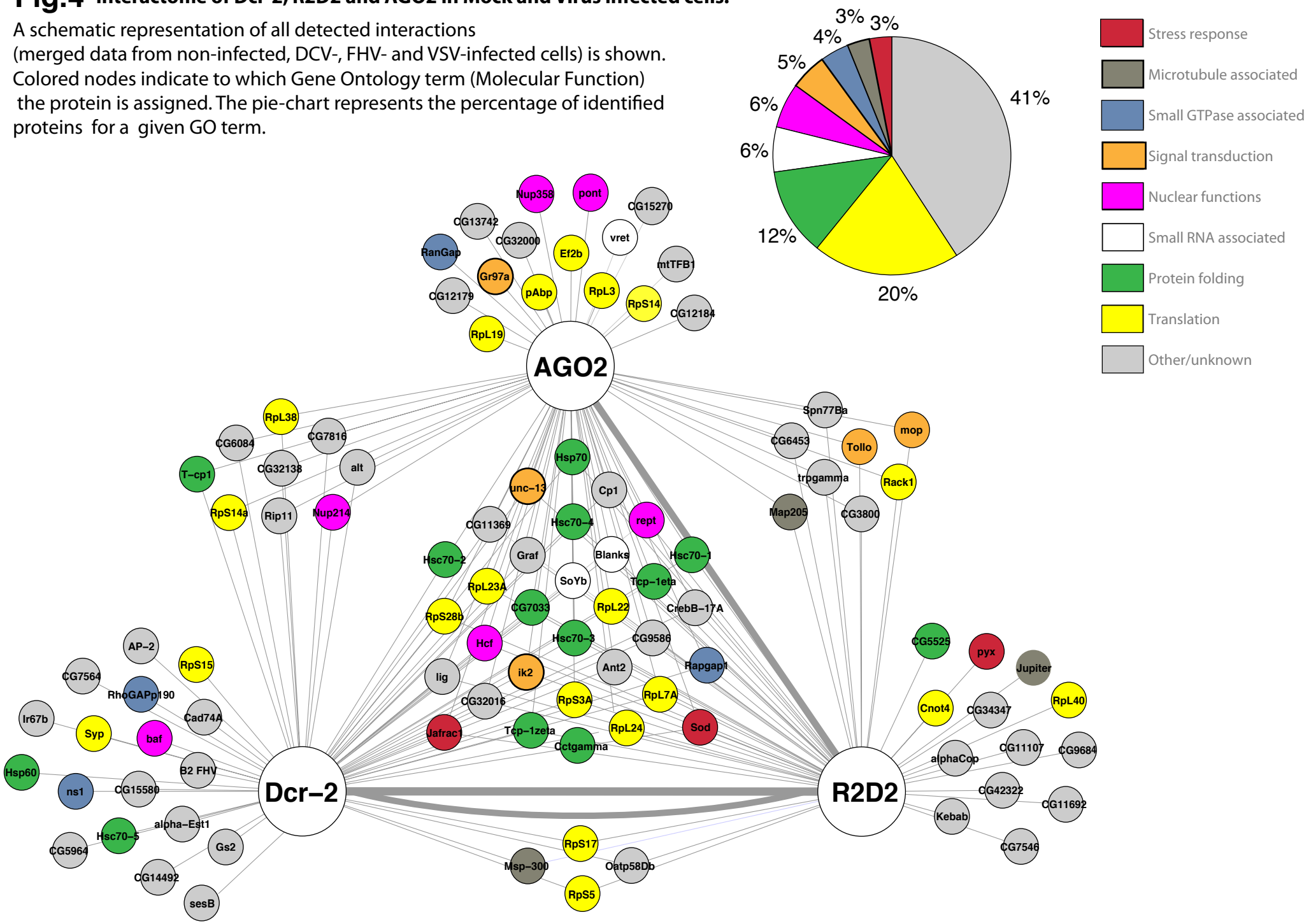

protein is the orthologue of the human protein IKK epsilon, which was found to co-purify with both SINTBAD and TBK1 and participates in IRF3 phosphorylation and activation (Fitzgerald et al., 2003) (Fig. 3.5). Importantly, Dm ik2 has no clear function in drosophila immunity assigned to date. Third, the orthologue of the drosophila Dcr-2 interacting protein nucleostemin (ns1) , GNL3, was found associated with PKR and OAS3 in human cells. Interestingly, as mentioned above, the orthologue of this protein in *C.elegans* is also present in the DCR-1 biochemical niche. Finally the poly-A binding protein (Pabp), which is important for poly-A dependent regulation of translation, was found to copurify with AGO2 in drosophila, while in humans in was found to be attached to PKR and OAS3.

In conclusion, this analysis permitted us to identify some evolutionarily conserved protein interactions. An in depth study of proteins that show up independently across species in different antiviral immune systems (e.g. Hcf, ns1) might uncover new, evolutionarily ancient, facets of antiviral immunity.

1.3.3 A gene ontology analysis of the identified interactants.

In total, we have identified 103 proteins interacting with Dcr-2, R2D2 or AGO2 in control or virus-infected S2 cells (Fig. 4 and Table 1- Chapter 1).

In order to facilitate the visualization and the analysis of the data, the open Source Cytoscape program was used to create images of the identified interactions in different conditions. Table1 (sheet 2) was used to construct the networks shown hereafter.

The gene ontology analysis of the identified proteins reveals a complex picture; the identified interactants are involved in very different molecular processes (Fig. 4). Interestingly, the most represented group for molecular function (20%) corresponds to molecules involved in translation, especially ribosomal proteins. This may not come as a surprise since the RNAi mechanism is known to partly interfere with the translation mechanism (Iwasaki and Tomari, 2009) and since no RNase treatment was used when the complexes were purified. The second most represented group is composed of molecules involved in “Protein Folding“ (16%). This family contains known chaperones (e.g. Hsp70, Hsc-70) but also chaperonins belonging to the TRiC/CCt complex (e.g. T-cp1, CCt γ). Concerning chaperones we note that the Hsc70-4, which participates in the

ATP-dependent loading of siRNA duplexes onto AGO2 and is required for the RNAi response (Iwasaki et al., 2010), was found to be pulled down with Dcr-2, R2D2 and AGO2 (Fig. 4). On the other hand, the observation that the chaperonins also interact with these three components has only been reported so far in the earlier mentioned Dcr-1 proteomic study in *C. elegans*, and no functional involvement of these proteins in the antiviral immunity has been described to date.

The third most represented category in the gene ontology, "small RNA associated", contained three recently identified factors important in small RNA regulation: (i) SoYb, which is associated with Dcr-2, R2D2 and AGO2 in S2 cells; SoYb encodes a protein with a DExD/H box helicase and two Tudor domains. This factor is related to the Yb protein, a protein acting in a different silencing pathway and controlling the biogenesis of the primary PIWI-interacting piRNAs (Olivieri et al., 2010); (ii) Vreteno, which we find associated to AGO2, is another Tudor domain containing protein that has been found to be required for piRNA-based transposon regulation in both germline and somatic gonadal tissues (Zavadil et al., 2011); (iii) Blanks, a recently described siRNA/dsRNA binding protein (Gerbasi et al., 2011), which we find here to be associated with R2D2 and AGO2 (Fig. 2). Finally, we were surprised to observe that 6% of the identified interactants have reported nuclear functions (e.g. Reptin, Hcf) (Fig. 2). Of note, while this project was ongoing, several groups have reported a nuclear function for Dcr-2 and AGO2 (Cernilogar et al., 2011; Moshkovich et al., 2011; Taliaferro et al., 2013).

1.4 A dynamic pattern of interactions

1.4.1 DCV infection remodels the siRNA pathway interaction network

We next analyzed the composition of the protein complexes assembled around Dcr-2, R2D2 and AGO2 upon viral infection. The first dataset (dataset 1) we obtained included information about the protein network formed by our three baits in non-infected condition (Control 1), or upon viral infection with DCV at two time points (8 and 16 hours). These early time points were chosen to analyze the influence of the stage of the infection cycle on the siRNA pathway interactome.

While the protein environment assembled around AGO2, Dcr-2 and R2D2 was composed of 25 proteins in non-infected condition (Fig. 5 and 6), the size of the complexes slightly increased upon DCV infection: 32 proteins were detected at 8 hours

Fig. 5. **Comparison of duplicated conditions**

A) Number of identified partners of Dcr-2,AGO2 and R2D2 in different conditions (Mock n=2 , or DCV infected at 8 and 16 hours)

B) 4-way Venn Diagram of the identified patners in Control 1, Control 2, DCV 8 hours or DCV 16 hours post-infection

A.

Condition	Number of partners
Control 1	25
Control 2	54
DCV 8 hours	32
DCV 16 hours	33

B.

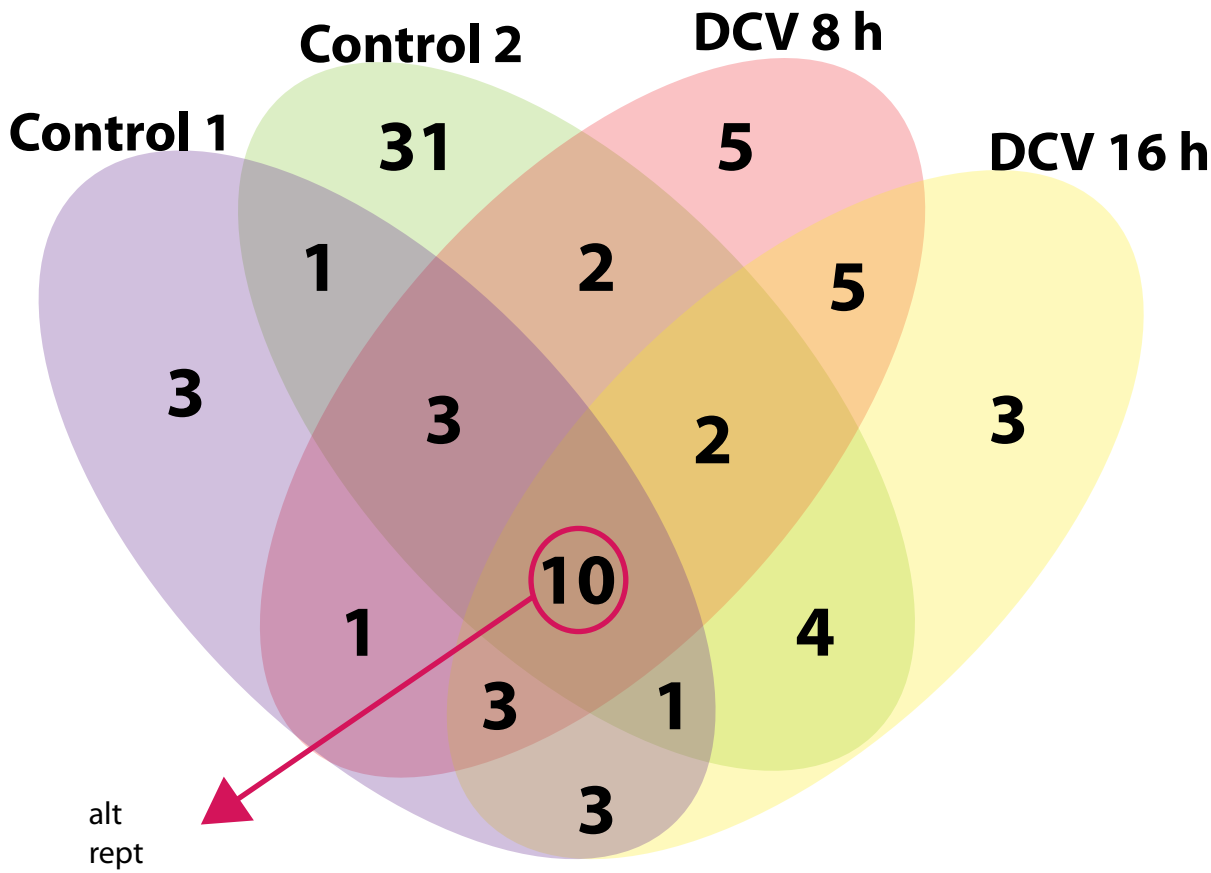

Fig. 6

Protein network assembled arround AGO2,Dcr-2 and R2D2 in Mock condition or at two timepoints of DCV infection (8 and 16 hours), generated from dataset1.

Non-infected (Control 1)

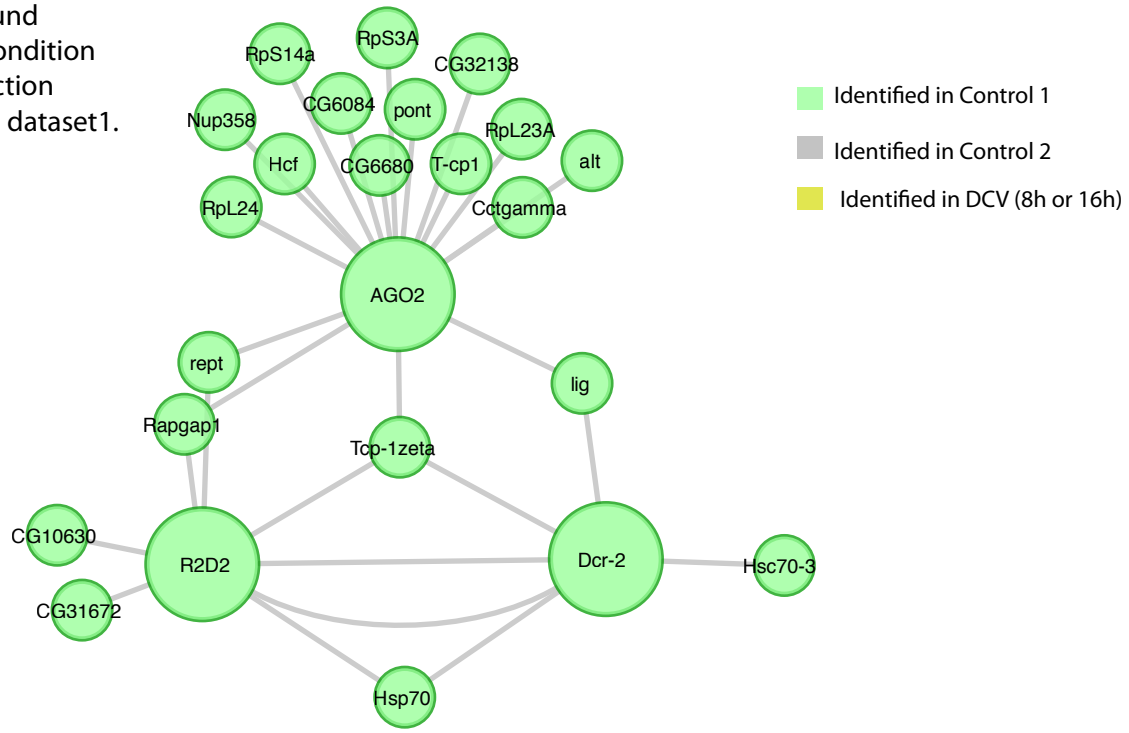

DCV infected 8 hours

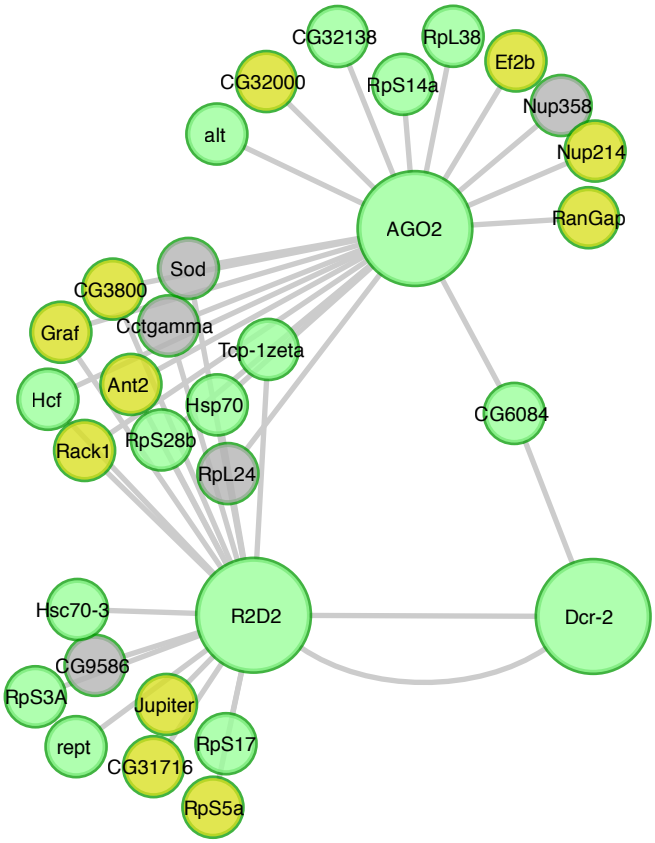

DCV infected 16 hours

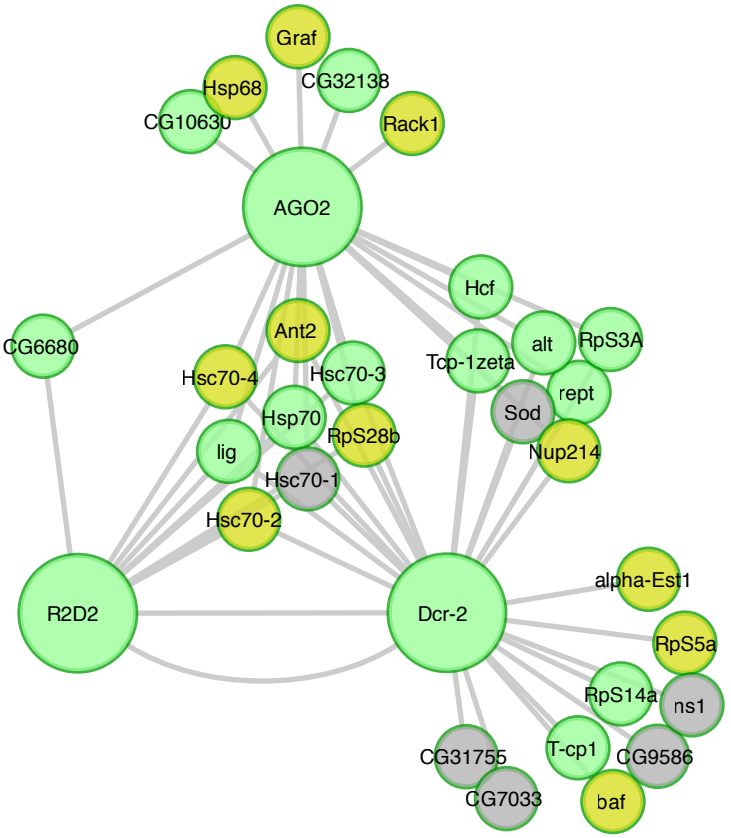

post-infection and 33 at 16 hours post-infection (Fig. 5 and 6). A total of 21 proteins were not detected in the non-infected control, but showed up after DCV infection (8 or 16 hours). Eight of these proteins were detected in the siRNA pathway interactome in non-infected conditions in the second dataset (Fig. 5), suggesting that these molecules may be constitutively present, but escaped detection in the first dataset. Interestingly however, the remaining 13 proteins were also absent from the non-infected samples in the second dataset (Fig. 5). The Venn Diagramm in Figure 5 further shows that most of the interactants detected in control 2, and not in control 1 (31 over a total of 54), were not present in DCV infected cells at 8 or 16 hours. Altogether, these data suggest that some proteins, shown in yellow in Figure 6, joined the siRNA interactome network upon DCV infection. Amongst these 13 proteins five were exclusively detected 8 hours post-DCV infection, three were only detected 16 hours post-DCV infection, and five (RACK1, Ant2, Nup214, Rps5a, Graf) were present at both time points.

Interestingly, we also observed changes in the pattern of interactions of the siRNA network during DCV infection. Indeed, a clustering of proteins around AGO2 and R2D2 is seen 8 hours post-DCV infection, compared to Control 1 (Mock) (Fig. 6), and this clustering appears to change over time, with many viral-induced interactions clustering around AGO2 and Dcr-2 16 hours post-DCV infection (Fig. 6). In addition, 8 proteins interact with Dcr-2, AGO2 and R2D2 at 16 hours post-DCV infection, whereas there were none at 8 hours post-infection and only one (Tcp1-zeta) in the non-infected condition. This suggests a reorganization of the molecular complexes operating in the antiviral siRNA pathway as the infection develops.

The conclusion we can draw from this analysis is that the components of the siRNA pathway are not static and that they dynamically reorganize their interaction networks once confronted to DCV infection. Consequently, we wanted to know if this was also true upon infection with other viruses (FHV and VSV). Therefore, we undertook a similar analysis of the network after infection with these two viruses.

Fig. 7 **Interaction Networks of AGO2, Dcr-2 and R2D2 upon FHV or VSV infection.**

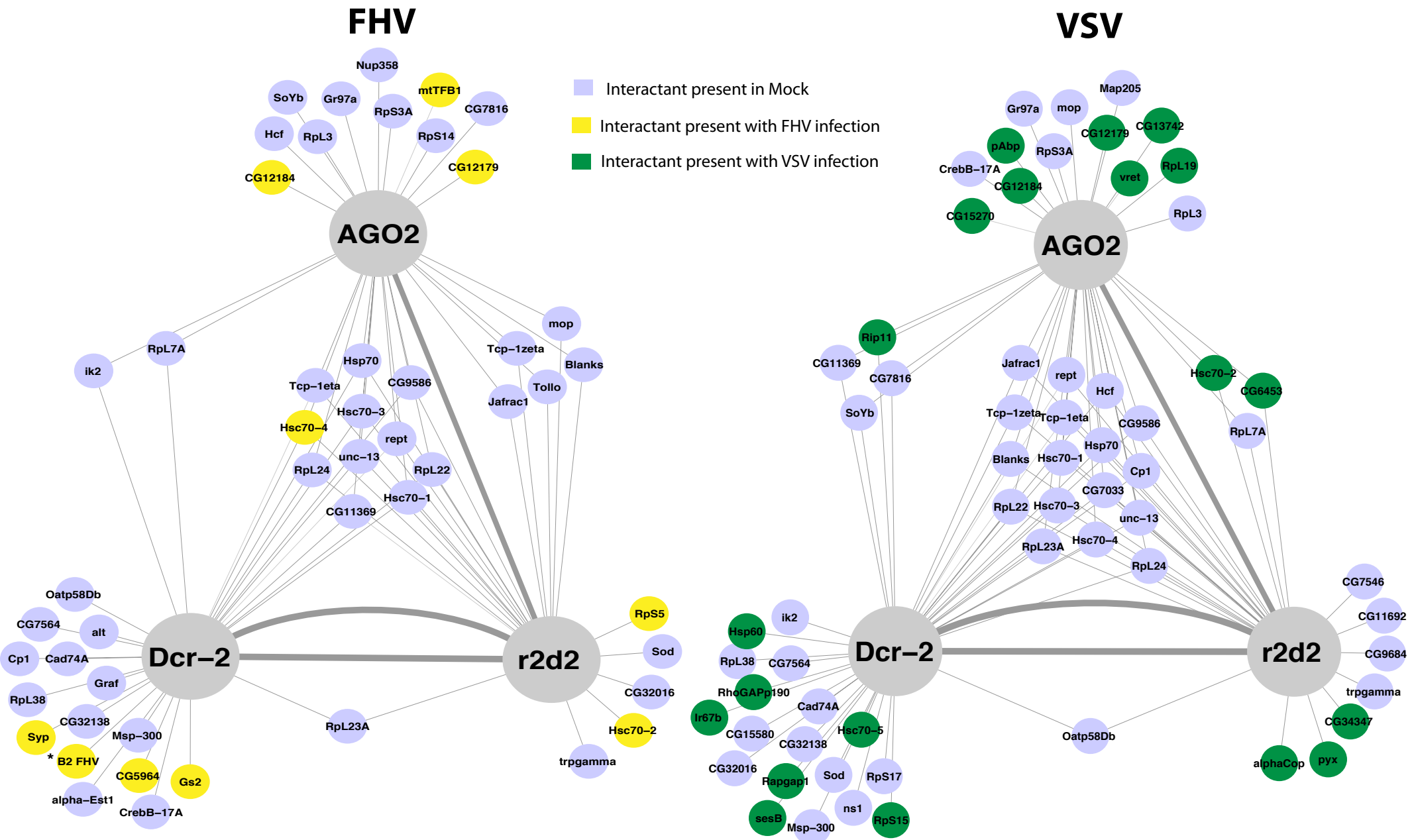

* B2 was the only protein from viral origin that was identified in the study.

Fig. 7.5 **Repartition of the presence or absence of partners pulled down with AGO2, Dcr-2 and R2D2 in different infections**

A) 3-way Venn Diagram representing the numbers of the identified partners of AGO2, R2D2, Dcr-2 when the cells were infected. B) 3-way Venn Diagram representing the numbers of the identified partners of AGO2, R2D2, Dcr-2 that were specific to viral infection (not present in Mock condition). C) Venn Diagram representing the numbers of the partners of AGO2,R2D2 and Dcr-2 that were present in Mock condition and that disappeared from the interaction network upon viral infection.

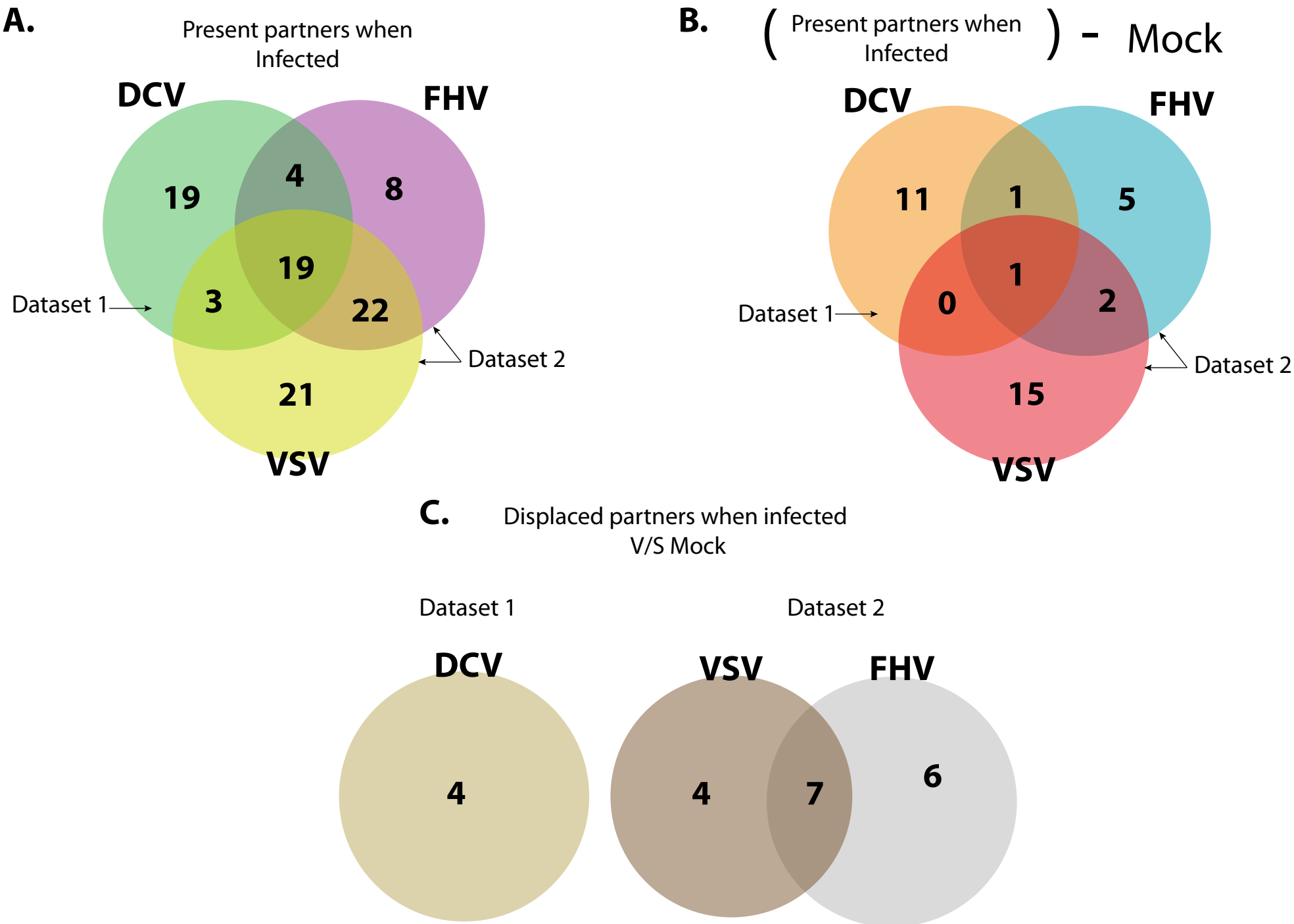

1.4.2 Virus-specific interactions of the siRNA interactome

For the analysis of the infection by FHV and VSV we merged the results of control 1 and control 2 to construct a network in non-infected conditions, which contained 64 proteins. The cells were challenged for 16 hours with FHV (MOI=1) or for 48 hours with VSV (MOI=10). The time points were picked after preliminary experiments on the replication kinetics of these different viruses. FHV replicated very fast whereas VSV replicated at slower rates (data not shown).

53 proteins were detected in the interactome after FHV infection and 65 after VSV infection. In agreement with our findings with DCV, FHV infection recruited 9 new protein partners to the network (Fig. 7 and 7.5), whereas VSV recruited 18 new protein partners (Fig. 7 and 7.5). Interestingly, further analysis shows that only one recruited protein (Hsc70-2) is common for the three viruses (Fig. 7.5). On the other hand many proteins were recruited to the network in a virus specific manner: 11 factors were DCV specific, 15 were VSV-specific and only 5 were FHV specific, including the viral protein B2 (Fig. 7.5 and 8).

The small number of proteins recruited by FHV might reflect the strength of its VSR. While VSV has no known VSR to date and DCV1-A have been shown to be a weak VSR (van Mierlo et al., 2012), the VSR from FHV, B2, is very potent. B2 might sequestrate the Dcr-2/R2D2 heterodimer preventing it from interacting with co-factors. Alternatively, the dsRNA binding protein B2 might prevent access of co-factors of R2D2 and DCR-2 to long or short dsRNA molecules.

Some of these virus-specific interactants made sense in light of the differences in the replication cycles of the viruses used in this study. These interactants are good candidates for host factors specifically recruited to the viral RNAs targeted by the siRNA pathway. Indeed, among the 5 FHV-specific interacting proteins, we note the presence of a mitochondrial protein (mtTFB1), in good agreement with the replication of FHV on mitochondrial membranes (Miller et al., 2001). Another example is the viral protein B2, which competes with Dcr-2 for the binding of viral dsRNA (Chao et al., 2005) (Fig. 8). Of similar interest is the observation that the poly(A) binding protein (PABP), which binds to the poly A tail of mRNAs and interacts with eIF4G and eIF4E bound to the 5' cap to initiate translation, is present only in the interactome of cells infected with VSV (Fig. 8). Indeed, unlike DCV and FHV, VSV mRNAs have both a 5' cap and a poly (A) tail. Altogether, these results indicate that in the course of viral infection, cellular proteins are

Fig. 8.

Identification of virus-specific induced interactions : (A) DCV-specific, (B) VSV-specific and (C) FHV-specific

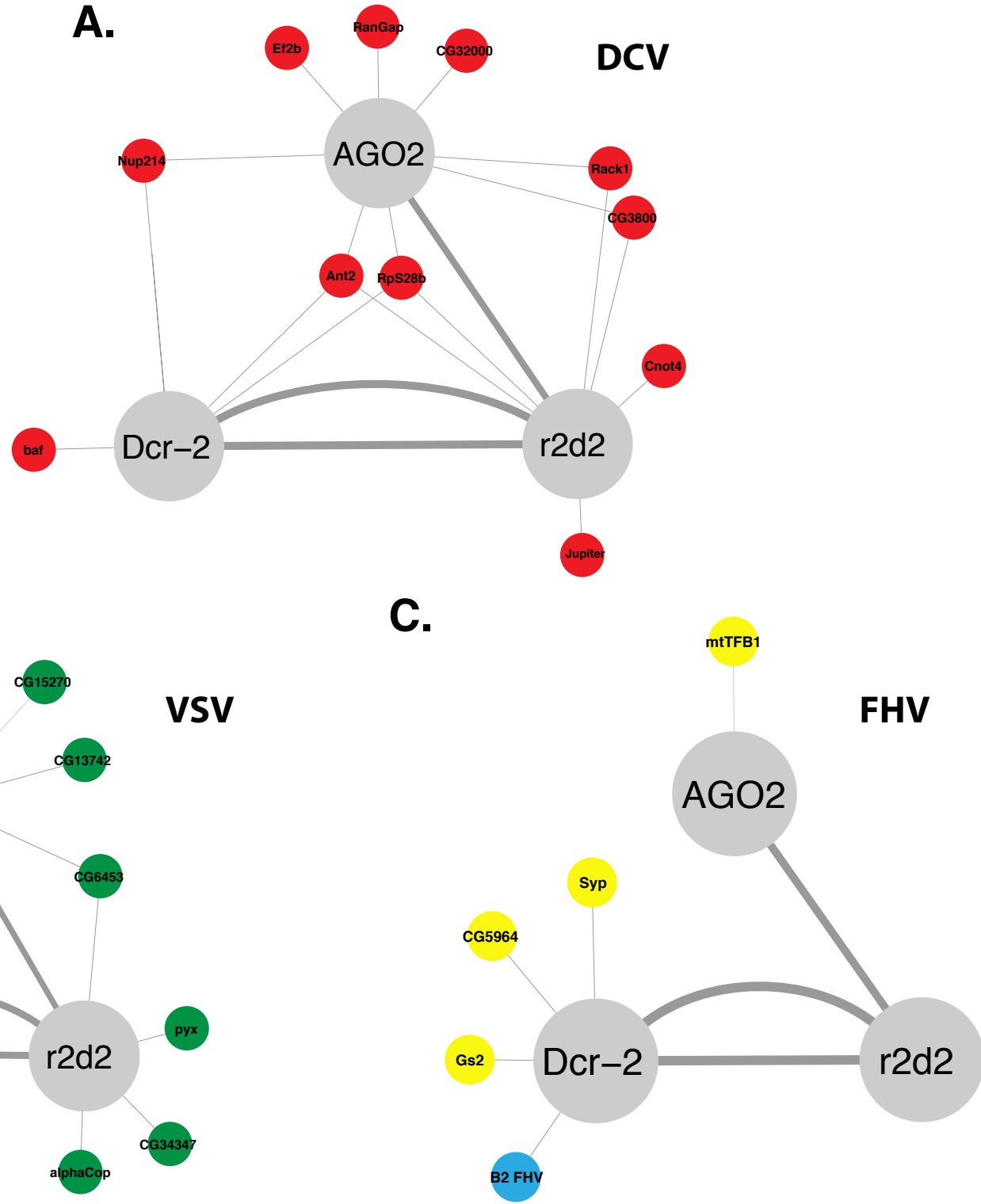

recruited by the core components of the siRNA pathway. These proteins may represent novel viral-induced components of the antiviral RNAi pathway, or cellular factors recruited by the virus to complete its infection cycle.

Conversely, we tried to see if there were proteins that were displaced (leaving the network) after viral infection (Fig. 7.5). This analysis showed that the number of proteins displaced from the network is lower than those recruited (Fig. 7.5, lower panel). In this analysis, the dataset 1 (DCV/control1) and dataset 2 (FHV/VSV/Control2) were examined separately. Four proteins found in Control 1 seemed to be displaced by DCV (Fig. 7.5). 11 proteins found in Control 2 were displaced by VSV and 13 proteins found in the same control were displaced by FHV. Interestingly, compared to VSV and DCV, FHV infection recruits the smallest number of proteins specifically to the three baits, and it conversely seems to displace the largest number of proteins from the network (13 proteins), consistent with the potency of its VSR B2. However, the displacement data stemming from Mass-Spec negative results (non-identified) should be interpreted carefully. In Mass Spectrometry experiments, the absence (non-identification) of a protein in a sample is less meaningful than the presence (identification) of this protein, because the non-identification could be due to various experimental artifacts (e.g. insufficient repetitions (n=1)).

In conclusion, this comprehensive proteomic study of the siRNA pathway revealed many new molecules that might play an important role in RNAi or in drosophila antiviral immunity in general. It further showed that some of these interactants are evolutionarily conserved and might be involved, not only in *D.m* antiviral immunity, but also in other eukaryotic immune systems (mammals and nematodes). Finally, this study illustrated that the siRNA pathway response to viral infection is not static but rather dynamic. This suggests that the substrate choice of Dcr-2, R2D2 and AGO2, and their potential interaction with VSRs, influence their interaction networks.
We next decided to assess the contribution of these identified factors in the control of viral replication in drosophila cells. Therefore, a RNAi screen strategy was employed and described hereafter.

Fig. 9 General RNAi-screening strategy

Gene-specific primers harboring the T7 promoter sequence were designed thanks to the E-RNAi algorithm. Touch-down PCR was performed with these primers to generate template DNA fragments that were *in vitro* transcribed thanks to the T7 DNA-dependant RNA polymerase. The *in vitro* transcription products were annealed to generate double stranded RNA. The genrated library of dsRNA was aliquoted in 96-well plates in triplicates. S2 cells were reverse-soaked with the dsRNA and incubated at 24 °C for 4 days to obtain an efficient knock-down.
After this incubation time, the cells were infected with DCV, FHV or VSV. The viral titers were then quantified by RT-QPCR or immuno-staining 16 hours post-infection for FHV and DCV and 48 hours for VSV. (See Materials and Methods)

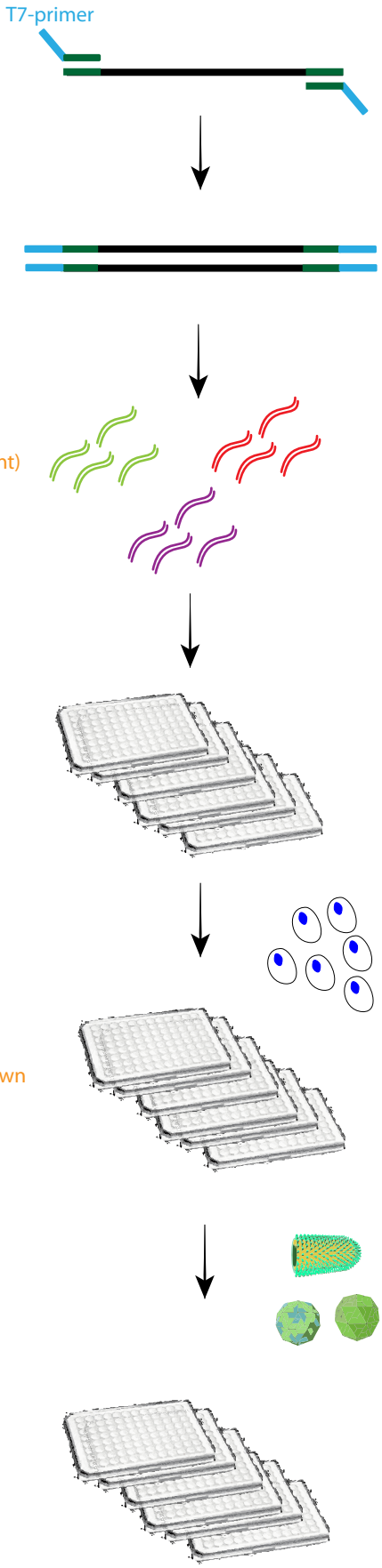

Lysis of cells followed by total RNA Reverse Transcription and Quantative PCR to determine viral titers (Cell to Ct from Ambion)

Fixing of cells and staining with DAPI and anti-capsid antibodies (only DCV and FHV)
Quantifying viral loads (normalised to DAPI) automatically in the INCELL1000 Analyser

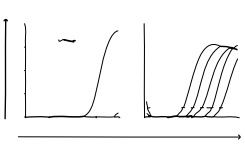

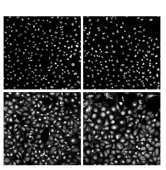

2. Functional analysis of the identified siRNA pathway co-factors

2.1 RNAi screen

2.1.1 Screen design and experimental procedure

Primers harboring the T7 polymerase sequence were designed thanks to the E-RNAi online tool. The primers were then used to generate template DNA for each gene of interest. *In vitro* T7 polymerase transcription was then used to generate ~100 dsRNAs targeting different genes. The dsRNA was quality-controlled on agarose gels, quantified and then aliquoted in 96-well cell culture plates (3µg/well). Each 96-well plate contained dsRNA against GFP (Mock) and a positive control dsRNA (dsAGO2). The same dsRNA was aliquoted in 6 independent wells for statistical stringency.

S2 cells were then reverse-soaked in these plates. After this treatment cells were challenged with different viruses. Different Multiplicity Of Infections (MOIs) were used: DCV MOI=1, VSV MOI=10 and FHV MOI=0,1. After 16 hours of infection for DCV and FHV cells were either fixed, for immunostaining, or lysed for a Reverse Transcription PCR (RT PCR) followed by Quantative PCR analysis (Fig. 9).

Cells were challenged by VSV for 48 hours and only a RT-QPCR was performed to quantify the viral genome (as the immunostaining experiments for FHV and DCV gave similar results to the RT-QPCR).

2.1.2 Screen data generation

Quantification of viral genomes by QPCR was performed with specific primers recognizing the viral genome sequence and amplification values were normalized to the values obtained for a housekeeping gene *RP49 (*See Materials and methods).

Quantifications of viral capsids were performed thanks to antibodies recognizing epitopes on DCV and FHV capsids respectively. Sixteen microscopy pictures revealing FITC signals were taken in each well. DAPI staining pictures were also captured for estimation of cell proliferation after the dsRNA treatment and for cell number normalization. This was performed on an automatic In Cell 1000 workstation at the Screening facility of IGBMC (See Material and Methods).

Fig. 10 **RNAi screen results of the 35 genes considered as hits.** Hits from screen showing a 2 fold change in viral titers for at least one virus and having shown no viability or proliferation defects upon knock-down. ns: non significant . Bars with no *ns* sign means that the difference is statistically significant (P<0.05).

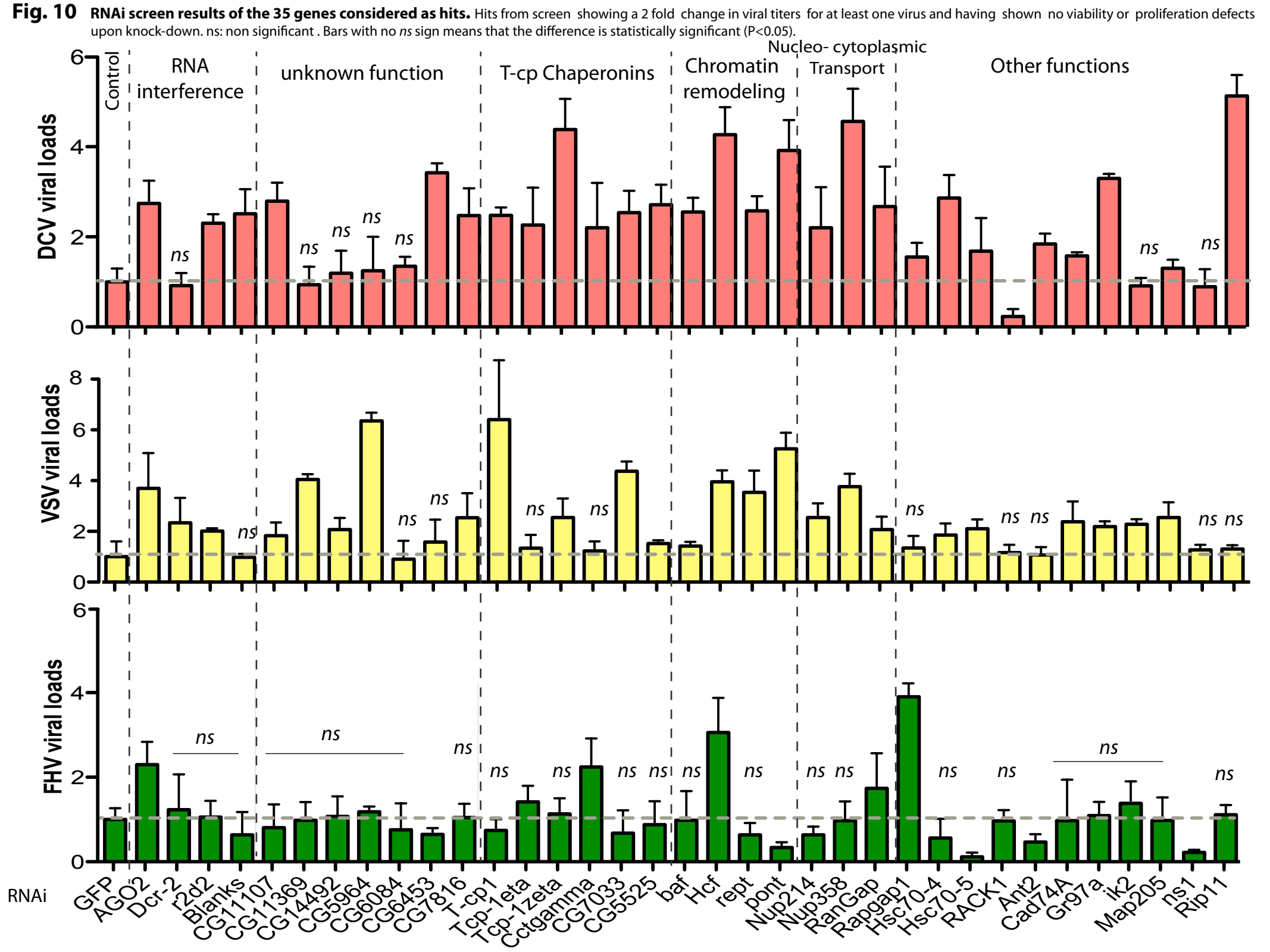

As each gene was tested in six independent wells, mean values and standard deviations were calculated and a two tailed t-test was performed, comparing the values obtained for a given tested gene and those obtained for the dsGFP treatment in the same plate.

The screen results are listed in Table 2. The table contains the proliferation index after each dsRNA treatment, calculated from the DAPI signal. dsGFP treatment was set to 100% (see Material and Methods). The Table 2 also contains the viability Z-scores obtained from Boutros et al (Boutros et al., 2004) , which reflects the effect of the dsRNA treatment on cell viability. A Z-score ≥ 3 means that the dsRNA treatment causes a cell death phenotype. Viral scores were calculated relative to the dsGFP treatment that was set to 1. Each score is followed by the two-tailed *t*-test value.

2.1.3 Screen Data Analysis

Two stringent selection criterions were set in order to determine the genes that strongly and significantly affect viral replication. First, we observed that the silencing of a subset of genes had a strong effect on the viability and proliferation of S2 cells (e.g. ribosomal proteins), complicating the conclusions we can draw from such results. We therefore discarded all the genes that had a Z-score ≥ 3 (cell viability defects) (Table 2). On the 103 genes tested, twelve had a Z-score ≥ 3, which left us with 88 genes. We also discarded genes affecting cell proliferation. They were identified by the DAPI nuclei/cell quantification we performed (See Materials and Methods).

17 genes showed a proliferation index under 50%, and were not further analyzed (Table 2). The remaining 71 genes for which the dsRNA treatment had no effect on cell viability or proliferation, were taken into consideration for their effect on viral replication.

Second, we sought to determine if the knock-down of the expression of a gene affects significantly viral replication. A cut-off of two-fold modification was chosen because knock-down of AGO2 consistently showed an increase in the viral titers by a factor of at least two. On the 71 genes left, 34 showed an increase or a decrease of two folds or more in the titer of at least one of the three tested viruses. The results obtained for these 34 genes were very consistent regarding the method used (immunostaining or RT-QPCR) (Table 2-Chapter 1, highlighted genes, Fig.10).

Fig. 11 **Repartition of the hits obtained from the functional screen,** according to virus phenotype (A) and the GO term Molecular Function (B).

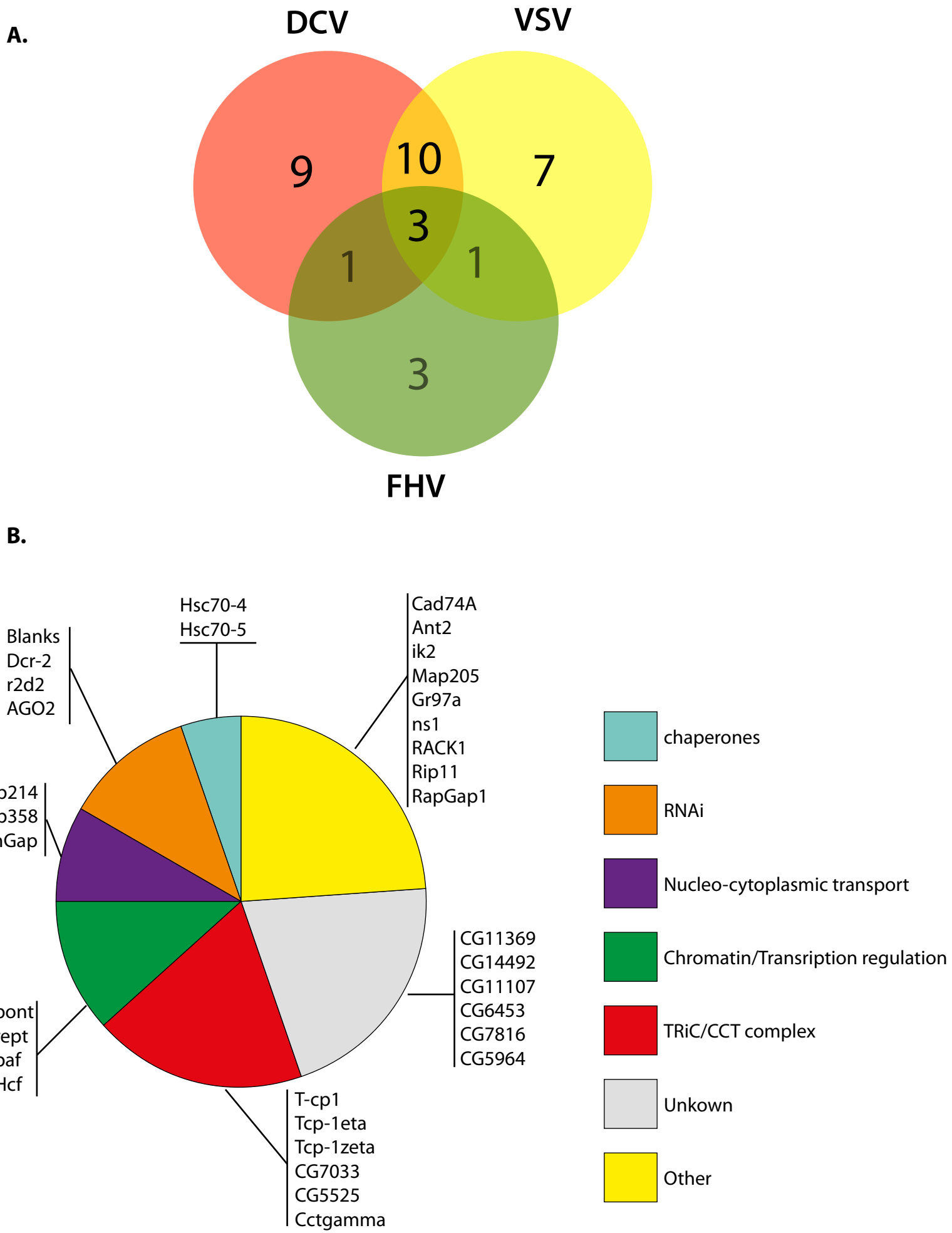

2.2 Screen Results

A gene ontology analysis of the results from the screen reveals that the 34 genes identified as “hits” cluster functionally in distinct gene families (Fig. 10 and 11). In general, the enrichment in the group of “hits” (Vinayagam et al., 2013) for a family of genes that are part of a particular functional category or pathway, has many advantages. First of all, such analysis is less prone to the inherent false positives and false negatives associated with the screen. For instance, a gene might be considered a false negative due to ineffective knockdown or as a false positive due to off-target effects; however, it is less likely that an entire group of genes could be falsely classified. The second advantage of such an enrichment analysis, improve confidence in the results by placing them in biological context and helps generate new hypothesis (Vinayagam et al., 2013).

The pie chart in Fig.11B represents the repartition of these 34 genes regarding their cellular functions. This chart reveals that three major functional groups of genes affect viral replication strongly and significantly: 1- six genes belonging to the Chaperonine T-cp1 family, 2- four genes involved in Chromatin/transcription regulation, 3 - four genes having a role in nucleocytoplasmic transport. In addition, six genes with unknown function and eight belonging to various gene families also affected viral replication significantly.
I will discuss hereafter the relevance of these results in light of viral replication and immunity.

2.2.1 CCT/TRiC Complex chaperonins

One major protein family that affects greatly viral replication is the CCT/TRiC chaperonin family of proteins (T-cp1, Tcp-1eta/zeta, CG7033, CG5525, Cctgamma) (Table 2-Chapter 1, Fig. 10 and 11). The knockdown of one of these proteins significantly affects the viral loads of the three studied viruses (Table 2-Chapter 1, Fig. 10). Thus, the effect of this family of proteins does not seem to be virus-specific, but rather general. The viral loads of all three viruses were affected when at least one of the mentioned chaperonin was knocked-down. This enrichment suggests that this family of proteins might play a major role in antiviral defense.

This CCT/TRiC complex forms an octamer, that is structurally conserved from archae to human (Cong et al., 2010; Ditzel et al., 1998). The CCT/TRiC complex provide favorable conditions for the correct folding of other proteins, preventing their aggregation (Yam et al., 2008). In particular, it has been shown that the chaperonin TRiC complex controls polyglutamine (polyQ) aggregation and toxicity, preventing aberrant folding and fibrillar aggregation of the Huntingtin protein, that is subjected to polyQ expansions in the context of Huntington disease (Kitamura et al., 2006; Tam et al., 2006; 2009). Interestingly, we note that *Drosophila* AGO2 protein harbors a polyQ rich domain (159 Q) in its amino-terminal (N-term) extremity (Hain et al., 2010). This polyQ rich N-term is a unique feature of AGO2, which is not present in other AGOs (AGO1, AGO3, PIWI or Aub). Moreover, this domain is subject to a very rapid evolution amongst drosophilidae when compared to other AGO2 domains (e.g. Mid, PIWI) (Hain et al., 2010). Interestingly, in the plant *Arabidopsis thaliana,* AGO1, which is important for both microRNA function and the antiviral siRNA function, contains a polyQ rich domain in its N-term (Shi et al., 2009). It has been proposed that this domain might play an important role in the antiviral activity of AGO2 in drosophila (Hain et al., 2010).

Taken together, these observations may explain the higher viral loads when one of the TRiC complex components is knocked-down. The TRiC complex might be essential for the prevention of the abnormal folding of the long polyQ stretch in AGO2. When this complex is disturbed, the polyQ might aggregate and consequently the antiviral function of AGO2 might be compromised.

In order to test this hypothesis, we began to construct experimental tools. Different AGO2-GFP fusion plasmids have been generated, either with wild-type AGO2

sequences or with truncated version of this protein (N-term of AGO2 (polyQ) fused to GFP, or AGO2 (Δ-polyQ) fused to GFP.

Different groups including ours have already observed a confined and particular localization of *dm*AGO2 in unknown sub-cellular bodies. We indeed observe this pattern when the WT AGO2-GFP fusion construct was over-expressed.

Furthermore, we observe that the aggregation is greatly enhanced when the AGO2 polyQ domain is expressed alone. On the other hand, when this polyQ domain is deleted from the protein, AGO2 seems to completely lose its sub-cellular localization (data not shown). We next plan to analyze the cellular distribution of these reporter proteins when components of the Tric Complex are knocked-down.

2.2.2 Chromatin/Transcription regulation factors

A second family of proteins, present in the nucleus and known to be involved in chromatin remodeling and gene transcription regulation struck our attention: Pontin, Reptin, Baf and Hcf (Fig. 10). Reptin and Hcf were found in the RNAi interactome in all conditions (mock or infected), Pontin was found only in mock-infected conditions while Baf interaction with the RNAi components seem to be induced by DCV (Fig. 6 and 7, Table 1). The effect of the knock-down on the viral replication was different for these four proteins: whereas Baf affected only DCV replication (Fig. 10), Reptin and Pontin seem to affect negatively the replication of DCV and VSV and Hcf affects negatively all three viruses (Fig. 10, Table 2).

Knowing that these four proteins are involved in a very broad and fundamental mechanism such as gene transcription, the effect seen on the viral replication may be due to a mechanism unrelated to the antiviral immunity. Therefore the effect we observe may be indirect. Hence, it is important to further characterize the biochemical significance of the binding of these proteins with RNAi components.

Interestingly, Ruvb-like 1 and 2 the homologues of Pontin and Reptin in mammals, were found to bind to human Ago-2 (Ameyar-Zazoua et al., 2012). It is important nonetheless to note that in order to detect RuvBL1 and 2 interacting with *Hs* Ago-2, the authors of this study have isolated nuclei extracts before immunoprecipitating Ago-2. It

is therefore important to try to isolate the nuclear fraction of AGO2 in our drosophila S2 system; this might enrich the Co-IP with the nuclear partners of AGO2.

At this point all the hypotheses one can emit are therefore speculative, because the nature of the biochemical interactions between these nuclear proteins and the RNAi components is still not well defined.

Regarding the potential biological significance of such a response it is interesting to note that a recent publication claiming that antiviral immunity against viral persistence in Drosophila is governed by reverse transcription of virally derived RNAs and their integration in the host's DNA. This finding is paradigm shifting (Goic et al., 2013). Therefore, one should consider the possibility that proteins like Pontin and Reptin, involved in various DNA metabolism pathways, such as DNA repair and recombination (Huen et al., 2010), might be involved in a DNA based defense mechanism against viral element. Moreover, a small RNA response at DNA break ends have been reported in *Drosophila* (Michalik et al., 2012). It is tempting to speculate that Pontin and Reptin might be involved in the regulation of a DNA silencing response (Qi et al., 2006).

Concerning Baf and Hcf, it is important to note several things; first, Baf's interaction with Dcr-2 was induced specifically by DCV infection (Fig. 8), and the knock-down of its expression affected only DCV viral loads (Fig. 10). Second, Hcf was found to interact with Dcr-2, AGO2 and R2D2 constitutively, and the viral infections, in most cases (expect DCV 16h time point), did not seem to displace it from the network (Fig. 6 and 7). Moreover, knock-down of Hcf, was the only one that affected replication of all three viruses (DCV, FHV, VSV) (Fig. 10). Curiously, Hcf human homologues HCF1 and HCF2 were identified as IRF1 and IRF2 interactants, in the interferon network mentioned earlier (Li et al., 2011) (Fig. 3.5). This is intriguing since the Drosophila genome does not encode any Interferon Regulatory Factors (IRFs).

Importantly, both Hcf and Baf are known to be transcription enhancers. Mammalian HCF1 is a transcription co-activator, recruited to specific DNA promoters (Vogel and Kristie, 2000; Whitlow and Kristie, 2009). Baf is a DNA-bridging protein, facilitating the physical clustering of transcription factors (Singhal et al., 2010).

Taken together, these observations, suggest that these two proteins (Hcf and Baf) might be involved in the parallel inducible antiviral response in Drosophila. In this case the viral RNA sensors (e.g. Dcr-2) might not transmit the message to the nucleus through messengers (e.g. IRFs in the mammalian systems), but they would rather interact directly with transcription regulators (Baf or Hcf). It would therefore be very interesting to

test if the depletion of these two genes would affect the induction of antiviral inducible genes like *vago*.

2.2.3 Nucleo-cytoplasmic transport proteins

Three genes involved in the nucleo-cytoplasmic transport showed strong and significant effects on viral replication (Table 2, Fig. 10). Two Nuclear Protein Complex (NPC) proteins, namely Nup214 and Nup358, and one Ras Superfamily members, RanGap.. These three proteins interact with Dcr-2, AGO2 and R2D2. Interestingly, the presence of two of them (RanGAP, and Nup214) was induced by the viral challenge, hinting at an active process. Interestingly, while the silencing of the three of them affects by at least two-folds the replication of DCV and VSV, only the knock-down of RanGap affects the replication of FHV (Fig. 10). This makes these three proteins direct or indirect players in the control of the viral loads. Interestingly, some viruses are known to express virulence factors that interfere with the nucleo-cytoplasmic transport. For example, the Influenza A NS1 protein, a major virulence factor, has been shown to target the RNA the NPC (Kuss et al., 2013).

However, in our case, the questions remain: why do we detect these proteins in the siRNA interactome? And how do they affect viral loads?

Many reports place these proteins at the cytoplasmic interface of the NPC (Köhler and Hurt, 2007). Intriguingly these proteins have been shown to be involved in HIV DNA import, RNA export and both protein import and export (Hutten and Kehlenbach, 2006; Rodriguez et al., 2012; Wälde and Kehlenbach, 2010; Zhang et al., 2010) .The existing literature on the role of these proteins in nucleo-cytoplasmic transport is rather contrasted. Therefore, no clear picture of how these proteins would control the viral loads can be drawn at the moment. We, hereafter, emit different hypotheses that might explain the observed phenotype and we propose some experiments to address their validity.

The first hypothesis would be that these proteins control the nuclear import of AGO2, R2D2 and Dcr-2 (Cernilogar et al., 2011; Wälde and Kehlenbach, 2010). This model would imply that the nuclear function of the siRNA pathway contribute to antiviral immunity (Goic et al., 2013).The weak points of this model is that no nuclear antiviral role of AGO2, Dcr-2 or R2D2 have been observed to date, and we detected no Importin

Fig 12 **Genes with unkown function showing a phenotype in the screen**

A) Viral loads of DCV, FHV and VSV upon the knock-down of indicated genes B) Uniprot predicted domains of CG7816,CG11107 and CG6453. *ns*: non significant. Bars without a *ns* label show a P-value<0.05

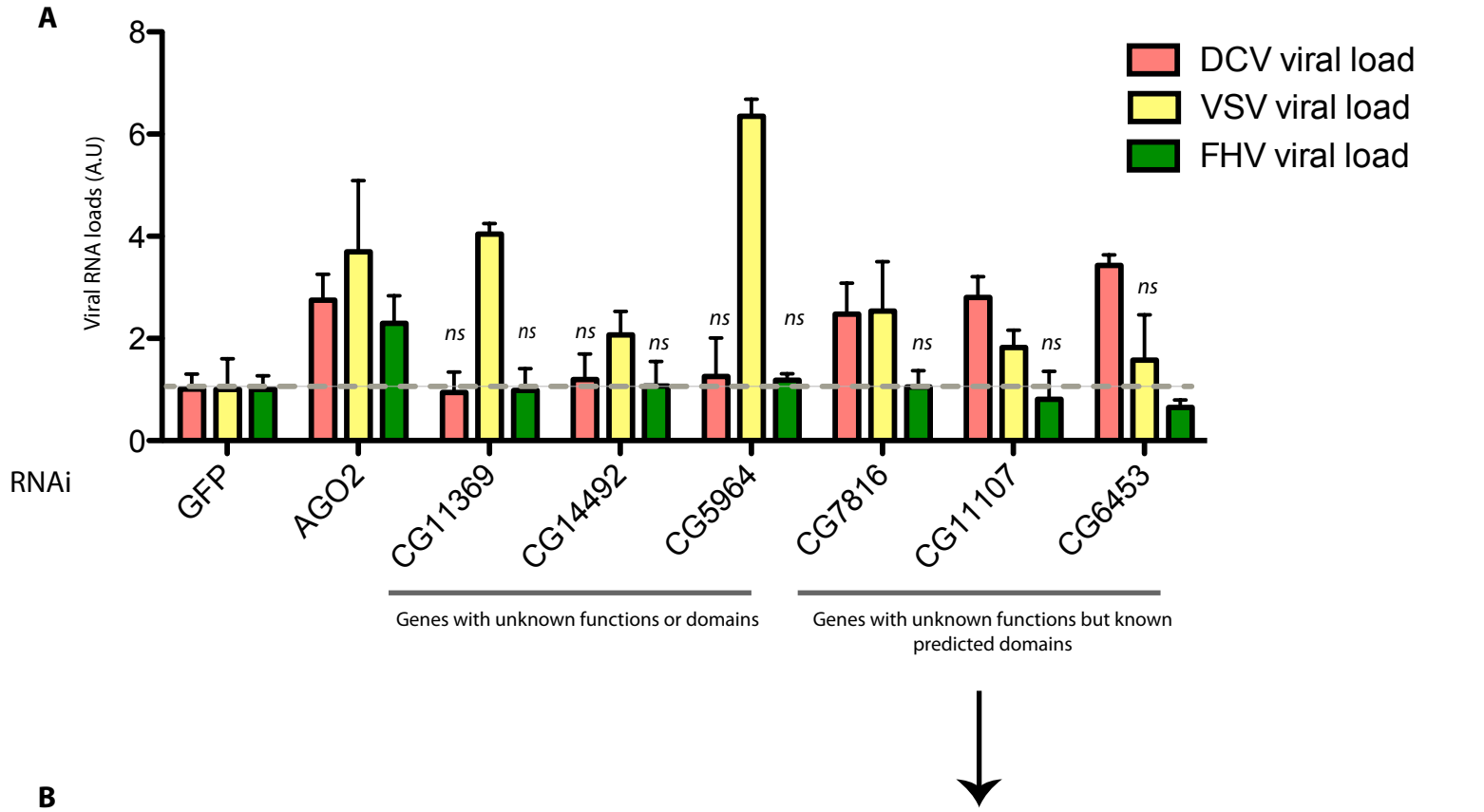

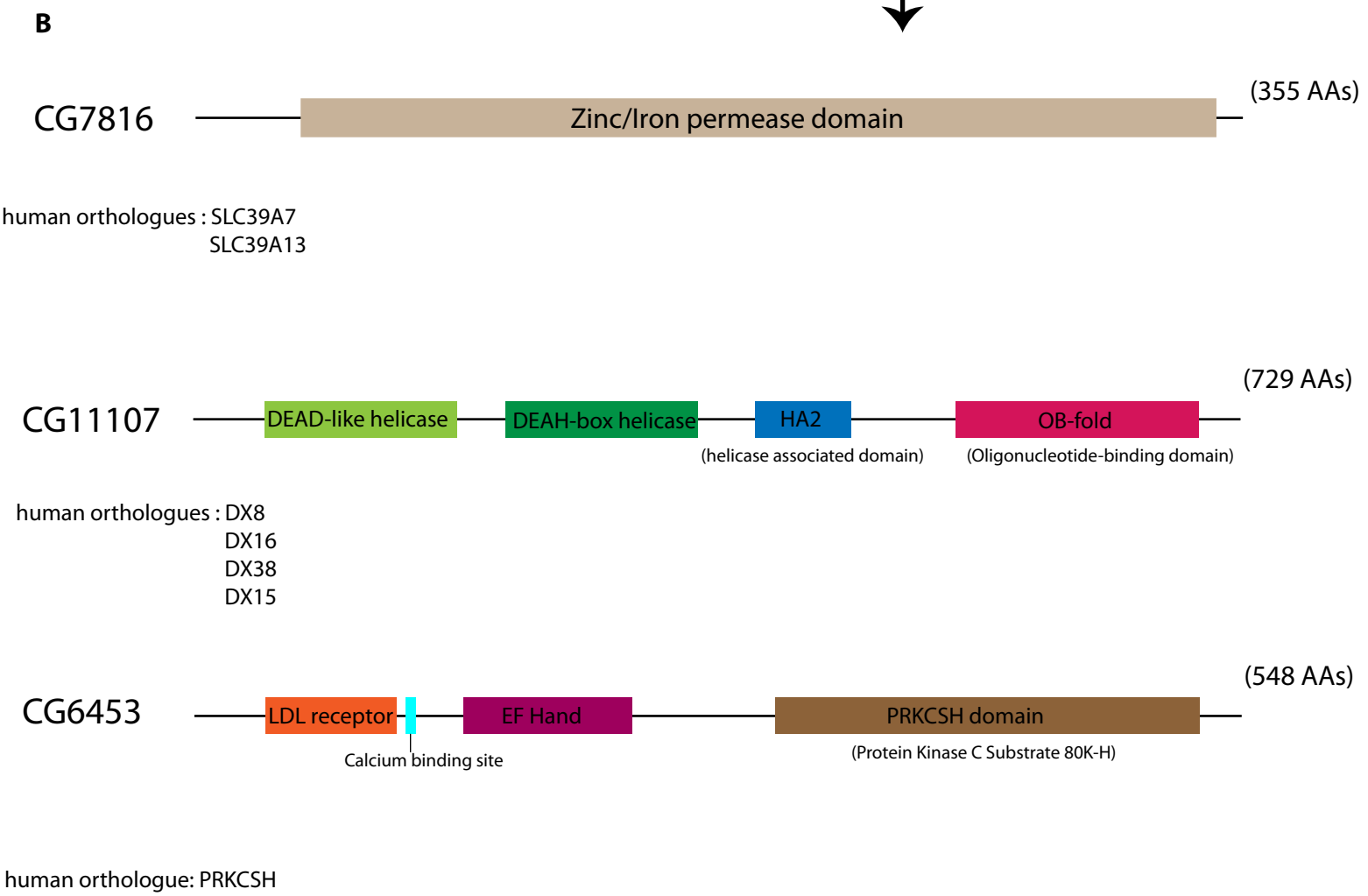

bound to AGO2, Dcr-2 and R2D2. This model can be nevertheless tested by different experiments. For instance, the cellular localization of AGO2, Dcr-2 or R2D2 can be carefully tracked upon Nup358, Nup214 or RanGap knock-down .

The second hypothesis, is that these proteins are important for the export of some antiviral small RNAs, the RISC complex would then get loaded with these RNAs at a perinuclear region. Intriguingly, Dcr-2 have already been observed by other members of the laboratory in peri-nuclear regions in some specific tissue (data not shown, Carine Meignin personal communication). If such a model is correct, this would then explain the interaction that AGO2, Dcr-2 and R2D2 might have with the cytoplasmic interface of the NPC (Nup214, Nup358 and RanGap). In this context, it is important to remention the recent study claiming that some virally derived small RNAs, transcribed from DNA in the nucleus, are important in the antiviral immune response in drosophila (Goic et al., 2013). Many experiments can be performed to assess the involvement of Nup358, Nup214 and RanGap in the specific export of such small RNAs.

The third and last explanation we imagine is that the effect we see on viral replication is completely indirect and results from a profound alteration in the cellular physiology when these important molecules are knocked-down. As the identified Nups and Ran/Gap are essential for the export of many mRNAs, a lot of different pathways can be affected, including the siRNA pathway. Interestingly, a report describes that the mammalian Dicer mRNA is exported through Exportin-5 (Bennasser et al., 2011). Therefore the effect we see on the viral replication when these proteins are knocked-down (RanGap, Nups) might be due to a inhibition in the export of some important cellular mRNAs, including Dcr-2 mRNA.

2.2.4 Genes with unassigned functions in Drosophila.

One of the most representative protein families corresponded to genes with unassigned functions (CG14492, CG5964, CG11369, CG11107, CG6453 and CG7816). CG14492, CG5964 and CG11369 affected only VSV replication (Fig. 12), these genes have unknown protein domains and seem to be drosophila specific.

Two other genes (CG11107 and CG6453) with unknown function but known protein features/domains affected DCV specifically: CG11107 contains a DEAD/DEAH box helicase domain and an ATP-binding domain; this gene has 4 human orthologues

Figure 13 - Heat-shock cognate proteins and infection A- Phylogenetic tree and multuple alignment of Hsc70s amino acid sequences with Clustal Omega
B- Interaction pattern of Hsc70s with AGO2, Dcr-2 and R2D2 upon viral infection
C- Effect of Hsc70s knock-down on viral loas.

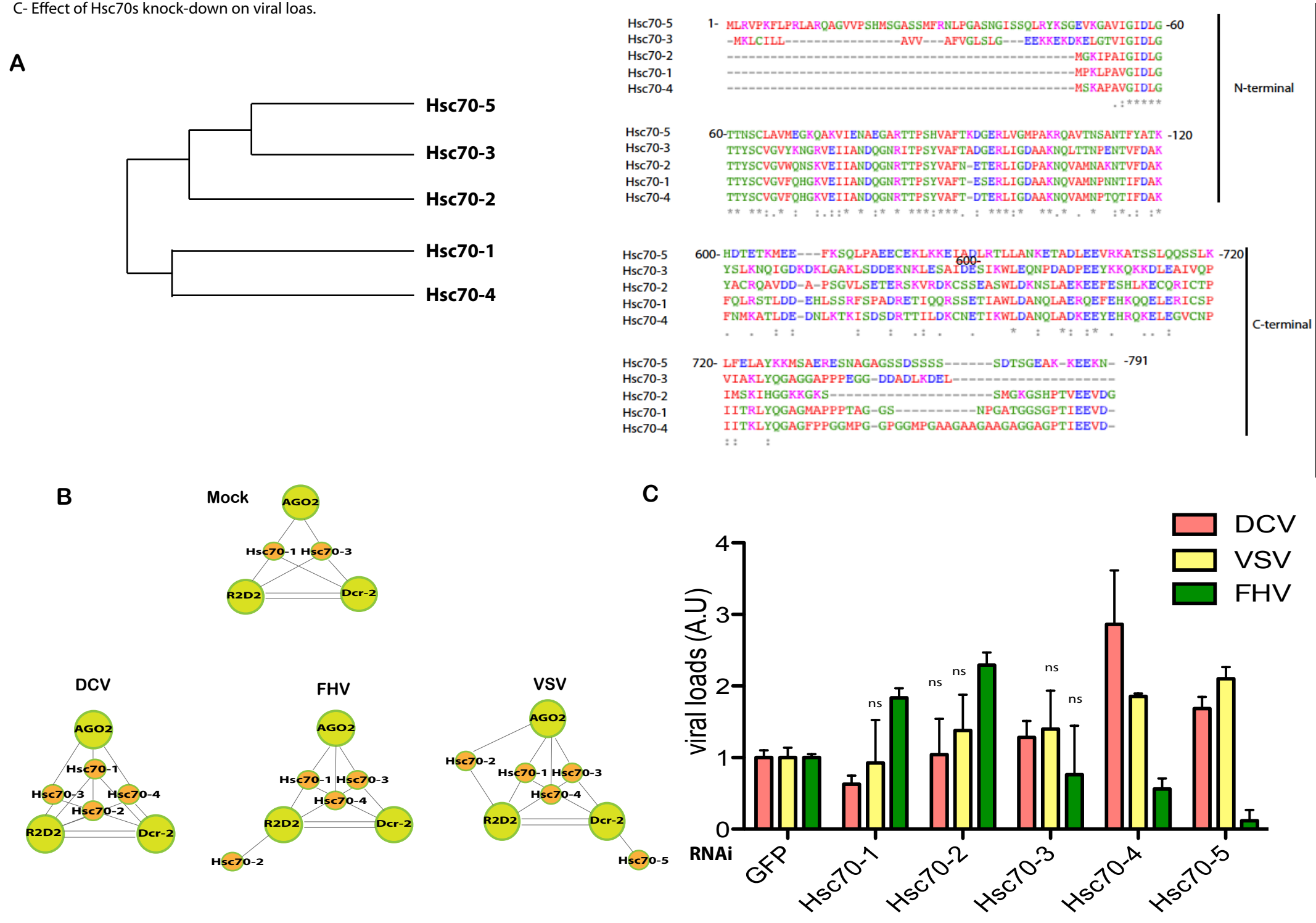

(DX8, DX15, DX16, and DX38). CG6453 contains many different domains including an EF-hand like domain; a Calcium binding site and a LDL receptor domain, this gene has one human orthologue called “protein kinase C substrate 80K-H“ or PRKCSH (Fig. 12). CG6453 have been tested in the lab *in vivo* thanks to a homozygous viable mutant line that was available. Preliminary survival data were encouraging, and these mutants seemed to succumb more rapidly to DCV infection with higher viral loads. Unfortunately, when the mutant line was crossed with a deficiency line the phenotype was lost, indicating that a secondary mutation was responsible for the observed phenotype. The other unknown genes would be worth investigating with new genetic tools (e.g. inducible shRNA with the Actin-Gal4; Gal80^{ts} system), because the homozygous mutant lines are unavailable.

2.2.5 Other classes of protein affecting viral replication

The heat-shock cognate-70 chaperones that are constitutively expressed (not necessarily induced by heat like Hsps) showed an interesting pattern. This family contains five proteins (Hsc70-1 to 5) that share an important amino acid sequence homology in the middle of their sequences (Fig. 13 A). Nevertheless, their N- and C-ter extremities slightly differ in their amino acid content. A phylogenetic tree generated after a Clustal Omega multiple alignment show that Hsc70-4 and Hsc70-5 are the most divergent (Fig.13A). These two proteins share nevertheless up to 52% of sequence identity when aligned pair-wise (data not shown).

We observed an interesting interaction pattern of these proteins with AGO2, Dcr-2 and R2D2 (Fig. 13B). Hsc70-1 and Hsc70-3 constitutively interacted with the three baits and were not displaced after viral infection. Hsc70-2 and Hsc70-4 joined the interactome when the cells were infected with all three viruses. Hsc70-5 was detected only when cells were infected with VSV. The depletion of these proteins affected mildly but significantly the viral replication (Fig. 13C). Depletion of both Hsc70-4 and Hsc70-5 increased DCV and VSV viral loads whereas the depletion of Hsc70-1 and Hsc70-2 affected positively only FHV replication (Fig. 13C). Intriguingly, the Hsc70-5 depletion decreased down to 90% FHV viral loads (Fig.13C). Interestingly however, consistent

with our data, different heat-shock chaperones have been shown to have either a positive or a negative effect on FHV replication (Weeks et al., 2009). Finally, our data suggest a substrate specific-role of these proteins, in light of their interaction with the Dcr-2, AGO2 and R2D2 upon viral infection. Importantly, studies relating Hsc70-3 and 4 to RNAi have already been published (Dorner et al., 2006). These proteins seem to be involved in the ATP-dependent RISC loading *in vitro* (Iwasaki et al., 2010). Therefore, investigating the specific role of Hsc70 proteins in antiviral defense is definitely a promising path.

3. Conclusion

Overall, the functional analysis of the siRNA pathway interactome reveals a number of putative novel players in antiviral immunity in Drosophila S2 cells.

Our observations and results lead us to the conclusion that the siRNA pathway components in drosophila are neither static, nor confined to a cellular compartment. We believe that different pools of Dcr-2, AGO2 and R2D2 complexes co-exist in the cell, and their function and localization might be dictated by their substrate choice. Our data indicate that the interactome analysis revealed a snapshot of all these different pools taken together.

Furthermore, our analysis showed the important role of the CCt/T-cp1 chaperonin family in the control of the viral loads. We emit the hypothesis proposing that this family of proteins might be involved in proper AGO2 folding. Our study also pinpointed an antiviral role for proteins with unknown functions or proteins involved in chromatin architecture, transcription regulation and nucleo-cytoplamsic transport. While some of these proteins affected different viruses (e.g. Hcf, RanGap), some were virus specific (Baf). Baf showed an interactant- and phenotype-specific pattern. This protein could therefore be a potential actor in the inducible antiviral response that co-exists with the broader siRNA mechanism. Finally, another protein behaving in a virus-specific manner elicited our curiosity, the Receptor of Activated protein C Kinase 1 (RACK1). RACK1 protein interacted with AGO2 and R2D2 specifically upon DCV infection and this protein seemed to be essential for DCV replication but not VSV or FHV (Table 2- Chapter 1, Fig. 10). In the second chapter of the thesis I describe how we addressed RACK1's specific proviral role.

III - Chapter 2 (Submitted Manuscript Draft)

Ribosomal protein RACK1 is a specific host factor required for IRES-mediated translation of fly and human viruses

Karim Majzoub[1], Mohamed Lamine Hafirassou[2,3], Yann Verdier[4], Carine Meignin[1,2], Stefano Marzi[5], Franck Martin[5], Hidehiro Fukuyama[1,6], Joëlle Vinh[4], Jules A. Hoffmann[1,2,7], Thomas F. Baumert[2,3,8,*], Catherine Schuster[2,3], Jean-Luc Imler[1,2,*]

[1]CNRS UPR9022, Institut de Biologie Moléculaire et Cellulaire, Strasbourg, France.

[2]Université de Strasbourg, Strasbourg, France.

[3]Inserm UMR1110, Institut de Virologie, Strasbourg, France.

[4]USR3149, ESPCI ParisTech, Paris, France.

[5]CNRS UPR9002, Institut de Biologie Moléculaire et Cellulaire, Strasbourg, France.

[6]INSERM Equipe Avenir, Institut de Biologie Moléculaire et Cellulaire, Strasbourg, France.

[7]Institut d'Etudes Avancées de l'Université de Strasbourg

[8]Pôle hépato-digestif, Hôpitaux Universitaires de Strasbourg, Strasbourg, France.

‡ To whom correspondence should be addressed: Thomas.Baumert@unistra.fr; JL.Imler@unistra.fr.

SUMMARY

Fighting viral infections is hampered by the scarcity of viral targets and their variability resulting in development of resistance. Viruses depend on cellular molecules for their life cycle, which are attractive alternative targets, provided that they are dispensable for normal cell functions. Using the model organism *Drosophila melanogaster*, we identify the ribosomal protein RACK1 as a cellular factor required for infection by the internal ribosome entry site (IRES)-containing virus *Drosophila* C virus (DCV). We further demonstrate that inhibition of RACK1 in human liver cells impairs hepatitis C virus (HCV) IRES-mediated translation and infection. Inhibition of RACK1 in *Drosophila* and human cells does not affect cell viability and proliferation, and RACK1-silenced adult flies are viable, indicating that this protein is not essential for general translation. Our findings demonstrate a specific function for ribosomal protein RACK1 in selective mRNA translation and uncover a promising target for the development of broad antiviral intervention.

INTRODUCTION

Viral infections are a significant threat for all living organisms. In humans, acute and chronic viral infections cause a wide spectrum of diseases, including life-threatening inflammation and cancer. A major challenge for the control of viral infections is that viruses, due to the small size of their genomes, offer few intrinsic targets either for recognition by the immune system or for inhibition by antiviral effector molecules. Furthermore, the error-prone viral polymerases allow RNA viruses to rapidly escape detection by the immune system and to resist the adverse effects of directly acting antiviral molecules. Significantly, viruses rely on numerous host factors for essential functions during their life cycle. These are not subject to rapid sequence changes and hence provide good alternative targets for antiviral therapy. Therefore, a central challenge is to identify cellular factors required for viral replication but dispensable for normal cell function.

RNA replication, transcription and translation are critical steps in the life cycle of RNA viruses, which involve interactions with host-cell molecules. In the model organism *Drosophila melanogaster*, the small interfering (si) RNA pathway targets viral RNAs. Indeed, flies mutant for the genes encoding the core components of this pathway, i.e. *Dicer-2*, *R2D2* and *Argonaute (AGO2)*, are more susceptible to viral infection than wild-type controls, and succumb with increased viral titers (Galiana-Arnoux et al., 2006; van Rij et al., 2006; Wang, 2006). Dicer-2 contains two RNase III domains and processes double stranded (ds) RNAs (e.g. viral replication intermediates) into 21 nucleotide (nt)-long siRNA duplexes. These are loaded onto AGO2, a central component of the RNA Induced Silencing Complex (RISC), and one of the strands (passenger strand) is discarded, while the other is used to guide the RISC towards complementary RNA molecules (e.g. viral RNAs; reviewed in (Ding, 2010; Galiana-Arnoux et al., 2006; van Rij et al., 2006; Wang, 2006)). The dsRNA binding protein R2D2 forms a heterodimer with Dicer-2 and helps directing it towards long dsRNAs (Cenik et al., 2011). In addition, R2D2 also participates in the loading of the siRNAs onto the RISC (Liu, 2003). Remarkably, several insect viruses have evolved mechanisms to counter the antiviral action of Dicer-2, R2D2 and AGO2 (Nayak et al., 2010; van Mierlo et al., 2012; van Rij et al., 2006; Wang, 2006; 2002). For example, the B2 protein from Flock House virus (FHV) binds dsRNAs and thus antagonizes Dicer-2 (Chao et al., 2005).

Two additional small RNA pathways have been described in flies, namely the Piwi interacting (pi)RNA pathway and the micro (mi)RNA pathway (reviewed in (Ghildiyal and Zamore, 2009; Ishizu et al., 2012; 2010)). They share with the siRNA pathway their requirement for small RNAs that direct Argonaute proteins (Piwi, Aubergine and AGO3 for piRNAs; AGO1 for miRNAs) towards their targets. Both the piRNA and siRNA pathways are important defense mechanisms against viruses and transposons (reviewed in (Ding, 2010)). On the other hand, the miRNA pathway is a fine-tuning mechanism modulating gene expression in both plants and animals (reviewed in (Bartel, 2009)). While the siRNA pathway is the main antiviral defense mechanism in plants, worms, and insects, no clear antiviral role has been assigned to the single Dicer protein encoded by mammalian genomes. Instead, an innate immune response based on interferon induction, together with adaptive immunity, mediates resistance to viral infections in vertebrates (Beutler et al., 2007). Interestingly however, viral infections can be modulated by miRNAs in mammals. Examples include viral miRNAs that regulate the transition from latent to lytic viral gene expression in large DNA viruses (e.g. Herpesviruses) (Umbach et al., 2008), and cellular miRNAs, such as the abundant hepatocellular miRNA miR122, required for efficient replication of hepatitis C virus (HCV) (2005).

Although the core components of the siRNA pathway have been well-characterized biochemically, *in vivo* studies are unveiling an added layer of complexity regarding their function and regulation (e.g. (Cernilogar et al., 2011; Marques et al., 2009; Okamura et al., 2009)). In particular, AGO2 and Dicer-2 appear to carry functions independent from RNA interference in some contexts *in vivo*. For example, AGO2, but not Dicer-2, regulates gene expression upon interaction with chromatin insulators (Moshkovich et al., 2011). Reciprocally, Dicer-2, but not AGO2, was shown to play a role in the induction of the antiviral molecule Vago upon viral infection in *Drosophila* or *Culex* mosquito cells (Deddouche et al., 2008; Paradkar et al., 2012). Hence, it is becoming apparent that in a physiological context, interaction of the core components of the siRNA pathway with cellular cofactors dictates their subcellular localization, and affects their substrate choice and function.

In order to gain insight into the protein environment of Dcr-2, R2D2 and AGO2 in the context of viral infections in *Drosophila*, and to identify novel host factors involved in the control of viral replication in this model organism, we have performed a proteomic

analysis of the complexes assembling around these three molecules in infected cells. The evolutionarily conserved ribosomal protein RACK1 copurified with AGO2 and R2D2 in cells infected by the picorna-like virus DCV, and we show here that this factor is mandatory for DCV replication, but largely dispensable for cell viability and proliferation. We further demonstrate that RACK1 is required for IRES-dependent translation in *Drosophila*, and in human hepatocytes, where this factor is an essential determinant of hepatitis C virus infection. Our data suggest that targeting RACK1 could effectively prevent HCV infection in hepatocytes, without affecting normal cell functions.

RESULTS

RACK1 copurifies with components of the siRNA pathway in DCV-infected cells

We performed a proteomic analysis of the siRNA pathway, which controls RNA virus infections in insects and interacts with viral RNA and associated proteins at crucial stages of the replication cycle (Figure S1)[1]. To identify the proteins interacting with the core components of the siRNA pathway, we used a biotin-tag affinity purification system, which allows high efficiency recovery of molecules expressed at physiological levels in *Drosophila* cells, using the exceptionally high affinity of avidin for biotin (de Boer et al., 2003). Dicer-2 (Dcr-2), R2D2 and AGO2 were tagged at the N- or C-terminus with a 15 amino-acid biotin-tag sequence, and stably expressed in a S2 derived cell line expressing the bacterial biotin ligase BirA3 (Fukuyama et al., 2012). Expression from the vectors is controlled by the baculovirus OpIE2 immediate early promoter, which is moderately active in *Drosophila* cells. BirA expressing cell lines transfected with the six expression plasmids (three proteins, tagged at their N- or C-terminal extremities) were selected for the interactome experiments. The tagged proteins and their associated partners were then extracted from cells either mock treated or infected by the RNA viruses DCV, FHV or Vesicular Stomatitis Virus (VSV). Samples (42 in total) were collected at the peak of viral production, and biotinylated proteins were recovered in single step affinity purification on Streptavidin coupled

[1] All data are available on PRIDE. Project name: 2012_DCV ; Accession numbers: 24806-24848 ;

FIGURE 1 RACK1 is required for DCV replication, but not for viability or proliferation in Drosophila cells.
(A) Interactome of Dcr-2, R2D2 and AGO2 in control and virus infected cells. A schematic representation of all detected interactions (merged data from non-infected, DCV-, FHV- and VSV-infected cells) is shown. The ribosomal proteins are shown in yellow. The dsRNA binding viral protein B2 is shown in blue. (B) Quantification by qRT-PCR of DCV viral RNA levels (top graph) and of cell numbers as estimated by DAPI staining (bottom graph) in cells treated with the indicated dsRNAs to induce silencing.The viability Z-scores indicated on the bars of the bottom panel are taken from (Boutros et al., 2004): a Z-score above 3 indicates that the depletion of the corresponding gene causes cell death. Cells treated with a dsRNA corresponding to GFP sequences are used as a reference. Data represent the mean and s.e.m. of at least three independent experiments. ns: non significant; * p<0.05.

A.

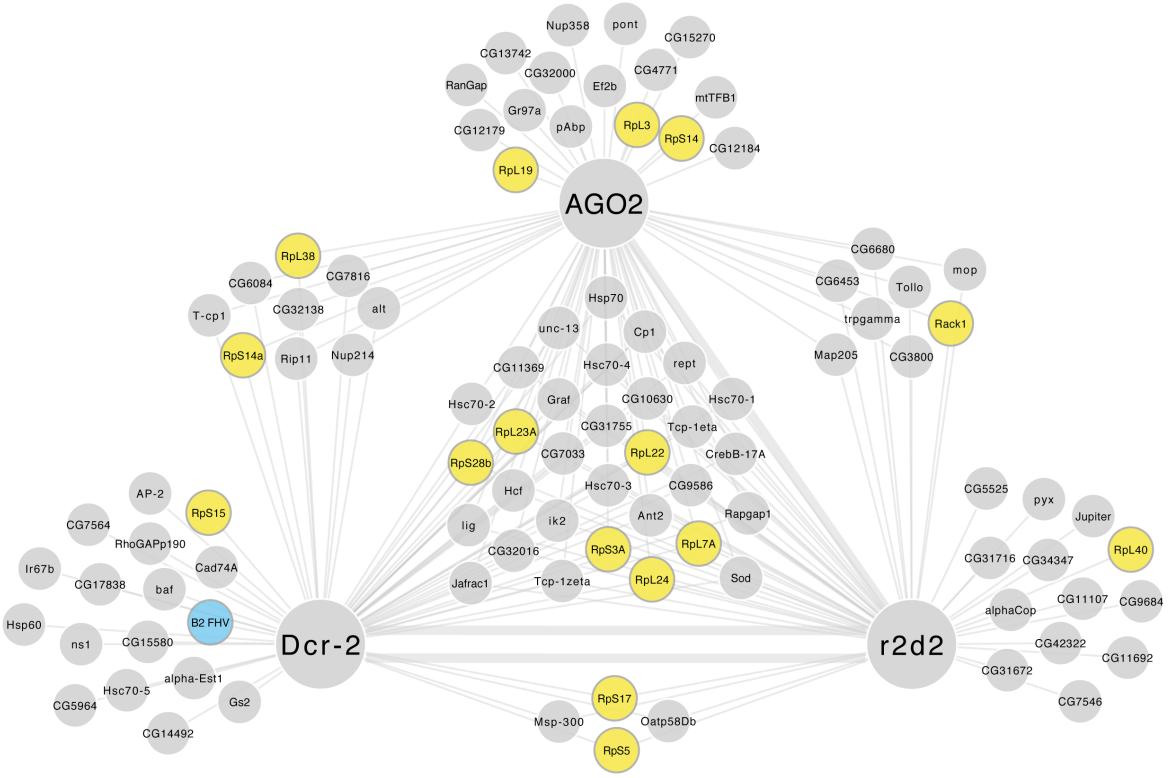

B.

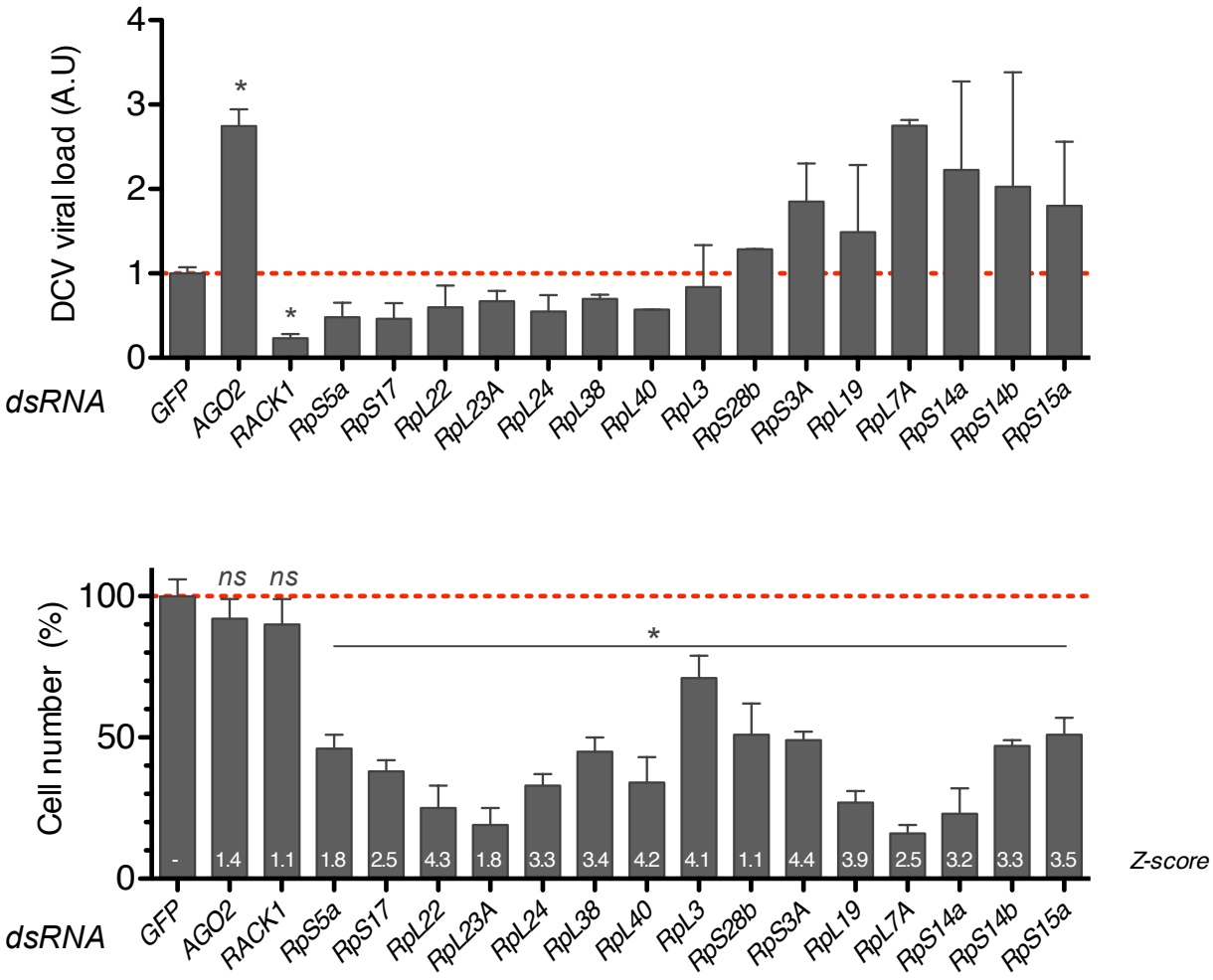

beads. The pulled down proteins were digested with trypsin and processed by NanoLC-FT ICR mass spectrometry (Figure S1) (Fukuyama et al., 2012).

We identified a total of 101 proteins interacting with Dcr-2, R2D2 or AGO2 in S2 cells, either non infected or challenged by DCV, FHV or VSV (see Figure 1A, Table S1). The cellular extracts were not treated with RNase, allowing the copurification with the protein baits Dicer-2, R2D2 and AGO2 of RNA-bound molecules. Examples include the viral suppressor of RNAi B2 from FHV, which competes with Dicer-2 for binding to dsRNA (Chao et al., 2005), and the recently described cellular dsRNA binding protein Blanks (Gerbasi et al., 2011) (Figure 1A). Among these RNA interacting proteins, we recovered 16 ribosomal proteins, of which RACK1 and RpS28b were only found in cells infected by DCV (Table S1).

RACK1 is required for *Dicistroviridae* infection of *Drosophila* cells

To address the functional relevance of this finding, we systematically depleted the 16 ribosomal proteins from S2 cells by RNAi, and tested DCV replication. Knockdown of most ribosomal genes affected cell viability or proliferation and did not yield interpretable results with regards to DCV infection (Figure 1B). By contrast, depletion of RACK1 (Figure S2A) did not affect cell viability, but resulted in a significant decrease of DCV titer in infected cells. Furthermore, RACK1 silencing did not affect replication of either FHV or VSV (Figure 2A,B), indicating that the RACK1-depleted cells are not only viable and able to proliferate, but can also support replication of other viruses. To test whether the effect of RACK1 was specific to DCV, or to the family to which it belongs, we infected cells with Cricket Paralysis Virus (CrPV), another member of the *Dicistroviridae* family. Replication of CrPV was also strongly impaired when RACK1 was depleted (Figure 2B).

We next confirmed these findings *in vivo*. RACK1 null mutant flies are not viable, indicating that RACK1 exerts developmental functions (Kadrmas et al., 2007). In agreement with this finding, silencing RACK1 expression with an shRNA driven by the broadly active *actin5C* promoter was embryonic lethal. When the thermosensitive Gal80 system was used to express the shRNA only in adult flies, development occurred normally and the adult flies expressed significantly reduced levels of RACK1 at the permissive temperature of 29°C (Figure 2C). The reduced levels of RACK1 did not affect the viability of the flies, although it reduced longevity by 20% at this temperature.

FIGURE 2. RACK1 is required for replication of DCV and CrPV, but not FHV and VSV

(A, B) S2 cells were treated with either control (GFP) or RACK1 dsRNA for 4 days, before challenge with DCV, FHV, VSV or CrPV. Viral infection was monitored by immunofluorescence 16h later using antibodies recognizing capsid proteins (A) or qRT-PCR (B).
(C) Silencing of RACK1 expression in transgenic flies expressing a small hairpin (sh) RNA targeting the 5' UTR from the RACK1 gene, using the Gal4-UAS system and the broadly expressed actin-Gal4 driver controlled by the thermosentitive (TS) tub-Gal80 repressor. A shRNA targeting the mCherry protein was used as a control. The life span of RACK1 depleted flies is shown in the bottom graph.
(D) RACK1 silenced flies infected by DCV after 5 days at 29°C show a decrease of the viral RNA and protein, as indicated by qRT-PCR and western blot. Data represent the mean and s.e.m. from at least three independent experiments.
ns: non significant; dpi: days post-infection; * p<0.05; ** p<0.01; *** p<0.001.

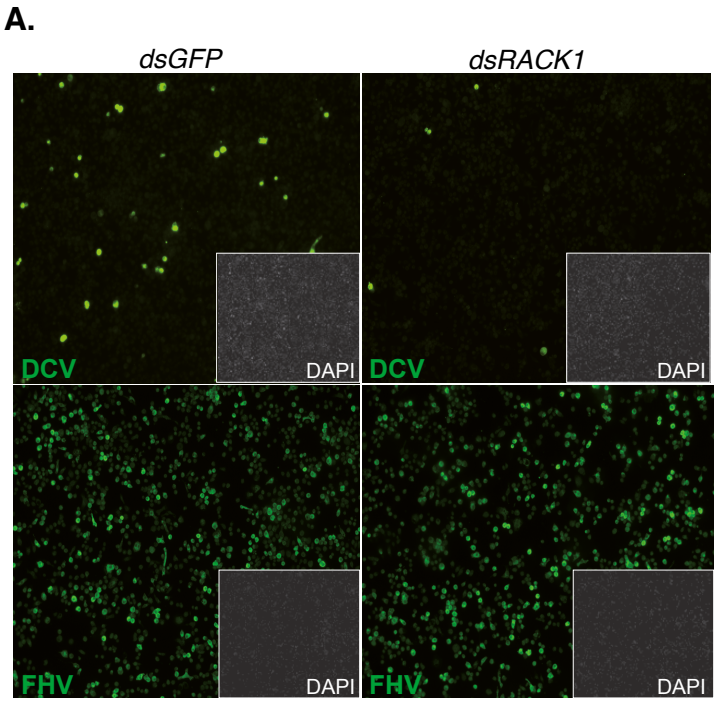

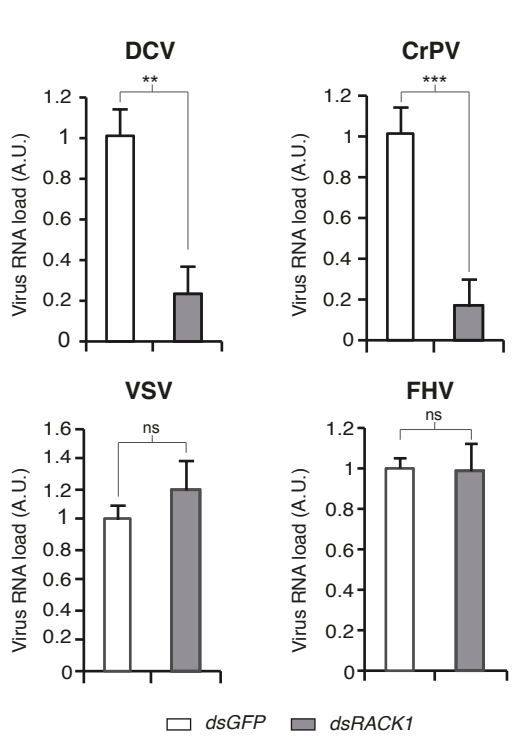

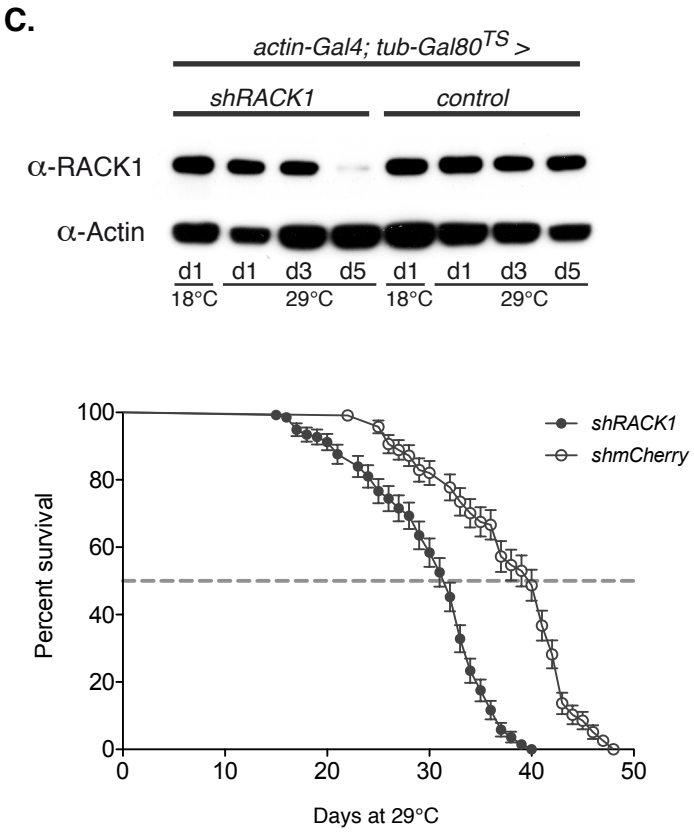

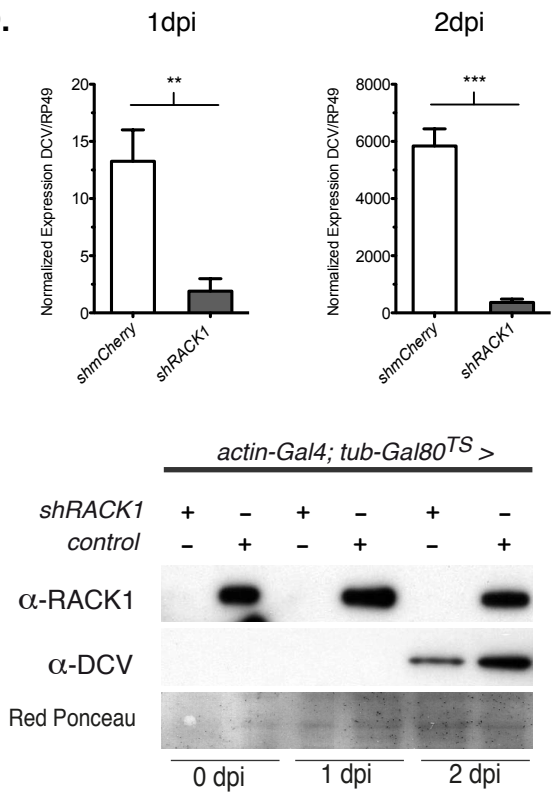

In addition, the eggs laid by RACK1-silenced females showed a phenotype similar to that of RACK1 mutants (Figure S2B) (Kadrmas et al., 2007). Thus, even though RACK1 is required during development, it appears to be largely dispensable in adult flies. As expected, when these flies were challenged with DCV, both viral RNA and capsid protein levels were reduced at 1 and 2 days post-infection compared to controls (Figure 2D). Overall, our data indicate that replication of the *Dicistroviridae* DCV and CrPV requires the ribosomal factor RACK1, which is otherwise dispensable for the viability of S2 cells and adult flies.

RACK1 is required for viral IRES-dependent translation

Our data indicate that RACK1 is required for a step of viral replication specific to *Dicistroviridae*. Whereas VSV and FHV use a canonical strategy of cap-dependent initiation of translation, DCV RNA recruits the 40S ribosomal subunit through IRES sequences to initiate its translation. Furthermore, although initially identified as a scaffolding protein involved in protein kinase C signaling, RACK1 is now recognized as a component of the 40S subunit of the ribosome (Coyle et al., 2009; Rabl et al., 2011; Sengupta et al., 2004). This suggested to us that RACK1 was required for viral translation. We first verified that RACK1 is indeed required at the ribosome level for CrPV replication. We silenced RACK1 expression in a stable cell line using an shRNA targeting the 5' untranslated region (Figure S2C), and observed a marked decrease in CrPV replication (Figure S2D). Transfection of a vector expressing wild-type RACK1 restored CrPV replication in these cells (Figure 3A). By contrast, expression of mutant proteins unable to interact with either RpS17 (D108Y) (Kuroha et al., 2010) or 18S rRNA (R38D/K40A) (Coyle et al., 2009) did not rescue CrPV replication (Figure 3A). We conclude that RACK1 is required in the 40S ribosomal subunit for CrPV replication.

To confirm that RACK1 is involved in translation from *Dicistroviridae* RNAs, we quantified the viral RNA present in polysomes from control S2 cells and from RACK1-silenced derivatives of these cells (Figure S2C). Ribosomes and polysomes from both cell lines were isolated through sucrose gradient centrifugation, and RNA was precipitated and analyzed by qRT-PCR. Depletion of RACK1 did not affect the amounts of *actin5C* mRNA, or of FHV RNA, in the polysome fractions (Figure 3B), in agreement with the observation that neither cell viability nor FHV replication is affected in the absence of RACK1. By contrast, a dramatic reduction of CrPV RNA was observed in

FIGURE 3. The ribosomal protein RACK1 is required for IRES-mediated translation.

(A) Stable S2 transformants expressing a shRNA targeting the 5' UTR of RACK1 were transfected with vectors expressing three versions of RACK1 (WT, R38D/K40E or D108Y). Expression of the transfected RACK1 was monitored by western blot using an antibody recognizing the N-terminal tag HA. The cells were infected with CrPV for 16h, and viral RNA loads were determined by qRT-PCR. Data represent the mean and s.e.m. from three independent experiments. The insert shows the position of the RACK1 residues R38, K40 (as green densities) and D108 (as cyan density) involved in interaction with the 40S subunit. ns: non significant; ** p<0.01. (B) Quantification of viral mRNA in polysomes from control (brown) vs RACK1-depleted (blue) cells. (C) RACK1 is required for translation regulated by the 5' IRES, but not the intergenic (IGR) IRES, of CrPV. The genome organization of CrPV is shown at the top. S2 cells were treated with dsRNAs corresponding to GFP (control), AGO2, eIF4E or RACK1 dsRNA for 3 days, before transfection of the indicated Luciferase reporters (5'CAP, IRESCrPV-IGR or IRESCrPV-5'). Luciferase activity was monitored 48h later. The ratio of the activity of the IRES-dependent luciferase and the 5' cap-dependent luciferase is plotted and normalized to the control for the three reporters. Data represent the mean and s.e. from six independent experiments. ns: non significant, * p<0.05, ** p<0.01.

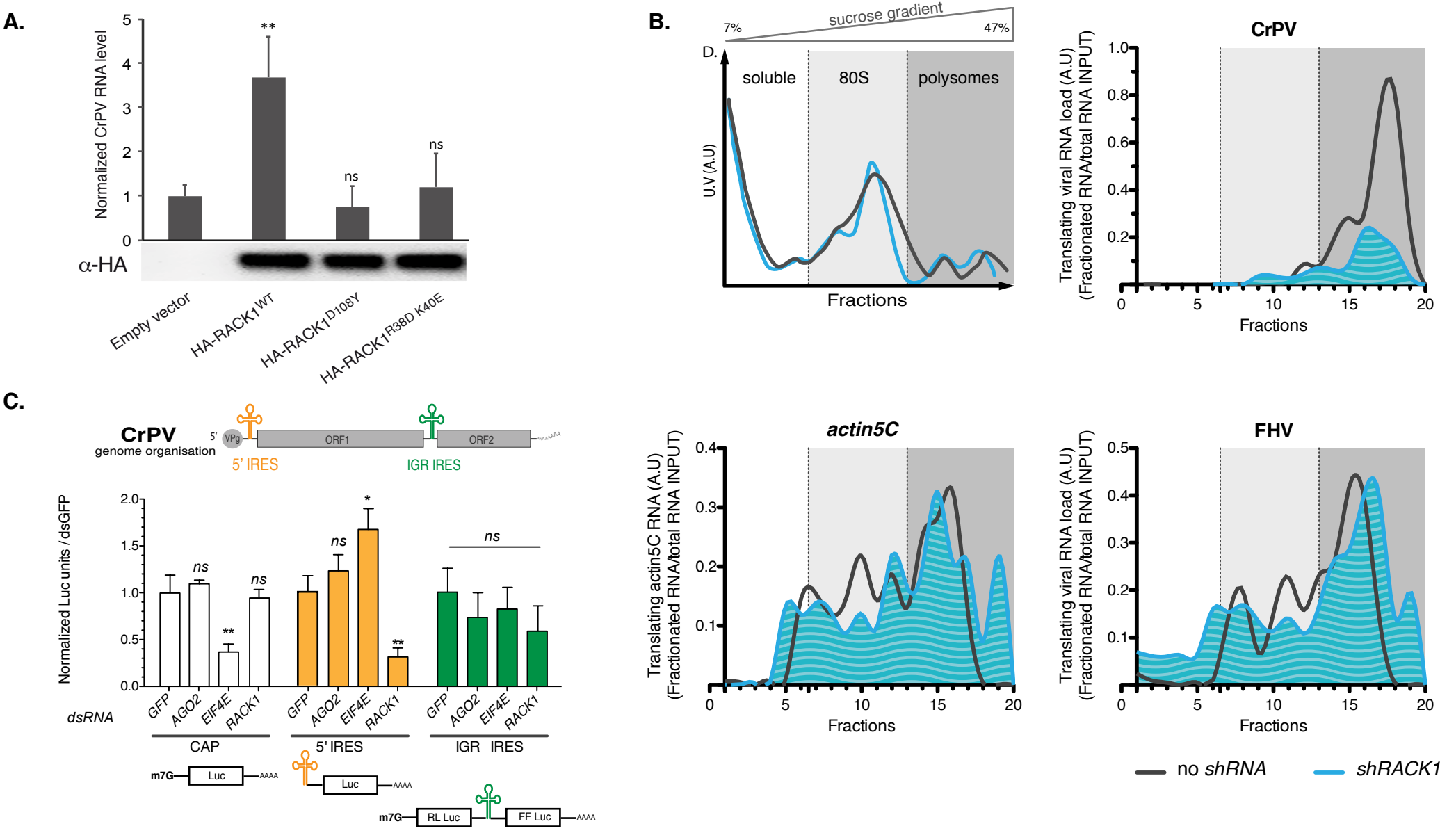

the polysome fraction when RACK1 was silenced (Figure 3B). Similar results were observed with DCV (data not shown). These results highlight the involvement of RACK1 in the translation of *Discistroviridae*.

Finally, we tested whether depletion of *RACK1* affected translation of Luciferase reporters placed under the control of the two IRES elements from CrPV (Figure 3C). Translation of a 5' cap-dependent RNA was not affected in the absence of RACK1, although it was affected when expression of eIF4E was knocked down. A significant reduction of translation was however observed for the 5' IRES reporter in RACK1 silenced cells. By contrast, translation driven by the intergenic (IGR) IRES (Jan and Sarnow, 2002; Spahn et al., 2004) was not affected by the level of RACK1 in the cells (Figure 3C).

RACK1 is an essential host factor for HCV infection

RACK1 is an evolutionarily strongly conserved factor, and we asked whether it plays a role in the translation driven by the IRES of a mammalian virus. To address this question, we chose hepatitis C virus (HCV), a major cause of liver disease and hepatocellular carcinoma with still unsatisfactory treatment options. HCV is a positive strand RNA virus member of the *Flaviviridae* family depending on a highly structured IRES for its translation (Spahn et al., 2001). Transfection of an siRNA targeting RACK1 markedly reduced expression of the protein in Huh7.5.1 cells, a hepatic cell line highly permissive for HCV infection (Figure 4A) (Lindenbach, 2005). Infection of RACK1-depleted Huh7.5.1 cells by cell culture-derived HCV (Jc1 strain) was strongly and significantly reduced, as revealed both by immunodetection of the viral core protein (Figure 4A) and the focus forming assay (Figure 4B). A similar inhibition of infection was observed for HCV Luc-Jc1, a well-characterized recombinant virus expressing a Luciferase reporter (Figure 4C). Inhibition of RACK1 was as efficient as the silencing of the key HCV host factors CD81 (Dorner et al., 2011) and Cyclophilin A (CypA) (Galiana-Arnoux et al., 2006; Kaul et al., 2009; van Rij et al., 2006; Wang, 2006) (Figure 4B,C). RACK1 silencing did not affect infection of cells by adenovirus-5, which does not use IRES-dependent translation (Figure 4D). We next depleted RACK1 in Huh7.5.1 cells containing the replicating reporter virus HCV Luc-Jc1, and observed a marked impairment of HCV replication (Figure 4E), demonstrating that RACK1 is required for HCV translation/replication rather than entry. Importantly, RACK1-specific siRNAs did

Figure 4. RACK1 is a specific host-factor required for IRES-mediated translation of HCV.
(A-D) Huh7.5.1 cells were transfected with siRNAs either control (siCTRL) or targeting RACK1 (siRACK1), CD81 (siCD81), Cyclophylin A (siCypA), HCV IRES (siHCV) or ribosomal protein RSP3 (siRibo), before infection three days later with HCV Jc1 (B), HCV Luc-Jc1 (C) or luciferase encoding adenovirus (D). Viral infection was monitored 3 days post-infection, by immunoblotting using antibodies recognizing HCV core protein (A); by counting foci forming units (ffu/ml) (B); or by quantifying luciferase activity (C, D). (E) HCV Luc-Jc1 replicating cells were transfected with siCTRL, two different siRNAs targeting RACK1 (siRACK1-1 and -2) or siCypA, and replication was monitored during 5 days by luciferase activity quantification. (F) Cell viability was measured during 5 days using MTT assay. (G, H) Huh7.5.1. cell lines stably expressing an IRES (IRESHCV-Luc) or a 5' cap-translated (CTRL-Luc) luciferase reporter gene (G) were transfected with siCTRL, siRACK1, siHCV or siRPS3. Translation was monitored 72h later by luciferase activity quantification. ** p<0.01; *** p<0.005.

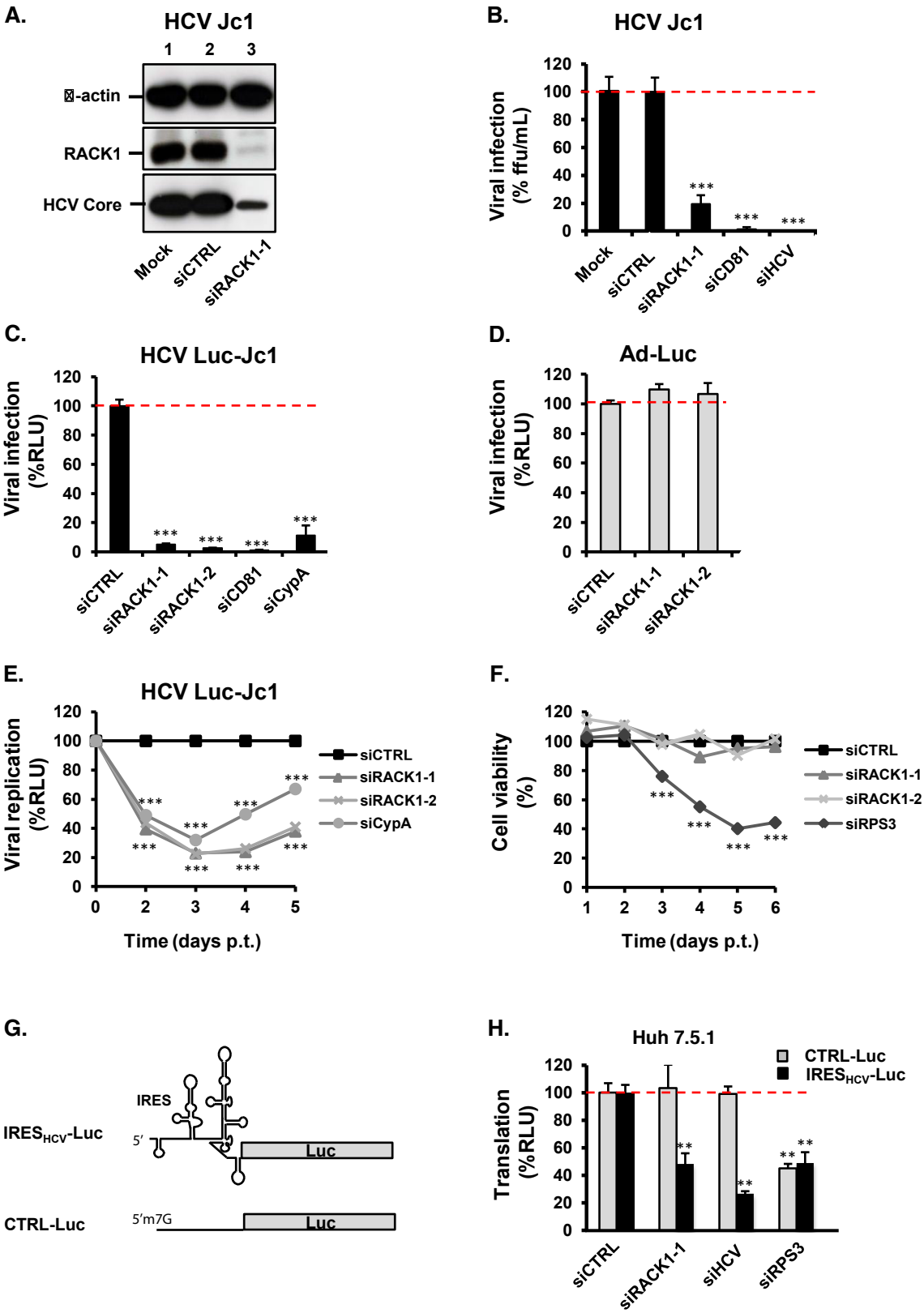

not affect cell viability, in contrast to silencing of the ribosomal protein RPS3 (Figure 4F).

To confirm that the inhibition of HCV replication is indeed mediated by the effect of RACK1 on IRES-mediated translation, we established stable cell lines expressing an $IRES_{HCV}$-luciferase reporter construct (Ding, 2010; Galiana-Arnoux et al., 2006; van Rij et al., 2006; Wang, 2006; Wolf et al., 2008) or a classical capped reporter gene (Figure 4G), and transfected these cells with RACK1-specific siRNAs. Silencing of RACK1 markedly and specifically decreased $IRES_{HCV}$-dependent translation, to a similar extent as an antiviral siRNA directed against the $IRES_{HCV}$ (Figure 4H). By contrast, silencing of ribosomal protein RPS3 inhibited translation from both IRES- and 5' cap-dependent reporter constructs (Figure 4H).

The effect of RACK1 on viral translation is independent of the miRNA pathway

While this work was in progress, two groups reported a role for RACK1 in miRNA function in both the model organism *Caenorhabditis elegans* and humans (Cenik et al., 2011; Jannot et al., 2011; 2011). Expression in S2 cells of two previously described miRNA reporters, *Par-6* and *nerfin-1* (Eulalio et al., 2007; Liu, 2003), was derepressed when RACK1 was silenced, indicating that in *Drosophila* as well, RACK1 can regulate miRNA function (Figure 5A,B). We note however that the derepression is much stronger for the miR1 reporter than for the miR9b reporter, suggesting that the role of RACK1 may be specific of a subset of miRNAs. By contrast, silencing of *Dcr-1* or *AGO1* derepressed equally well the two miR reporters (Figure 5A, B). To test whether miRNAs play a role in viral replication, we monitored accumulation of viral RNAs in cells depleted of *Dcr-1* or *AGO1*. Silencing of *Dcr-1* had no effect on the viral RNA load of the four viruses tested (Figure 5C). Silencing of *AGO1* did reduce to some extent CrPV and DCV RNA load. However, this reduction was variable in the case of DCV, and not to the extent of the reduction observed when *RACK1* is silenced for DCV and CrPV (Figure 5C). Thus, although the miRNA pathway may have a contribution in the replication of *Dicistroviridae*, our data suggest that the strong effect of RACK1 cannot be accounted for only by its effect on miRNA function. This was confirmed by the observation that silencing of *Dcr-1* or *AGO1* has no effect on translation driven by the $IRES_{CrPV\text{-}5'}$, unlike silencing of *RACK1* (Figure 5D).

FIGURE 5 The effect of RACK1 on viral translation is independent of the miRNA pathway

(A, B) RACK1 is required for miR1 and miR9b silencing. The structure of the Par-6 3' UTR and nerfin-1 3' UTR reporter constructs is represented on top, and the luciferase activity in cells silenced for the indicated genes is shown below. (C) Effect of the depletion of AGO1, Dcr-1 and RACK1 on replication in Drosophila S2 cells of CrPV, DCV, FHV and VSV. Cells were transfected with the indicated dsRNAs, and infected four days later. Viral RNA was extracted 24hpi, and quantified by qRT-PCR. (D) Silencing of AGO1 or Dcr-1 does not affect the activity of a Luciferase reporter gene controlled by the IRESCrPV-5' in Drosophila S2 cells. (E) Silencing of RACK1 affects the activity of the IRESHCV-luciferase reporter in miR122 deficient HEK-293T cells. Data represent the mean and s.e.m. of at least three independent experiments. ns: non significant; * p<0.05; ** p<0.01, *** p<0.001.

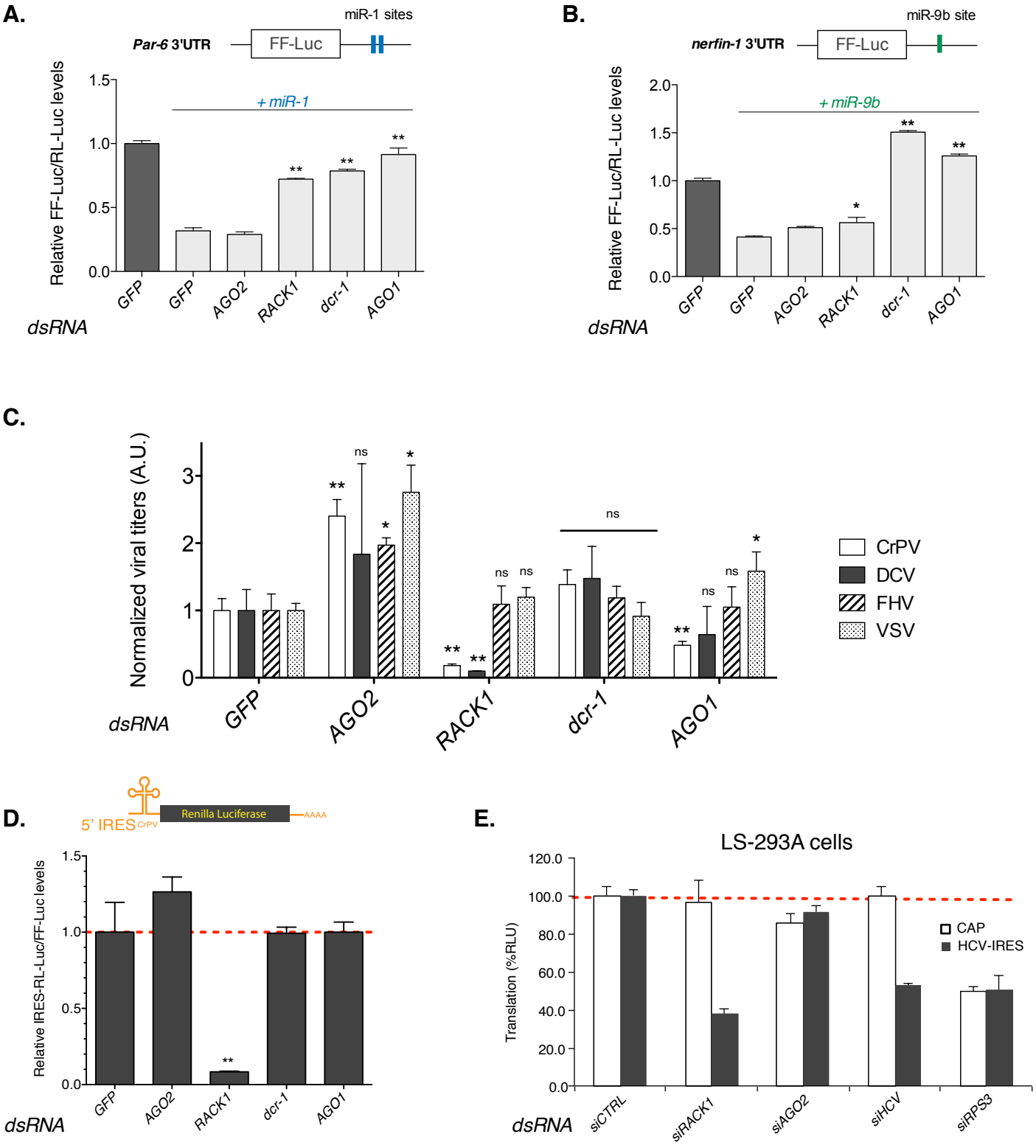

In mammalian hepatocytes, HCV translation depends on AGO2 and miR122 (Nayak et al., 2010; Roberts et al., 2011; van Mierlo et al., 2012; van Rij et al., 2006; Wang, 2006; 2002; 2013a). To determine whether the contribution of RACK1 to HCV translation was dependent on miR122, we turned to HEK-293T cells, which do not express this miRNA ((Chao et al., 2005; 2012a), Figure S3). Silencing RACK1 in these cells efficiently repressed translation driven by the $IRES_{HCV}$, suggesting that RACK1 and miR122 affect HCV translation by different mechanisms (Figure 5E). Thus, the role of RACK1 on $IRES_{HCV}$-dependent translation does not depend on miR122.

The position of RACK1 in the 40S subunit is consistent with an active role in HCV translation

To further characterize the involvement of RACK1 in $IRES_{HCV}$-mediated translation, we performed structural modeling analysis. Previous cryo-electron microscopy studies have highlighted the interaction of the 40S subunit with the HCV IRES, and have shown that binding of the HCV IRES triggers a pronounced conformational change in the small subunit of the ribosome (Ghildiyal and Zamore, 2009; Ishizu et al., 2012; Spahn et al., 2004; 2001; 2010). HCV IRES has been also visualized on the 80S human ribosome and RACK1 localized in its vicinity (Boehringer et al., 2005; Ding, 2010; Sengupta et al., 2004). The recent solving of the crystal structure of the small subunit of the ribosome at 3.9Å (Bartel, 2009; Rabl et al., 2011) and of the whole 80S at 3Å (Ben-Shem et al., 2011; Beutler et al., 2007) allows us to analyze the position of RACK1 in the 40S subunit in the absence or presence of the HCV IRES with pseudo-atomic details. RACK1 is located in close proximity to the IRES of HCV (Figure 6A). Although no direct contacts between RACK1 and $IRES_{HCV}$ could be observed, a recent study indicates that a peripheral domain of the translation initiation factor eIF3, which is required for $IRES_{HCV}$-dependent translation (Kieft, 2008; Umbach et al., 2008), is in contact with RACK1 (Figure 6B) (2005; 2013b). This domain may be the functional link between RACK1 and $IRES_{HCV}$-dependent translation. Furthermore, the conformational change triggered upon $IRES_{HCV}$ binding affects the region where RACK1 is located, supporting a functional link between $IRES_{HCV}$ and RACK1 (Figure 6A). By contrast, the $IRES_{CrPV\text{-}IGR}$, which does not depend on RACK1 (Figure 2C), interacts with a distinct site of the 40S subunit, directly contacting RpS25 (Figure 6C)

Figure 6 The position of RACK1 in the 40S subunit supports a role in HCV translation.

(A) Fitting of the atomic model of the 40S and IRESHCV to the 40S-IRES cryo-electron microscopy structure. The atomic model of the human 40S ribosome (pdb 3J3A and 3J3D (Anger et al., 2013)) and IRESHCV was fitted onto the cryo-electron microscopy density map of the complexes IRESHCV-40S at 20Å resolution (Spahn et al., 2001). RACK1 is in red, the 40S subunit in light transparent brown, and IRESHCV in blue. Other ribosomal proteins close to HCV IRES are in yellow (RpS17, RpS0, RpS26, RpS14, RpS5 and RpS28). RpS25 is in green. The changes on the 40S structure, observed upon IRESHCV binding, are in blue on the density map, close to RACK1. Information on IRESHCV model building and fitting are provided in the supplementary material.
(B) Cryo-electron microscopy structure of the 43S translation initiation complex (emd-5658; (Hashem et al., 2013)). 40S ribosomal subunit density is in light transparent brown, fitted RACK1 is in red. The eIF3 peripheral domain in contact with RACK1 is in violet. The densities for the core eIF3 domains, for the DHX29 factor and for the second peripheral domain of eIF3 contacting DHX29 are shown in grey. (C) Fitting of the atomic model of the 40S and IRESCrPV-IGR to the 40S-IRES cryo-electron microscopy structure. The atomic model of the human 40S ribosome and IRESCrPV-5' was fitted onto the cryo-electron microscopy density map of the complexes IRESCrPV-5'- human 40S ribosome at 20.3Å resolution (¬emd-1090; (Spahn et al., 2004)). Colors are as in panel A. The IRESCrPV-IGR atomic model is from (Schuler et al., 2006) (pdb 2NOQ).

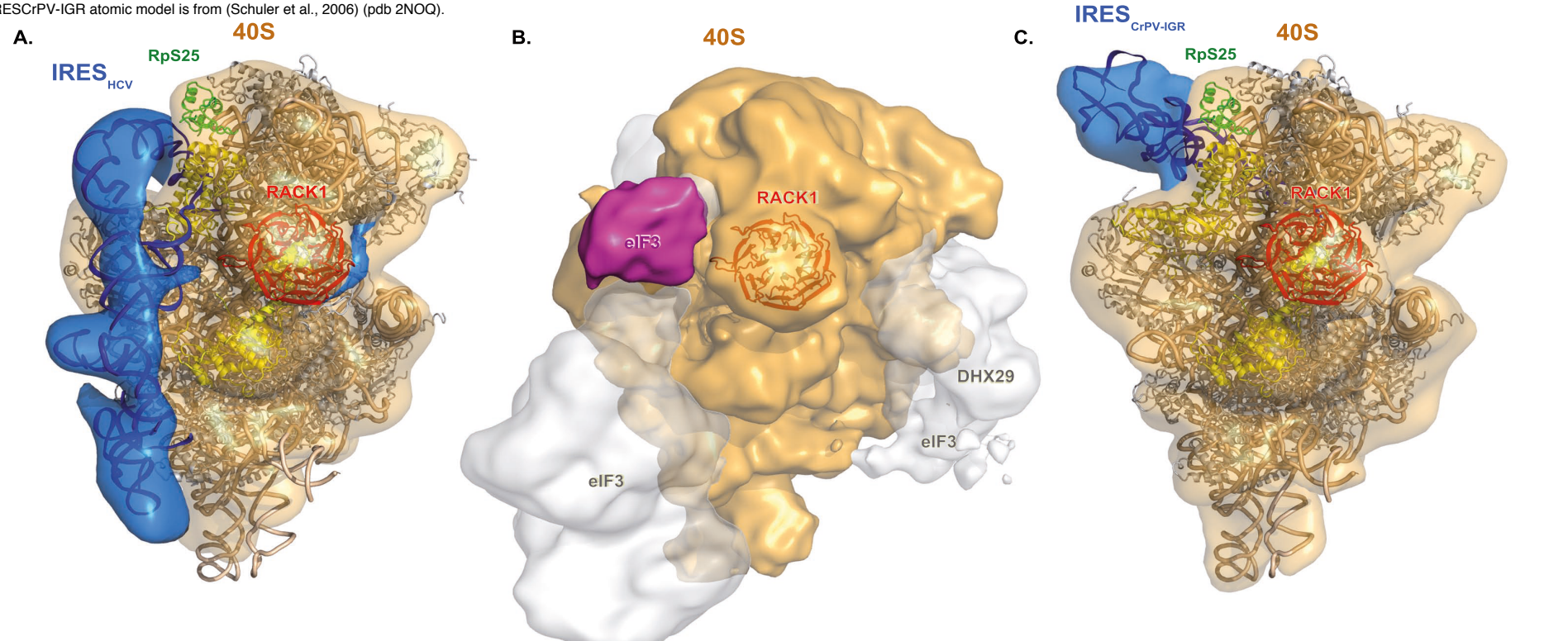

(Cernilogar et al., 2011; Marques et al., 2009; Okamura et al., 2009; Schüler et al., 2006; Spahn et al., 2004). Altogether, these structural observations confirm the critical role played by RACK1 in IRES-dependent translation.

DISCUSSION

Defining the protein niche of Dicer-2, R2D2 and AGO2 in infectious context

To identify novel host factors involved in the control of viral replication in *Drosophila*, we have used a broad proteomic approach based on a one-step purification technique taking advantage of the exquisite affinity of avidin for biotin. Using the three bait proteins Dicer-2, R2D2 and AGO2, we have identified 101 proteins, forming the core of a network of 188 protein interactions. The RNAi pathway is conserved during evolution and 16% of the interactants identified here were previously reported in studies on the interactome of Dicer, TRBP (an orthologue of R2D2) or AGO in worms and mammals (Chi et al., 2011; Duchaine et al., 2006; Moshkovich et al., 2011). Furthermore, in *Drosophila*, several proteins recently described for their involvement in RNA silencing, such as Hsc70-3 and -4 (Deddouche et al., 2008; Dorner et al., 2006; Iwasaki et al., 2010; Paradkar et al., 2012), Blanks (de Boer et al., 2003; Gerbasi et al., 2011), Sister of Yb and Vreteno (Fukuyama et al., 2012; Handler et al., 2011), were pulled-down together with Dicer-2, R2D2 and/or AGO2. Importantly, the comparison of the siRNA pathway interactome in cells uninfected or challenged with three different viruses revealed a dynamic pattern of interactions. The observed shift in the composition of the protein environment of the antiviral siRNA pathway probably reflects differences in the viral life cycles. This is illustrated by (i) the recovery of a mitochondrial protein, mtTFB1, with AGO2 only in cells infected by FHV, which replicates on the outer membrane of this organelle; (ii) the association of the poly(A) binding protein (PABP) (known to bind to the poly(A) tail of mRNAs and to interact with the eIF4F complex bound to the 5' cap to initiate translation) with AGO2 only in cells infected by VSV, the only virus used here expressing capped and poly-adenylated mRNAs; or (iii) the association of RACK1 with AGO2 and R2D2 only in cells infected by the IRES-containing virus DCV. Overall, the interactome dataset obtained in this proteomic analysis will be useful for future studies on the control of viral infections.

A new function for RACK1 in IRES-dependent translation

The RACK1 protein has been extensively studied during the last two decades, and shown to be involved in different aspects of cell regulation. RACK1 is an adapter protein, interacting with a variety of signaling molecules (e.g. PKC, Src, MAPK) (Arimoto et al., 2008; Fukuyama et al., 2012; Mamidipudi et al., 2004), and is a component of the 40S subunit of the ribosome (Chao et al., 2005; Coyle et al., 2009; Sengupta et al., 2004). RACK1 is thus ideally suited to connect signal transduction pathways to the regulation of translation (Gerbasi et al., 2011; Nilsson et al., 2004). Indeed, RACK1 was found to interact with the initiation factor eIF6, which associates with the 60S subunit of the ribosome, and prevents its association with the 40S subunit. RACK1-assisted phosphorylation by PKC of eIF6 was observed to trigger its release from the 60S subunit, thus promoting the formation of 80S active ribosomes (Ceci et al., 2003; Kadrmas et al., 2007).

Our data indicate that formation of active ribosomes is not strictly dependent on RACK1. Indeed, depletion of RACK1 does not affect cell viability of *Drosophila* S2 or human Huh7.5.1 cells in tissue culture. *In vivo* as well, translation can occur in the absence of RACK1, as lethality in *RACK1* mutant animals does not occur before larval stages for *Drosophila* and gastrulation in mice (Kadrmas et al., 2007; Volta et al., 2012). In agreement with this observation, translation of a 5' cap-dependent reporter was not affected in the absence of RACK1 in *Drosophila* and human cells. Nevertheless, the fact that *RACK1* mutant animals cannot complete their development suggests that this protein is required for the translation of some cellular mRNAs, in addition to viral IRES-containing RNAs. Interestingly, previous studies have highlighted the role of another protein from the 40S subunit of the ribosome, RpS25, in IRES-dependent translation (Coyle et al., 2009; Landry et al., 2009; Rabl et al., 2011; Sengupta et al., 2004). Performed on yeast and mammalian tissue-culture cells with IRES reporter assays, these experiments concluded that RpS25 is essential for the activity of two viral IRES, $IRES_{HCV}$ and $IRES_{CrPV\text{-}IGR}$. The mechanism used by RpS25 and RACK1 to promote translation is probably different for several reasons: (i) RpS25 is required for $IRES_{CrPV\text{-}IGR}$, unlike RACK1; (ii) in addition to IRES-dependent translation, RpS25 also mediates ribosome shunting in adenovirus (Hertz et al., 2013; Kuroha et al., 2010), whereas *RACK1* silencing does not affect adenovirus replication; (iii) structural data place RpS25

at a distance from RACK1 on the 40S subunit of the ribosome, providing an explanation for its importance on the activity of the $IRES_{CrPV\text{-}IGR}$. Several other ribosomal proteins (e.g. RpL38, RpL40) were recently proposed to be involved in specific translation of some 5' cap-dependent mRNAs (Coyle et al., 2009; Kondrashov et al., 2011; Lee et al., 2013), indicating that transcript-specific regulation can occur in the absence of IRES elements. Our data lend support to an evolving picture of the eukaryotic ribosome, which includes structurally peripheric components such as RACK1 involved in the modulation of translation of specific mRNAs.

A central unresolved issue is the nature of the *cis*-acting elements defining a possible "ribosome code" (Jan and Sarnow, 2002; Mauro, 2002; Spahn et al., 2004; Topisirovic and Sonenberg, 2011). In the case of RACK1, these *cis*-acting elements include viral IRES. Interestingly, the $IRES_{CrPV\text{-}IGR}$ is active in the absence of RACK1, unlike the $IRES_{CrPV\text{-}5'}$ or the $IRES_{HCV}$. This IRES (class I IRES) is capable on its own, without any initiation factors, of binding directly the 40S subunit and of recruiting the 60S subunit to form an active 80S ribosome, thus bypassing the loading of the initiator methionyl-tRNAi (Jan and Sarnow, 2002; Pestova et al., 2004; Spahn et al., 2001). By contrast, other IRES that have been characterized depend to varying degrees on a subset of initiation factors. For example, the function of $IRES_{HCV}$ (class II IRES) requires two canonical eIFs, eIF2 and 3, as well as Met-tRNAi (Kieft, 2008; Lindenbach, 2005). This suggests that the effect of RACK1 on translation initiation may require one of these factors. Interestingly, the eIF3 complex binds to the 40S ribosomal subunit, and to the $IRES_{HCV}$ (e.g. (Dorner et al., 2011; 2001)). Furthermore, RACK1 was shown to associate with one of the eIF3 subunits in order to assemble a translation pre-initiation complex in yeast (Kouba et al., 2012; 2013b). Thus, the effect of RACK1 on translation may be mediated through eIF3. Alternatively, the requirement for RACK1 may reflect the position of the IRES at the 5' extremity of the viral mRNA. In support of this hypothesis, the $IRES_{HCV}$ was not sensitive to RACK1 depletion when it was cloned in bicistronic reporters (data not shown).

RACK1 as a target for broad antiviral intervention

Our results open interesting therapeutic perspectives for chronic hepatitis C, a major cause of liver cirrhosis and cancer, for which antiviral resistance remains an

important challenge. Because HCV translation initiates viral genome neosynthesis via the formation of the replication complex, RACK1-mediated translation is a crucial step in virus propagation. Thus, RACK1 is a novel host target for antiviral therapy, which is complementary to other approaches targeting viral enzymes such as the protease, the polymerase or the nonstructural protein NS5A.

The current standard-of-care (SOC) for chronic genotype 1 HCV infection consists of pegylated interferon (IFN)-alfa, ribavirin and a protease inhibitor (2012b). A large number of other promising direct-acting antivirals (DAAs) are being evaluated in clinical trials. However, recent phase III randomized clinical trials demonstrate that limited response for distinct genotypes remains an important challenge in a significant fraction of patients (Jacobson et al., 2013; McPhee et al., 2013). Furthermore, difficult-to-treat patients, such as partial non-responders or null-responders to prior therapy, patients with advanced liver disease, HIV-coinfected or immune-compromised patients will most likely require additional or alternative approaches (Barreiro et al., 2012; Jacobson et al., 2013). A promising strategy to address antiviral resistance to SOC and DAAs are host-targeting agents (HTAs). Compared to the high variability of viral proteins targeted by DAAs, the variability of host factors targeted by HTAs is low (Nathan, 2012). By imposing a genetic barrier to resistance higher than that of DAAs, host-targeting agents may avoid emergence of viral escape variants. Indeed, we, and others, have shown that agents targeting host entry potently inhibit highly infectious escape variants of HCV (Fofana et al., 2010; Lupberger et al., 2011; Zhu et al., 2012). Given that HTAs interfere with host targets, one caveat is the possibly greater risk of cellular toxicity as compared to DAAs. Interestingly, our data obtained in cell culture models did not reveal any major toxicity linked to RACK1 inhibition. Thus, our proof-of-concept studies in state-of-the-art cell culture models open a highly attractive and innovative perspective to discover and develop small molecules targeting RACK1 for treatment of SOC-resistant chronic hepatitis C.

We note that several other viruses causing human disease use 5’ cap-independent mechanisms for the translation of their RNAs. These include HIV, enteroviruses such as poliovirus, rhinoviruses, cardioviruses such as EMCV, coxsackieviruses or aphtoviruses such as FMDV, hepatitis A virus (Martínez-Salas et al., 2008), which may also be sensitive to RACK1-targeting antiviral approaches. Animal viruses relying on IRES-mediated translation, which represent a significant economic

burden and for which treatment options are limited, or completely absent, such as pestiviruses (Peterhans et al., 2010), may also be sensitive to RACK1 inhibition. Therefore, the development of RACK1 inhibitors may have benefits for treating infections by human viruses other than HCV, and may even be relevant for veterinary medicine.

RACK1 and regulatory RNA functions

While this work was in preparation, two reports described a role for RACK1 in miRNA function in nematodes and human cells (Jannot et al., 2011; 2011). We confirm here that in *Drosophila* as well, RACK1 can affect miRNA function. However, the importance of the requirement for RACK1 for the silencing was variable depending on the tested miR reporter, suggesting that the requirement for RACK1 may be miR- or target-specific. The differences observed between the *in vivo* phenotypes of *RACK1* and *AGO1* or *Dicer-1* mutant flies support this hypothesis. Indeed, flies mutant for the miRNA pathway exhibit embryonic lethality (Lee et al., 2004; 2004b), whereas RACK1 mutants reach the larval stage (Kadrmas et al., 2007). Furthermore, shRNA-mediated conditional knockdown of AGO1 in adult flies resulted in rapid lethality, unlike silencing of RACK1 (data not shown). Based on our observation that RACK1 interacts with AGO2, it is possible that RACK1 preferentially affects the subset of miRNAs loaded onto AGO2.

Regarding viral infections, the fact that AGO2 interacts with RACK1 suggests the existence of a connection between translation and antiviral RNA interference. It raises the possibility that the siRISC complex inhibits translation of viral proteins. Based on *in vitro* experiments, it is generally assumed that AGO2 functions as a slicer, cleaving viral RNAs complementary to the guide siRNAs (Nayak and Andino, 2011), but direct evidence that AGO2 degrades viral RNAs *in vivo* is lacking. AGO2 can inhibit translation in some contexts, albeit by a different mechanism than AGO1. Interestingly, in *Drosophila*, AGO2 inhibits translation at the level of the 5' cap structure, competitively binding the cap-binding eIF4E protein and preventing its association with eIF4G and the 40S-bound initiation factor eIF3 (Iwasaki et al., 2009). An intriguing possibility is that binding to RACK1 allows AGO2 to also control translation of 5' cap-independent transcripts, as suggested by *in vitro* studies (Iwasaki and Tomari, 2009).

In summary, we have shown that the protein RACK1 is involved in translation of IRES-containing viral mRNAs and largely dispensable for translation of cellular mRNAs. Our findings comfort the ribosome code or ribosome filter hypothesis, and point to RACK1 as a promising tool to characterize the mechanism of transcript-specific translation and, in particular, the *cis*-acting elements modulating RNA translation in a RACK1-dependent manner. The identification of a ribosomal protein required for IRES-dependent translation of viral mRNAs further opens interesting perspectives for the design of a novel class of antiviral therapeutics targeting specific components of the ribosome, e.g RACK1.

Supplementary Figure 1.

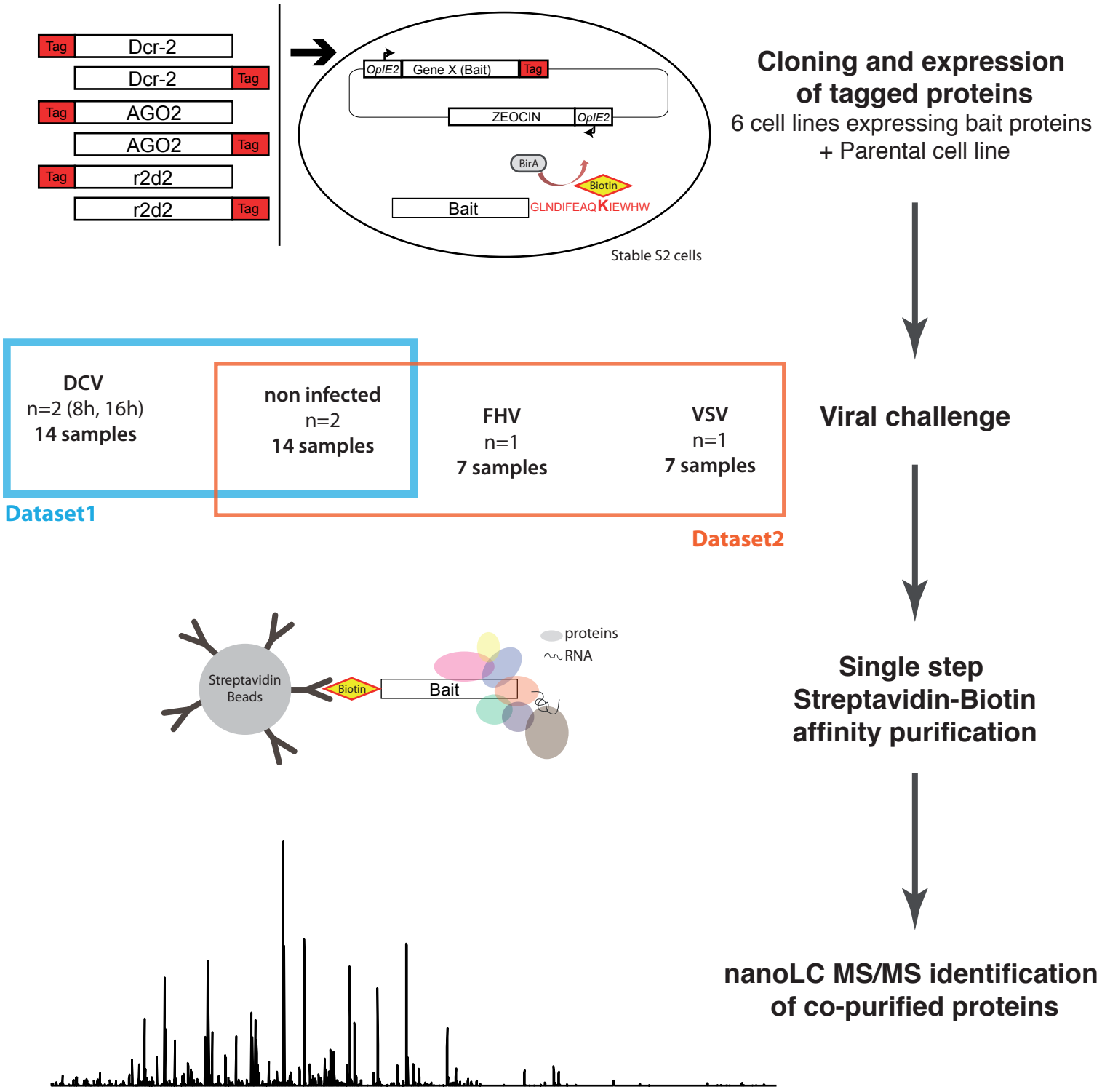

Fig. S1. Strategy used to define the siRNA pathway interactome. The bait proteins (Dcr-2, AGO2 and r2d2) were tagged at their amino- or carboxy-terminal extremities with a 15 amino-acid biotinylation target sequence (in red, with modified Lys in bold). S2 cells expressing the bacterial biotin ligase BirA were stably transfected with the corresponding expression constructs. Cells were then either non-infected or infected with DCV (8h and 16h), FHV (16h) or VSV (48h). Cell lysates were affinity purified in a single step on streptavidin beads, digested with trypsin, and analyzed by nanoLC MS/MS on a FT ICR mass spectrometer.

Figure S2

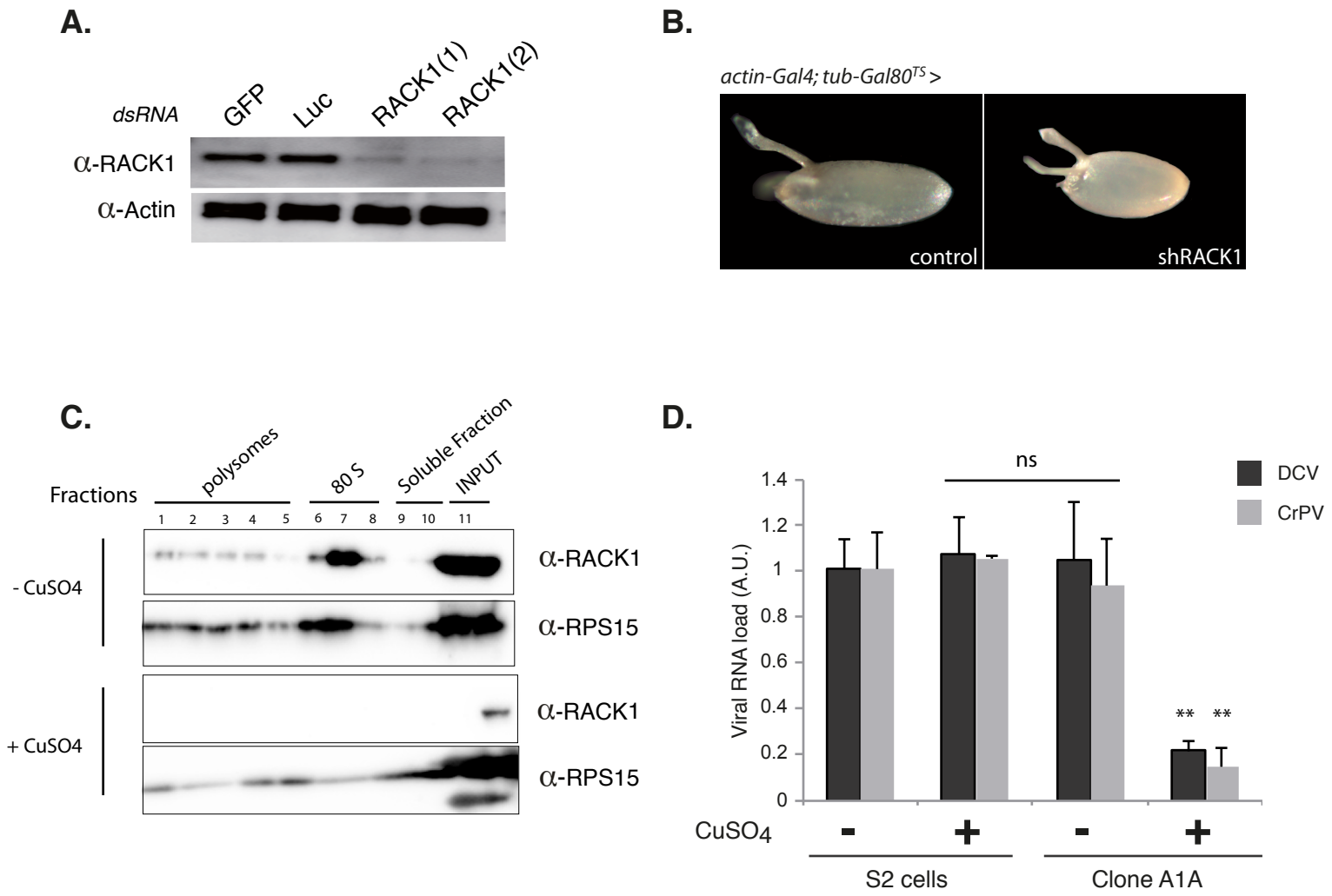

Fig. S2. Silencing of RACK1 expression in *Drosophila*. (A) RACK1 expression was silenced in S2 cells by incubating cells with two dsRNA targeting different regions of RACK1 for 4 days. RACK1 expression was monitored by western blot using specific anti-RACK1 antibodies. (B) Embryos laid by shRACK1 expressing females show a dorsalized phenotype, similar to RACK1 mutants. (C) Silencing of RACK1 with the same shRNA targeting the 5' UTR from the RACK1 gene as in panel B in stably transfected S2 cells. Expression of the shRNA is driven by the copper-inducible metallothionein promoter. Different polysomal fractions or Input proteins were probed for RACK1 expression and RPS15 (loading control). (D) Reduced viral replication of DCV and CrPV in shRACK1-expressing S2-A1A cells. Data show the mean and s.e.m. of three independent infections.(ns=non significant , ** $p < 0.01$)

Supplementary Figure 3

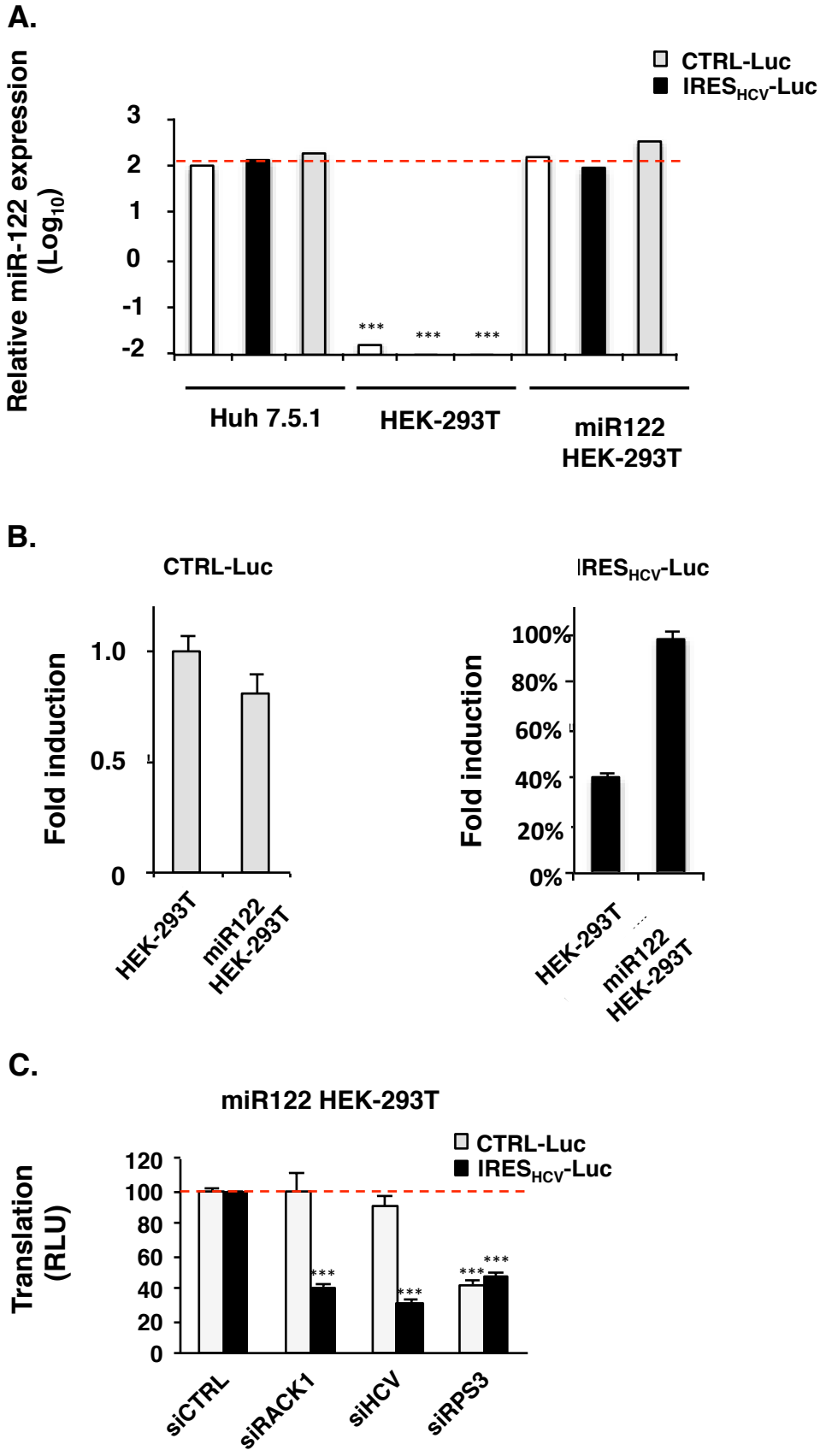

Fig. S2. miR122 complementation of HEK-293T cells stably transfected with an IRES$_{HCV}$-luciferase reporter construct (black bars) or a classical capped reporter gene (grey bars). A. miR122 quantification by quantitative RT-PCR in Huh 7.5.1, HEK-293T and miR122 complemented HEK-293T cells (miR122 HEK-293T), *** p <0.001. B. Translation level of capped or IRES dependent reporters in mir122-HEK-293T compared to miR122 deficient HEK-293T cells, translation was monitored 72h later by luciferase activity quantification. C. miR122 complemented HEK-293T cell lines stably expressing an IRES (IRES$_{HCV}$ -Luc) or a 5'cap-translated (CTRL-Luc) luciferase reporter gene were transfected with siCTRL, siRACK1, siHCV or siRPS3. Translation was monitored 72h later by luciferase activity quantification, *** p <0.001.

IV- Chapter 3

A proteomic analysis of RACK1 partners and their involvement in viral replication

IV - Chapter 3

A proteomic analysis of RACK1 partners and their involvement in viral replication

1. Introduction

Receptor of Activated C Kinase 1 (RACK1) is a highly conserved protein amongst eukaryotic species, containing seven WD40 beta-propeller domains(Nilsson et al., 2004). WD40 proteins are found in many macromolecular complexes in the cell, and are often considered as adaptor proteins, conferring adequate molecular platforms for other proteins. Therefore, it is not surprising that RACK1 has been detected in many interaction networks, including PKC, Src, Hif1-alpha, Jaks and STATs (Nilsson et al., 2004). RACK1 is not an enzyme so it cannot transmit signals by performing post-translational modification. Instead, it is considered to have a role in complex assembly; docking, scaffolding, stabilizing, or otherwise connecting elements of the complexes together (Ron et al., 2013). Interestingly, the recently solved crystal structures of different eukaryotic ribosomes, place RACK1 in the 40S ribosomal subunit, in stoichiometric quantities with other ribosomal components (Ben-Shem et al., 2011; Nilsson et al., 2004). These findings suggested the presence of a ribosomal pool of cytosolic RACK1, which might be involved in translation. Even though 400 publications listed in PubMed mention RACK1/GNB2L1 in their abstract, its exact function and how its signaling and ribosomal function could be connected remain elusive.

In Chapter 2, we describe a new ribosomal function of RACK1 in the IRES-mediated translation of viral mRNAs. This finding opens up many interesting and unaddressed questions: How does RACK1 interaction network behave upon infection with an IRES containing virus? Does RACK1 have co-factors involved in the viral IRES-mediated translation?

Fig 1. Experimental strategy of the pilot IP (A) .

The following scheme resumes the adopted strategy: transient expression of Tagged-RACK1 transgene, cell stimulation and lysis followed by the HA-precipitation of the complexes.Samples were then run on gel and subjected to MS/MS.

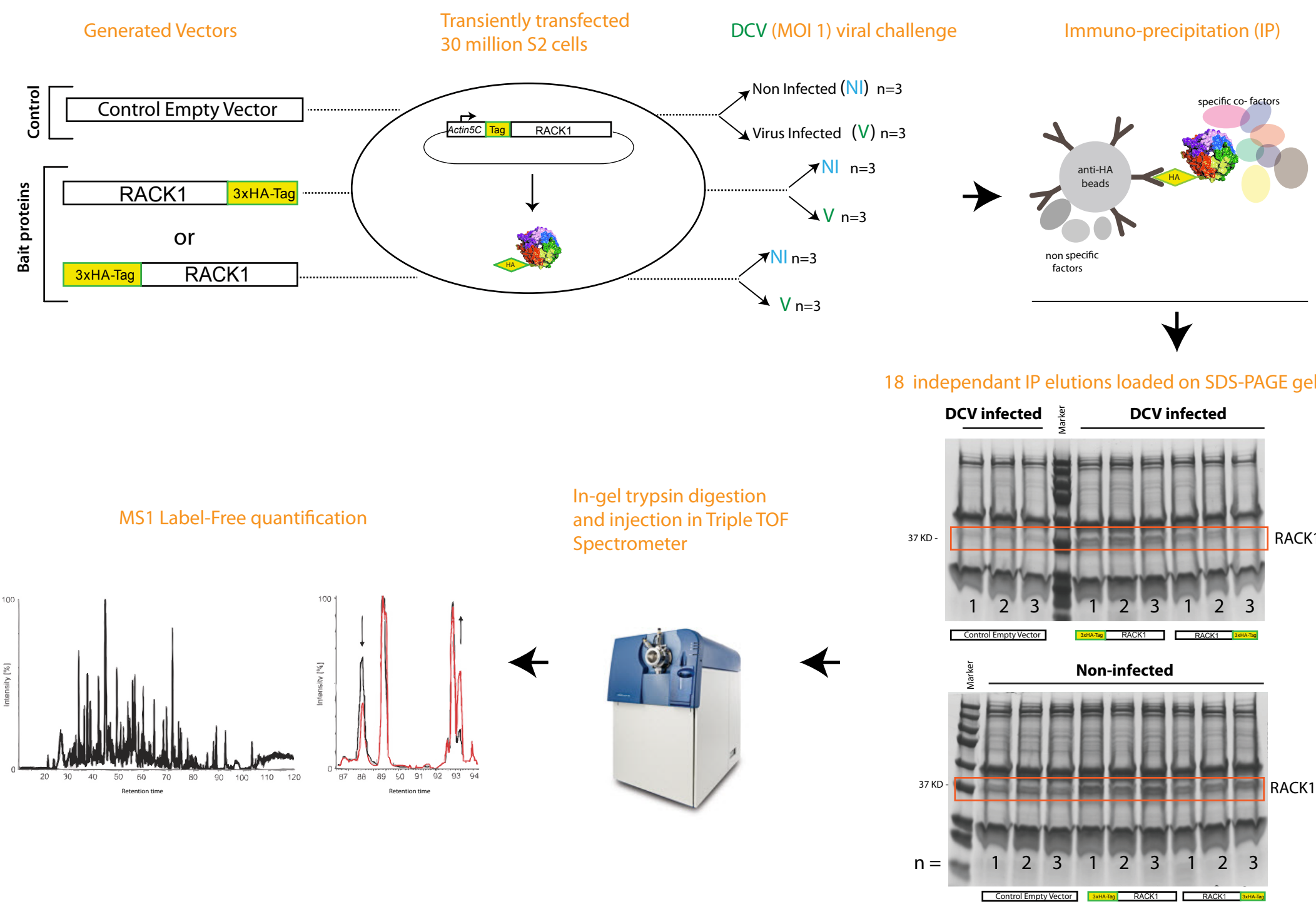

In order to tackle these questions, we decided to carry a proteomic analysis of RACK1 binding partners in normal or infectious contexts. Whereas RACK1 was recovered as a co-factor in many interactome studies (Gibson, 2012; Nilsson et al., 2004), we decided this time to use RACK1 as a bait to identify its interaction network. Briefly, we tagged RACK1 protein with different motifs and transiently expressed it in S2 cells, in mock or infected conditions (IRES-containing viruses). RACK1 was then immunoprecipitated and the pulled-down protein complexes were subjected to MS/MS on a triple TOF spectrometer (ABISciex). A total of 42 independent pull-down experiments with different conditions (IP incubation, HA or FLAG tag, N-ter or C-ter tag, control IPs, infection status) were subjected to MS/MS. Different strategies were adopted in order to obtain and analyse the data. For the 42 samples a label-free quantification strategy was used to assess the protein abundance status. 18 samples amongst the 42 were also subjected to the novel MS/MS ^{all} SWATH quantification method.
A selected number of identified co-factors was then tested in an RNAi screen for their contribution in the replication of different viruses, two IRES- containing viruses, CrPV and DCV, and two viruses that use a canonical cap-dependent translation mechanism (FHV and VSV).

2. Results

2.1 Optimisation of RACK1 pull-down

In a first pilot experiment, termed IP A, I pulled-down RACK1 and its co-factors were identified and quantified by the MS1 Label-Free method. I generated vectors containing *dm*RACK1 tagged N-terminally or C-terminally with a 3x hemagglutinin (HA) tag (Fig. 1). These vectors were then transiently transfected in S2 cells in 18 independent experiments: 6x with empty control vectors, 6x RACK1 HA-tagged in the N-terminus, 6x RACK1 HA-tagged in the C-terminus. 24 hours post-transfection half of the cells were infected with DCV (3x empty vector, 3x RACK1-HA N-term, 3x RACK1-HA C-term), and the other half was mock treated (Fig. 1). 16 hours post-infection the cells were lysed and the lysates were incubated with anti-HA-beads overnight (See Materials and Methods). The next day, the beads from 18 preparations were washed and the purified

Fig 2 **Immuno-precipitation optimization for low background.** The SDS-PAGE gel is loaded with eluates from different immuno-precipitation experiments of RACK1 Tagged with 3XFLAG in the N-term. Different salt concentrations in the buffer and different times of incubation of cell lysates with anti-FLAG beads were tested.

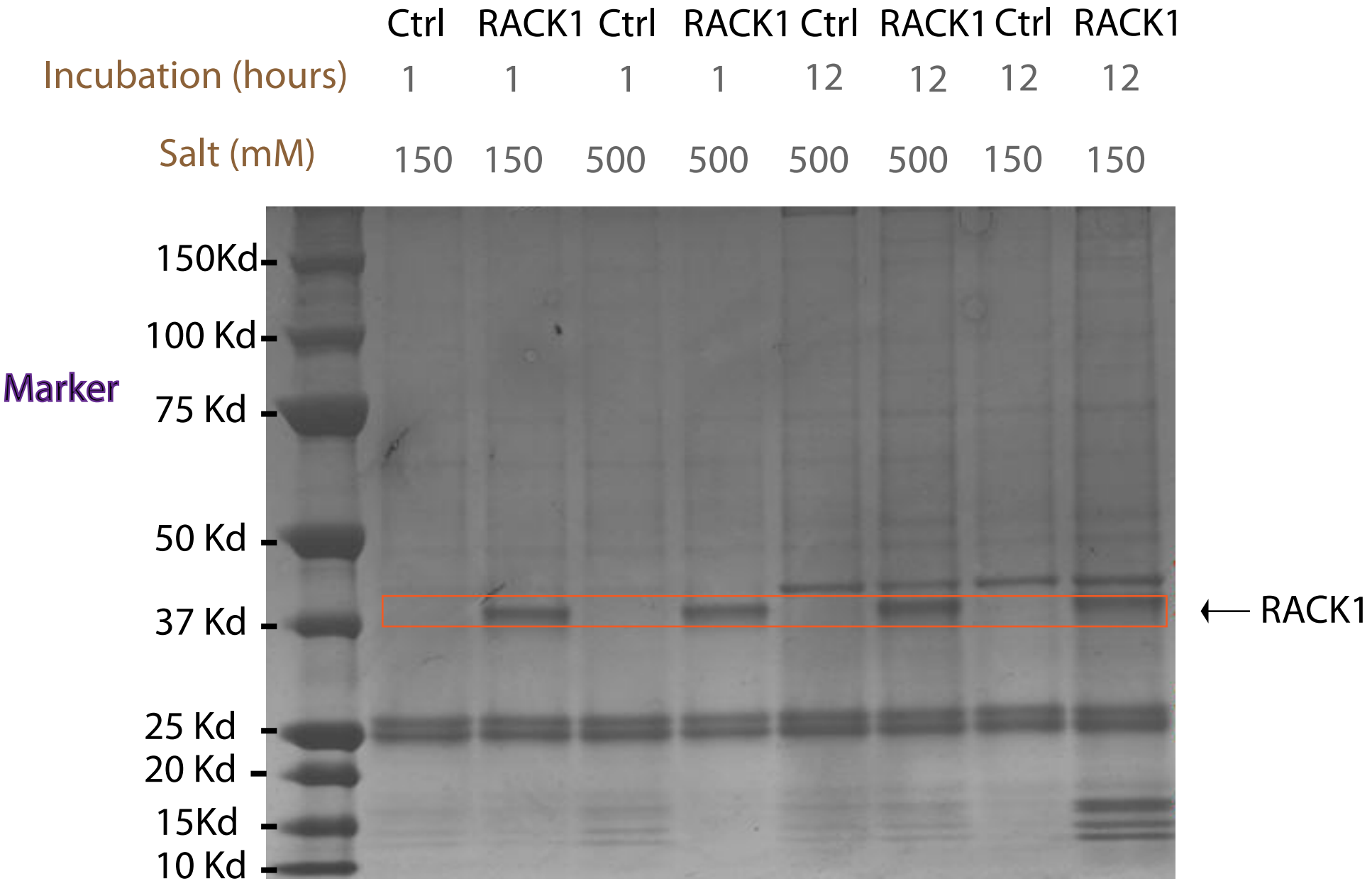

complexes were eluted and ran on a SDS-PAGE (Fig. 1). The obtained proteins were then trypsinised in-gel and injected in a Triple-TOF ABISciex (See Materials and Methods). The obtained Spectrums were then assigned to peptides using the *Drosophila melanogaster* SwissProt database.

This first pilot experiment permitted the identification of a large number of proteins (234 proteins in total), from which only a small fraction (26) was enriched in samples where RACK1 was over-expressed (Table 3-1). This result revealed the high sensitivity of the Triple-TOF machine. Furthermore, the important number of the identified non-specific factors (234-26= 208) indicated a high background noise. Indeed, the gel in Fig. 1 shows the presence of many protein bands, even in conditions where RACK1 was not overexpressed. This indicated that our immunoprecipitation conditions were not optimal.

I suspected that three parameters were influencing the attachment of non-specific factors to our pulled-down protein complexes. First, is the non-specific binding of complexes to the anti-HA-beads? I therefore turned to another tag (3xFLAG tag), and anti-FLAG-beads (anti-DYKDDDDK beads from CloneTech) optimized for minimal non-specific binding. The second parameter suspected is the time of incubation of the cell lysates with the antibody-coupled beads. Instead of incubating the beads with the cell lysates overnight, we reasoned that shorter incubation times could minimize the background noise. The third suspected parameter is the salt concentration in the washing buffers. I thought that a higher salt concentration in the washing buffer would discard non-stringent binders.

In order to test these different parameters, N- or C-terminal 3xFlag versions of RACK1 were generated and overexpressed in S2 cells. The lysates were then tested with anti-DYKDDDDK beads (Clonetech) with different incubation times (1 or 16 hours), and using two NaCl concentrations in the washing buffer (150mM or 500mM). The result was visualized on a SDS-PAGE with a Coomassie Blue staining (Fig. 2).

Figure 2 shows the protein migration pattern on SDS-PAGE of different conditions. One-hour incubation coupled to a 500mM NaCl washing buffer seemed to be the condition where minimal non-specific binding was occurring (Fig. 2).

These optimised conditions were then adopted for the next experiments**,** where 24 independent samples were prepared (IP B) (Fig. 3). I next included a new control to

Fig 3 **Experimental strategy .** The following scheme resumes the adopted optimised strategy with 2 different controls : transient expression of Tagged-RACK1 transgene, cell stimulation and lysis followed by the FLAG-precipitation of the complexes.Samples were then run on gel and subjected to MS/MS.

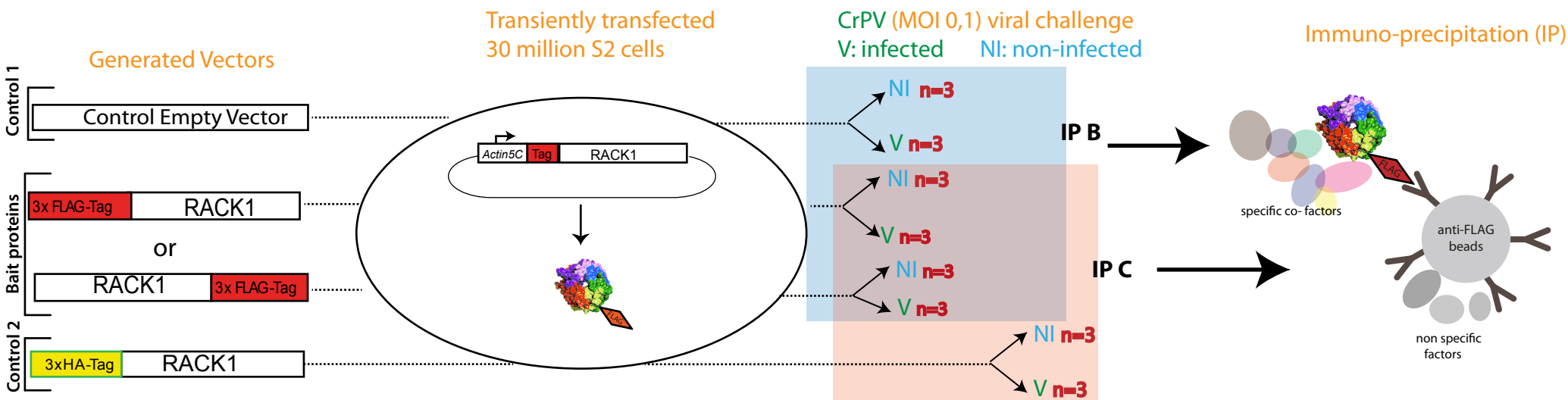

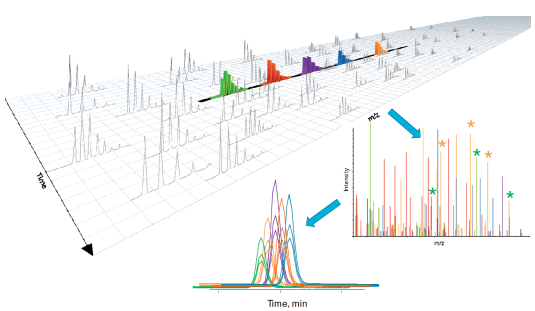

In-gel trypsin digestion and injection in Triple TOF Spectrometer

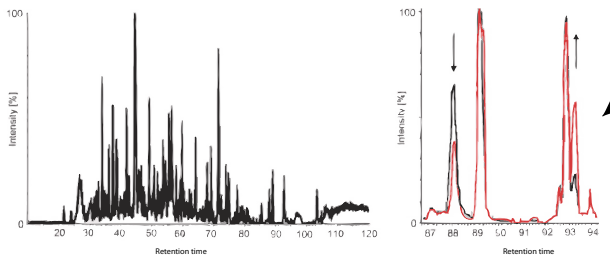

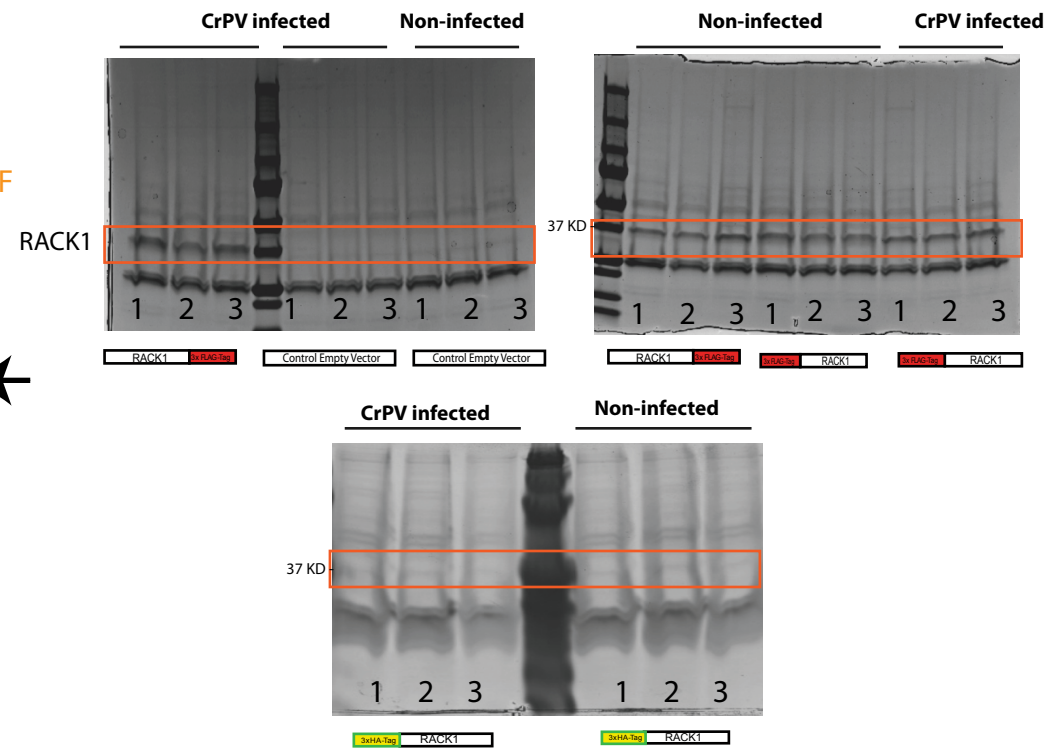

take into account the fact that the overexpression of RACK1 might induce some changes in the proteome of S2 cells. Therefore, I performed an additional immunoprecipitation on cells overexpressing the RACK1-HA tagged protein, which is insensitive to the pull-down with anti-FLAG beads (IP C) (Fig. 3).

In immunoprecipitations B and C, I also changed the virus used to infect the transfected S2 cells, and used CrPV instead of DCV. This virus, which also belongs to the *Dicistroviridae* family and requires RACK1 for its translation (see Chapter 2), is able to infect up to 90% of the cell population at 16 hours post-challenge, whereas DCV infects only ~10% of the cell population at this time point (data not shown). We reasoned that a cell population that is more uniformly infected would provide a clear picture of interactions induced by the virus.

2.2 Identification and quantification of RACK1 partners in different experimental set-ups

The purified protein complexes from different conditions were subjected to an in gel trypsin digestion, the digested peptides were then separated by nano-liquid chromatography coupled to electrospray Ionization, before being injected in the Triple-ToF ® Spectrometer from ABSciex. Survey MS spectrum were acquired and extracted peptide signals were then mapped across LC-MS measurements using their coordinates on the m/z and retention-time dimensions. The identified peptides were then used to perform a database search (*D. melanogaster* databank from Swissprot) using the ProteinPilot software (AB Sciex). The proteo-typic peptides were accordingly assigned to *D. melanogaster* proteins and validated with a 1% False Discovery Rate (FDR). The Label-Free quantification was carried out using the ABSciex package including PeakView and MarkerView softwares. Proteins validated with a FDR of 1% were loaded into PeakView. Reconstructed elution peak areas (XIC, eXtracted Ion Chromatogram) for each peptide, in each condition, were then exported to MarkerView and the peak areas were integrated and used as a quantitative measurement of the original peptide concentration (see Materials and Methods).

The numerical value assigned for a protein in a certain condition was the sum of all the integrated peaks, corresponding to different peptides, originating from the same protein. The mean and standard deviation of three independent values, corresponding to biological triplicates, from one condition (example: RACK1-HA N-terminal, non-infected)

Figure 4

A- Identification of RACK1 specific-cofactors

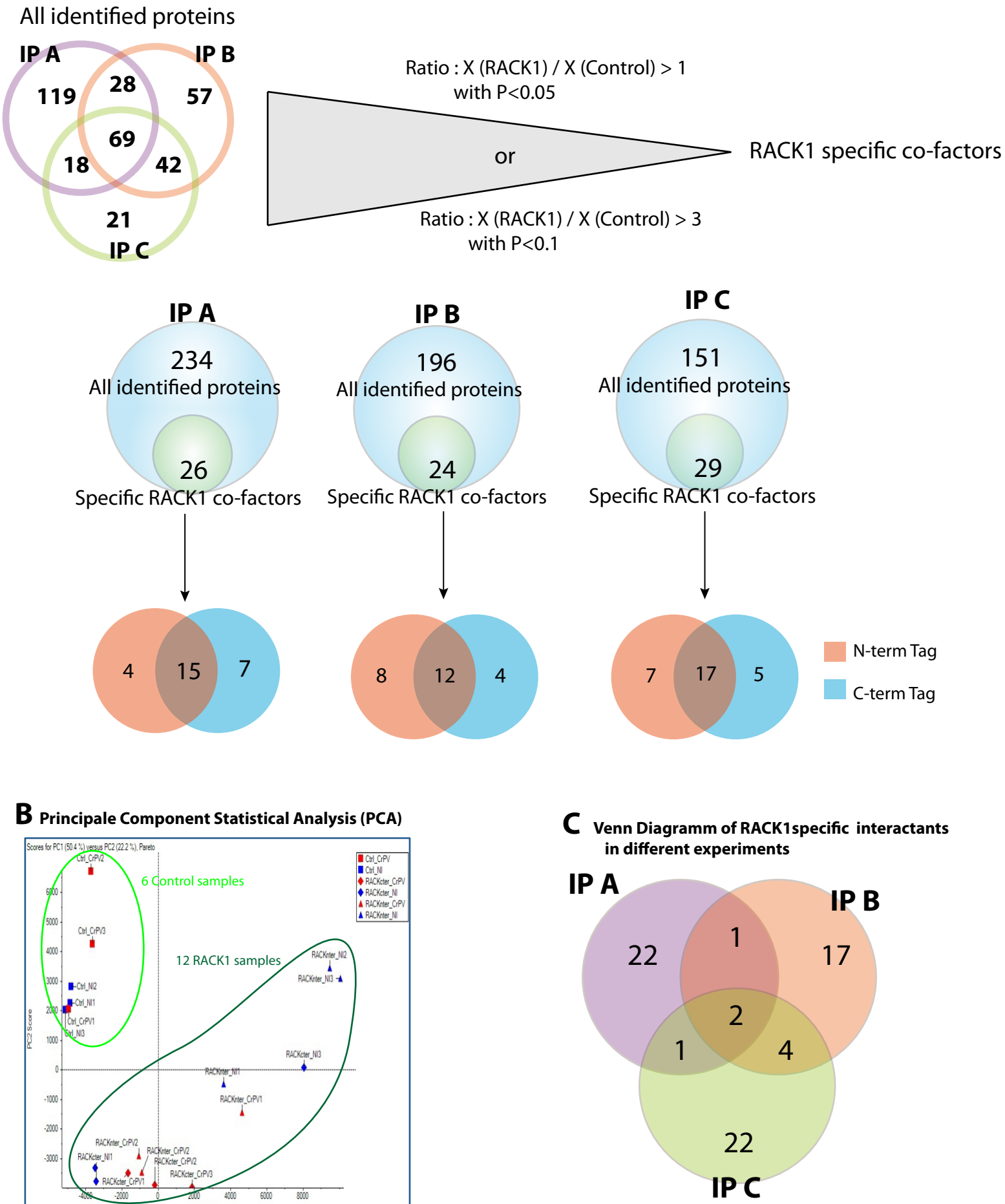

B **Principale Component Statistical Analysis (PCA)**

C **Venn Diagramm of RACK1specific interactants in different experiments**

was then used as a relative quantity (RQ) of the identified protein. The detailed results are explicated in Table 1- Chapter 3 (Tabs IP A, B or C- Label free).

In IP A, we identified the largest total number of proteins (234 proteins), compared to 196 proteins identified in IP B and 151 proteins identified in IP C (Fig. 4A). This was not surprising since IP A was not yet optimised for minimal background retrieval. Moreover, the percentage of proteins that were specifically detected in IP A was roughly 50% (119/234) compared to 29 % (57/196) in IP B and 14 % (21/151) in IP C (Fig. 4A), confirming the important background noise detected in IP A.

Then, I wanted to identify which of the detected proteins was a specific RACK1 co-factor. A protein was considered a specific-RACK1 co-factor if it was enriched in the condition where RACK1 was over-expressed and pulled-down, meeting therefore the following criterion:

1-The ratio X/Ctrl>2 in IP B and C and SWATH and >1 in IP A, where X is the RQ of an identified protein in condition A (ex: RACK-HA, N-ter, Non-infected) and Ctrl is the RQ of the same protein in the corresponding control condition (ex: empty vector, non infected). All the ratios corresponding to these criteria have a green label in Table 1-Chapter 3.

2-The P-value <0.05, Where P is the value of a two-tailed Student *t*-test between triplicates of condition A and triplicates of control condition (ex: *t*-test between three values from RACK-HA, N-ter, non-infected and three values from empty vector, non infected). All P values corresponding to these criteria have a yellow label in Table 3-1.

3- If a protein has a P-value <0.1 and a ratio X/Ctrl >3 it was considered as a RACK1 specific co-factors. The detection of RACK1 with a ratio = 3.8 and P-value of 0.36 in one of the samples (RACK1-C-ter IP C) (Table 3-1) incited us to loosen the P-value threshold (P <0.1) when the ratio is high.

Accordingly, I was able to identify 26, 24 and 29 proteins, which met the cited criterion, in IP A, B and C respectively. Importantly, the majority of these RACK1 co-enriched factors were identified with the two tagged versions of RACK1 (N- or C-ter) (Fig. 4A), Surprisingly, there was not an important overlap between the specific partners identified in the three experiments. Indeed, the Venn diagram in Figure 4C indicates that only two proteins (RACK1 and Cct-gamma) were common to the three analyses. Only one protein (aralar1) was found in both IP A and IP B, and only T-cp1 was found in both IP A and IP C, Hsp70Bb, Hsp26, Hsc70-4 and Hsc70-5 are the four common proteins to IP B and C (Fig. 4).

A very good reproducibility was observed, between the biological replicates (n= 3) in a given experiment, as illustrated by the Principle Component Analysis (PCA) shown in Fig. 4B. However, the low number of overlaps between IP A, B and C indicates a poor reproducibility between the experiments. IP A was expected not to share significant overlap with IP B and C, as it contained a significant amount of non-specific interactants. On the other hand, it was surprising that IP B and IP C shared only six RACK1 partners. This poor reproducibility can be attributed to the difference in the negative controls used in these two experiments, While in IP B the negative control was the transfection of an empty plasmid, IP C's negative control was the transfection of HA-RACK1 insensitive to the pull-down. The quantification of the identified proteins in the control sample is crucial, since the deduced quantity values are used as denominators to calculate the ratio that would determine if a protein is a specific factor or not. Therefore, my data show clearly that the overexpression of RACK1 is not neutral; such an overexpression could possibly affect the overall proteome of the transfected cells that would ultimately affect the quantities of the non-specific partners that are identified. Another parameter can possibly also explain the discrepancy between IP B and IP C: samples from IP C were stored for two months at 4°C before being injected in the Spectrometer. Although the RACK1 protein still had very good protein coverage in IP C, one cannot exclude that protein degradation can occur, which would affect the subsequent quantification.

Figure 5. Interaction network of RACK1 identified partners in Mock v/s Viral infection condition

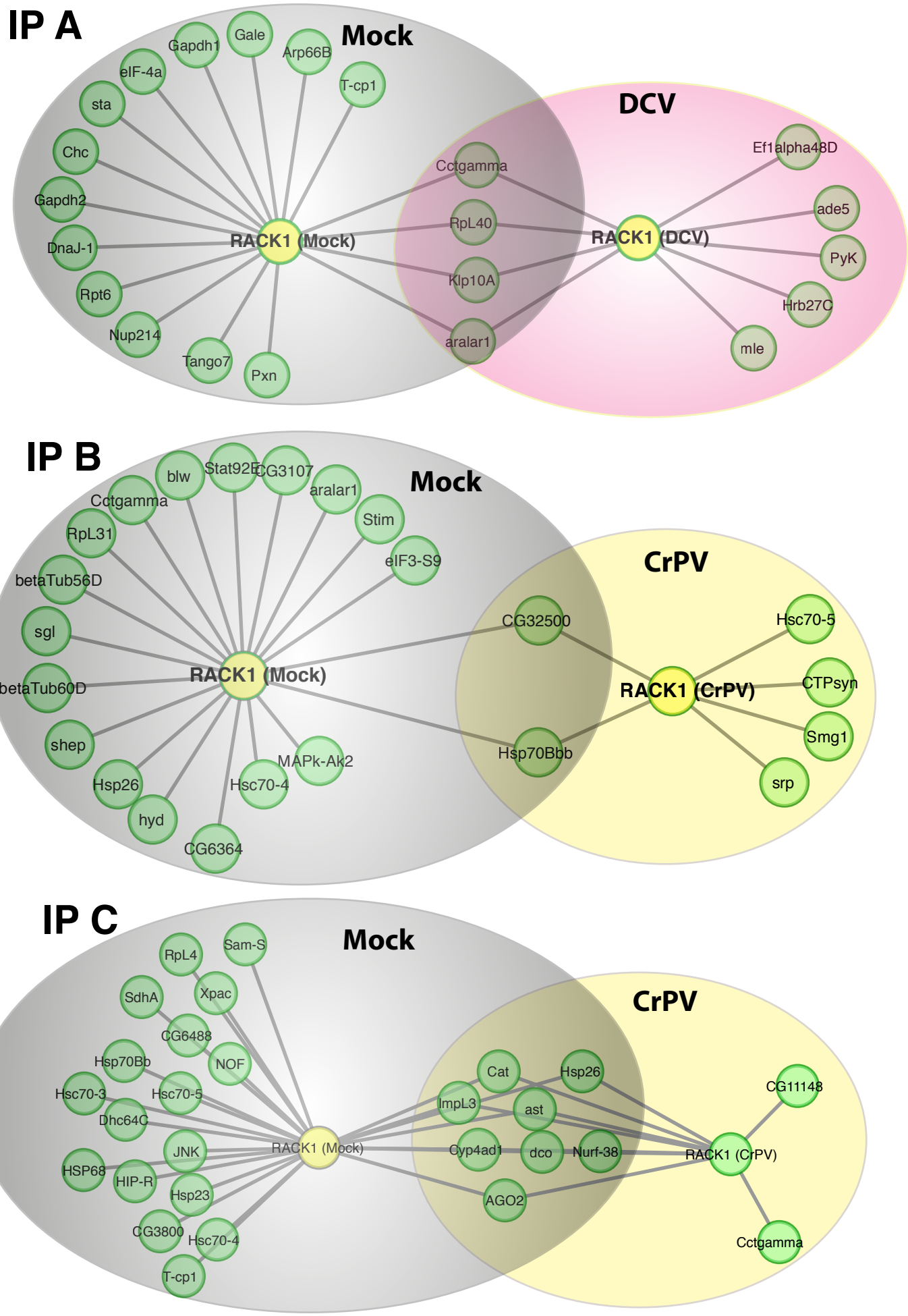

2.3 RACK1 specific co-factors in different experiments

In Figure 5 are depicted the interaction networks of RACK1 specific partners retrieved from IP A, B and C. As mentioned before, only few proteins interacting with RACK1 have been identified in both, IP B and IP C. These proteins are mostly chaperones (Hsp70Bb, Hsp26, Hsc70-4, Hsc70-5) involved in proper protein folding. However, a large number of chaperones or chaperonins that were not necessarily identified in each experiment were also identified (e.g. T-cp1, Hsc70-3, Hip-R) (Fig. 5). These interactions are not surprising since chaperones are known to assist the folding of proteins that are part of large molecular complexes. The surprising thing nonetheless, was the absence of some expected interactions. For instance, there were not a lot of ribosomal proteins identified (RpL31, RpL4 and RpL40). However, three proteins involved in translation initiation were detected (Fig. 5) (eIF-4a, eIF3-S9 and Tango7 (eIF3M)). This can possibly be attributed to the peripheral position of RACK1 in the ribosome and its involvement in translation initiation. Another expected class of interactants that was also absent is the family of Protein Kinases C from which RACK1 holds its name. However, many other kinases were detected with RACK1 (MAPk-Ak2, JNK, Smg1, Pyk, CG6364). It would be interesting to verify if these proteins also use RACK1 as an adaptor that increases their kinase activity.

Interestingly, the viral infection seems to affect negatively the number of RACK1 partners, shrinking the interaction network. While some partners were present in both Mock and infected conditions, the majority of RACK1 partners seem to disappear when the cells are infected with either DCV or CrPV. This can be due to the translational arrest these viruses cause soon after they infect the cells (Garrey et al., 2009; Ron et al., 2013). Of note, is the appearance of interactants that the viral infection seems to recruit? The interaction of four proteins with RACK1 appears to be induced by the viral infection. In the experiment IP B, CTPsyn, Smg1 and Srp show a ratio <1 in mock conditions, but this ratio becomes significantly greater than 1 when the cell are infected ($r > 1.5$). Moreover, the ratio of RACK1-CrPV/RACK1-non-Infected) of these proteins in the samples is significantly greater than 1, proving an enrichment of these proteins when the cells are infected with CrPV (Table 1-Chapter 3). Likewise, in IP C CG11148 seems to interact with RACK1 only when the cells are infected. The biological significance of these interactions can only be speculative for the moment. It is, however,

interesting to note, that one of these proteins interacting specifically with RACK1 upon CrPV infection is Smg1. Smg1 is a kinase that is involved in RNA non-sense mediated decay and is part of the mRNA surveillance complex (Gatfield et al., 2003). Further characterization of this interaction might unveil a new function of this protein in the regulation of viral mRNA translation.

Some other proteins (e.g. Cct-gamma) that appear in Fig. 5 to be present in RACK1's network upon infection only are close to our statistical threshold. One should be careful in analysing such interactions. Cct-gamma for instance appears in IP B to be interacting with RACK1 only in Mock conditions, where this protein has a ratio of 2.77 (RACK1 C-ter non infected / Control non infected) and a P-value of 0.02 (see Table 1-chapter 3, Fig. 5). A closer look at the ratio of this protein in infected conditions in IP B shows a ratio of 2.06 but a P-value of 0.22. This means that this protein was considered "not present" in infected condition because it simply did not pass our statistical threshold (Fig. 5). In IP C, Cct-gamma appears only in CrPV infected condition, where it passed the selection criterion (r>2.14, P-value=0.02). Likewise, a closer look at the values of this protein in Mock condition in the tab IP C- label free -Swiss Prot of Table 1- Chapter 3 reveals a 1.7 ratio and a P-value of 0.08, which explains why it was not considered as present in Mock condition (Fig. 5).

Finally, the detection of AGO2 interacting with RACK1 in IP C was reassuring since we were able to detect RACK1 after an AGO2 pull-down. Importantly, in mammalian cells a RACK1 - Ago-2 interaction was also shown (Jannot et al., 2011). Mammalian Ago-2. However, shares more similarity with *Drosophila* AGO1. This result also prompted us to consider this experiment (IP C) for further analysis.

2.4 IP C SwissProt v/s Uniprot analysis

Mass Spectrometry experiments rely on database interrogations for the identification of proteins. The spectra retrieved from such experiments are assigned to peptides originating from proteins contained in the interrogated database. Therefore, the size of a used database dictates which proteins are identified. Importantly, the spectra that do not correspond to a protein present in a given database are not assigned at all. We wanted

Figure 6 Comparison of the data generated in IP C after the interrogation of either Swissprot or Uniprot databases.

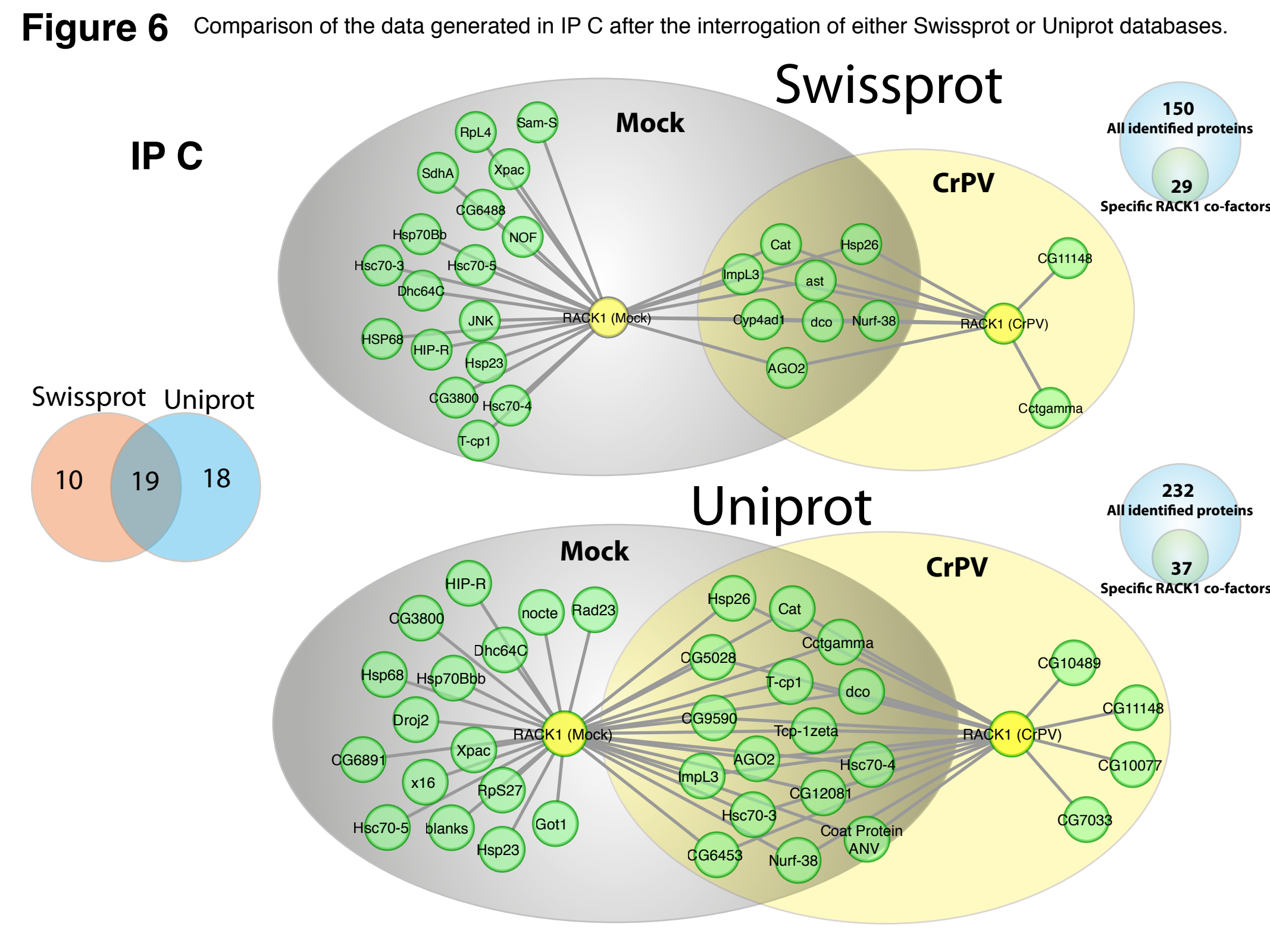

to make sure not to miss important interactants due to the use of only the SwissProt database in our interrogations. Therefore, we used the spectra generated in IP C and re-interrogated the Uniprot database, and determined the RACK1 specific interactants using the same algorithm as before.

While SwissProt is a manually curated and reviewed knowledgebase holding protein information and regarded as the 'gold standard' for annotation, UniProt offer additionally TrEMBL proteins (Translated EMBL) which are automatically annotated and not reviewed. Therefore Uniprot is a larger database compared to Swissprot.

The results of this new analysis are found in Table 1- Chapter 3, Tab IP C Uniprot and Figure 6.

47 proteins in total were identified after the interrogations of both databases and 19 proteins were in common between the SwissProt and Uniprot analysis (Fig. 6). The Uniprot analysis permitted the identification of 18 additional partners. Amongst these 18 partners, many had CG numbers assigned to genes of unknown function (e.g. CG9590, CG10489, CG6891, CG12081), three proteins were identified earlier in the siRNA interactome (CG7033, Tcp-1zeta and Blanks), and one viral protein belonging to the coat of American Noda Virus (ANV) (Fig. 6). ANV has a very similar sequence to FHV; therefore I suspect that this retrieved sequence comes from FHV that is possibly persistent in the S2 cells used. Surprisingly, 10 proteins that were earlier detected with the SwissProt analysis disappeared from the Uniprot analysis, and these were not proteins found in the first database and absent in the latter. As a matter of fact the Swissprot listing of proteins is included in the bigger Uniprot database. The reason for their disappearance stemed from the FDR statistical procedure that is typically set at 1%. To illustrate such a case I will take the JNK protein example. This protein appears as interacting with RACK1 (Fig. 6) in the SwissProt analysis but not in the Uniprot analysis. While there were 232 of total proteins selected from the Uniprot analysis after the FDR1% procedure, there were 150 of total proteins selected in the Swissprot analysis after the same procedure. The FDR 1% correction in the Uniprot analysis listed the JNK at position #259 > 232, therefore this protein was discarded. The FDR1% procedure in the SwissProt analysis positioned JNK at position #104 <150, therefore JNK was retained .

In conclusion, this comparative SwissProt v/s Uniprot analyses pointed out the importance of the choice of the database to be interrogated. Even thought a substantial computational power is required for such analyses; my data clearly advocate for

systematic Uniprot/SwissProt interrogations after data acquisition in general mass spectrometry protein identification procedures.

2.5 MS/MS^{all} SWATH (Sequential Windowed Acquisition of all Theoretical Fragment-ion spectra) quantification of RACK1 partners

We then took advantage of the power of the Triple TOF 5600 System, recently purchased and installed in the proteomic platform at the IBMC. This mass spectrometer enables a sensitive high-resolution quantitation with very fast acquisition speeds. A sequential 25 amu (atomic mass unit) windowed acquisition termed Sequential Windowed Acquisition of all THeoretical fragment-ion spectra (SWATH) interrogates a large mass range yielding a more complicated MS/MS spectra at each step. The major technical advantage of such a method resides in the fact that it enables the use of a larger number of values for the same protein.

Unlike the Label-free method that uses the average areas of spectra of peptides for quantification, the SWATH incorporates the areas of ion fragments. This is particularly important, since the accuracy is increased, when a protein is detected with just 1 or 2 peptides with a signal that is close to the background noise, and/or in case of the interference of another peptide with the same retention time (Aebersold et al.).

We chose IP C for the SWATH analysis – coupled to Uniprot database interrogation- as it was the most statistically robust experiment and contained the AGO2 protein.

The results of this analysis are listen in Table 1 within the Tab IP C-SWATH- Uniprot.

Interestingly, the overall ratios and P-values of the identified proteins improved significantly by the SWATH method. Therefore, we adjusted slightly the criterion determining if an identified protein is a RACK1-specific partner. Instead of considering a protein that has a ratio >1 (RACK1/control) as a specific RACK1 partner, we doubled this ratio threshold setting it at 2. We I therefore considered the proteins that had a ratio >2 and a P-value <0.05 or a ratio>3 and a P-value between 0.05 and 0.1. This filtering reduced the list of the total 235 proteins detected with a 1%FDR to 127 protein considered as specific RACK1 partners (Fig. 7A).

This result indicated that the list retrieved from the Label-Free approach roughly quadrupled with the SWATH analysis. While there were 93 new discovered proteins that

Fig. 7 Comparison of RACK1 partners in SWATH v/s Label Free experiments

A

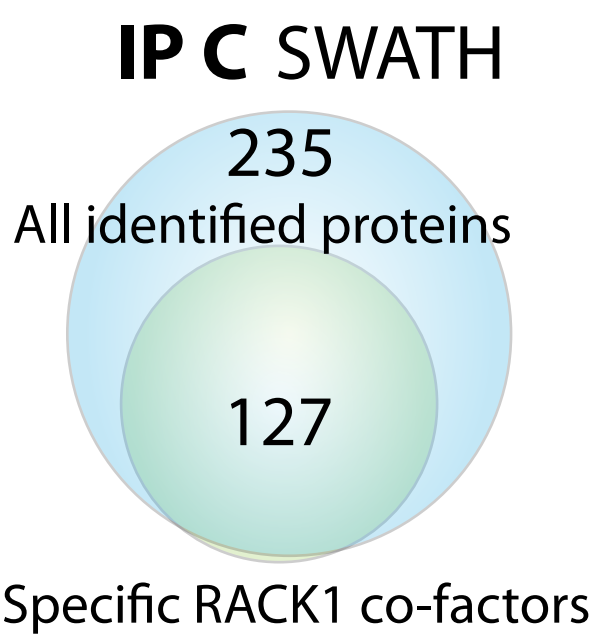

B

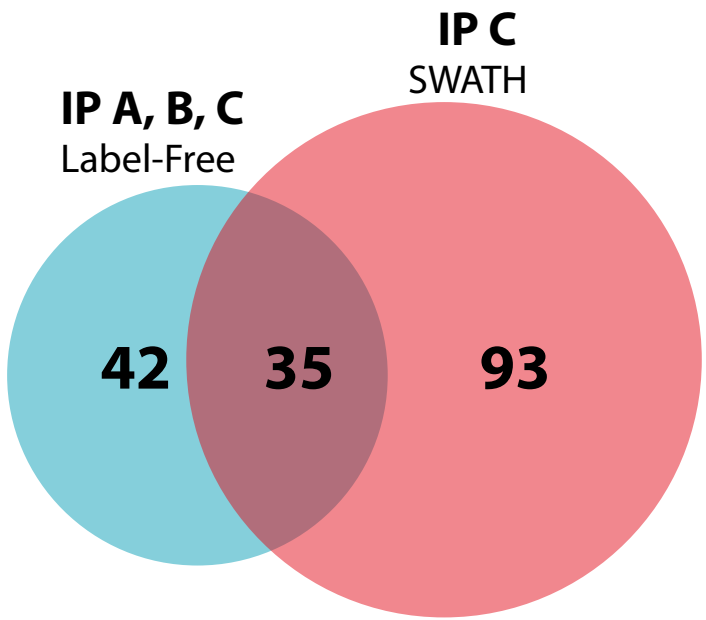

C

Condition	Number of partners
IP A SwissProt	26
IP B Swissprot	24
IP C Uniprot	37
SWATH IP C Uniiprot	127

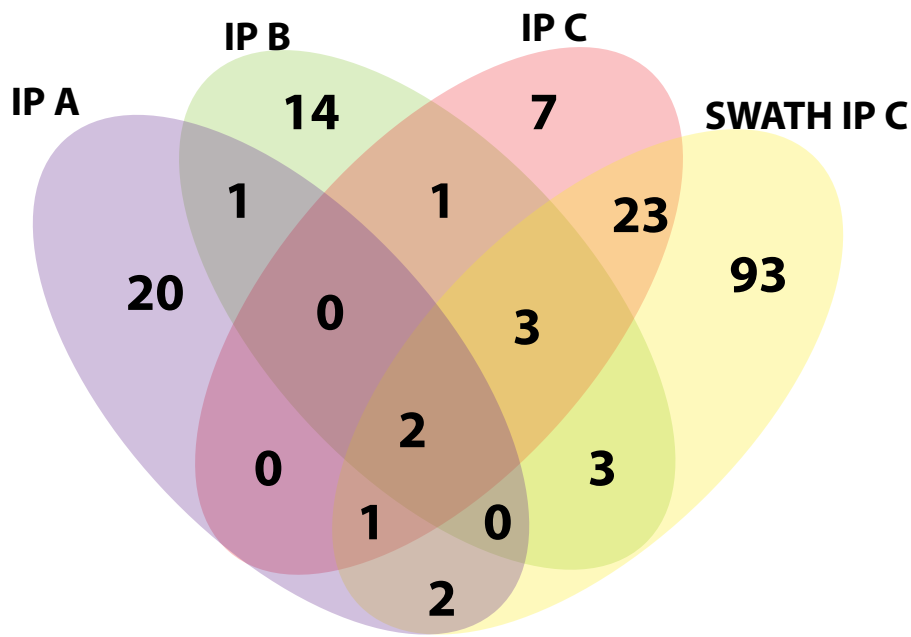

were never significantly enriched while using the Label-Free method, 35 proteins overlapped between the IP A, B, C Label-Free and the IP5 SWATH (Fig. 7B).
There were 43 proteins that were considered as significant with the IP A, B, C Label-free analysis and not with the SWATH (Fig. 7B). Amongst these 43 proteins, 36 were never identified in the IP C Label-Free (Fig. 7C) which made perfect sense, because the samples used in IP A and B were different from those used in IP C. Intriguingly however, 7 proteins that were enriched in the IP C Label-Free were absent from the SWATH analysis (maybe due to protein degradation over time).

A Gene Ontology clustering of the list of 127 proteins retrieved from the SWATH analysis was very insightful in regard to the different complexes in which RACK1 is possibly present (Fig. 8). Unlike the Label-Free experiments, the SWATH identified an important number of ribosomal proteins as significantly enriched in RACK1 samples.
There were 12 ribosomal proteins present (RpS27, RpL4, RpS18, RpS20, RpS14b, RpS17, RpL21, RpS28b, RpL40, RpS3, RpL22, RpL12). Moreover, many translation regulation factors were also identified (eIF-2alpha, Ef2b, eIF-4B, pAbp, Dp1, AGO2) (Fig. 8).
Interestingly, the clustering identified two more categories of proteins that might also be connected to the ribosomal function of RACK1: RNA binding proteins (Hrb27C, How, Lark, fl(2)d, Pen, Blanks) and RNA helicases (Bel, Hel25E).
As previously observed, a large number of factors involved in protein folding were also identified in the RACK1 network (e.g. Heat shock cognates and Chaperonins).
The other unveiled categories, that do not necessary relate to RACK1 ribosomal function, included general cell metabolism enzymes (e.g. RnrL, SdhA), cytoskeleton associated proteins (e.g. Map205, Jupiter, Tsr) and very few nuclear proteins (e.g. Xpac, Nurf-38). Importantly, roughly ~25% of the identified proteins were of unknown function (e.g. CG3800, CG9590) and surprisingly very few are involved in signal transduction pathways (Rab1, Polo and Pzg).
At last, the analysis of RACK1 partners in the infected conditions, show a reduction in the network of partners upon CrPV challenge, similar to the earlier observations in the Label-Free experiments. There was just one protein (Pzg) that seemed to be recruited to RACK1 upon CrPV infection (Fig. 8). However, a careful look at Table 1 IP C SWATH reveals a low-confidence in the fact that this interaction was truly induced by the virus. Pzg corresponding values in non infected conditions show ratios >2 but a P-value>0.05.

Fig. 8 A Gene Ontology clustering of RACK1 partners retrieved from the SWATH analysis

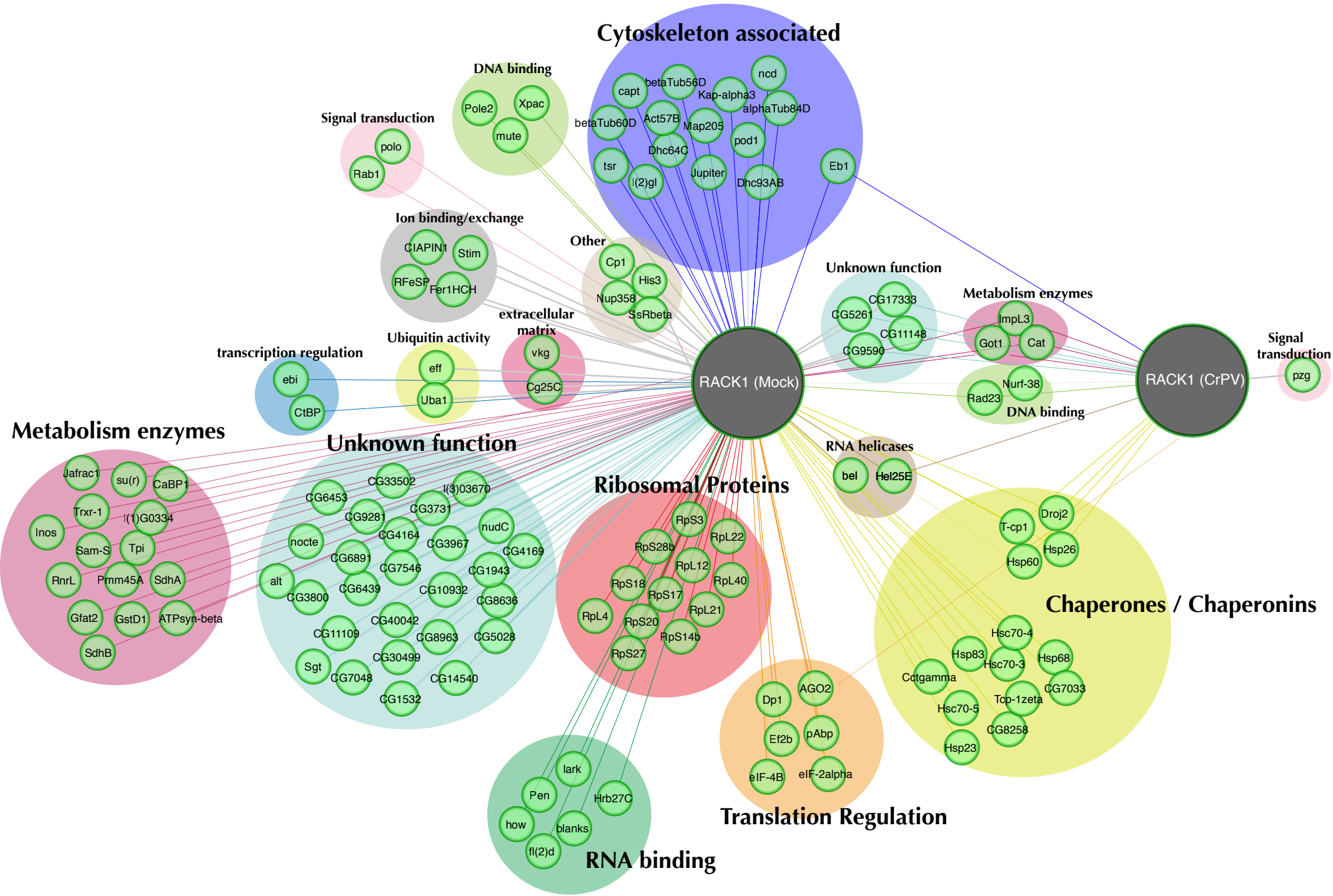

For this reason it was not considered as present in the mock conditions. Unfortunately, unlike IP B and IP C Label-Free, the SWATH analysis did not reveal high-confidence RACK1 partners that were specifically recruited upon CrPV infection.

Overall, our results show that the SWATH analysis increased significantly the sensitivity of protein detection and quantification. However, this method is very novel and has not been utilised in many studies yet. Therefore, it is hard to evaluate the confidence one can have in it. For the moment; the “gold standard“ quantification approach in Mass Spectrometry on a TripleQUAD instrument is the SRM/MRM and on a QTOF instrument it is still the Label-Free method. The TriplTOF instrument on which our SWATH analysis was performed is a hybrid between the TripleQUAD and the QTOF. The coming years will be crucial in determining if the SWATH is a reliable approach. The use of independent protein quantification approaches (e.g. SRM/MRM, western-blotting) to reproduce the SWATH results will help assessing the accuracy of this method.

2.6 An RNAi screen on a selected number of identified RACK1 partners

Next, I wanted to determine if any of the identified co-factors would show a phenotype similar to RACK1 regarding virus (IRES- or cap-dependent) replication.
Therefore, we adopted an approach similar to the one undertaken in Chapter 1, knocking-down the genes of interest by RNAi and quantifying viral replication of four different viruses: DCV, CrPV, FHV and VSV. The screen procedure (design and synthesis of dsRNA, cell soaking, viral infection and viral load quantifications) was identical to the one adopted in Chapter 1. However, the selection of the genes to test differed because the proteomic read-out was different (Label-Free/SWATH enrichment rather than the on/off MudPit method used in Chapter 1).

Our proteomic experiments generated an important amount of candidate genes. We selected only 50 candidates to test (including AGO2 and RACK1). These 50 were all at least detected with FDR1%. 45 of them (90%) were significantly enriched in RACK1 pull-down samples in at least one of the experiments, IP A, IP B, IP C Label-Free and IP C SWATH. The remaining 5 proteins amongst the 50 tested (RpL24, RpS25, Rm62, eIF3-S10 and RpL3) were not significantly enriched in RACK1 samples (4> ratio >1 but

Table 2. Functional screen of a selection of identified proteins. The left panel in the table resumes the identification status of the indicated protein in different experiments:
* means that a protein was detected and has a statistically significant enrichement in RACK1 pull-downs , ns means that a protein was detected without being significantly enriched in RACK1 pull-downs,
- means that a protein was not detected at all . The right panel shows the viral titers after knock-down of the indicated genes compared to Mock condition (dsRNA against GFP) that was set to 1.

Proteomic screen											Functional screen							
	Detection Status								Enrichement with RACK1 in SWATH		Effect of loss-of-function on viral replication							
	Label-Free			IP C SWATH	N-ter Tag	C-ter Tag	Mock	Infected										
Candidate	IP A	IP B	IP C						Ratio	P-value	DCV		CrPV		FHV		VSV	
RACK1	*	*	*	*	*	*	*	*	37	>0.05	**0,13**	**	**0,08**	**	0,94	ns	1,03	ns
AGO2	ns	ns	*	*	*	*	*	*	7.23	0.010	**1,90**	**	**1,54**	*	0,91	ns	**3,63**	***
Xpac	-	-	*	*	*	ns	*	ns	25.54	0.005	0,77	ns	0,99	ns	0,80	ns	0,98	ns
CG3800	-	ns	*	*	*	*	*	ns	75.11	0.001	0,80	ns	1,30	ns	0,77	ns	1,09	ns
CG9590	-	-	*	*	*	*	*	*	76.91	0.01	**0,73**	*	1,42	ns	0,79	ns	1,15	ns
Hsp26	ns	*	*	*	*	*	*	*	131.91	0.001	0,82	ns	1,04	ns	0,82	ns	1,08	ns
Nurf38	-	-	*	*	*	*	*	*	14.51	0.002	**1,46**	*	**2,42**	*	0,71	ns	**1,51**	*
RpS27	-	-	*	*	*	*	*	ns	21.71	0.024	1,02	ns	**2,14**	*	**1,99**	*	**4,40**	*
Hsp70	-	-	*	*	*	ns	*	ns	9.51	0.03	0,93	ns	0,79	ns	1,07	ns	1,20	ns
ImpL3	-	ns	*	*	*	*	*	*	22.41	0.007	0,77	ns	0,94	ns	**0,79**	*	**1,48**	*
Cat	ns	ns	*	*	*	*	*	*	42.41	0.002	**0,77**	*	0,99	ns	0,84	ns	1,14	ns
dco	-	ns	*	-	*	*	*	*	3.61 (Label-Free)	0.01	0,78	ns	1,50	ns	1,01	ns	1,49	ns
CG10630	-	-	*	*	*	*	*	ns	17.82	0.003	1,19	ns	0,83	ns	1,04	ns	1,08	ns
CG5028	-	-	*	*	*	*	*	*	7.92	0.012	0,77	ns	1,10	ns	0,89	ns	1,00	ns
Hsp23	-	ns	*	*	*	*	*	ns	19.01	0.012	0,99	ns	1,40	ns	1,13	ns	1,03	ns
T-cp1	*	*	*	*	*	*	*	*	6.45	0.04	**15,49**	***	**8,43**	***	**3,73**	***	**8,09**	***
Dhc64c	-	ns	*	*	*	*	*	ns	180.1	0.012	**5,15**	**	**1,71**	**	0,93	ns	1,34	ns
Got1	-	-	*	*	*	*	*	*	24.88	0.019	0,91	ns	0,72	ns	0,93	ns	1,24	ns
RpL24	ns	ns	-	-	ns	ns	ns	ns	3.63 (Label-Free)	0.39	**4,17**	*	**5,60**	***	**4,96**	***	**5,38**	***
CG11505	*	ns	ns	-	ns	*	*	ns	1.71 (Label-Free)	0.004	**1,74**	*	1,43	ns	1,28	ns	1,10	ns
Sam-S	ns	ns	*	*	*	*	*	ns	17.65	0.003	**2,99**	***	**3,07**	**	1,53	ns	**1,71**	**
RpS25	ns	ns	-	-	ns	ns	ns	ns	2.16 (Label-Free)	0.83	**1,93**	*	0,53	ns	**4,38**	***	**7,87**	***
Rm62	ns	ns	-	-	ns	ns	ns	ns	6.03 (Label-Free)	0.315	**6,42**	***	**6,45**	***	**2,83**	***	**5,70**	***
eIF-4a	*	ns	-	ns	*	*	*	ns	1.46 (Label-Free)	0.001	0,76	ns	**0,54**	**	0,72	ns	0,84	ns
RpL40	*	ns	ns	*	*	*	*	ns	8.29	0.0009	**3,30**	*	**5,39**	**	**1,79**	*	**0,52**	**
blw	ns	*	ns	ns	*	*	*	ns	4.21 (Label-Free)	0.053	1,19	ns	**1,23**	*	**0,66**	*	0,75	ns
Tango7	*	ns	-	-	ns	*	*	ns	2.71 (Label-Free)	0.016	**3,02**	***	**2,86**	**	1,31	ns	1,12	ns
eIF3-S9	ns	*	-	-	*	ns	*	ns	2.48 (Label-Free)	0.013	**2,79**	*	**6,09**	**	1,18	ns	1,20	ns
eIF3-S10	ns	ns	-	-	ns	ns	ns	ns	2.65 (Label-Free)	0.456	**2,14**	*	**3,27**	*	0,95	ns	0,75	ns
RpL3	ns	ns	-	-	ns	ns	ns	ns	6.57 (Label-Free)	0.394	**2,40**	*	**7,37**	**	1,51	ns	0,77	ns
Arp66B	*	ns	ns	ns	ns	*	*	ns	1.65 (Label-Free)	0.003	1,11	ns	1,20	ns	**0,63**	*	0,97	ns
CCTγ	*	*	*	*	*	*	*	*	6.16	0.005	**8,72**	***	**5,08**	***	**1,66**	*	0,87	ns
aralar1	*	*	-	-	*	*	*	*	6.14 (Label-Free)	0.0003	0,85	ns	**0,69**	**	0,82	ns	0,98	ns
RpL31	ns	*	ns	ns	ns	*	*	ns	8.80 (Label-Free)	0.0106	**2,17**	**	**5,54**	***	1,18	ns	**0,63**	*
CG12081	-	-	*	ns	*	*	*	*	4.185 (Label-Free)	0.036	1,06	ns	1,03	ns	1,00	ns	1,51	ns
nudC	-	-	ns	*	*	*	*	ns	9.47	0.001	**1,91**	**	**1,67**	*	1,04	ns	1,00	ns
SdhB	-	-	ns	*	*	ns	*	ns	3.67	0.0021	0,73	ns	0,82	ns	1,00	ns	1,00	ns
CG10077	-	-	*	ns	ns	*	ns	*	2.15	0.056	0,95	ns	0,78	ns	1,00	ns	1,03	ns
Hsp60	ns	ns	ns	*	*	*	*	*	16.15	0.006	**1,74**	**	1,16	ns	0,85	ns	0,96	ns
Hsp68	-	ns	*	*	*	*	*	ns	8.04	0.0041	0,94	ns	1,28	ns	0,53	ns	1,25	ns
Inos	ns	ns	ns	*	*	*	*	ns	8.36	0.0304	1,09	ns	1,17	ns	0,56	ns	1,24	ns
Hsp83	ns	-	ns	*	*	*	*	ns	6.18	0.002	**2,05**	***	1,56	ns	1,23	ns	**1,63**	*
Tub84D	ns	ns	ns	*	*	*	*	ns	23.32	0.0183	1,26	ns	1,15	ns	0,84	ns	0,99	ns
EF1a1	*	ns	ns	ns	*	ns	ns	*	1.68 (Label-Free)	0.014	2,25	ns	1,41	ns	1,14	ns	**1,53**	***
Hsc70-4	ns	*	*	*	*	*	*	ns	14.62	0.0049	**1,96**	***	**3,68**	**	0,97	ns	**1,34**	**
ncd	ns	ns	ns	*	*	*	*	ns	4.73	0.0037	**1,96**	**	**1,66**	**	0,71	ns	**1,72**	***
Hsc70-3	ns	ns	*	*	*	*	*	ns	6.36	0.002	**2,58**	*	**2,60**	***	1,07	ns	**1,18**	*
Hsc70-5	ns	*	*	*	*	*	*	*	3.51	0.012	**2,27**	*	**2,33**	***	1,04	ns	**1,27**	**
RnrL	ns	ns	ns	*	*	ns	*	ns	3.18	0.008	**5,32**	***	**4,48**	***	1,39	ns	**1,82**	***
Trxr1	-	ns	ns	*	*	ns	*	ns	3.82	0.0008	**2,16**	*	**1,39**	**	1,19	ns	1,39	ns

P-value >0.05). The rationale to include these five proteins in the analysis was hypothesis driven, as they seemed to constitute the perfect “usual suspects“ for a potential involvement in translation regulation.

The fifty genes selected and tested in Table 2 are listed. The results from both the proteomic and the functional RNAi screen are shown. The left part of the table (Proteomics) indicates in which IP the protein was significantly detected, with which RACK1 Tag and in which condition (Mock v/s Infected). The ratios and the P-values from the SWATH or the Label-Free are explicated. In the right part of the table (Table2) are listed the relative viral loads values (CrPV, DCV, FHV, VSV) after depletion of the indicated genes, followed by the statistical test result.
The knock-down of 27 out of the 50 tested genes show a significant two-fold change in the viral loads for at least one of the four viruses. The knock-downs that resulted in such changes are plotted in Figure 9. These 27 genes included RACK1 and AGO2, our positive controls. As expected RACK1 knock-down inhibits the replication of both DCV and CrPV, without affecting the viral loads of VSV and FHV. The knock-down of AGO2 increases DCV, CrPV and VSV replication, but had no effect on FHV (this observation is recurrent when the cells are persistently infected with FHV).
Amongst the tested genes, T-cp1, RpL24 and RpL40 affected the viral loads of all four viruses (Fig. 9). Rm62 as shown in Table 2 also affected the replication of the four viruses but this result was not reproduced when we used a second dsRNA to target this gene, which explains why we did not plot it in Figure 9.

There were five proteins (Dhc64C, Tango7, eIF3-S9, eIF3-S10, RpL3) other than RACK1 that affected significantly the replication of both CrPV and DCV without affecting VSV and FHV (Table 2-Chapter 3, Fig. 9). However the effect of the depletion of these proteins have opposite effect than RACK1, as they all showed enhanced CrPV and DCV viral loads, and no effect on FHV and VSV loads.
On the other hand there were no proteins that affected exclusively VSV and FHV replication (Fig. 9). However, the depletion of a number of proteins affected the replication of three viruses out of the four tested, and sometimes in opposite fashions. For example, the depletion of RpS25 caused a slightly enhanced replication of DCV (~2 fold) and a markedly enhanced replication of VSV and FHV (~4 to 8 folds), however RpS25 depletion negatively but non significantly CrPV replication (Table 3-2, Fig. 9).

Fig. 9 **Functional RNAi screen results.** The viral loads of the viruses were quantified by RT- QPCR and the relative amounts (relative to dsRNA GFP treatement) is plotted on the Y axis. The X axis indicates which dsRNA treatement was employed for gene knock-down. (ns: non significant t-test)

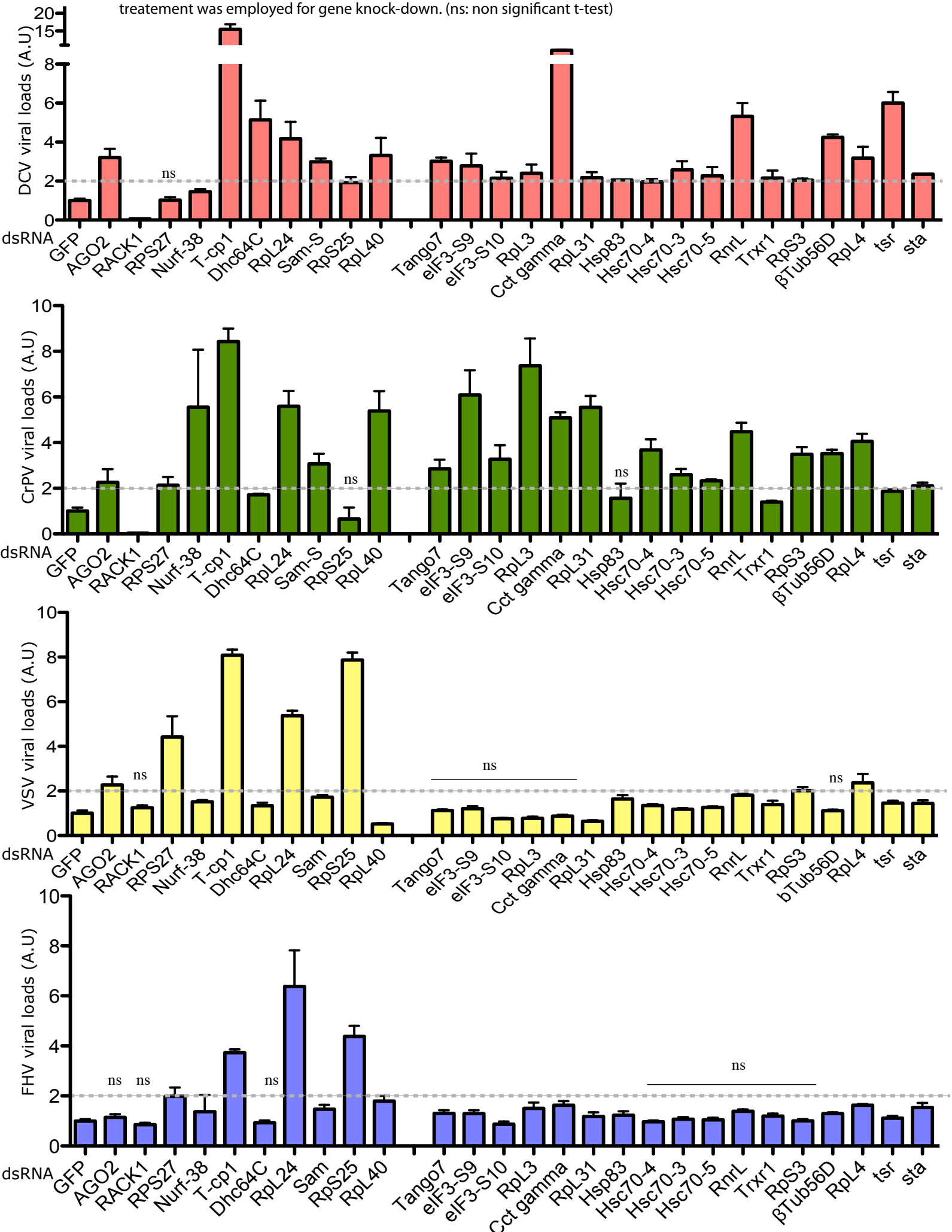

Another example is the Cct-gamma protein. The depletion of Cct-gamma caused an enhanced DCV and CrPV replication (~5 to 9 folds), and had only a slight effect on FHV replication (~1.6 fold) and no effect on VSV replication (Table 2-Chapter 3, Fig. 9).

Finally, we were unable to identify any protein that behaved like RACK1 regarding the replication of the 4 viruses. This analysis permitted, however, the identification of some translation associated proteins (ribosomal proteins or translation factors) like RpS25, RpL40, RpS27, RpL24 and RpL3 or eIF3-S9, and Tango7 (Table 2-Chapter 3, Fig. 9), that might be involved in specific viral translations. For instance, RpL40's depletion affected negatively the replication of VSV and had an opposite effect on the other three viruses, strengthening the recent finding concluding that this protein might be involved in VSV's cap-dependent translation (Lee et al., 2013) . However one should be cautious in the interpretation of these data. As mentioned in Chapter 1, the viability Z-score (Boutros et al., 2004) is an important factor to take into consideration in order to assess if the observed phenotype is significant or results from cell death. Interestingly, four of the hereupon mentioned ribosome related factors (RpS25, RpS27, eIF3-S9 and Tango 7) had a viability Z-score < 3, indicating that the knock-down of these proteins did not have an important effect on cell growth and viability.

Last, this analysis also confirmed the role that the T-cp chaperonins might have in antiviral immunity (T-cp1, Cct-gamma) (See Chapter-1).

3. Conclusion

We undertook here a functional proteomic analysis similar to the one described in Chapter 1, aiming to identify RACK1 co-factors that might be involved in IRES-viral replication.

In order to identify RACK1 partners, we used a standard Mass Spectrometry quantification method (Label-Free) and explored a novel technique enabled by the Triple-ToF (AbiSciex) machine, termed SWATH analysis. In the course of this analysis I was able to show, that different experimental factors, as well as, adjustments in the parameters of the Mass-Spec protein discovery strategy, can influence greatly the outcome of the results. Many factors turned out to be crucial throughout my analysis.

First, the experimental parameters that were important are the Tag and bead type on one hand and the bead-lysates incubation times, on the other hand. The choice of the negative control experiments turned out to be also a crucial parameter. An important lesson from the study is that in overexpression/ IP strategies one should take into account the nature of the negative controls because the overexpression of a protein might influence the overall proteome and consequently the retrieval of non-specific factors.
A second point that I recommend for future studies, is the use of stably rather than transiently transfected cell lines. The overexpression of a protein can induce artifactual interactions, moreover, it might be not suited to study the interaction of proteins like RACK1 that are part of huge molecular complexes like the ribosome.

The best negative control we propose, would then be a cell line that stably expresses a transgene harbouring a Tag that is insensitive to the antibody–coupled beads used for the pull-down of the “real baits“. Second I was able to point out that the database interrogation step influences also greatly the final read-out. Even thought, this step is computationally not trivial, I recommend parallel databases interrogations for future identification and quantification studies.

Finally, my functional RNAi screen was unable to identify any selected co-factor that phenocopied RACK1 depletion, in regard to viral replication (IRES v/s Capped viruses). This maybe due to several reasons. The first being the experimental strategy of transient over-expression that was adopted. Such a transient over-expression might be not sufficient for an optimal participation of RACK1 in proper ribosomal biogenesis. Therefore, the retrieved factors might reflect more faithfully the extra-ribosomal partners of RACK1 rather than the ribosomal ones. The second reason that might explain why I missed such RACK1-like factors is the selection of only 50 genes to test. Although our overall proteomic analysis identified around 170 significant RACK1 partners we only tested a subset of 50 genes. We might have missed the hunted factor. Nevertheless, I was able to identify some factors involved in viral specific translation/replication. For instance, I was able to reproduce the finding involving RpL40 in VSV-specific replication (Lee et al., 2013). Moreover, I find that the depletion of RpS25, that is known to affect the CrPV IGR IRES translation (Hertz and Thompson, 2011; Landry et al., 2009; Nishiyama et al., 2007), affected negatively (even thought not significantly) CrPV replication. However, the most intriguing finding is that, the depletion of RpL40 affects the replication of the IRES containing viruses (CrPV and DCV) exactly in the opposite fashion, and the depletion of RPS25 affects the replication of Capped viruses (FHV and VSV) exactly in the opposite fashion as well, enhancing in each case viral replication. This argues that the different ribosomal pools in the cell are occupied differently by each viral mRNA, and the depletion of some characteristic components of these ribosomal pools (e.g. RpL40, RpS25) disturbs the ribosomal occupancy pattern of viral mRNAs.

Last, the reason why factors giving a phenotype similar to RACK1 upon depletion, were not identified, might simply be because there are not any. The observed involvement of RACK1 in the regulation of IRES-mediated translation could be simply of a structural nature rather than a modulatory one. Following this logic, RACK1 might be important for the accommodation of specific mRNA on the ribosome. This hypothesis is plausible since RACK1 does not have any enzymatic function. Future Cryo-EM studies of RACK1 depleted ribosomes interacting with viral mRNAs would allow to address such a hypothesis.

V- Materials and Methods

Molecular cloning

cDNAs from the Dcr-2, AGO2 and r2d2 genes were amplified by standard PCR and inserted into a pDONR221 vector (Invitrogen) using the Gateway® cloning technology (see Primers table). The PCR fragments were recombined (BP reaction) with pDONR221 to obtain pENTRY-N-Dcr-2, pENTRY-N-AGO2, pENTRY-N-r2d2 or pENTRY-Dcr-2-C, pENTRY-AGO2-C and pENTRY-r2d2-C, and sequenced. An insect expression vector was then generated: the pDEST vectors pDEST-BIO-N or pDEST-BIO-C are based on the pIZ/V5-His (Invitrogen)- backbone and contain the biotin-tag sequence (encoding the GLNDIFEAQKIEWHE peptide) at the 5' or 3' end of the ccdB gene, a chloramphenicol resistance gene flanked by attR1 and attR2 sites, and DCV intergenic internal ribosomal entry site fused with a truncated cDNA encoding the transmembrane and cytoplasmic region of human CD4, to allow sorting of stably transfected cells. To construct the IRESCrPV-IGR reporter vector, the Renilla Luciferase- IRESCrPV-IGR - Firefly Luciferase cassette was amplified from the pSRT208 plasmid (Landry et al., 2009), with primers containing KpnI and NotI restriction sites, and inserted into the corresponding sites of the pACT5C-His vector. Regarding the IRESCrPV-5', cDNA was prepared from CrPV infected cells, and used as template for PCR with primers complementary to the IRESCrPV-5' (See Primers table). The PCR product was cloned in a pRL-ACT5C vector giving pACT5C- IRES5'CrPV - Renilla Luciferase. Importantly, the Met initiator codon of the Renilla Luciferase was deleted and replaced by the first 16 codons of the CrPV ORF1 protein. All plasmids were verified by sequencing.

The plasmid containing the shRNA targeting the 5'UTR of the RACK1 gene was constructed by annealing the two oligos pre-designed by the TRiP project (http://www.flyrnai.org/TRiP-TTR.html) (Ni et al., 2011) (see Table S2- Chapter 2) and flanked by SpeI and EcoRI restriction sites and ligating them between the corresponding sites of the Drosophila pMT-V5His vector (Invitrogen). Stable S2 cell lines bearing the plasmid were selected as described (Dimarcq et al., 1997).

The RACK1 variants (R38D K40E and D108Y) unable to bind to the ribosome

were constructed by site directed mutagenesis using the QuikChange® Site-Directed Mutagenesis Kit (Stratagene). The residues R38, K40, and D108 from Drosophila RACK1 correspond to the previously characterized residues R36, K38 and D109 from yeast RACK1 (Asc1p) (Coyle et al., 2009; Kuroha et al., 2010). Briefly, a wild-type RACK1 cDNA clone (ORF from DmRACK1 cloned in pDONR221) was used as a template for the PCR using the mismatched primers listed in the Primers Table. The DONOR clones were verified by sequencing, and then recombined using the Gateway LR reaction to pAHW plasmid (from the Drosophila Gateway collection) to express with the Actin5C promoter N-terminally HA tagged versions of RACK1 wt or mutants. The same DONOR clones were used to generate plasmids ready to inject in fly embryos (Genetic Services), for transgenesis based on the phiC31 system. The resulting vectors express RACK1 with an N-terminal HA tag, from the HSP promoter.

Reporter plasmids bearing the HCV IRES and the 14 first nucleotides of the HCV core sequence (nt 343 to 357) fused to a luciferase reporter gene (IRESHCV-Luc) or control plasmid expressing the luciferase reporter gene (CTRL-Luc) have been described (Wolf et al., 2008). IRESHCV-Luc and CTRL-Luc encode an IRES-translated mRNA and a cap-dependent mRNA, respectively (Figure 4G- Chapter 2). Plasmids were stably transfected into Huh7.5.1 cells using geneticin® (Sigma) selection. Cells were then reverse transfected with 10nM siRNA specific for RACK1 (siRACK1), HCV IRES (siHCV), ribosomal protein RPS3 (siRPS3) or with control siRNA (siCTRL). Three days later, IRES-mediated and cap-dependent translation were analyzed by luciferase activity of the reporter gene in cell lysates as described (Wolf et al., 2008).

Protein purification, identification and quantification by Mass Spectrometry

Dcr-2,AGO2 and R2D2

Cells expressing the bait proteins (AGO2, Dcr-2 and R2D2) were either mock infected or infected with DCV at multiplicity of infection (MOI) 1 for 8 or 16h, with FHV at MOI 0.1 for 16h or with VSV at MOI 10 for 48h. Protein purification and identification was performed as described (Fukuyama et al., 2012). Briefly, 20 million cells for each condition were lysed in 1mL of TNT buffer (50 mM Tris-HCl, pH7.5, 150 mM NaCl, 10% Glycerol, 1% Triton X-100, 100 mM NaF, 5 µM ZnCl2, 1mM Na3VO4, 10mM EGTA, pH8.0, Complete Protease Inhibitor Cocktail containing EDTA from Roche). Lysates were kept on ice for 30 min then centrifuged at 13,000 rpm for 30 min at 4°C. Supernatants were mixed with 150µl of prewashed streptavidin–sepharose beads and

incubated for 30 min at 4 °C in a rotative agitator. Beads were washed three times with 1mL Wash buffer I (50 mM Tris–HCl, pH7.5, 150 mM NaCl, 10% Glycerol, 0.1% Triton X-100, 100 mM NaF, 5µM ZnCl2, 1mM Na3VO4, 10mM EGTA, pH8.0), one time with 1mL Wash buffer II (Wash buffer I without Triton X-100), and suspended in 1mL Wash buffer II plus Complete Protease Inhibitor Cocktail containing EDTA. The on-beads tryptic digestion method was used on the purified samples (Fukuyama et al., 2012). After reduction/alkylation (DTT, 5mM final, 30 min, 56 °C/ Iodoacetamide 25mM final, 20 min in the dark), 10ng trypsin (modified sequencing grade, Roche) in 150mM ammonium carbonate was added and samples were incubated overnight at 37°C with shaking. Then, the reaction was stopped with 10µL 10% formic acid (FA). Peptides were recovered and the beads were discarded by filtering through C18 Tips (Proxeon). Peptides were eluted with 20µL 50% methanol, 5% FA. 5µL of peptides diluted 1:5 in water (5% of the total amount of material) were purified on a capillary reversed phase column (nano C18 Acclaim PepMap100 Å; 75µm internal diameter, 15cm length; Dionex), at a constant flow rate of 220nL.min-1, with a gradient 2% to 40% buffer B (water/acetonitrile/FA 10:90:0.1 (v:v:v)) in buffer A (water/ acetonitrile/FA 98:2:0.1 (v:v:v)) over 45min.

The first MS analysis was performed on a FT ICR mass spectrometer (LTQ-FT Ultra, ThermoFisher Scientific, San Jose, CA) with the top 7 acquisition method: MS resolution 60,000; mass range 500-2000 Th; followed by 7 MS/MS (LTQ) on the 7 most intense peaks, with a dynamic exclusion for 90s. The raw data were processed using Xcalibur 2.0.7 software and Mascot deamon. Each sample was first analyzed in triplicate then an exclusion list was added for three next runs. The database search was done on merged data using Mascot search engine (Matrix Science Mascot 2.3) on the 17D melanogaster database (16535 sequences) concatenated with protein sequences of DCV, FHV and VSV. Proteome Discoverer 1.3 (ThermoFisher Scientific) and Mascot were used to search the data and filter the results. The following parameters were used: up to 2 miss cleavages; MS tolerance 10ppm; MSMS tolerance 1Da; full tryptic peptides; partial modifications: carbamidomethylation (C), oxidation (M, H, W), Phosphorylation (Y).

Validation was performed on proteins identified using two filters: (1) only proteins identified with a FDR<1% (Peptide Validator Mascot significance threshold) and at least 1 peptide score above 30 were selected; (2) only proteins identified with 2 distinct sequences with ion score above 30, or 1 sequence with ion score above 30 with and a

MudPIT score above 49. Proteins identified by a peptide matching another protein were not taken into account and were filtered out for gene selection and subsequent validation tests. According to a preliminary study (data not shown), proteins that passed filter (2) and not filter (1) were manually checked: they were validated if the identified sequence was specific to the associated gene after control of the MS/MS spectrum (see Table S1). Protein that passed filter (1) and not the more stringent filter (2) were not considered. All proteomic raw data are available in the Pride database under accession numbers 24806- 24848 (http://www.ebi.ac.uk/pride).

RACK1

RACK1 immuno-precipitation (Chapter 3) was performed after the transient transfection (Effectene, Qiagen) of RACK1-3xHA or 3xFLAG tagged versions in 30 million cells in triplicates. The immuno-precipitation procedure was nearly identical to the one described above (same buffers). However, the incubation times of lysates/antibody-coupled beads was shorter for IP B and IP C (1 hour rather than overnight). The beads used were Anti-DYKDDDDK from Clonetech and Anti-HA from SIGMA. The elution of the immunoprecipitated baits and co-factors was performed with the Laemmli buffer. The eluates were then loaded on Bio-rad precasted SDS-PAGE gels and run on 100V for one hour.

Protein bands excised from the gels were transferred into 96-well microtitration plates. Gel slices were washed with three cycles of incubations in 25mM ammonium bicarbonate for 15 min and then in 25mM ammonium bicarbonate containing 50% (v/v) acetonitrile for 15 min. Samples were dehydrated with 100% acetonitrile and then reduced with 10mM DTT for 1 hour at 56°C. Proteins were then alkylated with 55mM iodoacetamide for 1 hour in the dark at room temperature. Gel pieces were washed again with the destaining solutions described above. 20ng of modified sequencing-grade trypsin (5ng/µL ; Promega, Madison, WI) in 25mM ammonium bicarbonate was added on each dehydrated gel piece. After 30 min of rehydratation at room temperature, 30µL of 25mM ammonium bicarbonate was added on gel pieces before digestion, overnight at 37°C. The resulting peptides were then extracted from the gel pieces in 30µL of 60% acetonitrile and 5% formic acid. The initial digestion and extraction supernatants from the same gel lane were pooled and vacuum-dried in a SpeedVac. The dried peptides were re-suspended in 15 µL of water containing 0.1% FA (solvent A). Peptide mixtures were analyzed using a NanoLC-2DPlus system (with nanoFlex

ChiP module; Eksigent, ABSciex, Concord, Ontario, Canada) coupled to a TripleTOF 5600 mass spectrometer (ABSciex) operating in positive mode. 5µL of each sample were loaded on a ChIP C-18 precolumn (300 µm ID x 5 mm ChromXP; Eksigent) at 2µL/min in solvent A. After 10min of desalting and concentration in the trap, the precolumn was switched online with the analytical ChIP C-18 analytical column (75µm ID x 15cm ChromXP; Eksigent) equilibrated in 95% solvent A and 5% solvent B (0.1% formic acid in ACN). Peptides were eluted by using a 5%-40% gradient of solvent B for 60 minute at a flow rate of 300 nL/min. The TripleTOF 5600 was first operated in data-dependant acquisition mode with Analyst software (ABSciex). Survey MS scans were acquired during 250 msec in the 400-1250 m/z range. Up to 20 of the most intense multiply charged ions (2+ to 5+) were selected for CID fragmentation, if they exceeded the 150 counts per second intensity threshold. Ions were fragmented using a collision energy spread of 45eV±15eV within a 50 ms accumulation time and an exclusion time of 15s. This so-called “Top20” method, with aconstant cycle time of 3.3s, was set in high-sensitivity mode. Each sample was submitted to a “Top20” discovery analysis followed by a SWATH-MS acquisition using an isolation width of 26 Da (1 Da window overlap for optimal efficiency). The method was constructed with 34 consecutive windows covering a 400-1250 mass range, with a constant cycle time of 3.5sec (250msec TOF-MS survey scan followed by the 34 SWATH windows with a 100msec accumulation time). To obtain an optimal mass accuracy, a beta-galactosidase digest (ABSciex) was injected before each sample using the “Autocal” feature in the batch mode from Analyst software: calibration was performed using the 10 more abundant peptides in MS mode and with the 729.xxx m/z precursor in MS/MS mode. Moreover, to prevent carry-over due to stationary phase memory, 2 consecutive washing runs were performed after each cycle of injections.

Data were searched against a D.melanogaster database. The complete proteome set from the UniProt database (released 2013) was added to human keratins and trypsin sequences and the final fasta file was created adding a decoy database with a Pearl script (Bruker). The first algorithm used was Mascot (version 2.2, Matrix Science, London, UK) through the ProteinScape package (Bruker). Peptide modifications allowed during the search were: N-acetyl (protein), carbamidomethylation(C) and oxidation (M). Mass tolerances in MS and MS/MS were set to 20 ppm and 0.5 Da, respectively, and the instrument setting was specified as ESI-QUAD-TOF. 2 trypsin miscleavages were allowed. Peptide identifications obtained from Mascot were validated with a peptide

FDR of 1% (individual identity scores varied between 34 and 38 for each data search). Paragon (ProteinPilot; ABSciex) was used as a second algorithm to perform database searches. The same UniProt D.melanogaster database was used and search parameters included a large set of biological modifications and the use of a decoy strategy to assess the false-discovery rate. The 18 raw data (.wiff) files acquired with the "Top20" Data-Dependent mode were submitted together to Paragon in order to create a single search result (.group) containing all the identified proteins and peptides validated with a FDR of 1%.

Then, a Label-free Quantification strategy was performed using Data-Dependant acquisitions. In the first instance, the quantification of proteins was carried out using the ABSciex package including PeakView and MarkerView softwares. Proteins validated with a FDR of 1% were loaded into PeakView using the Paragon result file: shared and modified peptides were removed, as well as peptides identified with a confidence lower than 0.95, to obtain a reliable and accurate quantification. For MS1 Data-Dependent acquisitions (Top20 discovery analyses), the following tolerances were used to extract ion chromatograms: 0.05 Dafor precursor masses and 2.5 min windows for retention times. Reconstructed elution peak areas (XIC, eXtracted Ion Chromatogram) for each peptide, in each condition, were then exported to MarkerView for further data processing. After a "Total Areas Sum" normalization, a Principal Component Analysis (Pareto) was performed to assess replicates reproducibility and samples correlation. Resulting tables were then submitted to a Student t-test: peptides and proteins validated with a p-value below 0.05 were considered as statistically significant. The behaviour from a specific peptide or a specific protein over the 18 samples was graphically visualized using the MarkerView individual profile plots. A mean area value for each of the 6 conditions was obtained by averaging the triplicates XICs, thus allowing the calculation of a ratio between 2 states (Immunoprecipitation/Control, Infected/Not-infected).

RNAi screen and viral titer quantification

Primers harboring the T7 polymerase sequence were designed thanks to the E-RNAi online tool. This tool permits the design of long dsRNA optimized for potency and off-target effects. The primers (Table primers) were then used to generate template DNA

for each gene of interest by touch-down PCR on complementary DNA (cDNA). Template size ranged from 300 to 600 nucletides (Fig. 9). The templates were verified on agarose gels for correct sizes. *In vitro* T7 polymerase transcription was then used to generate ~100 dsRNAs targeting different genes. The dsRNA was quality-controled on agarose gels, quantified and then aliquoted in 96-well cell culture plates (3ug/well). Each 96-well plate contained dsRNA against GFP (Mock) and a positive control dsRNA (dsAGO2). The same dsRNA was aliquoted in 6 independant wells for statistical stringency. S2 cells were then reverse-soaked in these plates, and kept with the dsRNA in media without serum for 1 hour. Complete medium was then added and cells were incubated for 4 days at 25°C for efficient silencing. After this treatment cells were challenged with different viruses. Different Multiplicity Of Infections (MOIs) were used : DCV MOI 1, VSV MOI 10 and FHV MOI 0,1. After 16 hours of infection for DCV and FHV cells were eather fixed , for immunostaining ,or lysed for a Reverse Transcription PCR (RT PCR) followed by Quantative PCR analysis (Fig. 9).

Cells were challenged by VSV for 48 hours and only a RT- QPCR was performed to quantify the viral genome as the QPCR and immunoblotting results were similar for DCV and FHV.

Viral RNA load was measured by qRT-PCR using the “Cell to Ct” SYBR green kit (Ambion), according to the manufacturer’s instructions, on a CFX384 Touch™ Real-Time PCR platform (Bio-Rad). The virus specific primers used in this

analysis are listed in Table Primers. Normalization was performed with the housekeeping gene RpL32. At least three independent biological replicates were performed for each experiment.

For DCV and FHV, immunofluorescence experiments were performed as follows:

infected cells were washed twice with PBS, then fixed for 10 min with a 4% solution of paraformaldehyde (PFA). Blocking was performed by incubation of the fixed cells with PBS supplemented with 10% FCS. Cells were then washed twice and incubated for 2h at room temperature with the primary antibody (@ DCV VP2 (Dostert et al., 2005) or FHV CP (Krishna et al., 2003), 1/5000). Cells were washed twice then incubated with an anti - rabbit FITC coupled secondary antibodies for 1h. Images were acquired using the InCELL1000 Analyzer workstation (GE LifeSciences). Image data processing was performed using the InCELL Analyzer software.

As each gene was tested in six independant wells, mean values and standard deviations were calculated and a two tailed t-test was performed, comparing the values

obtained for a given tested gene and those obtained for the dsGFP treatement in the same plate. The screen results are listed in Table 2- Chapter 1. The table contains the proliferation index after each dsRNA treatment, calculated thanks to the DAPI signal. DsGFP treatment was set to 100 %. The table contains the Z-scores obtained from Boutros et al (Boutros et al, 2004) that reflects the effect of the dsRNA treatment on cell viability.

A Z-score ≥ 3 means that the dsRNA treatment causes a cell death phenotype (Boutros et al, 2004). Viral scores were calculated relative to the dsGFP treatement that was set to 1. Each score is followed by the two tailed t-test value.

Two stringent selection criterion were set in order to determine the genes, that strongly and significantly, affect viral replication. First, we observed that the silencing of a subset of genes had a strong effect on the viability and proliferation of S2 cells (e.g ribosomal proteins), complicating the conclusions we can draw from such results. We, therefore, took advantage of the viability scores (Z-scores) published earlier by Boutros et al (Boutros et al, 2004), and discarded all the genes that had a Z-score ≥ 3 (cell viability defects) (Table 2). On the 101 genes tested twelve had a Z-score ≥ 3, which left us with 87 genes. We also discarded genes essential for cell proliferation. We took advantage of the DAPI nuclei/cell quantification we performed to assess this parameter. We assumed that the incubation of th cells with dsRNA against GFP for four days would not affect cell division nor proliferation. Knowing that the cells were seeded at the same numbers on day one (of the dsRNA treatment), the relative proliferation rate for a given condition was calculated by dividing the quantity of nuclei for a dsRNA condition X by the number of nuclei in the dsGFP treated wells. We, then multiplied this ratio by 100, setting dsGFP treatment at 100%. We discarded 17 genes that showed a proliferation index under 50 % (Table 2-Chpater 1). This left us with 70 genes where the dsRNA treatement had no effect on cell viability or proliferation. Second, we ought to determine if the knock-down of the expression of a gene affects significantly viral replication by at least two folds. This treshold was chosen because AGO2 knock-down showed consistently, an increase of at least two folds, in the viral titers. On the 70 genes left, 34 show an increase or a decrease of two folds, in titers of at least one of the three tested viruses, when compared to dsGFP. The results obtained for these 34 genes were very consistent regarding the method used (immunostaining or Q-PCR) (Table 2-Chapter 1, highlighted genes, and Fig.10).

Cell lines, transfection and luciferase assays

Drosophila S2 cells (Invitrogen) were transfected with plasmid DNAs by the CaPO4 precipitation method. 1F3 cells were obtained upon transfection of S2 cells with the pPAC-HA-BirA plasmid encoding the biotin ligase BirA, the Attacin A-luciferase reporter plasmid pJL169 and the puromycin selection plasmid pJL1. The expression vectors pDEST-BIOTIN-N-or-C Dcr-2, AGO2 and r2d2 were transfected into the parental 1F3 cell line and stable clones were selected firstly with zeocine (125 µg.mL-1) and puromycin (1 µg.mL-1), and secondly by flow cytometry monitoring the expression of hCD4 (clone RPAT4;
GE Healthcare). After three rounds of flow cytometry screenings, clones giving moderate and stable expression profiles were characterized by western blot for the expression of the tagged proteins. Stable cell lines containing the vector expressing the inducible shRNA targeting the 5'UTR of RACK1 were also selected with puromycine. The selected clones were subsequently tested for the depletion of RACK1 following the addition of CuSO4 (0.5mM) to the medium.
Reporter plasmids to monitor activity of the two CrPV IRES were transfected in Drosophila S2 cells soaked in dsRNA targeting GFP or RACK1. 48 hours later, cells were lysed and luciferase activity was measured with the Promega dual-luciferase assay, using a Berthold Luminometer. Reporter plasmid to monitor activity of the IRESHCV contained the IRES and the 14 first nucleotides of core sequences fused to the firefly luciferase reporter gene (IRESHCV-Luc), whereas the control plasmid expressed a 5' capdependent firefly luciferase reporter gene (CTRL-Luc), as described (Wolf et al., 2008). These reporter plasmids were stably transfected in Huh7.5.1 cells using geneticin® selection. The cells were then reverse transfected with 10nM siRNAs (Silencer® Select siRNA, Ambion) specific for either RACK1 (siRACK1), ribosomal protein RPS3 (siRibo) or control (siCTRL). Three days later, cell lysates were tested for IRES-mediated and capdependent translation using luciferase activity.

Toxicity assay

Cytotoxic effects of gene silencing on cells were assessed, day 1 to 6 post siRNA transfection, in triplicate by analyzing their ability to metabolize 3-(4,5-dimethylthiazol-2-yl)-2,5-diphenyltetrazolium bromide (MTT) (Sigma). Formazan crystals were solubilized 5 h after adding MTT (0.6mg.mL-1) as described (Lupberger et al., 2011).

Polysome profiling

S2-C7A or S2 cells ± 0.5mM CuSO4 were stimulated for 5 days then challenged with FHV (MOI 0.1) or CrPV (MOI 1). 16 hours post-infection cells were treated with 100µg/mL cycloheximide in PBS for 10 minutes and kept on ice. After centrifugation, cell pellets were frozen in liquid nitrogen. Then, lysis buffer containing 5mM HEPES, 100mM KCl, 10mM MgCl2, 0.1% Triton X-100, 2mM dithiothreitol, 100µg/mL cycloheximide, protease inhibitor and 1U/µL RNAsine, ajusted at pH 7.2 was added. After centrifugation, lysates were collected and put into 7-47% sucrose gradients containing 5mM HEPES, 100mM KCl, 10mM MgCl2, 0.1% Triton X-100 and 2mM dithiothreitol. Gradients and lysates were ultracentrifuged for 2h30 at 37,000 rpm and fractions were collected and monitored using BioRad Econo UV monitor.
RNAs from twenty polysomal fractions were precipitated with Guanidine-HCl 8M and absolute ethanol. Input and polysomal RNA were then purified with Macherey - Nagel RNA purification kit. RNAs were quantified and 200ng of RNAs of every fraction were used for reverse transcription. A quantitative PCR with specific primers was then performed. Quantification values of each fraction were normalized to the relative quantity of viral RNAs detected in the input of each condition.

HCV infection and replication assays

Huh7.5.1 human hepatoma cells were infected with cell culture-derived HCV (HCVcc) strains Jc1 and Luc-Jc1, half-maximal tissue culture infectious dose (TCID50 104 . mL-1 for both viruses)) as described (Lupberger et al., 2011; Pietschmann et al., 2006). 2 Two days before infection, gene silencing was performed by reverse transfection with 10 nM of siRNA (all Silence®Select siRNA, from Ambion®) specific for

RACK1 (siRACK1-1 : 5'-CAGGCUAUCUGAACACGGU-3' and siRACK1-2: 5'-CAAACACCUUUACACGCUA-3'), HCV host entry factor CD81 (siCD81) (Koutsoudakis et al., 2007), HCV replication factor Cyclophilin A (siCypA) (Kaul et al., 2009), HCV IRES (siHCV) (Dimitrova et al., 2008) or a nonspecific control siRNA (siCTRL) (Lupberger et al., 2011). Viral infection and RACK1 depletion was were analyzed by western blotting and quantified by counting of focus forming units (ffu)/mL following immunostaining using a HCV core-specific antibody (for HCV Jc1) (mAbC7-50, Affinity BioReagents, CO, USA) or by luciferase reporter gene expression in cell lysates (for Luc-Jc1), 3 days post incubation with virus as described (Koutsoudakis et al., 2007). For analysis of HCV replication experiments, Huh7.5.1 cells were electroporated with replication-competent HCV Luc-Jc1 RNA (Koutsoudakis et al., 2007). Three days later, cells were reverse transfected with the siRNAs described above. Viral replication was analyzed day 0 to 5 post transfection by quantification of luciferase activity (Benga et al., 2010).

miR122 quantification

Real time PCR quantification of mature miR-122 was performed using the miScript PCR System (Qiagen). Total RNA was isolated from the different cell lines by using the TRIzol® reagent (InvitrogenTM) and then subjected to reverse transcription step by using the miScript II RT Kit (Qiagen) with the miScript HiSpec Buffer, according to the manufacturer's recommendations. The obtained cDNA was used as a template in real time PCR experiment for mature microRNAs quantification, by using the miScript SYBR® Green PCR Kit (Qiagen) and the suitable miScript Primer Assays (miR-122 or RNU6). Each sample was assayed in triplicate for each single experiment. Real time PCR experiments were performed in the Corbett Rotor-Gene 6000 (Qiagen) and the data were analyzed in the Rotor-Gene software by using the comparative Ct (ΔΔCt) method.

Adenovirus infection

Recombinant adenovirus expressing a luciferase reporter gene under the CMV promoter (Ad-Luc) was transduced as described using an MOI of 2.5 (Wolf et al., 2008). Adenovirus cDNA was obtained from Vector Biolabs® (Philadelphia, USA). Gene silencing was performed as described above. Infection was analyzed 3 days post incubation with virus by quantification of luciferase activity.

Fly stocks

The TRiP lines (shRACK1 (#34693), shmCherry (#35787)) were obtained from the Bloomington Drosophila stock center. The drivers used were Actin5C-Gal4/CyO, Actin5C-Gal4/CyO; Tub-Gal80ts/TM6Tb. Transgenic lines for expression of HA-RACK1 wt or mutants were inserted at attP2 sites (68A4 on 3L) (Genetic Services). Expression of HA-RACK1 wt, but not the mutants, rescued the developmental defects of RACK11.8 null mutant flies (Kadrmas et al., 2007). All flies used were Wolbachia-free.

IRES – 40S structural model

To build the near-atomic resolution model of the HCV IRES – 40S complex, we used the cryoelectron microscopy (cryoEM) structure of the IRESHCV-40S (rabbit) complex at 20Å resolution (Spahn et al., 2001). An atomic model of the IRES structure (described thereafter) and the atomic model of the human ribosome obtained by cryoEM at 4.8Å resolution (Anger et al., 2013) were fitted inside its electron density. The obtained complete IRES-40S model provided the basis for the analysis of the IRESHCV interaction with the 40S ribosomal subunit, more specifically with the platform of the 40S, where RACK1 is located. Indeed, while for other regions of the ribosome a great variability is observed between different species (Ben-Shem et al., 2011), the platform is highly conserved and the main source of variability resides in the length of h26 of the 18S rRNA (Marzi et al., 2007). After having placed the 40S structure from human in the corresponding density of the rabbit 40S, an improved fitting was obtained using the UCSF Chimera package (Pettersen et al., 2004). As expected, the 40S platform showed a very good fitting.

Only fragments of the IRESHCV structure have been reported so far. We therefore

built a model of the IRES using the cryo-EM structure as a guide, as described (Berry et al., 2011). We used the structure of the individual domains from the IRESHCV, solved by NMR and X-ray crystallography (Berry et al., 2011; Collier et al., 2002; Kieft et al., 2002; Lukavsky et al., 2003; 2000; Rijnbrand et al., 2004) and the cryo-EM difference density map of the IRESHCV (Spahn et al., 2001) to produce a model of the IRESHCV including all major domains bound to the 40S ribosomal subunit. To correctly place the different domains in the IRES density, domains II (1P5P), IIId (1F84), JIIIabc (1KH6), IIIb (1KP7) and the central pseudoknot (3T4B) were manually modeled into the cryo-EM difference density as follows. Domain II has been placed at the top of the IRES , extending toward the ribosomal E-site followed by the central pseudoknot and the branching-out domain IIId. Domains JIIIabc and IIIb are located at the bottom of the IRES density. Figure 6 has been generated by PyMol (Molecular Graphics System, Schrödinger, LLC).

VI- References

Aebersold, R., Gstaiger, M., Malmström, L., and Hafen, E. SWATH MS is a novel technique that is based on data-independent acquisition (DIA) which aims to complement traditional mass spectrometry-based proteomics. (http://www.imsb.ethz.ch/researchgroup/malars/research/openswath)

Aliyari, R., Wu, Q., Li, H.-W., Wang, X.-H., Li, F., Green, L.D., Han, C.S., Li, W.-X., and Ding, S.-W. (2008). Mechanism of Induction and Suppression of Antiviral Immunity Directed by Virus-Derived Small RNAs in Drosophila. Cell Host and Microbe *4*, 387–397.

Ambros, V. (2003). MicroRNA pathways in flies and worms: growth, death, fat, stress, and timing. Cell.

Ambros, V., Lee, R.C., Lavanway, A., Williams, P.T., and Jewell, D. (2003). MicroRNAs and Other Tiny Endogenous RNAs in C. elegans. Current Biology *13*, 807–818.

Ameres, S.L., Horwich, M.D., Hung, J.H., Xu, J., Ghildiyal, M., Weng, Z., and Zamore, P.D. (2010). Target RNA-Directed Trimming and Tailing of Small Silencing RNAs. Science *328*, 1534–1539.

Ameyar-Zazoua, M., Rachez, C., Souidi, M., Robin, P., Fritsch, L., Young, R., Morozova, N., Fenouil, R., Descostes, N., Andrau, J.-C., et al. (2012). Argonaute proteins couple chromatin silencing to alternative splicing. Nature Structural & Molecular Biology 1–8.

Aravin, A.A., Hannon, G.J., and Brennecke, J. (2007). The Piwi-piRNA Pathway Provides an Adaptive Defense in the Transposon Arms Race. Science *318*, 761–764.

Aravin, A.A., Naumova, N.M., Tulin, A.V., Vagin, V.V., Rozovsky, Y.M., and Gvozdev, V.A. (2001). Double-stranded RNA-mediated silencing of genomic tandem repeats and transposable elements in the D. melanogaster germline. Current Biology *11*, 1017–1027.

Arimoto, K., Fukuda, H., Imajoh-Ohmi, S., Saito, H., and Takekawa, M. (2008).

Formation of stress granules inhibits apoptosis by suppressing stress-responsive MAPK pathways. Nature Cell Biology *10*, 1324–1332.

Babiarz, J.E., Ruby, J.G., Wang, Y., Bartel, D.P., and Blelloch, R. (2008). Mouse ES cells express endogenous shRNAs, siRNAs, and other Microprocessor-independent, Dicer-dependent small RNAs. Genes & Development *22*, 2773–2785.

Barreiro, P., Vispo, E., Labarga, P., and Soriano, V. (2012). Management and Treatment of Chronic Hepatitis C in HIV Patients. Semin Liver Dis *32*, 138–146.

Bartel, D.P. (2009). MicroRNAs: target recognition and regulatory functions. Cell *136*, 215–233.

Bellare, P., and Ganem, D. (2009). Regulation of KSHV lytic switch protein expression by a virus-encoded microRNA: an evolutionary adaptation that fine-tunes lytic reactivation. Cell Host and Microbe *6*, 570–575.

Ben-Shem, A., Garreau de Loubresse, N., Melnikov, S., Jenner, L., Yusupova, G., and Yusupov, M. (2011). The structure of the eukaryotic ribosome at 3.0 Å resolution. Science *334*, 1524–1529.

Bennasser, Y., Chable-Bessia, C., and Triboulet, R. (2011). Competition for XPO5 binding between Dicer mRNA, pre-miRNA and viral RNA regulates human Dicer levels. Nature Structural & Molecular Biology.

Bennasser, Y., Le, S.Y., Benkirane, M., and Jeang, K.T. (2005). Evidence that HIV-1 encodes an siRNA and a suppressor of RNA silencing. Immunity.

Berry, B., Deddouche, S., Kirschner, D., Imler, J.-L., and Antoniewski, C. (2009). Viral Suppressors of RNA Silencing Hinder Exogenous and Endogenous Small RNA Pathways in Drosophila. PLoS ONE *4*, e5866.

Beutler, B., Eidenschenk, C., Crozat, K., Imler, J.-L., Takeuchi, O., Hoffmann, J.A., and Akira, S. (2007). Genetic analysis of resistance to viral infection. Nature Reviews Immunology *7*, 753–766.

Boehringer, D., Thermann, R., Ostareck-Lederer, A., Lewis, J.D., and Stark, H. (2005). Structure of the Hepatitis C Virus IRES Bound to the Human 80S Ribosome: Remodeling of the HCV IRES. Structure *13*, 1695–1706.

Borsani, O., Zhu, J., Verslues, P.E., Sunkar, R., and Zhu, J.K. (2005). Endogenous siRNAs Derived from a Pair of Natural cis-Antisense Transcripts Regulate Salt Tolerance in Arabidopsis. Cell, 123(7):1279-91.

Boutros, M., Kiger, A.A., Armknecht, S., Kerr, K., Hild, M., Koch, B., Haas, S.A., Paro, R., Perrimon, N., Heidelberg Fly Array Consortium (2004). Genome-wide RNAi analysis of growth and viability in Drosophila cells. Science *303*, 832–835.

Brennecke, J., Aravin, A.A., Stark, A., Dus, M., Kellis, M., Sachidanandam, R., and Hannon, G.J. (2007). Discrete small RNA-generating loci as master regulators of transposon activity in Drosophila. Cell *128*, 1089–1103.

Brodersen, P., and Voinnet, O. (2006). The diversity of RNA silencing pathways in plants. Trends in Genetics *22*, 268–280.

Bronkhorst, A.W., Miesen, P., and van Rij, R.P (2013). Small RNAs tackle large viruses: RNA interference-based antiviral defense against DNA viruses in insects. Fly (Austin), 7(4).

Ceci, M., Gaviraghi, C., Gorrini, C., Sala, L.A., Offenhäuser, N., Carlo Marchisio, P., and Biffo, S. (2003). Release of eIF6 (p27BBP) from the 60S subunit allows 80S ribosome assembly. Nature Cell Biology *426*, 579–584.

Cenik, E.S., Fukunaga, R., Lu, G., Dutcher, R., Wang, Y., Hall, T.M.T., and Zamore, P.D. (2011). Phosphate and R2D2 Restrict the Substrate Specificity of Dicer-2, an ATP-Driven Ribonuclease. Molecular Cell 1–13.

Cernilogar, F.M., Onorati, M.C., Kothe, G.O., Burroughs, A.M., Parsi, K.M., Breiling, A., Sardo, lo, F., Saxena, A., Miyoshi, K., Siomi, H., et al. (2011). Chromatin-associated RNA interference components contribute to transcriptional regulation in Drosophila. Nature *480*, 391–395.

Czech B, Hannon GJ (2010). Small RNA sorting: matchmaking for Argonautes. Nat Rev Genet *12*, 19–31.

Chao, J.A., Lee, J.H., Chapados, B.R., Debler, E.W., Schneemann, A., and Williamson, J.R. (2005). Dual modes of RNA-silencing suppression by Flock House virus protein B2. Nature Structural & Molecular Biology *12*, 952–957.

Chi, Y.-H., Semmes, O.J., and Jeang, K.-T. (2011). A proteomic study of TAR-RNA binding protein (TRBP)-associated factors. Cell & Bioscience *1*, 9.

Chotkowski, H.L., Ciota, A.T., Jia, Y., Puig-Basagoiti, F., Kramer, L.D., Shi, P.-Y., and Glaser, R.L. (2008). West Nile virus infection of Drosophila melanogaster induces a protective RNAi response. Virology *377*, 197–206.

Chung, W.-J., Okamura, K., Martin, R., and Lai, E.C. (2008). Endogenous RNA Interference Provides a Somatic Defense against Drosophila Transposons. Current Biology *18*, 795–802.

Colpitts, T.M., Cox, J., Vanlandingham, D.L., Feitosa, F.M., Cheng, G., Kurscheid, S., Wang, P., Krishnan, M.N., Higgs, S., and Fikrig, E. (2011). Alterations in the Aedes aegypti Transcriptome during Infection with West Nile, Dengue and Yellow Fever Viruses. PLoS Pathog *7*, e1002189.

Cong, Y., Baker, M.L., Jakana, J., Woolford, D., Miller, E.J., Reissmann, S., Kumar, R.N., Redding-Johanson, A.M., Batth, T.S., Mukhopadhyay, A., et al. (2010). 4.0-A resolution cryo-EM structure of the mammalian chaperonin TRiC/CCT reveals its unique subunit arrangement. Proceedings of the National Academy of Sciences *107*, 4967–4972.

Conrad KD, Giering F, Erfurth C, Neumann A, Fehr C, Meister G, Niepmann M. (2013a). microRNA-122 Dependent Binding of Ago2 Protein to Hepatitis C Virus RNA Is Associated with Enhanced RNA Stability and Translation Stimulation. Plos One *8*, – e56272.

Covey, S.N. (1997). Plants combat infection by gene silencing. Nature, 385, 781 - 782.

Coyle, S.M., Gilbert, W.V., and Doudna, J.A. (2009). Direct Link between RACK1

Function and Localization at the Ribosome In Vivo. Molecular and Cellular Biology *29*, 1626–1634.

Crowley, T.E., Nellen, W., Gomer, R.H., and Firtel, R.A. (1985). Phenocopy of discoidin I-minus mutants by antisense transformation in Dictyostelium. Cell *43*, 633–641.

Cullen, B.R. (2009). Viral and cellular messenger RNA targets of viral microRNAs. Nature *457*, 421–425.

Czech, B., Malone, C.D., Zhou, R., Stark, A., Schlingeheyde, C., Dus, M., Perrimon, N., Kellis, M., Wohlschlegel, J.A., Sachidanandam, R., et al. (2008). An endogenous small interfering RNA pathway in Drosophila. Nature *453*, 798–802.

Czech, B., Zhou, R., Erlich, Y., Brennecke, J., Binari, R., Villalta, C., Gordon, A., Perrimon, N., and Hannon, G.J. (2009). Hierarchical Rules for Argonaute Loading in Drosophila. Molecular Cell *36*, 445–456.

Da Costa D, Turek M, Felmlee DJ, Girardi E, Pfeffer S, Long G, Bartenschlager R, Zeisel MB, Baumert TF (2012a). Reconstitution of the entire hepatitis C virus life cycle in nonhepatic cells. Journal of Virology *86*, 11919–11925.

Dawkins, R. (2006). The selfish gene.

de Boer, E., Rodriguez, P., Bonte, E., Krijgsveld, J., Katsantoni, E., Heck, A., Grosveld, F., and Strouboulis, J. (2003). Efficient biotinylation and single-step purification of tagged transcription factors in mammalian cells and transgenic mice. Proc Natl Acad Sci U S A *100*, 7480–7485.

de Carvalho Niebel, F., Frendo, P., Van Montagu, M., and Cornelissen, M. (1995). Post-transcriptional cosuppression of beta-1, 3-glucanase genes does not affect accumulation of transgene nuclear mRNA. Plant Cell, vol. 7 no. 3 347-358.

Deddouche, S., Matt, N., Budd, A., Mueller, S., Kemp, C., Galiana-Arnoux, D., Dostert, C., Antoniewski, C., Hoffmann, J.A., and Imler, J.-L. (2008). The DExD/H-box helicase Dicer-2 mediates the induction of antiviral activity in drosophila. Nature Immunology *9*, 1425–1432.

Deleris, A. (2006). Hierarchical Action and Inhibition of Plant Dicer-Like Proteins in

Antiviral Defense. Science *313*, 68–71.

Ding, S.-W. (2010). RNA-based antiviral immunity. Nature Reviews Immunology *10*, 632–644.

Ding, S.-W., and Voinnet, O. (2007). Antiviral Immunity Directed by Small RNAs. Cell *130*, 413–426.

Ditzel, L., Löwe, J., Stock, D., Stetter, K.O., Huber, H., and Huber, R. (1998). Crystal structure of the thermosome, the archaeal chaperonin and homolog of CCT. Cell, 93(1):125-38.

Dorner, M., Horwitz, J.A., Robbins, J.B., Barry, W.T., Feng, Q., Mu, K., Jones, C.T., Schoggins, J.W., Catanese, M.T., Burton, D.R., et al. (2011). A genetically humanized mouse model for hepatitis C virus infection. Nature *474*, 208–211.

Dorner, S., Lum, L., Kim, M., Paro, R., Beachy, P.A., and Green, R. (2006). A genomewide screen for components of the RNAi pathway in Drosophila cultured cells. Proceedings of the National Academy of Sciences *103*, 11880–11885.

Dostert, C., Jouanguy, E., Irving, P., Troxler, L., Galiana-Arnoux, D., Hetru, C., Hoffmann, J.A., and Imler, J.-L. (2005). The Jak-STAT signaling pathway is required but not sufficient for the antiviral response of drosophila. Nature Immunology *6*, 946–953.

Dölken, L., Krmpotic, A., Kothe, S., and Tuddenham, L, Tanguy M, Marcinowski L, Ruzsics Z, Elefant N, Altuvia Y, Margalit H, Koszinowski UH, Jonjic S, Pfeffer S (2010). Cytomegalovirus microRNAs facilitate persistent virus infection in salivary glands. Plos Pathogens, 6(10):e1001150 .

Duchaine, T.F., Wohlschlegel, J.A., Kennedy, S., Bei, Y., Conte, D., Jr., Pang, K., Brownell, D.R., Harding, S., Mitani, S., Ruvkun, G., et al. (2006). Functional Proteomics Reveals the Biochemical Niche of C. elegans DCR-1 in Multiple Small-RNA-Mediated Pathways. Cell *124*, 343–354.

Dunoyer, P., Himber, C., and Voinnet, O. (2005). DICER-LIKE 4 is required for RNA interference and produces the 21-nucleotide small interfering RNA component of the

plant cell-to-cell silencing signal. Nat Genet *37*, 1356–1360.

Elmayan, T., and Vaucheret, H. (1996). Expression of single copies of a strongly expressed 35S transgene can be silenced post-transcriptionally. Plant J *9*, 787–797.

Eulalio, A., Rehwinkel, J., Stricker, M., Huntzinger, E., Yang, S.F., Doerks, T., Dorner, S., Bork, P., Boutros, M., and Izaurralde, E. (2007). Target-specific requirements for enhancers of decapping in miRNA-mediated gene silencing. Genes & Development *21*, 2558–2570.

Fabian, M.R., and Sonenberg, N, Filipowicz W (2010). Regulation of mRNA translation and stability by microRNAs. Annu Rev Biochem. 2010;79:351-79.

Fabian, M.R., Mathonnet, G., Sundermeier, T., Mathys, H., Zipprich, J.T., Svitkin, Y.V., Rivas, F., Jinek, M., Wohlschlegel, J., Doudna, J.A., et al. (2009). Mammalian miRNA RISC Recruits CAF1 and PABP to Affect PABP-Dependent Deadenylation. Molecular Cell *35*, 868–880.

Félix, M.A., Ashe, A., Piffaretti, J., Wu, G., Nuez, I., and Bélicard, T. (2011). Natural and experimental infection of Caenorhabditis nematodes by novel viruses related to nodaviruses. Plos Biol, 9(1):e1000586.

Fitzgerald, K.A., McWhirter, S.M., Faia, K.L., Rowe, D.C., Latz, E., Golenbock, D.T., Coyle, A.J., Liao, S.-M., and Maniatis, T. (2003). IKKε and TBK1 are essential components of the IRF3 signaling pathway. Nature Immunology *4*, 491–496.

Fofana, I., Krieger, S.E., Grunert, F., Glauben, S., Xiao, F., Fafi Kremer, S., Soulier, E., Royer, C., Thumann, C., Mee, C.J., et al. (2010). Monoclonal Anti-Claudin 1 Antibodies Prevent Hepatitis C Virus Infection of Primary Human Hepatocytes. Gastroenterology *139*, 953–964.e954.

Förstemann, K., Horwich, M.D., Wee, L., Tomari, Y., and Zamore, P.D. (2007). Drosophila microRNAs Are Sorted into Functionally Distinct Argonaute Complexes after Production by Dicer-1. Cell *130*, 287–297.

Frohn, A., Eberl, H.C., Stöhr, J., and Glasmacher, E, Rüdel S, Heissmeyer V, Mann M, Meister G. (2012). Dicer-dependent and-independent Argonaute2 protein interaction

networks in mammalian cells. Molecular & Cellular Proteomics, 11(11):1442-56.

Fukuyama, H., Ndiaye, S., Hoffmann, J., Rossier, J., Liuu, S., Vinh, J., and Verdier, Y. (2012). On-bead tryptic proteolysis: An attractive procedure for LC-MS/MS analysis of the Drosophila caspase 8 protein complex during immune response against bacteria. Journal of Proteomics 75(15):4610-9.

Galiana-Arnoux, D., Dostert, C., Schneemann, A., Hoffmann, J.A., and Imler, J.-L. (2006). Essential function in vivo for Dicer-2 in host defense against RNA viruses in drosophila. Nature Immunology *7*, 590–597.

Garrey, J.L., Lee, Y.Y., Au, H.H.T., Bushell, M., and Jan, E. (2009). Host and Viral Translational Mechanisms during Cricket Paralysis Virus Infection. Journal of Virology *84*, 1124–1138.

Gasciolli, V., Mallory, A.C., Bartel, D.P., and Vaucheret, H. (2005). Partially Redundant Functions of Arabidopsis DICER-like Enzymes and a Role for DCL4 in Producing trans-Acting siRNAs. Current Biology, 15(16):1494-500.

Gatfield, D., Unterholzner, L., Ciccarelli, F.D., Bork, P., and Izaurralde, E. (2003). Nonsense-mediated mRNA decay in Drosophila: at the intersection of the yeast and mammalian pathways. The EMBO Journal *22*, 3960–3970.

Gerbasi, V.R., Preall, J.B., Golden, D.E., Powell, D.W., Cummins, T.D., and Sontheimer, E.J. (2011). Blanks, a nuclear siRNA/dsRNA-binding complex component, is required for Drosophila spermiogenesis. Proceedings of the National Academy of Sciences *108*, 3204–3209.

Ghildiyal, M., and Zamore, P.D. (2009). Small silencing RNAs: an expanding universe. Nature Reviews Genetics *10*, 94–108.

Gibson, T.J. (2012). RACK1 research–ships passing in the night? FEBS Letters, 586(17):2787-9.

Goic, B., Vodovar, N., Mondotte, J.A., Monot, C.E.M., Frangeul, L., Blanc, H.E., Gausson, V.E.R., Vera-Otarola, J., Cristofari, G., and Saleh, M.-C. (2013). RNA-mediated interference and reverse transcription control the persistence of RNA viruses

in the insect model Drosophila. Nature Immunology, 14(4):396-403.

Grundhoff, A., and Sullivan, C.S. (2011). Virus-encoded microRNAs. Virology, 411(2):325-43.

Gu, W., Shirayama, M., Conte, D., Vasale, J., Batista, P.J., Claycomb, J.M., Moresco, J.J., Youngman, E.M., Keys, J., Stoltz, M.J., et al. (2009). Distinct argonaute-mediated 22G-RNA pathways direct genome surveillance in the C. elegans germline. Molecular Cell *36*, 231–244.

Haasnoot, J., de Vries, W., Geutjes, E.J., and Prins, M, de Haan P, Berkhout B. (2007). The Ebola virus VP35 protein is a suppressor of RNA silencing. PLoS Pathog,3(6):e86.

Hain, D., Bettencourt, B.R., Okamura, K., Csorba, T., Meyer, W., Jin, Z., Biggerstaff, J., Siomi, H., Hutvagner, G., Lai, E.C., et al. (2010). Natural Variation of the Amino-Terminal Glutamine-Rich Domain in Drosophila Argonaute2 Is Not Associated with Developmental Defects. PLoS ONE *5*, e15264.

Hamilton, A. (2002). Two classes of short interfering RNA in RNA silencing. The EMBO Journal *21*, 4671–4679.

Handler, D., Olivieri, D., Novatchkova, M., Gruber, F.S., Meixner, K., Mechtler, K., Stark, A., Sachidanandam, R., and Brennecke, J. (2011). A systematic analysis of Drosophila TUDOR domain-containing proteins identifies Vreteno and the Tdrd12 family as essential primary piRNA pathway factors. The EMBO Journal *30*, 3977–3993.

Harada, H., Fujita, T., Miyamoto, M., Kimura, Y., Maruyama, M., Furia, A., Miyata, T., and Taniguchi, T. (1989). Structurally similar but functionally distinct factors, IRF-1 and IRF-2, bind to the same regulatory elements of IFN and IFN-inducible genes. Cell *58*, 729–739.

Hashem Y, des Georges A, Dhote V, Langlois R, Liao HY, Grassucci RA, Hellen CU, Pestova TV, Frank J (2013b). Structure of the Mammalian Ribosomal 43S Preinitiation Complex Bound to the Scanning Factor DHX29. Cell *153*, 1108–1119.

Hertz, M.I., Landry, D.M., Willis, A.E., Luo, G., and Thompson, S.R. (2013). Ribosomal

Protein S25 Dependency Reveals a Common Mechanism for Diverse Internal Ribosome Entry Sites and Ribosome Shunting. Molecular and Cellular Biology *33*, 1016–1026.

Hertz, M.I., and Thompson, S.R. (2011). Mechanism of translation initiation by Dicistroviridae IGR IRESs. Virology *411*, 355–361.

Heylbroeck, C., Pitha, P.M., and Hiscott, J. (1998). Virus-dependent phosphorylation of the IRF-3 transcription factor regulates nuclear translocation, transactivation potential, and proteasome-mediated degradation. Mol Cell Biol, 18(5):2986-96.

Hjelle, B., Ebel, G.D., Olson, K.E., and Blair, C.D. (2010). Comparison of Dengue virus type 2-specific small RNAs from RNA interference-competent and–incompetent mosquito cells. PLoS Negl Trop Dis, 4(10):e848.

Hoffmann, J.A. (2003). The immune response of Drosophila. Nature Cell Biology *426*, 33–38.

Hofmann WP, Zeuzem S (2012b). HEPATITIS C IN 2011 A new standard of care and the race towards IFN-free therapy. Nat Rev Gastroenterol Hepatol *9*, 67–68.

Huen, J., Kakihara, Y., Ugwu, F., Cheung, K.L.Y., Ortega, J., and Houry, W.A. (2010). Rvb1–Rvb2: essential ATP-dependent helicases for critical complexes. Biochem. Cell Biol. *88*, 29–40.

Hutten, S., and Kehlenbach, R.H. (2006). Nup214 is required for CRM1-dependent nuclear protein export in vivo. Molecular and Cellular Biology *26*, 6772–6785.

Ishizu, H., Siomi, H., and Siomi, M.C. (2012). Biology of PIWI-interacting RNAs: new insights into biogenesis and function inside and outside of germlines. Genes & Development , 1;26(21):2361-73.

Iwasaki, S., and Tomari, Y. (2009). Argonaute-mediated translational repression (and activation). Fly (Austin), 3(3):204-6.

Iwasaki, S., Kawamata, T., and Tomari, Y. (2009). Drosophila Argonaute1 and Argonaute2 Employ Distinct Mechanisms for Translational Repression. Molecular Cell *34*, 58–67.

Iwasaki, S., Kobayashi, M., Yoda, M., Sakaguchi, Y., Katsuma, S., Suzuki, T., and Tomari, Y. (2010). Hsc70/Hsp90 Chaperone Machinery Mediates ATP-Dependent RISC Loading of Small RNA Duplexes. Molecular Cel, 39(2):292-9.

Izant, J.G., and Weintraub, H. (1984). Inhibition of thymidine kinase gene expression by anti-sense RNA: a molecular approach to genetic analysis. Cell, 36(4):1007-15.

Izant, J.G., and Weintraub, H. (1985). Constitutive and conditional suppression of exogenous and endogenous genes by anti-sense RNA. Science *229*, 345–352.

Jacobson, I.M., Gordon, S.C., Kowdley, K.V., Yoshida, E.M., Rodriguez-Torres, M., Sulkowski, M.S., Shiffman, M.L., Lawitz, E., Everson, G., Bennett, M., et al. (2013). Sofosbuvir for Hepatitis C Genotype 2 or 3 in Patients without Treatment Options. N Engl J Med *368*, 1867–1877.

Jan, E., and Sarnow, P. (2002). Factorless ribosome assembly on the internal ribosome entry site of cricket paralysis virus. Journal of Molecular Biology *324*, 889–902.

Janeway, C.A. (1989). Approaching the Asymptote? Evolution and Revolution in Immunology. Cold Spring Harbor Symposia on Quantitative Biology *54*, 1–13.

Jannot, G., Bajan, S., re, N.J.G.E., Bouasker, S., Banville, I.H., Piquet, S., Hutvagner, G., and Simard, M.J. (2011). The ribosomal protein RACK1 is required for microRNA function in both C. elegans and humans. EMBO Report, 12(6):581-6.

Jopling CL, Yi M, Lancaster AM, Lemon SM, Sarnow P (2005). Modulation of hepatitis C virus RNA abundance by a liver-specific microRNA. Science *309*, 1577–1581.

Kadrmas, J.L., Smith, M.A., Pronovost, S.M., and Beckerle, M.C. (2007). Characterization of RACK1 function inDrosophila development. Dev. Dyn. *236*, 2207–2215.

Kaul, A., Stauffer, S., Berger, C., Pertel, T., Schmitt, J., Kallis, S., Lopez, M.Z., Lohmann, V., Luban, J., and Bartenschlager, R. (2009). Essential Role of Cyclophilin A for Hepatitis C Virus Replication and Virus Production and Possible Link to Polyprotein Cleavage Kinetics. PLoS Pathog *5*, e1000546.

Kawamata, T., Seitz, H., and Tomari, Y. (2009). Structural determinants of miRNAs for

RISC loading and slicer-independent unwinding. Nature *16*, 953–960.

Kawamura, Y., Saito, K., Kin, T., Ono, Y., Asai, K., Sunohara, T., Okada, T.N., Siomi, M.C., and Siomi, H. (2008). Drosophila endogenous small RNAs bind to Argonaute 2 in somatic cells. Nature *453*, 793–797.

Kemp, C., and Imler, J.L. (2009). Antiviral immunity in drosophila. Current Opinion in Immunology, 21(1):3-9.

Kemp, C., Mueller, S., Goto, A., and Barbier, V, Paro S, Bonnay F, Dostert C, Troxler L, Hetru C, Meignin C, Pfeffer S, Hoffmann JA, Imler JL (2013). Broad RNA Interference–Mediated Antiviral Immunity and Virus-Specific Inducible Responses in Drosophila. Journal of Immunol, 15;190(2):650-8.

Kieft, J.S. (2008). Viral IRES RNA structures and ribosome interactions. Trends in Biochemical Sciences *33*, 274–283.

Kieft JS, Zhou K, Jubin R, Doudna JA (2001). Mechanism of ribosome recruitment by hepatitis CIRES RNA. *7*, 194–206.

Kim, S.K., and Wold, B.J. (1985). Stable reduction of thymidine kinase activity in cells expressing high levels of anti-sense RNA. Cell, 42(1):129-38.

Kitamura, A., Kubota, H., Pack, C.-G., Matsumoto, G., Hirayama, S., Takahashi, Y., Kimura, H., Kinjo, M., Morimoto, R.I., and Nagata, K. (2006). Cytosolic chaperonin prevents polyglutamine toxicity with altering the aggregation state. Nature Cell Biology *8*, 1163–1169.

Kondrashov, N., Pusic, A., Stumpf, C.R., Shimizu, K., Hsieh, A.C., Xue, S., Ishijima, J., Shiroishi, T., and Barna, M. (2011). Ribosome-Mediated Specificity in Hox mRNA Translation and Vertebrate Tissue Patterning. Cell *145*, 383–397.

Kong, Y.W., Cannell, I.G., de Moor, C.H., Hill, K., Garside, P.G., Hamilton, T.L., Meijer, H.A., Dobbyn, H.C., Stoneley, M., Spriggs, K.A., et al. (2008). The mechanism of micro-RNA-mediated translation repression is determined by the promoter of the target gene. Proceedings of the National Academy of Sciences *105*, 8866–8871.

Kouba, T., Rutkai, E., Karaskova, M., and Valasek, L.S. (2012). The eIF3c/NIP1 PCI

domain interacts with RNA and RACK1/ASC1 and promotes assembly of translation preinitiation complexes. Nucleic Acids Research *40*, 2683–2699.

Köhler, A., and Hurt, E. (2007). Exporting RNA from the nucleus to the cytoplasm. Nat Rev Mol Cell Biol *8*, 761–773.

Kuroha, K., Akamatsu, M., Dimitrova, L., Ito, T., Kato, Y., Shirahige, K., and Inada, T. (2010). Receptor for activated C kinase 1 stimulates nascent polypeptide-dependent translation arrest. EMBO Report, 11(12):956-61.

Kuss, S.K., Mata, M.A., Zhang, L., and Fontoura, B.M.A. (2013). Nuclear imprisonment: viral strategies to arrest host mRNA nuclear export. Viruses *5*, 1824–1849.

Landry, D.M., Hertz, M.I., and Thompson, S.R. (2009). RPS25 is essential for translation initiation by the Dicistroviridae and hepatitis C viral IRESs. Genes & Development *23*, 2753–2764.

Lecellier, C.H. (2005). A Cellular MicroRNA Mediates Antiviral Defense in Human Cells. Science *308*, 557–560.

Lee, A.S.-Y., Burdeinick-Kerr, R., and Whelan, S.P.J. (2013). A ribosome-specialized translation initiation pathway is required for cap-dependent translation of vesicular stomatitis virus mRNAs. Proc Natl Acad Sci U S A. 110(1):324-9.

Lee, Y.S., Nakahara, K., Pham, J.W., Kim, K., He, Z., Sontheimer, E.J., and Carthew, R.W. (2004). Distinct Roles for Drosophila Dicer-1 and Dicer-2 in the siRNA/miRNA Silencing Pathways. Cell *117*, 69–81.

Lefebvre, G., Desfarges, S., Uyttebroeck, F., Muñoz, M., Beerenwinkel, N., Rougemont, J., Telenti, A., and Ciuffi, A. (2011). Analysis of HIV-1 expression level and sense of transcription by high-throughput sequencing of the infected cell. Journal of Virology *85*, 6205–6211.

Léger, P., Lara, E., Jagla, B., Sismeiro, O., Mansuroglu, Z., Coppée, J.Y., Bonnefoy, E., and Bouloy, M. (2013). Dicer-2- and Piwi-mediated RNA interference in Rift Valley fever virus-infected mosquito cells. Journal of Virology *87*, 1631–1648.

Li, F., and Ding, S.W. (2006). Virus counterdefense: diverse strategies for evading the

RNA-silencing immunity. Annual Review of Microbiology, 60:503-31.

Li H, Li WX, Ding SW (2002). Induction and suppression of RNA silencing by an animal virus. *296*, 1319–1321.

Li, S., Wang, L., Berman, M., Kong, Y.-Y., and Dorf, M.E. (2011). Mapping a Dynamic Innate Immunity Protein Interaction Network Regulating Type I Interferon Production. Immunity *35*, 426–440.

Li, W.X. (2004). Interferon antagonist proteins of influenza and vaccinia viruses are suppressors of RNA silencing. Proceedings of the National Academy of Sciences *101*, 1350–1355.

Lichner, Z. (2003). Double-stranded RNA-binding proteins could suppress RNA interference-mediated antiviral defences. Journal of General Virology *84*, 975–980.

Lin, X., Liang, D., He, Z., Deng, Q., Robertson, E.S., and Lan, K. (2011). miR-K12-7-5p encoded by Kaposi's sarcoma-associated herpesvirus stabilizes the latent state by targeting viral ORF50/RTA. PLoS ONE *6*, e16224.

Lindenbach, B.D. (2005). Complete Replication of Hepatitis C Virus in Cell Culture. Science *309*, 623–626.

Liu, J., Carmell, M.A., Rivas, F.V., Marsden, C.G., Thomson, J.M., Song, J.-J., Hammond, S.M., Joshua-Tor, L., and Hannon, G.J. (2004). Argonaute2 is the catalytic engine of mammalian RNAi. Science *305*, 1437–1441.

Liu, Q. (2003). R2D2, a Bridge Between the Initiation and Effector Steps of the Drosophila RNAi Pathway. Science *301*, 1921–1925.

Liu, X., Jiang, F., Kalidas, S., Smith, D., and Liu, Q. (2006). Dicer-2 and R2D2 coordinately bind siRNA to promote assembly of the siRISC complexes. Rna *12*, 1514–1520.

Lu, R., Maduro, M., Li, F., Li, H.W., Broitman-Maduro, G., Li, W.X., and Ding, S.W. (2005). Animal virus replication and RNAi-mediated antiviral silencing in Caenorhabditis elegans. Nature *436*, 1040–1043.

Lu, R., Yigit, E., Li, W.-X., and Ding, S.-W. (2009). An RIG-I-Like RNA Helicase Mediates Antiviral RNAi Downstream of Viral siRNA Biogenesis in Caenorhabditis elegans. PLoS Pathog *5*, e1000286.

Lupberger, J., Zeisel, M.B., Xiao, F., Thumann, C., Fofana, I., Zona, L., Davis, C., Mee, C.J., Turek, M., Gorke, S., et al. (2011). EGFR and EphA2 are host factors for hepatitis C virus entry and possible targets for antiviral therapy. Nat Med *17*, 589–595.

Machlin, E.S., Sarnow, P., and Sagan, S.M. (2011). Masking the 5' terminal nucleotides of the hepatitis C virus genome by an unconventional microRNA-target RNA complex. Proc Natl Acad Sci U S A *108*, 3193–3198.

Mamidipudi, V., Zhang, J., Lee, K.C., and Cartwright, C.A. (2004). RACK1 regulates G1/S progression by suppressing Src kinase activity. Molecular and Cellular Biology *24*, 6788–6798.

Marí-Ordóñez, A., Marchais, A., Etcheverry, M., Martin, A., Colot, V., and Voinnet, O. (2013). Reconstructing de novo silencing of an active plant retrotransposon. Nat Genet, 45(9):1029-39.

Marques, J.T., Kim, K., Wu, P.-H., Alleyne, T.M., Jafari, N., and Carthew, R.W. (2009). Loqs and R2D2 act sequentially in the siRNA pathway in Drosophila. Nature Structural & Molecular Biology *17*, 24–30.

Martínez-Salas, E., Pacheco, A., Serrano, P., and Fernandez, N. (2008). New insights into internal ribosome entry site elements relevant for viral gene expression. J. Gen. Virol. *89*, 611–626.

Matranga, C., and Pyle, A.M. (2010). Double-stranded RNA-dependent ATPase DRH-3: insight into its role in RNAsilencing in Caenorhabditis elegans. J Biol Chem. 13;285(33):25363-71.

Matzke, M.A., and Birchler, J.A. (2005). RNAi-mediated pathways in the nucleus. Nature Reviews Genetics, Jan;6(1):24-35.

Mauro, V.P. (2002). The ribosome filter hypothesis. Proceedings of the National Academy of Sciences *99*, 12031–12036.

McPhee, F., Hernandez, D., Yu, F., Ueland, J., Monikowski, A., Carifa, A., Falk, P., Wang, C., Fridell, R., Eley, T., et al. (2013). Resistance analysis of hepatitis C virus genotype 1 prior treatment null responders receiving daclatasvir and asunaprevir. Hepatology, 58(3):902-11.

Melton, D.A. (1985). Injected anti-sense RNAs specifically block messenger RNA translation in vivo. Proc Natl Acad Sci U S A; 82(1):144-8.

Michalik, K.M., Bottcher, R., and Forstemann, K. (2012). A small RNA response at DNA ends in Drosophila. Nucleic Acids Research *40*, 9596–9603.

Miller, D.J., Schwartz, M.D., and Ahlquist, P. (2001). Flock house virus RNA replicates on outer mitochondrial membranes in Drosophila cells. Journal of Virology, 75(23):11664-76.

Miyamoto, M., Fujita, T., Kimura, Y., Maruyama, M., Harada, H., Sudo, Y., Miyata, T., and Taniguchi, T. (1988). Regulated expression of a gene encoding a nuclear factor, IRF-1, that specifically binds to IFN-beta gene regulatory elements. Cell *54*, 903–913.

Moissiard, G., and Voinnet, O. (2006). RNA silencing of host transcripts by cauliflower mosaic virus requires coordinated action of the four Arabidopsis Dicer-like proteins. Proc Natl Acad Sci U S A *103*, 19593–19598.

Morazzani, E.M., Wiley, M.R., Murreddu, M.G., Adelman, Z.N., and Myles, K.M. (2012). Production of Virus-Derived Ping-Pong-Dependent piRNA-like Small RNAs in the Mosquito Soma. PLoS Pathog *8*, e1002470.

Moshkovich, N., Nisha, P., Boyle, P.J., Thompson, B.A., Dale, R.K., and Lei, E.P. (2011). RNAi-independent role for Argonaute2 in CTCF/CP190 chromatin insulator function. Genes & Development *25*, 1686–1701.

Mudge, J., Wilusz, J., Olson, K.E., and Blair, C.D. (2010). C6/36 Aedes albopictus cells have a dysfunctional antiviral RNA interference response. PLoS Neglected Tropical ….

Mueller, S., Gausson, V., and Vodovar, N. *et al* (2010). RNAi-mediated immunity provides strong protection against the negative-strand RNA vesicular stomatitis virus in Drosophila. Proc Natl Acad Sci U S A ; 107(45):19390-5.

Myles, K.M., Wiley, M.R., Morazzani, E.M., and Adelman, Z.N. (2008). Alphavirus-derived small RNAs modulate pathogenesis in disease vector mosquitoes.

Nathan, C. (2012). Fresh approaches to anti-infective therapies. Sci Transl Med *4*, 140sr2.

Nayak, A., and Andino, R. (2011). Slicer Activity in Drosophila melanogaster S2 Extract. In Methods in Molecular Biology, (Totowa, NJ: Humana Press), pp. 231–244.

Nayak, A., Berry, B., Tassetto, M., Kunitomi, M., Acevedo, A., Deng, C., Krutchinsky, A., Gross, J., Antoniewski, C., and Andino, R. (2010). Cricket paralysis virus antagonizes Argonaute 2 to modulate antiviral defense in Drosophila. Nature Structural & Molecular Biology, 17(5):547-54.

Nilsson, J., Sengupta, J., Frank, J., and Nissen, P. (2004). Regulation of eukaryotic translation by the RACK1 protein: a platform for signalling molecules on the ribosome. EMBO Reports *5*, 1137–1141.

Nishiyama, T., Yamamoto, H., Uchiumi, T., and Nakashima, N. (2007). Eukaryotic ribosomal protein RPS25 interacts with the conserved loop region in a dicistroviral intergenic internal ribosome entry site. Nucleic Acids Research *35*, 1514–1521.

Obbard, D.J., Gordon, K.H.J., Buck, A.H., and Jiggins, F.M. (2009). The evolution of RNAi as a defence against viruses and transposable elements. Philosophical Transactions of the Royal Society B: Biological Sciences *364*, 99–115.

Okamura, K., and Lai, E.C. (2008). Endogenous small interfering RNAs in animals. Nat Rev Mol Cell Biol, (9):673-8.

Okamura, K., Balla, S., Martin, R., Liu, N., and Lai, E.C. (2008). Two distinct mechanisms generate endogenous siRNAs from bidirectional transcription in Drosophila melanogaster. Nature Structural & Molecular Biology *15*, 581–590.

Okamura, K., Liu, N., and Lai, E.C. (2009). Distinct Mechanisms for MicroRNA Strand Selection by Drosophila Argonautes. Molecular Cell *36*, 431–444.

Okamura K, Ishizuka A, Siomi H, Siomi MC (2004b). Distinct roles for Argonaute proteins in small RNA-directed RNA cleavage pathways. Genes and Dev. *18*, 1655–

1666.

Olivieri, D., Sykora, M.M., Sachidanandam, R., Mechtler, K., and Brennecke, J. (2010). An in vivo RNAi assay identifies major genetic and cellular requirements for primary piRNA biogenesis in Drosophila. The EMBO Journal *29*, 3301–3317.

Otsuka, M., Jing, Q., Georgel, P., New, L., Chen, J., Mols, J., Kang, Y.J., Jiang, Z., Du, X., Cook, R., et al. (2007). Hypersusceptibility to vesicular stomatitis virus infection in Dicer1-deficient mice is due to impaired miR24 and miR93 expression. Immunity *27*, 123–134.

Otsuka M, Takata A, Yoshikawa T, Kojima K, Kishikawa T, Shibata C, Takekawa M, Yoshida H, Omata M, Koike K (2011). Receptor for Activated Protein Kinase C: Requirement for Efficient MicroRNA Function and Reduced Expression in Hepatocellular Carcinoma. Plos One *6*, –e24359.

Paradkar, P.N., Trinidad, L., Voysey, R., Duchemin, J.-B., and Walker, P.J. (2012). Secreted Vago restricts West Nile virus infection in Culex mosquito cells by activating the Jak-STAT pathway. Proc Natl Acad Sci U S A; 109(46): 18915-20.

Parameswaran, P., Sklan, E., Wilkins, C., Burgon, T., Samuel, M.A., Lu, R., Ansel, K.M., Heissmeyer, V., Einav, S., Jackson, W., et al. (2010). Six RNA Viruses and Forty-One Hosts: Viral Small RNAs and Modulation of Small RNA Repertoires in Vertebrate and Invertebrate Systems. PLoS Pathog *6*, e1000764.

Perrat, P.N., DasGupta, S., Wang, J., Theurkauf, W., Weng, Z., Rosbash, M., and Waddell, S. (2013). Transposition-driven genomic heterogeneity in the Drosophila brain. Science *340*, 91–95.

Pestova, T.V., Lomakin, I.B., and Hellen, C.U.T. (2004). Position of the CrPV IRES on the 40S subunit and factor dependence of IRES/80S ribosome assembly. EMBO Reports *5*, 906–913.

Peterhans, E., Bachofen, C., Stalder, H., and Schweizer, M. (2010). Cytopathic bovine viral diarrhea viruses (BVDV): emerging pestiviruses doomed to extinction. Vet. Res. *41*, 44.

Pfeffer, S., Sewer, A., Lagos-Quintana, M., Sheridan, R., Sander, C., Grässer, F.A., van Dyk, L.F., Ho, C.K., Shuman, S., Chien, M., et al. (2005). Identification of microRNAs of the herpesvirus family. Nature *2*, 269–276.

Qi, D., Jin, H., Lilja, T., and Mannervik, M. (2006). Drosophila Reptin and Other TIP60 Complex Components Promote Generation of Silent Chromatin. Genetics *174*, 241–251.

Qi, X., Bao, F.S., and Xie, Z. (2009). Small RNA deep sequencing reveals role for Arabidopsis thaliana RNA-dependent RNA polymerases in viral siRNA biogenesis. PLoS ONE *4*, e4971.

Rabl, J., Leibundgut, M., Ataide, S.F., Haag, A., and Ban, N. (2011). Crystal Structure of the Eukaryotic 40S Ribosomal Subunit in Complex with Initiation Factor 1. Science *331*, 730–736.

Ratcliff, F., Harrison, B.D., and Baulcombe, D.C. (1997). A similarity between viral defense and gene silencing in plants. Science, 276(5318):1558-60.

Roberts, A.P.E., Lewis, A.P., and Jopling, C.L. (2011). miR-122 activates hepatitis C virus translation by a specialized mechanism requiring particular RNA components. Nucleic Acids Research *39*, 7716–7729.

Rodriguez, M.S., Dargemont, C., and Stutz, F. (2012). Nuclear export of RNA. Biology of the Cell *96*, 639–655.

Ron, D., Adams, D.R., Baillie, G.S., and Long, A. (2013). RACK1 to the future–a historical perspective. Cell Commun Signal;11:53.

Rosenberg, U.B., Preiss, A., Seifert, E., and Jäckle, H. (1985). Production of phenocopies by Krüppel antisense RNA injection into Drosophila embryos.Nature ;313(6004):703-6.

Ruby, J.G., Jan, C.H., and Bartel, D.P. (2007). Intronic microRNA precursors that bypass Drosha processing. Nature *448*, 83–86.

Saito, K., Nishida, K.M., Mori, T., and Kawamura, Y. (2006). Specific association of Piwi with rasiRNAs derived from retrotransposon and heterochromatic regions in the

Drosophila genome. Genes Dev. ;20(16):2214-22.

Saito, K., Sakaguchi, Y., Suzuki, T., and Suzuki, T. (2007). Pimet, the Drosophila homolog of HEN1, mediates 2′-O-methylation of Piwi-interacting RNAs at their 3′ ends. Genes Dev. ;21(13):1603-8.

Saleh, M.-C., Tassetto, M., van Rij, R.P., Goic, B., Gausson, V., Berry, B., Jacquier, C., Antoniewski, C., and Andino, R. (2009). Antiviral immunity in Drosophila requires systemic RNA interference spread. Nature *458*, 346–350.

Saleh, M.-C., van Rij, R.P., Hekele, A., Gillis, A., Foley, E., O'Farrell, P.H., and Andino, R. (2006). The endocytic pathway mediates cell entry of dsRNA to induce RNAi silencing. Nature Cell Biology *8*, 793–802.

Sarkies, P., and Miska, E.A. (2013). RNAi pathways in the recognition of foreign RNA: antiviral responses and host–parasite interactions in nematodes. Biochem Soc Trans.; 41(4):876-80.

Scherer, L.J., and Rossi, J.J. (2003). Approaches for the sequence-specific knockdown of mRNA. Nat Biotechnol *21*, 1457–1465.

Schott, D.H., Cureton, D.K., and Whelan, S.P. (2005). An antiviral role for the RNA interference machinery in Caenorhabditis elegans. Proc Natl Acad Sci U S A. 20;102(51):18420-4.

Schüler, M., Connell, S.R., Lescoute, A., Giesebrecht, J., Dabrowski, M., Schroeer, B., Mielke, T., Penczek, P.A., Westhof, E., and Spahn, C.M.T. (2006). Structure of the ribosome-bound cricket paralysis virus IRES RNA. Nature Structural & Molecular Biology *13*, 1092–1096.

Sengupta, J., Nilsson, J., Gursky, R., Spahn, C.M.T., Nissen, P., and Frank, J. (2004). Identification of the versatile scaffold protein RACK1 on the eukaryotic ribosome by cryo-EM. Nat Struct Mol Biol *11*, 957–962.

Shi, H., Chamond, N., Djikeng, A., Tschudi, C., and Ullu, E. (2009). RNA interference in Trypanosoma brucei: role of the n-terminal RGG domain and the polyribosome association of argonaute. Journal of Biological Chemistry *284*, 36511–36520.

Shuai, K., and Liu, B. (2003). Regulation of JAK-STAT signalling in the immune system. Nature Reviews Immunology *3*, 900–911.

Singhal, N., Graumann, J., Wu, G., Araúzo-Bravo, M.J., Han, D.W., Greber, B., Gentile, L., Mann, M., and Schöler, H.R. (2010). Chromatin-Remodeling Components of the BAF Complex Facilitate Reprogramming. Cell *141*, 943–955.

Siomi, M.C., Saito, K., and Siomi, H. (2008). How selfish retrotransposons are silenced in Drosophila germline and somatic cells. FEBS Letters *582*, 2473–2478.

Song, R., Hennig, G.W., Wu, Q., Jose, C., Zheng, H., and Yan, W. (2011). Male germ cells express abundant endogenous siRNAs. Proc Natl Acad Sci U S A ;108(32):13159-64.

Souza-Neto, J.A., Sim, S., and Dimopoulos, G. (2009). An evolutionary conserved function of the JAK-STAT pathway in anti-dengue defense. Proceedings of the National Academy of Sciences *106*, 17841–17846.

Spahn, C.M.T., Jan, E., Mulder, A., Grassucci, R.A., Sarnow, P., and Frank, J. (2004). Cryo-EM visualization of a viral internal ribosome entry site bound to human ribosomes: the IRES functions as an RNA-based translation factor. Cell *118*, 465–475.

Spahn, C., Kieft, J.S., Grassucci, R.A., and Penczek, P.A. (2001). Hepatitis C Virus IRES RNA-Induced Changes in the Conformation of the 40S Ribosomal Subunit. Science, 291(5510):1959-62.

Stam, M., de Bruin, R., Kenter, S., van der Hoorn, R.A.L., van Blokland, R., Mol, J.N.M., and Kooter, J.M. (1997). Post-transcriptional silencing of chalcone synthase in Petunia by inverted transgene repeats. Plant J *12*, 63–82.

Stephenson, M.L., and Zamecnik, P.C. (1978). Inhibition of Rous sarcoma viral RNA translation by a specific oligodeoxyribonucleotide. Proc Natl Acad Sci U S A. 1; 75(1):285-8.

Subramanian, S., and Steer, C.J. (2010). MicroRNAs as gatekeepers of apoptosis. J Cell Physiol. ;223(2):289-98.

Tabara, H., Grishok, A., and Mello, C.C. (1998). RNAi in C. elegans: soaking in the

genome sequence. Science, 16;282(5388):430-1.

Tabara, H., Sarkissian, M., Kelly, W.G., Fleenor, J., Grishok, A., Timmons, L., Fire, A., and Mello, C.C. (1999). The rde-1 Gene, RNA Interference, and Transposon Silencing in C. elegans. Cell *99*, 123–132.

Takeuchi, O., and Akira, S. (2008). RIG-I-like antiviral protein in flies. Nature Immunology *9*, 1327–1328.

Taliaferro, J.M., Aspden, J.L., Bradley, T., Marwha, D., Blanchette, M., and Rio, D.C. (2013). Two new and distinct roles for Drosophila Argonaute-2 in the nucleus: alternative pre-mRNA splicing and transcriptional repression. Genes & Development *27*, 378–389.

Tam, S., Geller, R., Spiess, C., and Frydman, J. (2006). The chaperonin TRiC controls polyglutamine aggregation and toxicity through subunit-specific interactions. Nature Cell Biology *8*, 1155–1162.

Tam, S., Spiess, C., Auyeung, W., Joachimiak, L., Chen, B., Poirier, M.A., and Frydman, J. (2009). The chaperonin TRiC blocks a huntingtin sequence element that promotes the conformational switch to aggregation. Nature Structural & Molecular Biology *16*, 1279–1285.

Topisirovic, I., and Sonenberg, N. (2011). Translational Control by the Eukaryotic Ribosome. Cell *145*, 333–334.

Umbach, J.L., Kramer, M.F., Jurak, I., Karnowski, H.W., Coen, D.M., and Cullen, B.R. (2008). MicroRNAs expressed by herpes simplex virus 1 during latent infection regulate viral mRNAs. Nature,454(7205):780-3.

Vagin, V.V. (2006). A Distinct Small RNA Pathway Silences Selfish Genetic Elements in the Germline. Science *313*, 320–324.

Van der Krol, A.R., Mur, L.A., Beld, M., and Mol, J.N. (1990). Flavonoid genes in petunia: addition of a limited number of gene copies may lead to a suppression of gene expression. Plant Cell, 2(4):291-9.

van Mierlo, J.T., Bronkhorst, A.W., Overheul, G.J., Sadanandan, S.A., Ekström, J.-O.,

Heestermans, M., Hultmark, D., Antoniewski, C., and van Rij, R.P. (2012). Convergent Evolution of Argonaute-2 Slicer Antagonism in Two Distinct Insect RNA Viruses. PLoS Pathog *8*, e1002872.

van Rij, R.P., Saleh, M.C., Berry, B., Foo, C., Houk, A., Antoniewski, C., and Andino, R. (2006). The RNA silencing endonuclease Argonaute 2 mediates specific antiviral immunity in Drosophila melanogaster. Genes & Development *20*, 2985–2995.

Vargason, J.M., Szittya, G., Burgyan, J., and Hall, T. (2003). Size selective recognition of siRNA by an RNA silencing suppressor. Cell, ;115(7):799-811.

Vaucheret, H. (2008). Plant argonautes. Trends in Plant Science, 3(7):350-8.

Vinayagam, A., Hu, Y., Kulkarni, M., Roesel, C., Sopko, R., Mohr, S.E., and Perrimon, N. (2013). Protein complex-based analysis framework for high-throughput data sets. Science Signaling, *6(264):rs5.*

Vogel, J.L., and Kristie, T.M. (2000). The novel coactivator C1 (HCF) coordinates multiprotein enhancer formation and mediates transcription activation by GABP. The EMBO Journal *19*, 683–690.

Voinnet, O. (2013). How to become your own worst enemy. Nature Immunology, 14(4):315-7.

Voinnet, O., Li, W.X., Ji, L.H., Ding, S.W., and Baulcombe, D.C. (1998). Viral pathogenicity determinants are suppressors of transgene silencing in Nicotiana benthamiana. The EMBO Journal, Nov 16;17(22):6739-46.

Voinnet, O. (2005). Non-cell autonomous RNA silencing. FEBS Letters *579*, 5858–5871.

Voinnet, O., and Baulcombe, D.C. (1997). Systemic signalling in gene silencing. Nature *389*, 553–553.

Volta, V., Beugnet, A., Gallo, S., Magri, L., Brina, D., Pesce, E., Calamita, P., Sanvito, F., and Biffo, S. (2012). RACK1 depletion in a mouse model causes lethality, pigmentation deficits and reduction in protein synthesis efficiency. Cell. Mol. Life Sci. *70*, 1439–1450.

Wang, X.H. (2006). RNA Interference Directs Innate Immunity Against Viruses in Adult Drosophila. Science *312*, 452–454.

Wälde, S., and Kehlenbach, R.H. (2010). The Part and the Whole: functions of nucleoporins in nucleocytoplasmic transport. Trends in Cell Biology *20*, 461–469.

Weaver, B.K., Kumar, K.P., and Reich, N.C. (1998). Interferon regulatory factor 3 and CREB-binding protein/p300 are subunits of double-stranded RNA-activated transcription factor DRAF1. Molecular and Cellular Biology, 18(3):1359-68.

Wee, L.M., Flores-Jasso, C.F., Salomon, W.E., and Zamore, P.D. (2012). Argonaute Divides Its RNA Guide into Domains with Distinct Functions and RNA-Binding Properties. Cell *151*, 1055–1067.

Weeks, S.A., Shield, W.P., Sahi, C., Craig, E.A., Rospert, S., and Miller, D.J. (2009). A Targeted Analysis of Cellular Chaperones Reveals Contrasting Roles for Heat Shock Protein 70 in Flock House Virus RNA Replication. Journal of Virology *84*, 330–339.

Whitlow, Z.W., and Kristie, T.M. (2009). Recruitment of the Transcriptional Coactivator HCF-1 to Viral Immediate-Early Promoters during Initiation of Reactivation from Latency of Herpes Simplex Virus Type 1. Journal of Virology *83*, 9591–9595.

Wilkins, C., Dishongh, R., Moore, S.C., Whitt, M.A., Chow, M., and Machaca, K. (2005). RNA interference is an antiviral defence mechanism in Caenorhabditis elegans. Nature *436*, 1044–1047.

Wolf, M., Dimitrova, M., Baumert, T.F., and Schuster, C. (2008). The major form of hepatitis C virus alternate reading frame protein is suppressed by core protein expression. Nucleic Acids Research *36*, 3054–3064.

Wu, Q., Luo, Y., Lu, R., Lau, N., Lai, E.C., Li, W.X., and Ding, S.W. (2010). Virus discovery by deep sequencing and assembly of virus-derived small silencing RNAs. Proceedings of the National Academy of Sciences *107*, 1606–1611.

Yam, A.Y., Xia, Y., Lin, H.-T.J., Burlingame, A., Gerstein, M., and Frydman, J. (2008). Defining the TRiC/CCT interactome links chaperonin function to stabilization of newly made proteins with complex topologies. Nat Struct Mol Biol *15*, 1255–1262.

Ye, K., Malinina, L., and Patel, D.J. (2003). Recognition of small interfering RNA by a viral suppressor of RNA silencing. Nature, 426(6968):874-8.

Ye, X., and Liu, Q. (2008). Expression, purification, and analysis of recombinant Drosophila Dicer-1 and Dicer-2 enzymes. Methods Mol. Biol. *442*, 11–27.

Yeung, M.L., Bennasser, Y., Watashi, K., Le, S.-Y., Houzet, L., and Jeang, K.-T. (2009). Pyrosequencing of small non-coding RNAs in HIV-1 infected cells: evidence for the processing of a viral-cellular double-stranded RNA hybrid, 37(19):6575-86.

Zambon, R.A., Vakharia, V.N., and Wu, L.P. (2006). RNAi is an antiviral immune response against a dsRNA virus in Drosophila melanogaster. Cell. Microbiol. *8*, 880–889.

Zamecnik, P.C., and Stephenson, M.L. (1978). Inhibition of Rous sarcoma virus replication and cell transformation by a specific oligodeoxynucleotide. Proc Natl Acad Sci U S A. 1; 75(1):280-4.

Zavadil, J., Sachidanandam, R., and Hannon, G.J. (2011). Vreteno, a gonad-specific protein, is essential for germline development and primary piRNA biogenesis in Drosophila. Development ;138(18):4039-50.

Zhang, R., Mehla, R., and Chauhan, A. (2010). Perturbation of Host Nuclear Membrane Component RanBP2 Impairs the Nuclear Import of Human Immunodeficiency Virus -1 Preintegration Complex (DNA). PLoS ONE *5*, e15620.

Zhang, X., Yuan, Y.R., Pei, Y., Lin, S.S., and Tuschl, T. (2006). Cucumber mosaic virus-encoded 2b suppressor inhibits Arabidopsis Argonaute1 cleavage activity to counter plant defense. Genes Dev. Dec 1;20(23):3255-68.

Zhu, H., Wong-Staal, F., Lee, H., Syder, A., McKelvy, J., Schooley, R.T., and Wyles, D.L. (2012). Evaluation of ITX 5061, a scavenger receptor B1 antagonist: resistance selection and activity in combination with other hepatitis C virus antivirals. J. Infect. Dis. *205*, 656–662.

VII- Tables and Supplementary Data

- Table 1 (MS/MS) - Chapter 1 and Chapter 2 is attached as an excel file
- Table 1- Chapter 3 is attached as an excel file.

Functional Screen of the 101 interactants

Table 2- Chapter 1	RNAi			
GENE (Flybase ID)[1]	*Viability Z score* [2]	*Cell Number (%)* [3]	*DCV score* [4]	*t-test* [5]
GFP	-	100	1	-
AGO2	1.4	92	2.74376223720	5.6184604024E-13
alpha-Est1	0.1	111	1.08805443300	0.619499958459464
alphaCop	1.5	29	4.834565E+00	0.968330272819136
alt	0.1	54	1.12277233607	0.262553361649425
Ant2	0.5	58	1.84385067465	0.00299673300221
AP-2	0.1	42	1.12084698068	0.278999517521408
baf	0.4	102	2.55093733870	2.0182676183E-06
Cad74A	0.2	123	1.57657962195	0.057078859179
Cctgamma	0.4	68	2.202463768	0.004413193
CG10630 (Blanks)	0.9	131	2.51059242676	0.0032961566327
CG11107	0.8	66	2.79372844634	0.00188641241591988
CG11369	0.8	67	0.93698448684	0.680481972128114
CG11692	Unknown	Not tested	Not tested	Not tested
CG12179	0	87	1.40809492031	0.34048086492716
CG12184	0.6	48	1.20756390169	0.0373120067972119
CG13742	Unknown	42	0.96309086787	0.722564830905856
CG14492	0.2	51	1.19231208159	0.659767679824442
CG15270	0.1	58	1.64512502422	0.0199097625300767
CG15580	0	79	1.67523390841	0.0508345943573773
CG17838	0.2	92	1.20024921239	0.0488845536501619
CG31672	0.4	54	0.91967891866	0.164063377103243
CG31716	0.8	82	0.87812416733	0.00039845328487042
CG31755	0.6	94	1.81389034852	1.19527282337951E-07
CG32000	0.9	52	0.96376232347	0.004738375
CG32016	0.6	57	1.10475632504	0.390031172800262
CG32138	0.5	92	1.07699298633	0.395646557344053
CG34347	3.6	45	1.34237947002	0.0106724332691523
CG3800	0.4	83	1.56749821727	4.47438704064442E-08
CG42322	0.3	67	1.94979027951	0.00480097625110899
CG4771 (vreteno)	0.2	40	0.89140999759	0.296878539170924
CG5525	0.5	59	2.71043873670	9.95561281214434E-10
CG5964	0.3	41	1.24786207765	0.137660434194129
CG6084	0.4	60	1.34817331728	0.00834229722351772
CG6453	1	80	3.42018881921	2.02749840277922E-12
CG6680 (Spn77Ba)	0.1	34	1.51078337970	0.0132457650663528
CG7033	0.6	95	2.53859746992	5.33322149381657E-13
CG7546	0.4	57	1.93228497474	1.51612775247272E-06
CG7564	0.6	51	1.96155589219	3.02629616573759E-06
CG7816	0.5	59	2.47004850155	0.00317037473611717
CG9586	0.3	81	1.41284229965	0.028380123881846
CG9684	0.4	64	0.93834894	0.003849475
Cp1	0.8	47	1.66782239405	0.000106425240877014
CrebB-17A	0.1	34	1.28670976339	0.0384435250482816

Functional Screen of the 101 interactants

Dcr-2	1.3	114	0.91885850745	0.000994704604490258
	RNAi			
GENE (Flybase ID)[1]	***Viability Z score [2]***	***Cell Number (%) [3]***	***DCV score [4]***	***t-test [5]***
Ef2b	0.1	27	2.39151915365	7.3045367154E-(
Gr97a	0.1	112	3.29720008955	0.007038060902
Graf	0.4	59	1.12045635802	0.512528125930
Gs2	0.3	122	1.77638168824	0.000758963736
Hcf	0.2	51	4.26819004753	2.141141976933
Hsc70-1	0.8	86	0.62669753962	0.018355291060
Hsc70-2	0.5	128	1.04054562273	0.682011583488
Hsc70-3	2.9	92	1.28019474204	0.081866261245
Hsc70-4	2.8	122	2.86036463157	5.58146743695E
Hsc70-5	0.5	51	1.68433891769	0.001874266703
Hsp60	0.5	40	2.17163344191	3.1260391368E-(
Hsp70Aa	Unknown	51	1.19287406720	0.217319925597
ik2	0.3	50	0.91281258804	0.614490482693
Ir67b	0.3	Not tested	Not tested	Not tested
Jafrac1	0.5	75	1.21620315172	0.286823824245
Jupiter	0.6	91	0.78408191408	0.000742275886
lig	1.6	104	0.51598598068	1.24413710671E
Map205	1.4	53	1.30282051282	0.0025842385087
mop	0.5	74	1.96822222222	0.0041533266387
Msp-300	Unknown	89	1.38479613136	0.092176033524
mtTFB1	0.1	72	1.05814800328	0.661611892087
ns1	1.8	67	0.89159420289	0.5506874780486
Nup214	0.8	70	2.20374639079	8.22966271132E
Nup358	0.2	82	4.56314433444	3.8080196620E-1
Oatp58Db	0.5	83	1.56024695336	0.000961772307
pAbp	3.0	31	2.93597057072	0.020468530035
pont	0.3	86	3.91813801509	7.36238398840E
pyx	1	87	1.93621091023	0.003885128014
r2d2	0.8	112	2.30348946704	0.042832465422
RACK1	1.1	90	0.23411571918	6.00413732271E
RanGap	Unknown	55	2.67043917316	0.000994458980
Rapgap1	0	50	1.55280219185	0.026748156933
rept	0.1	73	2.57880786511	1.0932301623E-(
RhoGAPp190	0.2	81	1.69923181086	0.338164431046
Rip11	Unknown	81	5.12766422534	0.028422939234
RpL19	3.9	27	1.49010764670	0.101430695124
RpL22	4.3	25	0.59933195979	0.009911050554
RpL23A	1.8	19	0.66963596964	2.25979613970E
RpL24	3.3	33	0.54863428826	0.001513537326
RpL3	4.1	71	0.83834976573	0.215751103736
RpL38	3.4	45	0.69783208189	0.001066520971
RpL40	3.2	34	0.57105138882	0.001981235312
RpL7A	2.5	16	4.75179487179	0.0662218795344

Functional Screen of the 101 interactants

	RNAi			
GENE (Flybase ID)[1]	***Viability Z score [2]***	***Cell Number (%) [3]***	***DCV score [4]***	***t-test [5]***
RpS14a	3.2	23	3.22794871794	9.51E-06
RpS14b	3.3	47	2.02755555555	0.000263114
RpS15Aa	3.5	51	1.80230305417	0.0377671
RpS17	2.5	38	0.46445533738	1.18824E-05
RpS28b	1.1	51	1.28641156896	0.002328334
RpS3A	4.4	49	1.84983978376	6.90E-08
RpS5a	1.8	46	0.48010877788	4.71E-06
Sod	0.4	90	1.99770427556	0.00446331
T-cp1	0.4	65	2.47702934569	2.63E-08
Tcp-1eta	0.3	53	2.26494576371	2.80E-06
Tcp-1zeta	0.7	73	4.38305520934	0.00035195
Tollo	0.7	45	1.29348345	0.04749589
trpgamma	0.5	128	1.57536631000	0.009340957
unc-13	0.1	41	1.43389493	0.06839483

[1] List of genes tested by RNAi for DCV viral load.

[2] Z-score for viability as determined by Boutros et al, Science (2004) ;303(5659):832-5. Z>2.9 indicated that the depletion of the gene causes cell viability defects.

[3] DAPI positive cells were counted automatically using the INCELL 1000 Analyzer software after 4 days of RNAi treatment. The number represents the percentage of DAPI-positive cells compared to wells treated with dsRNA targeting GFP. We considered that a gene affects cell viability or proliferation when the value was <50%.

[4] Fold increase in DCV, VSV or FHV RNA measured by Q RT-PCR by comparison to cells treated with control dsGFP. Immunostaining quantifications are not shown (Data 80% similar to Q RT-PCR results)

5 Student t-test of three independent experiments for the corresponding dsRNA treatment.

* Highlighted in Grey or in Red are genes affecting DCV, VSV or FHV titers more than 2 folds (up or down, P<0,05) in both Q RT-PCR and immunostaining quantification ,without affecting cell viability or proliferation.

Functional Screen of the 101 interactants

	RNAi			
GENE (Flybase ID) [1]	***VSV score*** [4]	***t-test***	***FHV score*** [4]	***t-test***
GFP	1		1	
AGO2	3.693481242	0.0000166786	2.299446E+00	3.E-03
alpha-Est1	0.910006793	0.4904923620	1.302246E+00	4.E-02
alphaCop	4.792988726	0.0003712522	4.440697E-02	2.E-04
alt	1.443346493	0.0384687317	5.418632E-01	6.E-03
Ant2	1.067618321	0.6861864377	4.664047E-01	1.E-02
AP-2	0.796510849	0.3870209244	1.111558E+00	4.E-01
baf	1.418404446	0.0234309899	9.841653E-01	9.E-01
Cad74A	2.382150093	0.0007120827	9.741268E-01	8.E-01
Cctgamma	1.227525268	0.012748149	2.243345636	0.04734954
CG10630 (Blanks)	0.97836827	0.9434548282	6.370837E-01	2.E-02
CG11107	1.826467745	0.0005333437	8.071018E-01	1.E-01
CG11369	4.042979984	0.0093839399	9.840557E-01	9.E-01
CG11692	Not tested	Not tested	not tested	not tested
CG12179	1.541159909	0.0465570671	1.010598E+00	9.E-01
CG12184	0.749562587	0.3538166631	1.350028E+00	1.E-02
CG13742	0.851332143	0.5354094498	1.636377E+00	8.E-03
CG14492	2.070833069	0.0011934976	1.070128E+00	6.E-01
CG15270	1.146030158	0.5714490596	1.325662E+00	4.E-02
CG15580	1.901791875	0.0015021532	7.952587E-01	1.E-01
CG17838	1.03115974	0.7683137554	9.318447E-01	7.E-01
CG31672	1.080009037	0.5997429532	7.310430E-01	8.E-02
CG31716	1.191225529	0.2831674071	1.195332E+00	3.E-01
CG31755	1.281576987	0.0624609859	8.258523E-01	2.080E-01
CG32000	1.24554236	0.1542355491	1.110896E+00	5.E-01
CG32016	1.222873517	0.1938201825	5.950582E-01	1.E-02
CG32138	1.176852623	0.4192473964	1.137031E+00	3.E-01
CG34347	2.197119622	0.0001324608	6.477258E-01	4.E-02
CG3800	1.499974188	0.0302131901	1.276134E+00	7.E-02
CG42322	2.003486268	0.0266757708	1.294585E+00	4.E-02
CG4771	1.711655829	0.0291440323	1.022278E+00	9.E-01
CG5525	1.518379892	0.0177234624	8.778695E-01	4.E-01
CG5964	6.350144273	0.0000001947	1.181387E+00	2.E-01
CG6084	0.905434126	0.6339549412	7.564461E-01	8.E-02
CG6453	1.575908	0.1132243190	6.474244E-01	3.E-02
CG6680	1.14222354	0.4004561545	7.900258E-01	1.E-01
CG7033	4.373426413	0.0117886988	6.784327E-01	5.E-02
CG7546	1.211236518	0.2305248836	7.135308E-01	5.E-02
CG7564	1.13618378	0.4063201698	1.048747E+00	7.E-01
CG7816	2.534964434	0.0026423392	1.047799E+00	8.E-01
CG9586	1.25836462	0.1347019918	1.925087E+00	9.E-02
CG9684	1.110527997	0.4981483444	9.030046E-01	4.E-01
Cp1	1.367440234	0.0516093861	3.275242E-01	6.E-04
CrebB-17A	0.927670665	0.7115142610	4.590404E-01	3.E-03

Functional Screen of the 101 interactants

Dcr-2	2.340071661	0.0011699169	1.233893E+00	3.E-01
	RNAi			
GENE (Flybase ID)[1]	***VSV score***	***t-test***	***FHV***	***t-test***
Ef2b	5.113783856	0.000544852	0.089437526	7.8176E-07
Gr97a	2.185301439	4.26583E-05	1.092165285	0.44248025
Graf	1.351872441	0.080440355	1.890229179	0.0152009
Gs2	1.808469107	0.030794967	0.696094076	0.08127928
Hcf	3.958271351	0.004743836	3.055413199	0.00015604
Hsc70-1	0.923952078	0.635028585	1.834918574	0.03720099
Hsc70-2	1.37837682	0.06952961	2.291976291	0.03545011
Hsc70-3	1.397691039	0.135855042	0.761143421	0.23309628
Hsc70-4	1.855839869	0.001400849	0.560576582	0.07631215
Hsc70-5	2.100815625	0.001562955	0.117953131	0.00041571
Hsp60	1.158037618	0.499487857	0.765547423	0.04697429
Hsp70Aa	1.451603746	0.219547235	2.311526142	0.32035089
ik2	2.275328749	0.000597628	1.383122961	0.08291834
Ir67b	not tested	not tested	not tested	not tested
Jafrac1	1.17977951	0.332839373	1.147892546	0.40952396
Jupiter	0.974165831	0.858413439	0.955442251	0.76246488
lig	1.180021066	0.274861723	0.849419631	0.36975559
Map205	2.548634798	0.002124311	0.976905597	0.733751043
mop	1.234355245	0.18484689	0.7345465	0.0634645
Msp-300	1.51479281	0.012034812	0.927203304	0.62810704
mtTFB1	1.980507079	0.003983376	0.73462989	0.12506605
ns1	1.272176705	0.133585675	0.224084209	0.000560382
Nup214	2.542970155	4.51628E-05	0.637589871	0.01871279
Nup358	3.761891046	0.000155998	0.973041862	0.83404306
Oatp58Db	1.309292053	0.069816152	0.974865737	0.86121215
pAbp	5.087021673	0.000154597	0.384333636	0.00426336
pont	5.254902063	2.85921E-06	0.336775197	0.00069206
pyx	1.796447759	0.006641542	1.217664281	0.13332608
r2d2	2.014127801	0.003210615	1.057537723	0.73341746
RACK1	1.160721807	0.428096658	0.9679406	0.038594
RanGap	2.069448484	0.001555646	1.739940521	0.03612306
Rapgap1	1.348812907	0.126700353	3.900868362	0.01850515
rept	3.533570206	2.04992E-05	0.635749163	0.1906879
RhoGAPp190	1.606539102	0.019182667	1.354441171	0.06492908
Rip11	1.307619799	0.15904237	1.114784831	0.45558087
RpL19	4.655249038	8.31091E-06	0.074682008	0.00017049
RpL22	2.104059448	0.000975225	0.152604997	0.00016956
RpL23A	2.519154857	3.11895E-05	0.077763998	8.1711E-05
RpL24	1.296465631	0.105744545	0.205539165	0.00511771
RpL3	0.753637601	0.213328356	0.45712258	0.0043128
RpL38	2.753080354	0.000947231	0.087298846	9.1435E-05
RpL40	0.605031438	0.002916116	0.134217198	0.00012201
RpL7A	7.981741626	0.000106556	0.079808873	7.28128E-07

Functional Screen of the 101 interactants

	RNAi			
GENE (Flybase ID)[1]	***VSV score***	***t-test***	***FHV***	***t-test***
RpS14a	6.184898706	0.001481629	0.689374322	0.020573136
RpS14b	3.404790298	0.000802851	0.312776877	0.000883073
RpS15Aa	7.657067273	0.000128312	0.727198696	0.057147464
RpS17	2.638367253	0.000185636	0.181032848	0.00019419
RpS28b	3.356596756	0.002956375	0.148662374	0.000150522
RpS3A	3.454102307	1.0729E-05	0.059826104	7.6207E-05
RpS5a	2.549998735	1.10983E-05	0.062069486	7.75733E-05
Sod	1.104470415	0.60015012	1.058563872	0.734705443
T-cp1	6.406955762	2.25126E-05	0.741026463	0.075878034
Tcp-1eta	1.33945417	0.189176438	1.415386151	0.052614696
Tcp-1zeta	2.545368792	0.004807509	1.134984993	0.325811246
Tollo	2.283765451	0.000152064	1.358813378	0.129542136
trpgamma	1.098462988	0.441275741	1.05216754	0.752207359
unc-13	1.067026049	0.781513557	1.183671773	0.147902504

Primers Table	
	Sequence
DCR-2,AGO2 and r2d2 cloning primers	
R2d2 C-ter fusion forward (gateway)	5'-GGGGacaagtttg tac aaa aaagcaggctGCCACCATG GAT AACAAGTCAGCCGTATCTGCTC-3'
R2d2 C-ter fusion Reverse	5'-GGG Gac cac ttt gta caa gaa agc tgg gtC AATCAACATGGTGCGAAAATAGTC-3'
R2d2 N-ter fusion forward(gateway)	5'-GGGG aca agt ttg tac aaa aaa gca ggc tTC GATAACAAGTCAGCCGTATCTGCTC-3'
R2d2 N-ter fusion Reverse	5'-GGGGaccactttgtacaagaaagctgggtCTTATCACTA TTAAATCAACATGGTGCGAAAATAG-3'
N-ter fusion Dicer-2 FWD	5'-GGGG aca agt ttg tac aaa aaa gca ggc tTC GAAGATGTGGAAATCAAG CCTCGCG-3'
N-ter fusion Dicer-2 REV	5'-GGGGaccactttgtacaagaaagctgggtCTTATCACTA TTAGGCGTCGCATTTGCTTAGCTGC-3'
C-ter fusion Dicer-2 FWD	5'-GGGGacaagtttg tac aaa aaagcaggctGCCACCATG GAAGATGTGGAAATCAAG CCTCGCGGC-3'
C-ter fusion Dicer-2 REV	5'-GGG Gac cac ttt gta caa gaa agc tgg gtC GGCGTCGCATTTGCTTAGCTGCTGAAG-3'
N- ter fusion Ago-2 FWD	5'-GGGG aca agt ttg tac aaa aaa gca ggc tTC GGAAAAAAAGATA AGAACAAGAAAGGAGG-3'
N-ter fusion Ago-2 REV	5'-GGGGaccacttt gtacaagaaagctgggtCTTATCACTA TCA GACAAAGTACATGGGGTTTTTCTTC ATG-
C-ter fusion Ago-2 FWD	5'-GGGG acaagttt gtac aaa aaa gca ggc t GC CAC CATG GGAAAAAAAGATA AGAACAAGAAAGG-
C-ter fusion Ago-2 REV	5'-GGG Gac cac ttt gta caa gaa agc tgg gtC GACAAAGTACATGGGGTTTTTCTTC-3'
CrPV IRES 1 cloning	
Forward primer containing an EcoRI site:	GGAATTCtttaataagtgttgtgcagat
the reverse primer complementary to the 5'end of the CrPV ORF1 containing a BstbI site:	AAAAttcgaaGAGTTGATGTTGTTGGTTGCG.

shRNA against RACK1 5'UTR cloning primers	
Forward :	ctagtagtTAGCAAATAATATAAACTCAAtagttatattcaagcataTTGAGTTTATATTATTTGC
Reverse :	aattcgcTAGCAAATAATATAAACTCAAtatgcttgaatataactaTTGAGTTTATATTATTTGC
RACK1 mutagenesis primers :	
R38D K40E Fwd	ccataatttcggcctccgatgacgagaccctgatcgtgtgg
R38D K40E Rev	ccacacgatcagggtctcgtcatcggaggccgaaattatgg
D108Y Fwd	cttcgagggacacactaagtatgttttgtcggttgccttct
D108Y Rev	agaaggcaaccgacaaaacatacttagtgtgtccctcgaag
RACK1 dsRNA primers	
Fwd Primer 1	taatacgactcactatagggAAGACCATCAAGCTGTGGAA
Rev Primer 1	taatacgactcactatagggGCTCCTCAACGGTCTTCTTG
Fwd Primer 2	taatacgactcactatagggCTCGCCCAACCACTCCAACC
Rev Primer 2	taatacgactcactatagggCGCAGCTCCTCAACGGTCTTCT
Q-PCR primers	
DCV Fwd	TCATCGGTATGCACATTGCT
DCV Rev	CGCATAACCATGCTCTTCTG
FHV Fwd :	TTTAGAGCACATGCGTCCAG
FHV Rev	CGCTCACTTTCTTCGGGTTA
CrPV Fwd	GCTGAAACGTTCAACGCATA
CrPV Rev	CCACTTGCTCCATTTGGTTT
RP49 Fwd	GACGCTTCAAGGGACAGTATCT
RP49 Rev	AAACGCGGTTCTGCATGAG
Primers for RNAi screen	
Hsp68 fwd	taatacgactcactatagggCAGGCAACAAAGGATGCTG
Hsp70Aa fwd	taatacgactcactatagggAAACTGGTTGTTGCGGTAGG
RpL24 fwd	taatacgactcactatagggCTAACCCCATTTCGGCAATA
Hsc70-1 fwd	taatacgactcactatagggGAAGGCGAAGTTGGTAGCAG
Cctgamma fwd	taatacgactcactatagggCACCTGCAGTCCCAGCTTAG
Graf fwd	taatacgactcactatagggATGAATAGCTCGGGCGGT
CG9586 fwd	taatacgactcactatagggCAGCTGTTCCGCTGTCAAC
Act57B fwd	taatacgactcactatagggTGACGATGAAGTTGCTGCTC

CG3983 fwd	taatacgactcactatagggGGAACGCGAACAGAACAAGT
Hsp70Ba fwd	taatacgactcactatagggCATTCCGTGCAAGCAGACTA
RanGap fwd	taatacgactcactatagggCTTGCCGAATCCTTCAAGC
RpS17 fwd	taatacgactcactatagggGTGAAGAAGGCCGCTAAGGT
Act88F fwd	taatacgactcactatagggCAGATGTGGATCTCGAAGCA
Rapgap1 fwd	taatacgactcactatagggTTGAAAACATTCTTCGTGCG
Hcf fwd	taatacgactcactatagggTGTCGGATGCTTTGTTTTTG
alphaTub85E fwd	taatacgactcactatagggTTATGGTTGACAACGAGGCA
r2d2 fwd	taatacgactcactatagggTTTTTGACAAAGCGGCATAA
CG31716 fwd	taatacgactcactatagggCCGCAAGCCTCTAGCAATA
CG32000 fwd	taatacgactcactatagggAGTTAAAGGGTGTCCTGCCC
Hsc70-4 fwd	taatacgactcactatagggCTGTGGCCTACGGTGCTG
RpL23A fwd	taatacgactcactatagggGAGCTGGATGAGTCGGAAAG
AGO2 fwd	taatacgactcactatagggCGCTACACGATCGAAATCAA
Dcr-2 fwd	taatacgactcactatagggCTTTTTGGACATGGTCACCC
RpS3A fwd	taatacgactcactatagggGTTTTCTCGCAAGGACTGGT
CG3800 fwd	taatacgactcactatagggGAGGAGGAAGAGGGCAAAG
Tcp-1zeta fwd	taatacgactcactatagggCCCTTGCCGATCTGCTTAC
CG7033 fwd	taatacgactcactatagggACACCAATTGATCGCGTTTT
CG10630 fwd	taatacgactcactatagggTGCCCTTATGGTTTTGAATGA
RpS28b fwd	taatacgactcactatagggACCGCTCAACTTCCTTTTTG
pont fwd	taatacgactcactatagggCTGGTTCCCGGAGTTCTCTT
CG31755 fwd	taatacgactcactatagggTAACCATGGCCATCCCTTAC
alt fwd	taatacgactcactatagggGTAAACCTAAAGCATGCCCC
CG31672 fwd	taatacgactcactatagggGGATATCTAACCCCACGCAA
betaTub60D fwd	taatacgactcactatagggACTTTACACGGAGGCACGTC
Act79B fwd	taatacgactcactatagggCCGCACCAAACTAACCAAAC
alphaTub84B fwd	taatacgactcactatagggAGTCCAAGCTGGAGTTCGC
betaTub56D fwd	taatacgactcactatagggGGCCAAGGGTCATTACACAG
Ef2b fwd	taatacgactcactatagggCAACATGTCTGTGATTGCCC
sesB fwd	taatacgactcactatagggGTGGCGTGGACAAGAACAC
RpS14a fwd	taatacgactcactatagggTTGATATCCGGTTAACGCAA
Jupiter fwd	taatacgactcactatagggCGACCAATCCACGAACAATA
RpS5a fwd	taatacgactcactatagggAATAGATCGCAAAGCCCTCA
Sod fwd	taatacgactcactatagggAAGGTCTCCGGTGAGGTGT
Hsc70-2 fwd	taatacgactcactatagggCACCTTCGACGTCTCCGTA
baf fwd	taatacgactcactatagggAGATGTGTTGTTGCATTTTCG
betaTub97EF fwd	taatacgactcactatagggGTGCAGAGCAAGAACAGCAG
RpL38 fwd	taatacgactcactatagggGATGCGCGTGCTGTAAAAAT
Hsp70Bc fwd	taatacgactcactatagggTCAACGTAAAGCAGTCCGTG
Act87E fwd	taatacgactcactatagggTCTGAGGCAACACCTACACG
RpS3 fwd	taatacgactcactatagggGTCGTGCTTGCTATGGTGTG
Nup358 fwd	taatacgactcactatagggGCTACAGTAGGCTGAACCCG
Hsp70Bb fwd	taatacgactcactatagggCTCAGAACAGCAGCTGAACG

alpha-Est1 fwd	taatacgactcactatagggAACGCCCACCTACCTGTACC
RpS3 fwd	taatacgactcactatagggTAACCTCAAAGCAGATGGGC
Nup358 fwd	taatacgactcactatagggGTTAATGGCCCAAAAGCAGA
Hsp70Bb fwd	taatacgactcactatagggAACTCACACACAATGCCTGC
lig fwd	taatacgactcactatagggAAAACCTTTCCGTCCTCTCC
CG32138 fwd	taatacgactcactatagggGCCTTCAGGGTGTCTTGTGT
CG8258 fwd	taatacgactcactatagggGAGCTGCTGCGTCTAGGAAT
T-cp1 fwd	taatacgactcactatagggCACAGTGACCAACGATGGAG
alphaTub84D fwd	taatacgactcactatagggTCTTTAAATTTCCCACCGGC
Act42A fwd	taatacgactcactatagggGCTACGTGGCCTTGGACTT
Act5C fwd	taatacgactcactatagggCATTGTGCACCGCAAGTG
Hsp70Bbb fwd	taatacgactcactatagggATCGGGGTGGAGTATAAGGG
Hsc70-3 fwd	taatacgactcactatagggCGGCACCTTCGATGTCTC
CG6680 fwd	taatacgactcactatagggGTCACTCAGCTGATGCTCGT
rept fwd	taatacgactcactatagggCAAGATCGCCGGAAGATGTA
Nup214 fwd	taatacgactcactatagggCCGCAGCAATGTGAACCT
RpS27 fwd	taatacgactcactatagggCAGCACCCCAACTCGTACTT
CG6084 fwd	taatacgactcactatagggCAAGGGTCAGGTCACCGAG
Ant2 fwd	taatacgactcactatagggGTGCAGGGCATCGTCATCTA
Hsp68 rev	taatacgactcactatagggCGGCTCACCTTCGAGTAGA
Hsp70Aa rev	taatacgactcactatagggGCAGGCATTGTGTGTGAGTT
RpL24 rev	taatacgactcactatagggCGAAAGGTGTTTACCGCTTG
Hsc70-1 rev	taatacgactcactatagggTACGTGGTACCAAGATCAATGC
Cctgamma rev	taatacgactcactatagggCCCTTCTTGTACTCCAGCGA
Graf rev	taatacgactcactatagggCTCCTTGCGCATTGCAGTAT
CG9586 rev	taatacgactcactatagggGGATGGCTCTGTAGCCACTT
Act57B rev	taatacgactcactatagggCTTATGAAAGTGATTCGGGCA
CG3983 rev	taatacgactcactatagggGGTTGGCCTGATCCTGTGT
Hsp70Ba rev	taatacgactcactatagggTCCACGGACTGCTTTACGTT
RanGap rev	taatacgactcactatagggCTGCCTTCTTCTCCAAAGCTA
RpS17 rev	taatacgactcactatagggCGACCAAAGTTGTTGGTGTT
Act88F rev	taatacgactcactatagggATTTGGCTTTCAATTCACTGAC
Rapgap1 rev	taatacgactcactatagggCGTGCCACCAATGTGTAGG
Hcf rev	taatacgactcactatagggCCGAAGACGACCATTAGCTC
alphaTub85E rev	taatacgactcactatagggTCGAACTTGTGATCCAGACG
r2d2 rev	taatacgactcactatagggGTGTTTGGCATCACGCTTC
CG31716 rev	taatacgactcactatagggCTCGACAATTGCCTCGTTG
CG32000 rev	taatacgactcactatagggATGTCAGCTACATTTGCCATCTT
Hsc70-4 rev	taatacgactcactatagggTTGGAGAGACGACCCTTGTC
RpL23A rev	taatacgactcactatagggTGATGCACACCTTCTTCTGG
AGO2 rev	taatacgactcactatagggTATACCCTTGGAGCGCTTTG
Dcr-2 rev	taatacgactcactatagggTGAACGCCAATATTCATGAGG
RpS3A rev	taatacgactcactatagggCTTGCGATTGCTGAGCATAA
CG3800 rev	taatacgactcactatagggCCTGATTCTTCGCTTTTTCA
Tcp-1zeta rev	taatacgactcactatagggCGATGCCCTTCTGGTTGAT

CG7033 rev	taatacgactcactatagggCTTCAGACGCATCACAGCAT
CG10630 rev	taatacgactcactatagggAAGGGTGCATATTCTTCCATGT
RpS28b rev	taatacgactcactatagggGCTTCTTCTTCTCCGCGAAA
pont rev	taatacgactcactatagggCACATCTGATGAGCCGGG
CG31755 rev	taatacgactcactatagggCCACTCAAGGTTGATGAATCG
alt rev	taatacgactcactatagggGCTGGGTTTTAAATTCATTTGC
CG31672 rev	taatacgactcactatagggTTTCCTTTGGATTCCTCTGG
betaTub60D rev	taatacgactcactatagggCAAGAGAAGTACTGCACACGAA
Act79B rev	taatacgactcactatagggGTACATGGCCGGGGAGTT
alphaTub84B rev	taatacgactcactatagggGGGATCGCACTTGACCATCT
betaTub56D rev	taatacgactcactatagggTGAAGAAGTGAAGACGTGGG
Ef2b rev	taatacgactcactatagggCCGTCATCGTTATAGGTGGC
sesB rev	taatacgactcactatagggGCACGGTATCGAAGGGATAG
RpS14a rev	taatacgactcactatagggGGACGAAGGTGTCGTTGAAG
Jupiter rev	taatacgactcactatagggGGATTGCGTGAATCGAGTTT
RpS5a rev	taatacgactcactatagggATCAGCTTCTTGCCGTTGTT
Sod rev	taatacgactcactatagggATTGAACCTCAAAGGTTGCG
Hsc70-2 rev	taatacgactcactatagggCCCACCAGGACCACATCAT
baf rev	taatacgactcactatagggGCACACCTCCTTCATCCAGT
betaTub97EF rev	taatacgactcactatagggATCGAACTCCACTTCGTCGT
RpL38 rev	taatacgactcactatagggAAACAAATTTATCGCGAACCA
Hsp70Bc rev	taatacgactcactatagggTTGGCTTTAGTCGACCTCCT
Act87E rev	taatacgactcactatagggTTGGCTACTGGCTGTTTTCA
RpS3 rev	taatacgactcactatagggGTCTCGACATAGTCGTTGCAC
Nup358 rev	taatacgactcactatagggTCGCAGGTTGAAGACTTGCT
Hsp70Bb rev	taatacgactcactatagggTAGTCTGCTTGCACGGAATG
alpha-Est1 rev	taatacgactcactatagggATACATGCATACAAACTCCCCC
RpS3 rev	taatacgactcactatagggATCTCCCGAATGGATCATCA
Nup358 rev	taatacgactcactatagggGCGTTTTCTGCAGGCATT
Hsp70Bb rev	taatacgactcactatagggTCGAAGATAAGCACATTGCG
lig rev	taatacgactcactatagggTGCATCATTTGCAATTCCTC
CG32138 rev	taatacgactcactatagggGCTTTCGTCCTCAGCGATT
CG8258 rev	taatacgactcactatagggGGCCATCAGACCGTATTTGT
T-cp1 rev	taatacgactcactatagggCCACAACCATGGCTGAGAAG
alphaTub84D rev	taatacgactcactatagggCTGACTCTGCGGGCGTAT
Act42A rev	taatacgactcactatagggGAGATCCACATCTGCTGGAAA
Act5C rev	taatacgactcactatagggTGTTGTTGGTGTGTGTGTGG
Hsp70Bbb rev	taatacgactcactatagggTAGCCGGTTGTCAAAGTCCT
Hsc70-3 rev	taatacgactcactatagggCACCGACCAGCACAATCTC
CG6680 rev	taatacgactcactatagggCCTTCAGGCAGGGCTTTTA
rept rev	taatacgactcactatagggGACCCAGCTTGTTGACCTTT
Nup214 rev	taatacgactcactatagggGGATTCCAGAGGAGCTGGAC
RpS27 rev	taatacgactcactatagggTTGCACACACAAGAGCTTCC
CG6084 rev	taatacgactcactatagggTAATCAACCGGCGAGTACAG
CG32016 fwd	taatacgactcactatagggCGAAAAGACCGTAGAAGCCA

Hsc70-5 fwd	taatacgactcactatagggGCTGAAGGGCCATTGAAATA
unc-13 fwd	taatacgactcactatagggATTCGGCTACAGTCCACAAT
tsr fwd	taatacgactcactatagggTATTCGCTTGCACAGGTACG
CG4771 fwd	taatacgactcactatagggTTGTGGGTCCCAACATAAGG
RpL24 fwd	taatacgactcactatagggAAACAGTGCCCCTGCTAATG
Jafrac1 fwd	taatacgactcactatagggCCGAGTTCCGCAAGATCAAT
CG6453 fwd	taatacgactcactatagggCTTGGCATGCGTAGACCAG
RpL7A fwd	taatacgactcactatagggAGGCCAAAGAAGAAGCCAGT
CG7546 fwd	taatacgactcactatagggGATCGATTGCGCTGACAATA
Cp1 fwd	taatacgactcactatagggTGGAGCACCGCAAGAACTAT
alphaCop fwd	taatacgactcactatagggGTGGGCTTGATGACCACCTA
RpL3 fwd	taatacgactcactatagggTCTTTTCCGTTTTACACGTCTG
RpL40 fwd	taatacgactcactatagggTGCGTGGTGGTATCATTGAG
CG9684 fwd	taatacgactcactatagggACGGCAGCAGACAAAGTACC
CG5525 fwd	taatacgactcactatagggCACCATCCTGAAGCAGATGA
RpS17 fwd	taatacgactcactatagggCCAAGACGGTGAAGAAGGC
CrebB-17A fwd	taatacgactcactatagggAAATTGAAGCGGAAACGGTA
CG7564 fwd	taatacgactcactatagggCATTTTAGAACATCCTCACGCA
Map205 fwd	taatacgactcactatagggACCCTCGATTTCTTGCTACA
CG34347 fwd	taatacgactcactatagggCTCTGACCTCTGACCCCG
RpL22 fwd	taatacgactcactatagggCGTTCACTTTTCCAAGGCAT
RpL23A fwd	taatacgactcactatagggAAGATCCGCACCAACGTG
CG32016 rev	taatacgactcactatagggCACTGAACCATTCAGGTTCTTC
Hsc70-5 rev	taatacgactcactatagggGCTGTAGAATCTTCCCGCAA
unc-13 rev	taatacgactcactatagggGCAGCTTTTCCCAAAATTGA
tsr rev	taatacgactcactatagggAAATTGGCGATCTCAACAGG
CG4771 rev	taatacgactcactatagggTCCTGTATGTCTCGCTGCAT
RpL24 rev	taatacgactcactatagggCGAAAGGTGTTTACCGCTTG
Jafrac1 rev	taatacgactcactatagggCAGACCTCGCCGTACTTGTC
CG6453 rev	taatacgactcactatagggACCTTGAAATCGTCTGTGCTC
RpL7A rev	taatacgactcactatagggTCCAGAGGATCAACATCGTG
CG7546 rev	taatacgactcactatagggTGCTCCCTCACTTGTTATAGCTT
Cp1 rev	taatacgactcactatagggGCAGTGTCCCTGATCCTTGA
alphaCop rev	taatacgactcactatagggCAGACGCGAATACTGCGAT
RpL3 rev	taatacgactcactatagggGGTGCCGAGAACTTACGATG
RpL40 rev	taatacgactcactatagggCTGTGCCTTGGCAGCAAAT
CG9684 rev	taatacgactcactatagggTCGTAATGTGTTTGACCCGA
CG5525 rev	taatacgactcactatagggACCACCTTGGAGTTCAACGA
RpS17 rev	taatacgactcactatagggGTCGACCTCGATGATGTCCT
CrebB-17A rev	taatacgactcactatagggCCAAAGGAGGCTTTGAAGTG
CG7564 rev	taatacgactcactatagggGGACAGCAGTCGAGCAGAA
Map205 rev	taatacgactcactatagggCGGAGAACATGGTGACATTG
CG34347 rev	taatacgactcactatagggCGCTCCAAAAACACACACAC
RpL22 rev	taatacgactcactatagggATTGAGGCTAGCCCGAAGTT
RpL23A rev	taatacgactcactatagggCGCACATAGGCCTTCTTCTG

Ef1alpha48D fwd	taatacgactcactatagggGGAACCCTCTACCAACATGC
AP-2 fwd	taatacgactcactatagggGAGGGATGGTGTCGTCGT
CG15270 fwd	taatacgactcactatagggGCCCCCATTAAGTCGAGATT
Hsp60 fwd	taatacgactcactatagggCAACGGTGATCAGGCCAT
CG12184 fwd	taatacgactcactatagggGATCGAATAAGGATTTCCCCA
CG13742 fwd	taatacgactcactatagggGTCCGAAAACCATGATAGCC
Ef1alpha100E fwd	taatacgactcactatagggAGAAGATCGGCTACAATCCG
Tcp-1eta fwd	taatacgactcactatagggGAAAGGGGGAAGGATAAGTTTTT
RpS5b fwd	taatacgactcactatagggAAAGTGACAGCTCCTTTTACCG
CG14492 fwd	taatacgactcactatagggTTTCTGCAGCTGAAGTTTGC
Ir67b fwd	taatacgactcactatagggGGGATTGTGGTTTGGTGGT
ik2 fwd	taatacgactcactatagggGAGGAGGATCAAGAGGGGC
CG11107 fwd	taatacgactcactatagggCTTCAAACTGGTGAGTAAAACCG
CG17838 fwd	taatacgactcactatagggTTTGCAACAAACACCCATTG
CG15580 fwd	taatacgactcactatagggCTTTCAACGCACAAACAAACA
Cad74A fwd	taatacgactcactatagggAGTTTGTTTTGCATTTCGGC
Gs2 fwd	taatacgactcactatagggCGTGTTCCAGTAACGCTTCC
CG5964 fwd	taatacgactcactatagggCCTGTTCGATTATTTTCGTTGC
trpgamma fwd	taatacgactcactatagggGAGAAGAAGTTCCTGCTGGC
Oatp58Db fwd	taatacgactcactatagggAAGGCCGCTATTCGCTATCT
mtTFB1 fwd	taatacgactcactatagggGCTTTGGGTGTCTCCGTTT
CG12179 fwd	taatacgactcactatagggAGCAGCTCGCAAAAGGAGT
pAbp fwd	taatacgactcactatagggAATCCATCCGGTCCGTAAAG
CG11369 fwd	taatacgactcactatagggGGCGGGAGACACCAAAAT
Msp-300 fwd	taatacgactcactatagggCTGAGCCAAAGCCAAGAAAA
RpL19 fwd	taatacgactcactatagggCCCATTCCAGGTCAGAACAT
RpS15Ab fwd	taatacgactcactatagggTCCTGACCGTGATGATGAAG
RpS15Aa fwd	taatacgactcactatagggTTTTTCCTTCCGTTTCCCTT
Gr97a fwd	taatacgactcactatagggATTGTGTGGCGGGCATTTAT
pyx fwd	taatacgactcactatagggCTGCGAAGGTGGAAAGTGG
Rip11 fwd	taatacgactcactatagggGTGTCGCGCGTGATTAAA
CG7816 fwd	taatacgactcactatagggTTGTATTTTCCGCACGGC
RhoGAPp190 fwd	taatacgactcactatagggGGAGGGGGAGAGAAAGGAT
CG42322 fwd	taatacgactcactatagggGCACTTGCTCAGGCATATCA
RpS14b fwd	taatacgactcactatagggCATCGAGGATGTGACCCCTA
CG9311 fwd	taatacgactcactatagggGGCTGCTCTTCTTACGGGAG
CG3983 fwd	taatacgactcactatagggGTGTGGGCGATGTAAAGGAT
Ef1alpha48D rev	taatacgactcactatagggGCCAATTTTGTACACATCCTG
AP-2 rev	taatacgactcactatagggTGTGCTTTTCACAAAATGTCG
CG15270 rev	taatacgactcactatagggAACCTACAGGCAAATTTCATTCA
Hsp60 rev	taatacgactcactatagggCGAGGAGTTGATGAAGTACGG
CG12184 rev	taatacgactcactatagggAATTGGCCGGCTACATTAAA
CG13742 rev	taatacgactcactatagggTACCCGGAATCGTCGATGTA
Ef1alpha100E rev	taatacgactcactatagggGTCGATCAAGCACTTGCCCT
Tcp-1eta rev	taatacgactcactatagggCTTCCTTCTCTGGCATGAGC

RpS5b rev	taatacgactcactatagggGGCATTGTGGTAACGACATC
CG14492 rev	taatacgactcactatagggGGCAACAGGTTGTTCGAGTA
Ir67b rev	taatacgactcactatagggCGCTGTGCAACAATATTTGA
ik2 rev	taatacgactcactatagggATGCACCAGCTTGTTATCCC
CG11107 rev	taatacgactcactatagggACCATGCTGATCGCAACTTT
CG17838 rev	taatacgactcactatagggGATGACGATGATGATGTATCCAA
CG15580 rev	taatacgactcactatagggTTCCGTTCGCTGTATAGGTTC
Cad74A rev	taatacgactcactatagggCAGTGCCGTTAGGTATCCGT
Gs2 rev	taatacgactcactatagggCTTTTGCTGTCGTGTGGAAC
CG5964 rev	taatacgactcactatagggGCTGGCGTCTCAAAGAAGTT
trpgamma rev	taatacgactcactatagggGTTGATCAGCAACTCCACCA
Oatp58Db rev	taatacgactcactatagggGGCCCCTGAAAATTGAGAAG
mtTFB1 rev	taatacgactcactatagggCCTGTTGTGCAACGACTTCA
CG12179 rev	taatacgactcactatagggTGGCCTGCGAGAACTTATCT
pAbp rev	taatacgactcactatagggGAACTTGTCAAAAAGTCCCGA
CG11369 rev	taatacgactcactatagggCGCCAAGCGTCTCTTTTTAG
Msp-300 rev	taatacgactcactatagggTTGCTAACTCTGCGTCCTCA
RpL19 rev	taatacgactcactatagggTTCGCAGTACCCTTACGCTT
RpS15Ab rev	taatacgactcactatagggTGTTGGTCCACTTCTCGATG
RpS15Aa rev	taatacgactcactatagggCGGCATTTACCTGGATTTGT
Gr97a rev	taatacgactcactatagggCCGCCGAAGAAGCAATTAT
pyx rev	taatacgactcactatagggGTGATATTGCTGCATGTGTGG
Rip11 rev	taatacgactcactatagggGAAGGTCCTGCCTTTCGTTT
CG7816 rev	taatacgactcactatagggCTCTGCGTGGGTTAAACGTA
RhoGAPp190 rev	taatacgactcactatagggAGATTTCCTTTGCCGCAGTA
CG42322 rev	taatacgactcactatagggGGGGAGACTAACTCCGTGCT
RpS14b rev	taatacgactcactatagggGCCCTTGCCACTGCATTTAT
CG9311 rev	taatacgactcactatagggCCCATCTGACGCTTCTCCT
CG3983 rev	taatacgactcactatagggTCATAGTACTCACCCATTCTGGC

Résumé détaillé en francais

Etude de l'interactome de la voie des siRNA dans l'organisme modèle *Drosophila melanogaster*

Etat de la question :

La voie de l'ARN interférence (ARNi), en particulier celle des siRNA, constitue la défense antivirale majeure chez les plantes, les nématodes et les insectes. Le génome de l'organisme modèle *Drosophila melanogaster* code pour trois protéines, Dcr-2, AGO2 et R2D2, indispensables à cette voie. Les mouches mutantes pour une de ces trois protéines sont plus susceptibles et succombent plus rapidement aux infections virales comparées aux mouches sauvages. Beaucoup d'études biochimiques entreprises durant les dernières années ont permis d'obtenir une image assez précise de la fonction moléculaire de ces trois protéines *in vitro*. Cependant, plusieurs études *in vivo* ont révélé une réalité plus complexe, probablement liée à l'association de ces molécules avec des co-facteurs. Le but de ma thèse était d'identifier ces co-facteurs et d'étudier leur fonction, notamment dans un contexte infectieux.

Question posée

Quels sont les co-facteurs protéiques de la voie des siRNA dans un contexte infectieux chez la drosophile ? Quelle est la contribution de chacun de ces co-facteurs dans le contrôle de la charge virale ?

Approches expérimentales

<u>Etude protéomique de l'environnement de Dcr-2, AGO2 et R2D2</u>

Dcr-2, AGO2 et R2D2 ont été étiquetés par génie génétique avec un tag de 16 acides aminés, reconnu par la biotin-ligase BirA , qui permet leur biotinylation. Des lignées de cellules S2 stables exprimant chacune de ces protéines ont été sélectionnées et soumises ensuite à des infections par trois virus à ARN ayant des caractéristiques et des sites de

réplication différents: le virus C de la Drosophile (DCV) (*Dicistroviridae*), le virus de la stomatite vésiculaire (VSV) (*Rhabdoviridae*) et le Flock House virus (FHV) (*Nodaviridae*). Au pic d'infection, les cellules ont été lysées et les protéines d'intérêts purifiées grâce à la grande affinité de la biotine pour la streptavidine. Les complexes récupérés ont été analysés par spectrométrie de masse afin d'identifier les cofacteurs associés. L'analyse protéomique a été réalisée dans le cadre d'une collaboration avec le laboratoire de Joëlle Vinh à l'ESPCI ParisTech (Paris).

Etude fonctionelle par criblage ARN interférence

Des ARN double brins, ciblant spécifiquement l'expression de chacune des protéines identifiées, ont été synthétisées *in vitro* grâce à une stratégie employant la polymérase T7. Ces ARN doubles brins ont été ensuite transfectés dans les cellules afin d'inhiber l'expression des gènes cibles. Quatre jours après ce traitement les cellules ont été infectées par VSV, DCV ou FHV. La charge virale a été ensuite quantifiée, 16h post-infection pour DCV et FHV et 48 post-infection pour VSV. La quantification des charges virales s'est faite par Transcription Réverse suivie de QPCR (PCR quantitative), ou immuno-marquage des capsides virales.

Résultats

La spectrométrie de masse a permis d'identifier 101 molécules interagissant avec la voie des siRNA. 16 % des protéines identifiées ont déjà été trouvé associées à Dicer , Argonaute ou TRBP (homologue de R2D2 chez les mammifères) dans d'autres organismes. En outre, plusieurs molécules de drosophiles impliquées dans des mécanismes d'ARN interférence ont été identifiées. Ces observations constituent une validation de la méthode employée. Une observation intéressante découlant de cette analyse était que les complexes s'associant à Dcr-2, R2D2 et AGO2 sont modifiés en réponse à l'infection virale. En outre, un certain nombre de ces changements sont spécifiques du virus utilisé.

Le criblage RNAi nous a ensuite permis d'identifier beaucoup de facteurs cellulaires qui influencent la réplication virale négativement, de la même manière que AGO2. Ces facteurs représentent de bons candidats pour être des régulateurs de la voie de l'ARN interférence antivirale chez la drosophile. Trois familles de gènes ayant des effets importants sur la réplication virale se dégagent : (i) les chaperonines de type TriC/CCT (T-cp1, CCt gamma, CG7033 ,T-cp zeta) , (ii) les gènes nucléaires impliqués dans la

transcription et l'organisation générale de la chromatine (pontine, reptine, hcf) et (iii) les gènes impliqués dans le transfert nucleo-cytoplasmique (RanGap, RapGap, Nup358, Nup214). L'inhibition par RNAi de la plupart de ces gènes n'affecte pas la viabilité cellulaire, un facteur important à prendre en compte pour l'analyse des résultats.

Le criblage a permis également d'identifier des gènes pro-viraux. Parmi ces gènes beaucoup étaient des protéines ribosomales. L'inhibition de la plupart des protéines ribosomales a cependant un effet très fort sur la viabilité des cellules, ce qui rend l'interprétation des résultats délicate. Une protéine en particulier a toutefois suscité notre intérêt en raison de son caractère non indispensable pour la viabilité cellulaire, la protéine RACK1 (Receptor of Activated Kinase C 1).

RACK1 est une protéine localisée dans la plateforme de la sous-unité 40S du ribosome. Curieusement, l'inhibition de RACK1 n'affecte ni la viabilité des cellules ni leur prolifération, mais a un effet négatif fort sur la réplication de DCV et un autre virus de la même famille, le Cricket Paralysis Virus (CrPV). En revanche, les réplications de FHV et de VSV ne sont pas affectées par l'inhibition de RACK1. Ces observations nous ont conduit à émettre l'hypothèse que RACK1 serait indispensable à la traduction et à la réplication des virus contenant un élément IRES (Internal Ribosomal Entry Site) (i.e. : DCV, CrPV) et serait dispensable à la traduction des virus utilisant une coiffe 5' pour leurs traductions (i.e. : VSV et FHV).

Afin de tester cette hypothèse trois approches complémentaires on été employées. Premièrement nous avons pu démontrer que le pool de RACK1 situé dans le ribosome est responsable du phénotype observé, et cela en créant des mutations ponctuelles dans RACK1 qui affectent sa liaison au ribosome. Dans des expériences de sauvetage, les mutants RACK1 ne pouvant se fixer au ribosome n'ont pas pu stimuler la réplication de CrPV, contrairement à la version sauvage de la protéine. La deuxième approche consistait à utiliser des gènes rapporteurs luciférase contenant un IRES ou une coiffe 5'. Nous avons observé que le rapporteur contenant une coiffe 5' n'est pas affecté par la déplétion de RACK1 contrairement à celui qui contient l'IRES de CrPV. La troisième approche était de quantifier les messagers viraux dans les ribosomes engagés dans la traduction dans des cellules contenant ou pas RACK1, grâce à la méthode des profils de polysomes. La quantité des l'ARNm de FHV dans les polysomes n'est pas modifiée par l'inhibition de RACK1, contrairement aux ARNm de CrPV et de DCV.

Nous avons alors contacté l'équipe de Thomas Baumert à l'Institut de Virologie de Strasbourg, afin de tester l'implication de RACK1, une protéine fortement conservée au cours de l'évolution, dans la réplication d'un virus de mammifères à IRES, le virus de l'Hépatite C (VHC). Nos collaborateurs ont pu montrer que la présence de RACK1 était cruciale pour la traduction et la réplication du VHC, un virus qui constitue une menace majeure pour la santé humaine. Le mécanisme impliquant RACK1 dans la traduction IRES-dépendante est donc conservé au cours de l'évolution. Ainsi, en ciblant cette protéine de l'hôte, on peut inhiber la réplication virale sans affecter la viabilité cellulaire.

Des études antérieures ont montré que la présence d'une mutation homozygote dans le gène RACK1 est létale à des stades avancés du développement embryonnaire chez la souris et des stades larvaires chez la mouche. Nous avons montré par des expériences de génétique chez la drosophile qu'une copie de RACK1 incapable de se lier au ribosome est incapable de sauver le phénotype développemental causé par une mutation non-sens de RACK1. Ces observations indiquent que RACK1 joue un rôle dans la traduction d'une certaine classe d'ARNm endogènes au cours du développement.
La dernière partie de mon travail de thèse a consisté à employer la méthode du profil de polysomes suivie d'une analyse par puces à ADN pour identifier les ARNm dont la traduction dépend de RACK1. Les résultats sont en cours d'analyse.

Conclusions

L'étude entreprise a permis d'identifier 101 cofacteurs de Dcr-2, Ago2 ou r2d2. Certains de ces co-facteurs ont un effet antiviral (i.e. : Chaperonines TriC/CCT), et d'autres un effet proviral (i.e. : RACK1). Nous avons ensuite pu montrer que RACK1 est un facteur cellulaire spécifique, indispensable à la traduction des génomes viraux contenant une séquence IRES. Ainsi RACK1 serait une cible idéale pour le traitement des infections causées par des virus contenant des IRES, en utilisant par exemple des ARNsi inhibant son expression. Une demande de brevet US provisionnel a été déposée en ce sens.

Perspectives

Des hypothèses expliquant l'implication de certaines familles de gènes identifiées, dans l'immunité antivirale, peuvent être testées. Par exemple, nous soupçonnons l'implication des chaperonines TriC/CCT dans le bon repliement de l'extrémité amino-terminale riche en glutamine de AGO2. Des outils ont été mis en place pour tester cette hypothèse rapidement.

Concernant RACK1, l'interrogation du transcriptome, ainsi que du traductome va permettre d'identifier les ARNm qui dépendent de cette protéine ribosomale pour leur traduction. L'identification de tels ARNm permettrait de prévenir les effets secondaires que pourrait avoir une thérapie antivirale ciblant RACK1. En élargissant la palette des ARNm régulés par RACK1 et en ouvrant l'étude de leurs séquences 5' et 3' UTR, elle lèverait également un voile sur la nature du « code ribosome » qui permet la traduction spécifiques de certains ARNm chez les eucaryotes.

Résumé (Abstract) en français

La voie de l'ARN interférence (ARNi), en particulier celle des siRNA, constitue la défense antivirale majeure chez les plantes, les nématodes et les insectes. Le génome de l'organisme modèle *Drosophila melanogaster* code pour trois protéines, Dcr-2, AGO2 et R2D2, indispensables à cette voie. Les mouches mutantes pour une de ces trois protéines sont plus susceptibles et succombent plus rapidement aux infections virales comparées aux mouches sauvages. Beaucoup d'études biochimiques ont permis d'obtenir une image assez précise de la fonction moléculaire de ces trois protéines *in vitro*. Cependant, plusieurs études *in vivo* ont révélé une réalité plus complexe, probablement liée à l'association de ces molécules avec des cofacteurs. Ce manuscrit décrit les approches adoptées afin d'identifier les partenaires protéiques de la voie des siRNA et d'étudier leurs rôles, notamment dans un contexte infectieux. Dcr-2, AGO2 et R2D2 ont été étiquetés par génie génétique avec un tag de 16 acides aminés, reconnu par la biotin-ligase BirA, qui permet leur biotinylation après leurs transfections dans les cellules S2. Les cellules transfectées ont été ensuite soumises à différentes infectiones virales, notamment avec le virus C de la Drosophile (DCV) (*Dicistroviridae*), le virus de la stomatite vésiculaire (VSV) (*Rhabdoviridae*) ou le Flock House virus (FHV) (*Nodaviridae*). Les cellules ont été ensuite lysées au pic de l'infection et les complexes protéiques purifiés et analysés par spectrométrie de masse.

La spectrométrie de masse a permis d'identifier 101 molécules interagissant avec la voie des siRNA. 16 % des protéines identifiées ont déjà été trouvé associées à Dicer , Argonaute ou TRBP (homologue de R2D2 chez les mammifères) dans d'autres organismes. En outre, plusieurs molécules de drosophiles impliquées dans des mécanismes d'ARN interférence ont été identifiées. Une observation intéressante découlant de cette analyse était que les complexes s'associant à Dcr-2, R2D2 et AGO2 sont modifiés en réponse à l'infection virale. En outre, un certain nombre de ces changements sont spécifiques du virus utilisé. Le criblage fonctionnel par RNAi des molécules identifiées a permis d'identifier beaucoup de facteurs cellulaires qui influencent la réplication virale négativement. Trois familles de gènes ayant des effets importants sur la réplication virale se dégagent : (i) les chaperonines de type TriC/CCT (T-cp1, CCt gamma, CG7033 ,T-cp zeta) , (ii) les gènes nucléaires impliqués dans la transcription et l'organisation générale de la chromatine

(pontine, reptine, hcf) et (iii) les gènes impliqués dans le transfert nucleo-cytoplasmique (RanGap, RapGap, Nup358, Nup214). Le criblage a, également, permis d'identifier des gènes pro-viraux. Une protéine en particulier a toutefois suscité notre intérêt la protéine RACK1 (Receptor of Activated Kinase C 1). L'inhibition de RACK1 n'affecte ni la viabilité des cellules ni leur prolifération, mais a un effet négatif fort sur la réplication de DCV et un autre virus de la même famille, le Cricket Paralysis Virus (CrPV). En revanche, les réplications de FHV et de VSV ne sont pas affectées par l'inhibition de RACK1. Ultérieurement, nous avons pu prouver grâce à des expériences complémentaires que RACK1 et un facteur de l'hôte indispensable à la traduction et la réplication des virus possédants une séquence IRES (Internal Ribosomal Entry Site) dans leurs génomes, tel que DCV et CrPV. En outre, cela était vrai pour un virus humain à IRES, le virus de l'Hépatite C (VHC). En effet, l'inhibition de RACK1 dans des hépatocytes humains a causé une forte diminution du titre de VHC. Ainsi RACK1 serait une cible idéale pour le traitement des infections causées par des virus contenant des IRES.

En conclusion, cette étude a pu identifier plusieurs gènes ayant une fonction antivirale. Ces facteurs représentent de bons candidats pour être des régulateurs de la voie de l'ARN interférence antivirale chez la drosophile. Cette étude a également pu caractériser un gène pro-viral, RACK1, qui constitue une cible idéale pour des thérapies visant à combattre l'infection des virus à IRES.